Phenotypic and genomic diversity of *Sclerotinia sclerotiorum* L. de Bary in Canada

Laura Esquivel Garcia

Plant Science Department

Macdonald Campus of McGill University

21111 Lakeshore, Sainte Anne de Bellevue, Québec H9X 3V9

April 2024

A thesis submitted to McGill University in partial fulfillment of the requirements of the degree of Master of Science

Contents

ACKNOWLEDGMENTS

I would like to express my gratitude to my supervisor, Dr. Valerio Hoyos-Villegas for his support and guidance throughout my research journey. His expertise was instrumental in shaping this work.

I am also beyond grateful first to my home country for providing the funding to continue with my professional journey through the National Council of Science and Technology (CONACYT), Agriculture and Agri-Food Canada (AAFC) for providing the funds to perform my research, and to MITACS through their Global Research Award (GRA) for providing the funding for a research exchange at Curtin University in Australia, which was substantial for completing my research.

I extend my heartfelt appreciation to Dr. Mark Derbyshire who played a significant role in the bioinformatics component of my research, his patience and kind words motivated me in my academic journey. During my internship in his lab, I earned valuable knowledge and met many inspiring people, so I want to also thank his team at the Centre for Crop and Disease Management who were always keen to provide their support.

I am also thankful to Dr. Jaqueline Bede, who agreed on being part of my committee and put her time to provide feedback during my committee meetings.

I am grateful to my friends and colleagues for their constructive feedback, help, and the insightful discussions, which enriched the quality of this work.

Lastly, I would like to thank my family for their unwavering love, encouragement, and understanding, especially during the hardest times and uncertainty. Their belief in me has been a constant source of motivation.

ABSTRACT:

Sclerotinia sclerotiorum L. de Bary (*Ss*), the causal pathogen of white mold disease, poses a significant threat to global agricultural production, affecting a broad spectrum of plant species, including the economically important common bean (*Phaseolus vulgaris* L.). Understanding the genetic diversity and pathogenicity of *Ss* is crucial for developing effective disease management strategies.

In this study, we conducted a phenotypic dual trait analysis focusing on categorizing the isolates based on their compatibility reactions by establishing Mycelial Compatibility Groups (MCGs) and determining aggressiveness levels by assessing the disease-inducing capability of a population of 39 *Ss* isolates collected across Canada. These isolates were tested on two common bean germplasms: the susceptible cultivar Beryl and the moderately resistant landrace G122.

Upon pairing all isolates by challenging them against each other, we established 18 MCGs among a small population of 39 *Ss* isolates, suggesting high genetic diversity. Aggressiveness of isolates was assessed using *in planta* inoculation, allowing for categorization of *Ss* isolates by aggressiveness levels, as determined by the statistical analysis of STAUDPC mean values in the susceptible cultivar.

To complement the phenotypic analysis, we sequenced two *Ss* genomes using Nanopore sequencing technologies. This approach provided long reads, which are more effective in identifying large structural variants (SVs) compared to traditional short-read sequencing methods. Aided by long reads generated data we obtained high-quality, contiguous genome assemblies. By utilizing the generated assemblies, we followed a pipeline and compared the genome of two *Ss* isolates. The pipeline was part of a rapid approach that enabled the identification of large SVs utilizing bioinformatic tools tailored for long-reads that enabled the identification of SVs. These SVs were spotted in intergenic regions influencing overall genomic architecture. Our genomic analysis revealed significant insights into the genetic differences between two *Ss* genomes. The use of long-read sequencing technology allowed us to capture genomic variations that are often missed by short-read methods, providing a more comprehensive understanding of the pathogen's genome. This knowledge is essential for developing targeted disease management strategies and for breeding resistant common bean cultivars.

Overall, this study highlights the importance of combining phenotypic and genomic analysis to understand the complexity of *Ss* pathogenicity. Our integrated approach underscores the importance of maintaining diverse and representative isolates in disease management studies to accurately assess and mitigate the threat posed by *Ss*. This research provides a foundation for developing targeted strategies to combat white mold disease and protect global agricultural production.

RÉSUMÉ

Sclerotinia sclerotiorum L. de Bary (*Ss)*, l'agent pathogène responsable de la moisissure blanche, constitue une menace importante pour la production agricole mondiale, affectant un large spectre d'espèces végétales, y compris le haricot commun (*Phaseolus vulgaris* L.) d'importance économique. Comprendre la diversité génétique et la pathogénicité du *Ss* est crucial pour développer des stratégies efficaces de gestion de la maladie.

Dans cette étude, nous avons effectué une analyse phénotypique à deux caractères axés sur la catégorisation des souches en fonction de leurs réactions de compatibilité en établissant des groupes de compatibilité mycélienne (MCG) et en déterminant les niveaux d'agressivité en évaluant la capacité d'induire la maladie d'une population de 39 souches *Ss* collectés à travers le Canada. Ces souches ont été testés sur deux cultivars de haricot commun : le sensible Beryl et le G122 possedant résistance intermédiaire (IR).

En appariant toutes les souches en les confrontant les uns aux autres, nous avons établi 18 MCGs parmi une petite population de 39 souches *Ss*, ce qui suggère une grande diversité génétique. Les tests des souches pour la détermination de l'agressivité des souches a été évalué à l'aide d'une inoculation *in planta* permettant la catégorisation des souches de *Ss* par niveaux d'agressivité, comme déterminé par leur analyse statistique des valeurs moyennes STAUDPC dans le cultivar sensible.

Pour compléter l'analyse phénotypique, nous avons séquencé deux génomes *Ss* à l'aide des technologies de séquençage Nanopore. Cette approche a fourni des lectures longues, qui sont plus efficaces pour identifier les grandes variantes structurelles (SV) par rapport aux méthodes traditionnelles de séquençage à lecture courte. Aidé par de longues lectures de données générées, nous avons obtenu des assemblages génomiques contigus et de haute qualité. En utilisant les assemblages générés, nous avons suivi un pipeline robuste et comparé le génome de deux souches *Ss*. Le pipeline faisait partie d'une approche rapide qui a permis l'identification de grandes SV à l'aide d'outils bioinformatiques adaptés aux données de lecture longue qui ont permis l'identification de SV. Ces SVs ont été repérés dans des régions intergéniques et il est suggéré qu'ils influencent l'architecture génomique des génomes analysés. Notre analyse génomique a révélé des informations significatives sur la diversité génétique entre deux génomes de *Ss*. L'utilisation de la technologie de séquençage à lecture longue nous a permis de capturer les variations génomiques

qui sont souvent manquées par les méthodes à lecture courte, offrant ainsi une compréhension plus complète du génome de l'agent pathogène. Ces connaissances sont essentielles pour élaborer des stratégies ciblées de gestion des maladies et pour sélectionner des cultivars de haricots communs résistants.

Dans l'ensemble, cette étude met en évidence l'importance de combiner les analyses phénotypiques et génomiques pour comprendre la complexité de la pathogénicité de *Ss*. Notre approche intégrée souligne l'importance de conserver des suches diversifiés et représentatifs dans les études de gestion des maladies afin d'évaluer et d'atténuer avec précision la menace posée par *Ss*. Cette recherche constitue une base pour l'élaboration de stratégies ciblées visant à lutter contre la pourriture blanche et à protéger la production agricole mondiale.

LIST OF ABBREVIATIONS

AFLP: Amplified Fragment Length Polymorphism

ANOVA: Analysis of Variance

CWDEs: Cell Wall Degrading Enzymes

HTS: High Throughput Sequencing

HGT: Horizontal Gene Transfer

IDM: Integrated Disease Management

IGRs: Intergenic Regions

MAS: Marker-assisted selection

MCG: Mycelial Compatibility Group

ML: Machine Learning

OA: Oxalic Acid

PCD: Programmed Cell Death

PCWDEs: Plant cel wall-degrading enzymes

QDR : Quantitative Disease Resistance

QTL : Quantitative Trait Loci

ROS: Reactive Oxygen Species

RAPD: Random Amplification of Polymorphic DNA

SMRT: Single-Molecule Real-Time

SRAP: Sequence-Related Amplified Polymorphism

Ss: *Sclerotinia Sclerotiorum*

SSRs: Simple Sequence Repeats

SNPs: Single Nucleotide Polymorphism

TEs: Transposable Elements

SVs: Structural Variants

WGS: Whole Genome Sequencing

LIST OF FIGURES

LIST OF TABLES

CONTRIBUTION TO KNOWLEDGE

- *Sclerotinia sclerotiorum* L. de Bary IN CANADA: PHENOTYPING TRAITS FOR EPIDEMIOLOGICAL INSIGHTS.

This chapter integrates phenotypic and genotypic analyses to explore the relationship between Mycelial Compatibility Groups (MCGs), and aggressiveness variation in *Ss* isolates. The key contributions to knowledge from this chapter include:

1) Comprehensive Phenotypic Characterization: The chapter provides a detailed characterization of *Ss* MCGs and isolates aggressiveness. This information is crucial for breeding programs aimed at developing resistant cultivars and for tailoring management practices to specific pathogen populations.
2) High genetic diversity in *Ss*: In this chapter the establishment of MCGs led us to the conclusion that the reproduction dynamics in *Ss* is a subject of crucial interest in new populations. We encountered high genetic diversity in a small population, highlighting the need to keep exploring *Ss* biology as a measure for tailoring management strategies.
3) Classification system for MCGs: While there are diverse classification systems based on different approaches, a consensus has not been set to classify MCGs. In our study we suggest that a classification system is applied to classify MCGs based on frequency and geographic dispersal. We suggest that this classification system facilitates in the decision making for research directions in population structure studies.

- CHARACTERIZATION OF STRUCTURAL VARIANTS IN *Sclerotinia sclerotiorum* L. de Bary WITH NANOPORE WHOLE-GENOME SEQUENCING.

This chapter presents significant advancements in the genomic characterization of *Sclerotinia sclerotiorum* (*Ss*) by employing long-read sequencing technology. The primary contributions to knowledge from this chapter are as follows:

1) High-Quality Genome Assemblies: By utilizing Nanopore whole-genome sequencing, we generated highly contiguous genome assemblies of two *Ss* isolates. This approach overcame the limitations of short-read sequencing, providing a more accurate and comprehensive view of the *Ss* genome
2) Identification of Structural Variants (SVs): Our study identified 106 large structural variant (SV) insertions using a whole-genome alignment approach with the Sniffles2 variant caller. This contribution is crucial for understanding the genomic architecture and variation within *Ss* populations. Although the results need further exploration, they offer a preliminary view of genomic variation dynamics particularly in non-coding regions.
3) Insights into Genomic Diversity: Our findings highlight the genomic diversity and complexity of *Ss*, which are essential for developing effective disease management strategies. This work sets a new standard for genomic studies in phytopathogenic fungi, demonstrating the utility of long-read sequencing in capturing genomic variations that are often missed by traditional short-read methods.

1.1. INTRODUCTION

Common bean (*Phaseoulus vulgaris* L.) is a crucial legume crop globally, serving as a significant source of protein, fiber, vitamins, and minerals for millions of people, particularly in developing countries. Its versatility in cultivation and nutritional makes it a staple food and an essential component of sustainable agricultural systems (Myers & Kmiecik, 2017). However, the production of common beans is increasingly threatened by biotic stresses, which severely impact yield and quality. Among these biotic stresses, fungal pathogens, such as *Sclerotinia sclerotiorum* (Lib.) de Bary *(Ss*), present a great challenge.

Sclerotinia sclerotiorum, the causal pathogen of the white mold disease in common bean (*Phaseolus vulgaris* L.), is a devastating fungus with necrotrophic behavior (Gerard et al., 2011; McDonald & Boland, 2004) . White mold is a major threat in various bean production areas, prompting efforts to improve resistance to this disease. However, resistance elucidation remains challenging due to the need for a detailed characterization of pathogenic determinants involved in its development (Dong et al., 2015). Damage caused by *Ss* varies among populations from different regions (Otto-Hanson et al., 2011). *Ss* isolates demonstrate variation in different phenotypic traits. This variation in phenotype causes a wide range of responses. Such is the case of aggressiveness among *Ss* (Willbur et al., 2017). Despite attempts to develop resistant cultivars, existing information on resistance against *Ss* is limited to a few isolates, failing to represent genetically diverse isolates across a wide geography (Hoffman et al., 2002; Kim & Diers, 2000).

Although genetic diversity studies have been routinely performed, they often lack comprehensive representation and standardization. They are based on molecular markers or high-throughput techniques based on short reads and often fail to capture important sources of genomic variation by introducing sequencing and alignment bias (Aldrich-Wolfe et al., 2015; Cubeta et al., 1997; Hambleton et al., 2002; Liu et al., 2018; Sharma et al., 2015).

Despite ongoing efforts to develop resistant cultivars, the current characterization of genomic variation driving white mold disease in Canadian pulse crops remains outdated and incomplete. Therefore, this study aimed to perform a comprehensive investigation, combining both phenotypic and genomic analysis, to unravel the intricate genomic landscape on two *Ss* isolates. By utilizing advanced long-read sequencing technologies, this study aimed to generate high-quality genome assemblies to facilitate the understanding of the genomic diversity underlying *Ss*. Additionally, we

sought to establish a correlation between phenotypic traits, such as Mycelial Compatibility Group reactions (MCGs), pathogen aggressiveness, and structural genomic variation, providing valuable insights for tailored crop breeding strategies aimed at fighting *Ss* genotypes responsible for significant yield losses in Canadian pulse crops.

To effectively address the central thesis, the Objectives, and Hypothesis are outlined as follows:

General Objective: To investigate *Sclerotinia sclerotiorum* (Lib.) de Bary *(Ss)* dynamics in a Canadian population, integrating phenotypic dual-trait analysis and advanced long-read genotyping.

Objective 1: Establish phenotypic diversity in a *Ss* Canadian population.

Objective 1.1. Establish Mycelial Compatibility Groups among collected samples.

Hypothesis: Isolates with geographic closeness will display compatible responses, whereas isolates geographically distant will be incompatible.

Objective 1.2. Aggressiveness determination of isolates and recording responses of current germplasm of partial resistance.

Hypothesis: Isolates will display differential aggressiveness levels in both susceptible and moderately resistant germplasm.

Objective 2: Implementing Whole Genome Sequencing (WGS) genotyping with long-reads to identify structural variants.

Hypothesis: Nanopore reads will enable the identification of large structural variants.

CHAPTER 1: LITERATURE REVIEW

1.1. Common bean importance, origin, and worldwide production.

Common bean (*Phaseolus vulgaris* L.) is an important pulse crop cultivated and consumed worldwide (Broughton et al., 2003). Common beans are important due to their high levels of proteins and carbohydrates. They also contain vital components such as micronutrients and vitamins, making them an appealing food source in the fight against malnutrition (Sathe, 2002).

The common bean emerged from two separate gene pools: The Mesoamerican and the Andean gene pools (Debouck & Smartt, 1995). The former contains four races: Jalisco, Durango, Central America, and Guatemala. The latter, on the other hand, contains three races: Nueva Granada, Chile, and Peru (Beebe et al., 2001; Bitocchi et al., 2013; Bitocchi et al., 2017).

Common bean is cultivated in more than 100 countries worldwide with a global production of 28.35 million tons harvested from an area of 36.79 million hectares as per the latest report from 2022. The top producers of common bean include India, Brazil, Myanmar, and the United Republic of Tanzania with an annual production of 6.61, 2.84, 2.66, and 1.34 million tons respectively as observed in Figure 1.

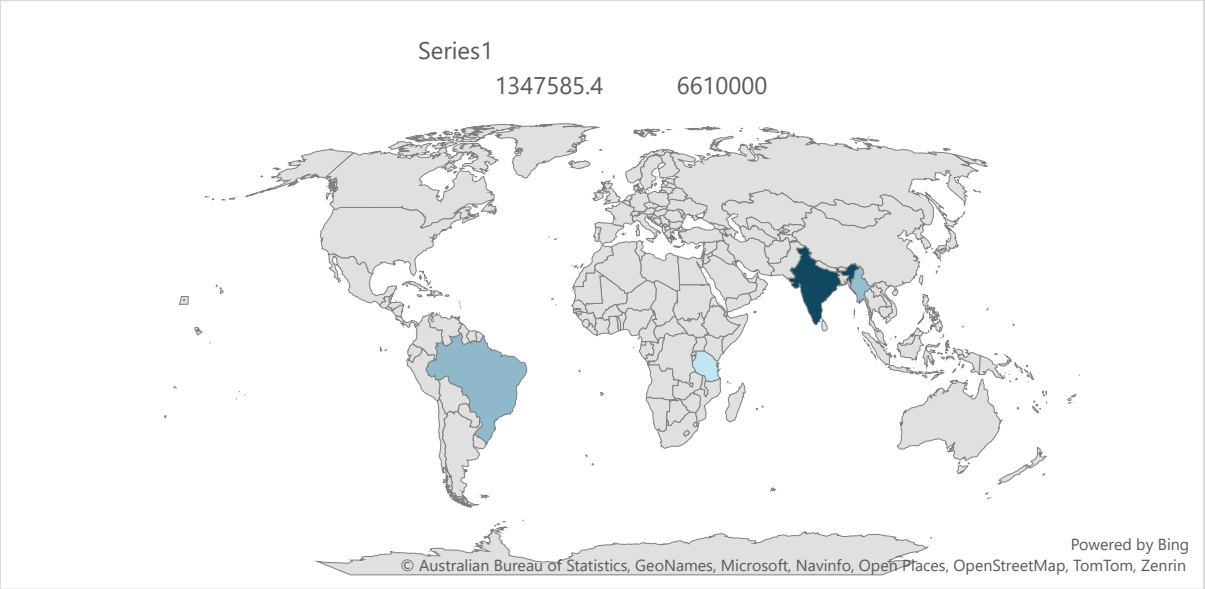

Figure 1. Top 5 common bean producing countries (2021-2022). This map illustrates the top five common bean producing countries, showcasing production quantities with color gradients representing production volume. Darker colors indicate higher production, while lighter shades denote lower production levels. Data is measured in tons, providing a comparative view of each country's production for the last reported period in FAOSTAT. India leads the production with 6.61 million tons, while the United Republic of Tanzania ranks fifth with 1.34 million tons.

Canada is also key player in the global common bean production, contributing significantly to the overall output of this important crop. Annually, Canada produces approximately 312,994 tons of common beans, which accounts for about 1.10% of the total global production. In fact, Canada is one of the leading contributors to the Americas' collective bean production. According to statistics from 2021-2022, the Americas collectively produced 26.3% of the world's beans, second only to Asian countries. This highlights the crucial role that Canada plays in meeting the growing demand for common beans, both domestically and internationally (FAOSTAT, 2024). This is depicted in Figure 2.

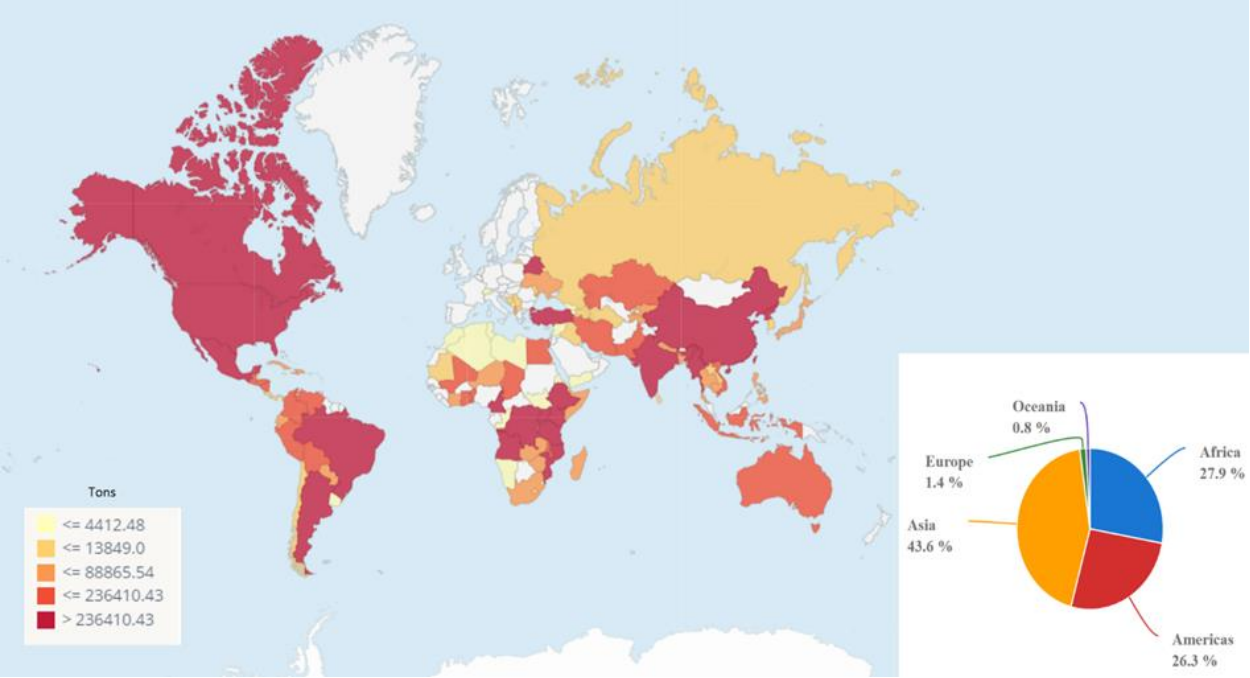

Figure 2. Production quantities of dry bean by country. Customized from FAOSTAT consulted in March 2024. Visual representation presents worldwide dry bean production, with varying color gradients indicating production volume, from light yellow for lower production to deep red for higher production levels. Production quantities are measured in metric tons. Additionally, accompanying the map is a bar chart illustrating the percentage contribution of each continent to the overall global production of common beans.

As awareness of the health benefits associated with common bean consumption continues to rise, so does their popularity among consumers (Nchanji & Ageyo, 2021; Rodríguez et al., 2022). Countries like the United States, Mexico, and Brazil have long embraced beans as dietary staple, but now, emerging countries are also recognizing the nutritional value and versatility of these pulse crop influencing their acceptance as part of their diet (Bitocchi et al., 2017; FAOSTAT, 2024; King et al., 2024). This trend towards increased consumption not only reflect the growing appreciation for beans' nutritional benefits but also presents significant opportunities for further expansion of bean cultivation and trade.

1.2. Common bean and research in developing biotic stress resistance

Despite the prevailing emphasis on increasing common bean production, the bean industry faces a critical challenge from biotic stresses. Research to tackle biotic stresses affecting staple crops is a top priority for plant breeders (Miklas et al., 2006). By addressing these challenges, plant scientists also align with the Food and Agriculture Organization's (FAO) current agenda to fight malnutrition by 2030 (FAO, 2024), with the common bean representing a promising option. Hence, it is crucial to address the biotic stresses that common beans face throughout their growth cycle, especially in regions with the highest production worldwide, where emerging problems threaten common bean production areas.

Common beans, like other crops, face numerous biotic stresses, including diseases caused by pathogens such as fungi, bacteria, viruses, and pests, which pose significant challenges, as reported by Singh and Schwartz (2010).

White mold, caused by the fungal pathogen *Ss,* has represented one of the most devastating diseases affecting common beans (Steadman, 1983). Substantial research has been done regarding the fight against *Ss* in common beans and other pulses. This research encompasses various approaches tailored to understanding the pathogen's biology, host-pathogen interactions, biological control, genomics, and molecular markers, breeding for resistance, and developing effective management strategies. Studies have explored the genetic diversity, pathogenicity factors, and mechanisms of infection of *Ss* in canola and common bean embracing advanced Machine Learning (ML) algorithms enhancing epidemiological studies (Shahoveisi et al., 2022). On a similar basis, investigations have examined the mechanisms of physiological resistance of white mold in common beans (Miklas et al., 2013). Research involving environmentally friendly options for controlling *Ss* has also been a topic of interest. Such is the case of the exploration of beneficial

microorganisms like *Trichoderma spp.* (Vinale et al., 2014) and *Pseudomonas chlororaphis* (Nandi et al., 2017) in reducing disease incidence and severity. In addition, studies that support integrated disease management (IDM) have been a crucial topic, as they are believed to offer the best outcomes when fighting fungal pathogens (O'Sullivan et al., 2021). Comprehensive disease management requires an understanding of the multifaceted nature of the pathogen. As the threat evolves, it becomes imperative to address its broad host range and its capacity to infect and thrive on various host tissues.

1.3. *Sclerotinia sclerotiorum* L. de Bary: a cosmopolitan threat with a necrotrophic behaviour

White mold is considered among the main fungal diseases affecting bean production worldwide attributed to its cosmopolitan behavior. The definition of *Ss* as a cosmopolitan pathogen lies in its ability to infect more than 425 plant species in 74 families, including cultivated plants like common bean, and non-cultivated plant species alike (Derbyshire et al., 2022)

The disease is endemic and widespread in North and South American countries, observed especially during seasonally cooler and more humid environmental conditions (Miklas et al., 2013). Although the disease occurs in cool and moist areas, its incidence has been highly reported in hot and dry localities when the season favors such conditions, meaning this is a widely distributed fungal disease all over the globe, which consistently agrees with its previously described cosmopolitan presence (Saharan & Mehta, 2008).

Ss is commonly transmitted to the host by inoculum present in the soil in the form of black hard structures called sclerotia, or through the deposition of inoculum transported by the wind (ascospores) which deposit on aerial plant organs. Additionally, *Ss* has been considered a fungus

with prototypical necrotrophic pathogenesis, surviving from dead plant cells. As a necrotrophic pathogen, *Ss* uses its arsenal of toxins, and cell wall-degrading enzymes that facilitate the penetration into the cell wall, which is key to the initiation of the infection process (Bolton et al., 2006; Glazebrook, 2005; Horbach et al., 2011). However, recent studies have demonstrated the adaptability of this pathogen in its lifestyle, with the ability to display an early biotrophic phase on its host, with the early infection on living plant cells, later transitioning to its typical necrotrophic behavior (Kabbage et al., 2015), which has sparked debates about a more accurate lifestyle suggesting it will be better described as a hemibiotroph serving as a fungal model for a predominant asexual reproduction system, producing inoculum that persists over time, and sexual sporulation (Joelle et al., 2011). Understanding *Ss* biology is crucial to defeating the disease, which is why studying how it manifests with an impact in common beans is a priority.

1.4. White mold symptoms and its impacts in common bean

From over 60 names used to refer to the diseases caused by *Ss* in different crops, the term adopted for the disease symptoms observed in common beans is “white mold” (Saharan & Mehta, 2008). The term “white mold” is mostly attributed to the presence of a white fluffy mycelium at the early stages of infection on aerial plant parts, a feature that lasts only some days until it finally gives place to the rise of the most persistent inoculum which is key in *Ss* success (Rollins Jeffrey & Dickman Martin, 2001). In broad terms, white mold affects all aerial plant parts (stems, flowers, and pods), and first manifests as a water-soaked, to brown appearance. The infection does not follow a specific pattern but instead forms irregularly through the infected parts, later developing into fluffy white mycelial growth, giving the disease its characteristic appearance (Kabbage et al., 2015). As the infection progresses, the affected tissues get a necrotic appearance leading to stem rot, wilting with imminent death (Boland & Hall, 1994). Humid conditions are favorable for the

symptoms to expand along the tissue; hence it has been observed that the disease often thrives in temperate regions during periods of high rainfall or irrigation (Boland & Hall, 1994). The infection in plant organs develops with some particularities. In affected flowers mycelium formation with a cotton appearance is observed. In vegetative organs such as pods, branches, leaves, and stems, damages are first observed as watery small dark green spots, that rapidly increase in size until they finally produce fatal outcomes to the entire organ.

Ss, the causal pathogen of the white mold disease, is responsible for substantial yield and quality losses in common beans (Gerard et al., 2011; McDonald & Boland, 2004). Losses attributed to *Ss* in common bean can vary depending on several factors such as disease severity of the *Ss* population present in a region, cultural practices, and environmental conditions. Globally, *Ss* is known to provoke significant yield losses. It is estimated that each year, losses caused by white mold range from 20% to as high as 100% under favorable weather conditions in susceptible cultivars (Purdy, 1979; Schwartz & Singh, 2013). Similarly, del Río et al. (2004) analyzed protected and non-protected plots with 34% to 50% and 73% to 76% disease incidence respectively, in navy bean in North Dakota. In Alberta, Canada, it was observed that disease incidence in common bean varied depending on market class with pinto beans, on average, having the highest disease incidence (33%) followed by great Northern (15%), black (10%), red (6%), and yellow (5%) (Reich et al., 2023).

Overall, the evidence highlights the critical importance of implementing effective disease management strategies to mitigate yield losses in common beans. Understanding the epidemiology of *Ss* is key to minimizing its impact on crop yields.

1.5. *Sclerotinia sclerotiorum* life cycle

The life cycle of *Ss* is complex and consists of several stages that contribute to the pathogens' ability to infect and spread within common bean crops. *Ss's* ability to disseminate and its persistent behavior to infect a wide range of plant species all over the world is attributable in great measure to the capacity to produce sclerotia that can survive in the soil for several years. Starting from sclerotia as the primary inoculum in the life cycle, sclerotia germinate either myceliogenically, giving place to the asexual cycle of reproduction, or carpogenically to initiate the sexual cycle where apothecia are produced out of sclerotia and release ascospores which are usually responsible for stem infection causing great yield losses (Boland & Hall, 1994; Derbyshire & Denton-Giles, 2016; Kabbage et al., 2015). Once it has infected the plant, the fungus colonizes host tissues with an arsenal of toxins and cell wall-degrading enzymes followed by the formation of mycelial mats that spread and produce new sclerotia (Kabbage et al., 2015). The fact that *Ss* poses a dual reproduction system is what helps its survival influencing population structure. Regulation of sexual sporulation is classified as homothallic (self–fertile) hence, a single ascospore could complete the whole cycle. Dispersal of *Ss* is via air-borne ascospores, which will eventually germinate in the presence of water and develop as hyphae helped by exogenous nutrients. Appressoria derive from hyphae and penetrate plant surfaces producing plant infection (de Abreu et al., 2019; Joelle et al., 2011).

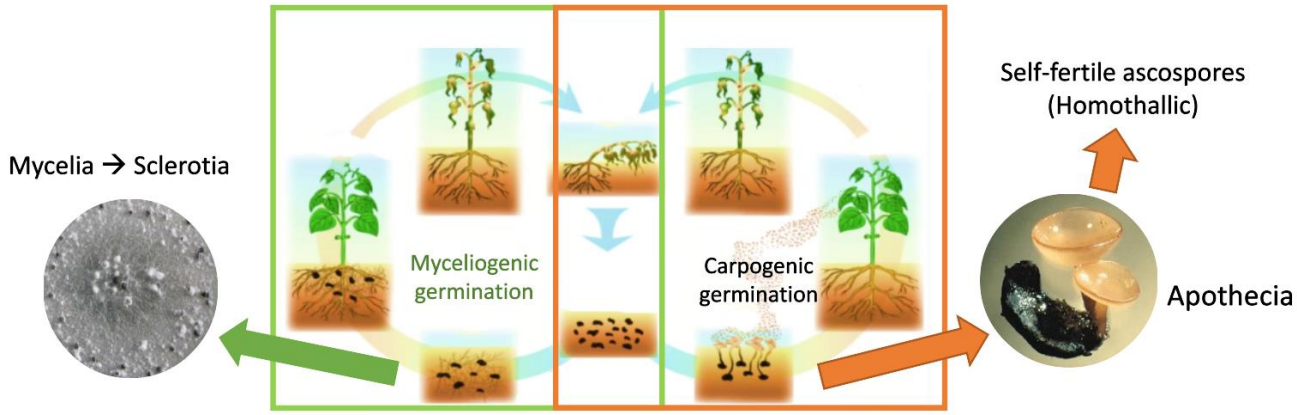

Figure 3. Myceliogenic and carpogenic germination of *Sclerotinia sclerotiorum* on common bean. Sclerotia are dark, hardened structures that remain dormant in the soil. Depending on weather conditions, sclerotia can germinate myceliogenically, producing hyphae that directly infect plant tissues, or carpogenically, forming mushroom-like structures called apothecia, that release ascospores and to infect aerial plant parts. Adapted from: de Abreau et al., 2019 and Amselem et al., 2011.

1.6. Sclerotia as a persistent inoculum

The life cycle, colonization, and sclerotia formation of *Ss* allow this phytopathogenic fungus to persist in the soil and infect subsequent bean crops, making it a major challenge for disease management (Boland & Hall, 1994; Kabbage et al., 2015).

Sclerotia are hard, asexual, resting structures produced by *Ss,* which can survive for years in soil (Bae & Knudsen, 2007; Smith et al., 2015). Not only do their melanized and compact attributes help sclerotia to remain dormant in the soil for extended periods, but this also benefits their survival, resisting adverse environmental conditions such as drought and extreme temperatures (Bolton et al., 2006). Sclerotia germinate in two ways: carpogenically to form apothecia from which ascospores are liberated, or vegetatively to produce hyphae (Erental et al., 2008).

Sclerotia production is important in an economical context, as sclerotia are persistent resting and dissemination structures of *Ss* (Bolton et al., 2006). Sclerotia development has traditionally been classified into three distinct stages, based on macroscopically evident

characteristics: (1) initiation -the appearance of small distinct initial forms of interwoven hyphae, (2) development -an increase in size, and (3) maturation -characterized by surface delimitation, internal consolidation, and pigmentation, and often associated with droplet secretion (Bolton et al., 2006; Townsend & Willetts, 1954). These phases are accompanied by both morphological and biochemical differentiation. The initiation and maturation stages of sclerotial development are affected by numerous factors, such as photoperiod, temperature, oxygen concentration, mechanical factors, and nutrients (Chet & Henis, 1975).

1.7. Host-pathogen interactions.

Significant progress has been made in understanding host-fungal interactions in recent years. Notably, advances have been made specifically for pathosystems involving *Ss*, focusing on either the molecular mechanisms of fungal virulence or plant quantitative disease resistance (QDR) (Mbengue et al., 2016).

On the fungal side, *Ss* is a necrotrophic phytopathogen, which uses a variety of pathogenicity factors to facilitate infection of their plant hosts (Kabbage et al., 2015; Oliver & Ipcho, 2004). *Ss* takes advantage of the nutrients present in dead tissue to start the infection process, whose initiation is characterized by the early production of oxalic acid and cell wall-degrading enzymes (CWDEs), such as specific isoforms of polygalacturonase (SSPG1) and protease (ASPS), at the expanding edge of the lesion (Hegedus & Rimmer, 2005). Oxalic acid (OA) plays complex and diverse roles in the infection process and is central to pathogenesis as demonstrated by Godoy et al. (1990). The authors found that when non-pathogenic, oxalic acid-deficient mutants were used to inoculate the aerial organs of common beans (leaves, stems, and pods), these mutants failed to produce disease symptoms, did not produce sclerotia, and exhibited low expression of pectinases

and cellulases. This indicates that both sclerotia formation and the expression of certain plant cell wall-degrading enzymes (PCWDEs) depend on the presence of OA. The main roles of oxalic acid are the suppression of plant defenses, the induction of plant programmed cell death (PCD), the deregulation of guard cell function, and calcium detoxification (Hegedus & Rimmer, 2005). According to Bateman and Beer (1965), *Ss* colonizes and causes adverse effects in its host mainly because its oxalic acid exerts a direct toxic effect through acidification of the environment. At a decreased pH level, the resistance of the host is reduced through the enhancement of PCWDEs efficiency (Favaron et al., 2004; Wang et al., 2009; Wei & Clough, 2016).

The importance of OA in pathogenicity is also emphasized by its ability to strongly chelate biologically important cations such as calcium, iron, manganese, magnesium, nickel, aluminum, and coopper, affecting their solubility and thus availability. OA is also able to destabilize cytoplasmic and chloroplast membranes, which aids in tissue maceration (Dutton & Evans, 1996).

In addition to OA, *Ss* also secretes extracellular proteins able to macerate tissues and degrade cell wall components, best known as PCWDEs. The fungus produces polysaccharide depolymerases and glucosidases, necessary to degrade the important structural cell wall polysaccharides, cellulose, pectin, and hemicellulose. The level of these enzyme activities correlates with the development of disease symptoms (Riou et al., 1991).

When it comes to hosts' defenses against fungal pathogens, plants exert localized responses associated with an oxidative burst and a generalized systemic response mediated by signaling molecules. The result of the oxidative burst is the formation of reactive oxygen species (ROS) that form a toxic barrier to pathogen invasion. The pathogen fights to overcome the effects of ROS and it foremost achieves to suppress the oxidative burst thanks to OA and enzymes, such as superoxide dismutase and catalase that serve to deplete ROS (Cessna et al., 2000; Mayer et al., 2001).

Moreover, Guo and Stotz (2007) found that several signaling pathways including jasmonic acid, salicylic acid, and ethylene signaling were also involved in regulating defense against *Ss* in a study with the plant model *Arabidopsis*. In attempts to obtain a more comprehensive insight into *Ss*-host interactions, some studies on molecular and biological processes involved in both pathogenesis and plant defense have been conducted in *Arabidopsis* and other crops like soybeans.

1.8. Understanding *Sclerotina sclerotiorum* epidemiology through the study of phenotypic traits

The multifaceted nature of *Ss* is widely acknowledged as the primary challenge in breeding programs. In the case of most fungal diseases, the main reason for the frequent breakdown of effective resistances is the inability to tailor the breeding varieties to the array of factors influencing the dynamics that regulate each population (Kumar & Verma, 2019).

Ss's complex epidemiology has sparked a special interest among plant pathologists constituting the first step headed towards breeding efforts. Understanding the wide array of genetic and phenotypic traits that regulate the pathogen's epidemiology is crucial to developing effective breeding strategies.

Ss has been described using different approaches including morphological characters (Rathi et al., 2018; Willetts et al., 1980), mycelial compatibility grouping (Kohn et al., 1991), differences in aggressiveness of isolates by geographical region (Bolton et al., 2006; Otto-Hanson et al., 2011), pathogenicity factors (Sharma et al., 2015), genetics (Lehner et al., 2015). Some other studies have even made progress in understanding the pathosystem at the plant level as well by studying the importance of cell wall-degrading enzymes and other secreted proteins (McCaghey et al., 2019). Combining the results from these studies provides breeders with the guidelines for selecting disease-resistant germplasm by targeting specific resistance mechanisms observed in specific plant

material, hence, getting as much information as possible enables the optimization of breeding strategies for durable resistance.

Thus, phenotypic traits such as mycelial compatibility groups (MCGs), aggressiveness, and morphology influence *Ss* epidemiology, hence investigations involving these traits are a priority when describing a new population.

1.9. Mycelial Compatibility Groups (MCGs): Its importance in genetic studies and common bean breeding

Genetic diversity is commonly observed among fungal pathogens. Sources of such diversity include but are not limited to mutation and recombination (Burdon & Silk, 1997). The first introduction of the term mycelial compatibility for *Ss* was done towards the end of the 20th century when Kohn et al. (1991) aimed at developing the protocol to characterize genetic diversity through mycelial compatibility.

The use of mycelial compatibility groups (MCGs) has been included among the tools to measure the population diversity of fungi. This technique is a quick phenotypic marker used widely for genotyping *Ss* populations (Schafer & Kohn, 2006). It is also a commonly used approach to characterize clonal lineages and to assess the genetic diversity of fungal pathogens such as *Ss*. MCGs are phenotypes determined by a multilocus-controlled self-recognition system and can be observed macroscopically (Carbone et al., 1999). This macroscopic marker consists of co-culturing two or more isolates together in the same medium to assess if the isolates challenged can anastomose together and grow as a single colony showing fused growth, with no reaction line. On the other hand, incompatible isolates display an obvious contact zone characterized by reduced growth, dead cells, or sparse mycelia indicating the limits of mycelia growth for each challenged isolate (Kohn et al., 1990). While rating the compatibility reactions of isolates appears to be a

straightforward process, some difficulties exist when performing rating. Firstly, MCG testing presents the difficulty of misinterpretation of the contact zone often producing a barrage line (sparse mycelia) when challenging different fungal isolates. This barrage line might be indeed one of four possible states: no contact, hyphal contact without fusion, fusion with subsequent killing; and fusion with a stable heterokaryon (Carling, 1996), but the lack of methods to resolve this ambiguity were a main constrain until the introduction of methods utilizing complementary auxotrophic nitrate to accurately assess the heterokaryon formation (Puhalla, 1985). The most remarkable difficulty of MCG testing is the confounding scoring of compatibility. Some research has been done to facilitate this routine marker. In their study Schafer and Kohn (2006), deemed it necessary to enhance the protocol first suggested by Kohn et al. (1991) for assessing the *Ss* mycelial reactions. This improvement consisted in testing different growth media, and concentrations of red food coloring to amend the medium. Their experimentation yielded an optimized, reproducible, enhanced option to enhance the barrage line for incompatible reactions and hence, a more accurate macroscopic rating: the use of a PDA medium amended with red food coloring. The study of MCGs is of special interest in *Ss* variability since it has been argued that a relationship exists between different MCG and genotypically different strains as demonstrated by Kohn et al. (1991), and most recently by Liu et al. (2018).

1.10. Aggressiveness determination: Delving into *Sclerotinia sclerotiorum* pathogenicity

An integral part of comprehending host-pathogen interactions involves grasping the dynamics unfolding at all levels. Plant pathologists have demonstrated substantial interest in unraveling the complex dynamics of plant pathogens, particularly focusing into the quantitative dimension, which has shaped the term ‘aggressiveness’. Aggressiveness is a quantitative measure

to determine the ability of a pathogen to infect and cause disease in host plants (Pariaud et al., 2009). Additionally, it has been stressed that the term 'virulence' and aggressiveness which are often confounded, differ in definition. The former refers to the ability of a pathogen to infect a host, while the latter encompasses virulence but extends beyond it, as it might also involve assessing the severity of the disease and considering factors such as a pathogen's growth rate and overall impact of the pathogen on host fitness and yield (Van der Plank, 1984).

Aggressiveness, a quantitative measure of the pathogen's damage to the host, may be measured on different scales. The decision on which scale to use is defined by the research question. For example, aggressiveness can measure a variety of quantitative traits, which are considered aggressiveness components: infection efficiency, latent period, spore production rate, infectious period, and lesion size.

When attempting to understand an *Ss* population, the primary need is to pinpoint differences in aggressiveness responses in the host to isolates. Lesion size is the quantitative trait that is measured as an aggressiveness component in common bean breeding programs against *Ss*.

1.11. Genetic basis of *Sclerotinia sclerotiorum* resistance in common bean

A useful tool to determine the aggressiveness of isolates in the context of *Ss* and common bean is artificial inoculation under a controlled environment. Several studies have been performed describing different methods for inoculation aiming to mimic a natural field infection (Gupta et al., 2020; Han et al., 2024). A widely used inoculation method preferred among common bean breeders for its reproducibility is the cut-stem technique otherwise known as straw-inoculation described by Petzoldt and Dickson (1996). Initially used in screening to identify common bean cultivars with physiological resistance against *Ss*, it is now widely preferred among inoculation methods to mimic the natural occurrence of infection and hence, determine aggressiveness levels in *Ss* isolates. The

aggressiveness determination utilizing techniques such as cut-stem inoculation serve as useful tools to understand isolates and establish relationships between host and pathogen. Aggressiveness determination through cut-stem inoculation consists of cutting the main stem of plants that reached the 3rd to 4th trifoliate and immediately after putting into contact the lesion zone with PDA plugs containing the mycelia inoculum. This method has helped determine isolates aggressiveness in different common bean production areas where *Ss* is a problem.

In common bean, different diseases are controlled by incorporating integrated disease management measures. In the fight against white mold, it is not an exception. Although there is abundant evidence of control measures against *Ss* they all have their own constrains ranging from damages to the environment to costly measures (O'Sullivan et al., 2021). Deployment of cultivars with durable resistance remains at the top options to fight this persistent pathogen (McDonald & Linde, 2002; Mundt, 2014; Singh & Schwartz, 2010). However, in common bean only partial resistance has been achieved (Miklas et al., 2014).

Common bean genetics studies have identified resistance loci and explored genetic diversity to develop resistant cultivars. Additionally, functional genomics approaches have served the genetic studies by elucidating the molecular mechanisms, aiding in the development of improved bean cultivars (Joelle et al., 2011; Karandeni Dewage et al., 2022; Miklas et al., 2006; Singh & Schwartz, 2010).

In a broad sense, resistance is recognized to be qualitative or quantitative in nature, which refers to the phenotypic expression of this trait, and the way in which it is inherited (Niks et al., 2015). The genetic basis of *Ss* resistance in common bean is a complex mix of multiple genes and genetic factors. Common bean cultivars may possess quantitative or polygenic resistance against *Ss*, involving the combined effect of multiple genes with small individual effects (Nelson et al.,

2018). Inheritance to white mold resistance differs from single inheritance, in the number of quantitative trait loci (QTL) involved. In common bean, white mold resistance involves more than ten QTLs contributing in most of the cases with small to moderate effects. Genes against white mold in common bean represent a varying degree of resistance, they are inherited in a quantitative manner and are often challenging to identify and manipulate. Despite the difficulty in identifying resistance genes, progress has been achieved using QTL mapping and meta-QTL analysis. Recent studies, such as those conducted by Vasconcellos et al. (2017), have utilized advanced genomic tools like SNP markers and dense linkage maps to pinpoint resistance QTLs with greater precision. This study has enabled researchers to identify consensus QTLs across different environments and genetic backgrounds, consolidating multiple individual QTLs into stable meta-QTLs. These meta-QTLs not only provide more reliable targets for marker-assisted selection (MAS) but also help in understanding the underlying genetic mechanisms of resistance.

Furthermore, common bean plants may exhibit qualitative or major gene resistance against *Ss*, involving specific resistance genes that confer strong resistance against specific pathogen isolates or strains (Miklas et al., 2001).

Our understanding of resistance to *Ss* in common bean is far from complete, but several studies have contributed towards elucidating its basis with important contributions. In 2011, Soule et al. (2011) aided by DNA markers and genetic mapping described genomic regions linked to white mold resistance. Recently, there has been a growing interest in physiological resistance, and the study of QTLs associated with disease avoidance are resulting in the registration of cultivars with partial resistance (Miklas et al., 2014).

Although constant breeding efforts are being conducted, some challenges slow down breeding progress. Firstly, breeding against white mold is characterized by challenging screening

disrupted by environmental variability (low heritability), lack of characterization of the pathogen's biology, and lack of ability to gather information on pathosystem phenotypes associated with resistance (Ender & Kelly, 2005; Kolkman & Kelly, 2002).

1.12. Genetic variation in *Sclerotinia sclerotiorum.*

Disease resistance remains at the top of disease management options to contribute to the fight against fungal plant pathogens (McDonald & Linde, 2002; Singh & Schwartz, 2010). However, genetic variation in plant pathogens potentiates their ability to overcome acquired host resistance, and it has become a subject of major interest among plant pathologists. Genetic variation in pathogenicity genes and genome evolution are believed to confer pathogens the mechanisms for their rapid adaptations (Grandaubert et al., 2019).

Various genetic diversity analysis tools based on molecular methods like microsatellite loci (also known as simple sequence repeats SSRs), random amplification of polymorphic DNA (RAPD), microsatellite haplotypes, sequence-related amplified polymorphism (SRAP), amplified fragment length polymorphism (AFLP) and genome sequencing have been used widely to analyze the *Ss* genetic diversity (Aldrich-Wolfe et al., 2015; Cubeta et al., 1997; Hambleton et al., 2002; Liu et al., 2018; Sharma et al., 2018; Sirjusingh & Kohn, 2001; Tok et al., 2016). These molecular tools come with some limitations. For example, sequencing technologies based on short sequences pose challenges for genome assembly, including the difficulty of sequencing repetitive sequences and producing fragmented genomes (Treangen & Salzberg, 2011; Wang et al., 2021). In the case of molecular markers, while they offer a useful tool to detect variation, each of them bases their identification on specific regions of DNA, thus not allowing a point of comparison (Oliveira & Azevedo, 2022).

Fungi possess varying genomes among and between individuals of the same species (Potgieter et al., 2020). Several factors play a role and influence genomic variability in fungal pathogens. Among them, factors as transposable elements (TEs) and genome compartmentalization play an important role. Compartmentalization of the fungal genome has long been recognized as a challenging yet crucial aspect of genomic studies (Möller & Stukenbrock, 2017; Santana et al., 2014). This organizational complexity significantly influences genomic variability, particularly concerning the identification and characterization of structural variants (SVs).

With the advent of novel sequencing technologies, there is growing consensus that the most effective method for investigating genomic variation involves the generation of high-quality assemblies with minimal fragmentation (Simpson & Pop, 2015). This approach entails leveraging sequencing platforms that facilitate seamless assembly by producing longer reads, enhancing assembly efficiency. Moreover, the ability of longer reads to span entire genomic regions, including repetitive regions, ensures the creation of genome assemblies with fewer gaps. Additionally, genomic variants whose identification was traditionally challenging has remarkably been improved with the introduction of long-read sequencing technologies. Long-read sequencing, such as that provided by nanopore technology, produces significantly longer reads compared to traditional short-read sequencing methods. Nanopore sequencing works by threading single DNA or RNA molecules through a nanopore (a tiny biological pore) and measuring changes in ionic current to determine the sequence of bases (Jain et al., 2016).

Nanopore sequencing can generate reads that span entire structural variants (SVs), allowing these variants to be captured within a single read. Consequently, nanopore sequencing results in more precise genome assemblies and provides deeper insights into genome architecture.

These advancements are especially valuable for understanding the role of SVs in fungal pathogens (Pollard et al., 2018)

1.13. Structural Variation, Definition, and significance in genomic variation

The term structural variation (SV) refers to regions of DNA that display differences in number, orientation, or chromosomal location between individuals (Wellenreuther et al., 2019). SVs were first identified by Alfred Sturtevant with the spotting of inversions in *Drosophilla melanoganster* (Sturtevant, 1913). Ever since SVs were first recognized, many remarkable findings have been reported in the field of SVs. One of the most outstanding reports of SVs granted Barbara McClintock a Nobel Prize in 1983 with her contributions on the discovery of transposable elements in maize (McClintock, 1931; McClintock, 1950). Such is the contribution of SVs to the overall genomic variation that the focus is being shifted from traditional SNPs identification towards unexplored larger alterations in the genomic architecture (Sanchis-Juan et al., 2018; Xia et al., 2017). Although it remains to be acknowledged that SNPs are the most common polymorphisms found at the genomic level, the number of base pairs affected by SVs is three times higher compared to SNPs, and hence SV's research is an intriguing yet poorly understood field (Wellenreuther et al., 2019).

Traditionally, SVs were believed to comprise 1000 base pairs. However, with the incorporation of novel sequencing techniques, the definition has been shaped and now recognizes SVs as spanning to genomic variation over 50 base pairs (Mahmoud et al., 2019). In some populations, SVs are present at significant frequencies, and there is evidence that they can contribute to shaping the genomic architecture of fungal plant pathogens, influencing various biological processes and traits essential for pathogenicity and adaptations (Kronenberg et al., 2018)

SVs contribute significantly to genomic diversity and plasticity, allowing fungal pathogens to adapt rapidly to environmental changes and host defenses. SVs can affect gene expression, disrupt coding sequences, and create novel gene functions, enhancing the pathogens' ability to infect and overcome host resistance mechanisms (Gorkovskiy & Verstrepen, 2021).

1.14. Case Studies of Structural Variants in Fungal Pathogens

Structural Variants (SVs) hold considerable influence over the genome architecture and adaptative capabilities of fungal pathogens (Badet et al., 2020; Langner et al., 2021). While studies on genomic variations in *Ss* abound, research specifically targeting SVs is a field under exploration. Despite limited research on SVs in this species, broader research across fungal pathogens underscores the pivotal role of SVs in driving genetic diversity, adaptation, and pathogenicity.

The detailed mechanisms underlying SV-mediated genomic rearrangements and their functional implications in fungal pathogenesis await thorough exploration (Hartmann, 2022).

Understanding the role of SVs in fungal pathogens is crucial for grasping their adaptability and virulence. In various fungal pathogens, structural variants have demonstrated significant influence over diverse traits and contribute substantially to the pathogen’s virulence and adaptation.

Several case studies highlight the significant impact of SVs on the evolution and pathogenicity of these organisms. For instance, research on *Zymoseptoria tritici* reveals how SVs contribute to the emergence of virulent strains by enabling rapid adaptation to host defenses and environmental changes (Amezrou et al., 2024)

In a recent study, Durak and Ozkilinc (2023) emphasized how differences in SVs dynamics between two *Molininia* species contributed to genome evolution and pathogenicity, with each

species exhibiting unique patterns of SVs that correlate with their specific ecological niches and host interactions.

Moreover, a study by Zaccaron and Stergiopoulos (2024) demonstrated that SVs in the tomato pathogen *Cladosporium fulvum* contribute to its ability to overcome host resistance genes. This occurs through gene gain or loss events. These events contribute to the genomic stability and plasticity of fungal pathogens, allowing them to rapidly adapt to changing environments and host defenses.

Despite their importance in contributing to genomic diversity, SVs are still poorly understood. This is partly due to the limitations of high-throughput techniques that rely on short-read sequencing. These techniques can introduce bias, overlook SVs, and are often costly (Pollard et al., 2018).

While previous standard genotyping methods failed to detect such important components of genomic variation, the study of SVs has been enhanced by increasing high-quality genome assemblies with long-read sequencing (Everhart et al., 2020; Marx, 2023). One approach is suggested for capturing large SVs: Whole Genome Assemblies. It has been demonstrated that this approach enables the recovery of large SVs (Simpson & Pop, 2015). This method provides a more comprehensive view of the genome, allowing researchers to identify complex variations that were previously missed. As a result, it has become a crucial tool in advancing our understanding of genomic diversity and its implication for evolution, disease resistance an adaptation (Potgieter et al., 2020).

As the multifaceted fungal plant pathogen *Ss* continues to threaten global production, it is in the best of our interests to produce information that can explain important host-pathogen

interactions with the aim of contributing on breeding efforts. For this reason, the present study describes our efforts to elucidate the genomic repertoire of SV in *Ss* isolates collected in Canada to give steps towards the battle against a devastating pathogen.

1.15. REFERENCES

Aldrich-Wolfe, L., Travers, S., & Nelson, B. J. (2015). Genetic Variation of *Sclerotinia sclerotiorum* from Multiple Crops in the North Central United States. *PLOS ONE*, *10*(9). https://doi.org/https://doi.org/10.1371/journal.pone.0139188

Amezrou, R., Ducasse, A., Compain, J., Lapalu, N., Pitarch, A., Dupont, L., Confais, J., Goyeau, H., Kema, G. H. J., Croll, D., Amselem, J., Sanchez-Vallet, A., & Marcel, T. C. (2024). Quantitative pathogenicity and host adaptation in a fungal plant pathogen revealed by whole-genome sequencing. *Nature Communications*, *15*(1), 1933. https://doi.org/10.1038/s41467-024-46191-1

Badet, T., Oggenfuss, U., Abraham, L., McDonald, B. A., & Croll, D. (2020). A 19-isolate reference-quality global pangenome for the fungal wheat pathogen Zymoseptoria tritici. *BMC Biology*, *18*(1), 12. https://doi.org/10.1186/s12915-020-0744-3

Bae, Y. S., & Knudsen, G. R. (2007). Effect of sclerotial distribution pattern of Sclerotinia sclerotiorum on biocontrol efficacy of Trichoderma harzianum. *Applied Soil Ecology*, *35*(1), 21-24. https://doi.org/https://doi.org/10.1016/j.apsoil.2006.05.014

Bateman, D. F., & Beer, S. V. (1965). Simultaneous Production and Synergistic Action of Oxalic Acid and Polygalacturonase during Pathogenesis by Sclerotium Rolfsii. *Phytopathology*, *55*, 204-211. https://www.ncbi.nlm.nih.gov/pubmed/14274523

Beebe, S., Rengifo, J., Gaitan, E., Duque, M. C., & Tohme, J. (2001). Diversity and Origin of Andean Landraces of Common Bean. *Crop Science*, *41*(3), 854-862. https://doi.org/https://doi.org/10.2135/cropsci2001.413854x

Bitocchi, E., Bellucci, E., Giardini, A., Rau, D., Rodriguez, M., Biagetti, E., Santilocchi, R., Spagnoletti Zeuli, P., Gioia, T., Logozzo, G., Attene, G., Nanni, L., & Papa, R. (2013). Molecular analysis of the parallel domestication of the common bean (Phaseolus vulgaris) in Mesoamerica and the Andes. *New Phytologist*, *197*(1), 300-313. https://doi.org/https://doi.org/10.1111/j.1469-8137.2012.04377.x

Bitocchi, E., Rau, D., Bellucci, E., Monica, R., L, M. M., Gioia, T., Santo, D., Nanni, L., Attene, G., & Papa, R. (2017). Beans (Phaseolus ssp.) as a Model for Understanding Crop Evolution. *Frontiers in Plant Science*, *8*. https://doi.org/https://doi.org/10.3389/fpls.2017.00722

Boland, G. J., & Hall, R. (1994). Index of plant hosts of Sclerotinia sclerotiorum. *Canadian Journal of Plant Pathology*, *16*(2), 93-108. https://doi.org/10.1080/07060669409500766

Bolton, M. D., Thomma, B. P. H. J., & Nelson, B. D. (2006). Sclerotinia sclerotiorum (Lib.) de Bary: biology and molecular traits of a cosmopolitan pathogen. *Molecular Plant Pathology*, *7*(1), 1-16. https://doi.org/https://doi.org/10.1111/j.1364-3703.2005.00316.x

Broughton, W. J., Hernández, G., Blair, M., Beebe, S., Gepts, P., & Vanderleyden, J. (2003). Beans (Phaseolus spp.) – model food legumes. *Plant and Soil*, *252*(1), 55-128. https://doi.org/10.1023/A:1024146710611

Burdon, J. J., & Silk, J. (1997). Sources and Patterns of Diversity in Plant-Pathogenic Fungi. *Phytopathology®*, *87*(7), 664-669. https://doi.org/10.1094/PHYTO.1997.87.7.664

Carbone, I., Anderson, J. B., & Kohn, L. M. (1999). Patterns of Descent in Clonal Lineages and Their Multilocus Fingerprints Are Resolved with Combined Gene Genealogies. *Evolution*, *53*(1), 11-21. https://doi.org/10.2307/2640916

Carling, D. E. (1996). Grouping in Rhizoctonia Solani by Hyphal Anastomosis Reaction. In B. Sneh, S. Jabaji-Hare, S. Neate, & G. Dijst (Eds.), *Rhizoctonia Species: Taxonomy, Molecular Biology, Ecology, Pathology and Disease Control* (pp. 37-47). Springer Netherlands. https://doi.org/10.1007/978-94-017-2901-7_3

Cessna, S. G., Sears, V. E., Dickman, M. B., & Low, P. S. (2000). Oxalic Acid, a Pathogenicity Factor for Sclerotinia sclerotiorum, Suppresses the Oxidative Burst of the Host Plant. *The Plant Cell*, *12*(11), 2191-2199. https://doi.org/10.1105/tpc.12.11.2191

Chet, I., & Henis, Y. (1975). Sclerotial Morphogenesis in Fungi. *Annual Review of Phytopathology*, *13*(Volume 13), 169-192. https://doi.org/https://doi.org/10.1146/annurev.py.13.090175.001125

Cubeta, M. A., Cody, B. R., Kohli, Y., & Kohn, L. M. (1997). Clonality in Sclerotinia sclerotiorum on Infected Cabbage in Eastern North Carolina. *Phytopathology®*, *87*(10), 1000-1004. https://doi.org/10.1094/phyto.1997.87.10.1000

de Abreu, M. J., Leite, M. E., Ferreira, A. N., & de Souza, E. A. (2019). Phenotypic and genotypic characterization of single isolate-derived monoascospore strains of Sclerotinia sclerotiorum from common bean. *Tropical Plant Pathology*, *44*(6), 533-540. https://doi.org/10.1007/s40858-019-00304-0

Debouck, D. G., & Smartt, J. (1995). "Beans," in Evolution of Crop Plants. *Ed. J. Smartt (Harlow: Longman), 287-294*.

del Río, L. E., Venette, J. R., & Lamey, H. A. (2004). Impact of White Mold Incidence on Dry Bean Yield Under Nonirrigated Conditions. *Plant Disease*, *88*(12), 1352-1356. https://doi.org/10.1094/PDIS.2004.88.12.1352

Derbyshire, M. C., & Denton-Giles, M. (2016). The control of sclerotinia stem rot on oilseed rape (Brassica napus): current practices and future opportunities. *Plant Pathology*, *65*(6), 859-877. https://doi.org/https://doi.org/10.1111/ppa.12517

Derbyshire, M. C., Newman, T. E., Khentry, Y., & Owolabi Taiwo, A. (2022). The evolutionary and molecular features of the broad-host-range plant pathogen Sclerotinia sclerotiorum. *Molecular Plant Pathology*, *23*(8), 1075-1090. https://doi.org/https://doi.org/10.1111/mpp.13221

Dong, S., Raffaele, S., & Kamoun, S. (2015). The two-speed genomes of filamentous pathogens: waltz with plants. *Curr Opin Genet Dev*, *35*, 57-65. https://doi.org/10.1016/j.gde.2015.09.001

Durak, M. R., & Ozkilinc, H. (2023). Genome-Wide Discovery of Structural Variants Reveals Distinct Variant Dynamics for Two Closely Related Monilinia Species. *Genome Biology and Evolution*, *15*(6), evad085. https://doi.org/10.1093/gbe/evad085

Dutton, M. V., & Evans, C. S. (1996). Oxalate production by fungi: its role in pathogenicity and ecology in the soil environment. *Canadian Journal of Microbiology*, *42*(9), 881-895. https://doi.org/10.1139/m96-114

Ender, M., & Kelly, J. D. (2005). Identification of QTL Associated with White Mold Resistance in Common Bean. *Crop Science*, *45*(6), 2482-2490. https://doi.org/https://doi.org/10.2135/cropsci2005.0064

Erental, A., Dickman, M. B., & Yarden, O. (2008). Sclerotial development in Sclerotinia sclerotiorum: awakening molecular analysis of a “Dormant” structure. *Fungal Biology Reviews*, *22*(1), 6-16. https://doi.org/https://doi.org/10.1016/j.fbr.2007.10.001

Everhart, S., Gambhir, N., & Stam, R. (2020). Population Genomics of Filamentous Plant Pathogens—A Brief Overview of Research Questions, Approaches, and Pitfalls. *Phytopathology®*, *111*(1), 12-22. https://doi.org/10.1094/PHYTO-11-20-0527-FI

FAO. (2024). *Putting a number on hunger: different measures for different purposes.* . https://www.fao.org/interactive/state-of-food-security-nutrition/en/

FAOSTAT. (2024). *Dry bean production data 2021-2022. Food and Agriculture Organization of the United Nations. Retrieved from* http://www.fao.org/faostat/en/#data/QCL.

Favaron, F., Sella, L., & D'Ovidio, R. (2004). Relationships Among Endo-Polygalacturonase, Oxalate, pH, and Plant Polygalacturonase-Inhibiting Protein (PGIP) in the Interaction Between Sclerotinia sclerotiorum and Soybean. *Molecular Plant-Microbe Interactions®*, *17*(12), 1402-1409. https://doi.org/10.1094/MPMI.2004.17.12.1402

Gerard, P., Peter, S., Darren, R., & Chris, G. (2011). The interaction of annual weed and white mold management systems for dry bean production in Canada. *Canadian Journal of Plant Science*, *91*(3), 587-598. https://doi.org/10.4141/cjps10127

Glazebrook, J. (2005). Contrasting Mechanisms of Defense Against Biotrophic and Necrotrophic Pathogens. *Annual Review of Phytopathology*, *43*(Volume 43, 2005), 205-227. https://doi.org/https://doi.org/10.1146/annurev.phyto.43.040204.135923

Godoy, G., Steadman, J. R., Dickman, M. B., & Dam, R. (1990). Use of mutants to demonstrate the role of oxalic acid in pathogenicity of Sclerotinia sclerotiorum on Phaseolus vulgaris. *Physiological and Molecular Plant Pathology*, *37*(3), 179-191. https://doi.org/https://doi.org/10.1016/0885-5765(90)90010-U

Gorkovskiy, A., & Verstrepen, K. J. (2021). The Role of Structural Variation in Adaptation and Evolution of Yeast and Other Fungi. *Genes (Basel)*, *12*(5). https://doi.org/10.3390/genes12050699

Grandaubert, J., Dutheil, J. Y., & Stukenbrock, E. H. (2019). The genomic determinants of adaptive evolution in a fungal pathogen. *Evolution Letters*, *3*(3), 299-312. https://doi.org/10.1002/evl3.117

Guo, X., & Stotz, H. U. (2007). Defense Against Sclerotinia sclerotiorum in Arabidopsis Is Dependent on Jasmonic Acid, Salicylic Acid, and Ethylene Signaling. *Molecular Plant-Microbe Interactions®*, *20*(11), 1384-1395. https://doi.org/10.1094/MPMI-20-11-1384

Gupta, N. C., Sharma, P., Rao, M., Rai, P. K., & Gupta, A. K. (2020). Evaluation of non-injury inoculation technique for assessing Sclerotinia stem rot (Sclerotinia sclerotiorum) in oilseed Brassica. *J Microbiol Methods*, *175*, 105983. https://doi.org/10.1016/j.mimet.2020.105983

Hambleton, S., Walker, C., & Kohn, L. M. (2002). Clonal lineages of Sclerotinia sclerotiorum previously known from other crops predominate in 1999-2000 samples from Ontario and Quebec soybean. *Canadian Journal of Plant Pathology*, *24*(3), 309-315. https://doi.org/10.1080/07060660209507014

Han, V.-C., Michael, P. J., Crockett, R., Swift, B., & Bennett, S. J. (2024). Effective, consistent, and rapid non-contact application methods for seedling basal stem infection by Sclerotinia sclerotiorum. *Plant Disease*. https://doi.org/10.1094/PDIS-11-23-2412-SC

Hartmann, F. E. (2022). Using structural variants to understand the ecological and evolutionary dynamics of fungal plant pathogens. *New Phytologist*, *234*(1), 43-49. https://doi.org/https://doi.org/10.1111/nph.17907

Hegedus, D. D., & Rimmer, S. R. (2005). Sclerotinia sclerotiorum: When "to be or not to be" a pathogen? *FEMS Microbiology Letters*, *251*(2), 177-184. https://doi.org/10.1016/j.femsle.2005.07.040

Hoffman, D. D., Diers, B. W., Hartman, G. L., Nickell, C. D., Nelson, R. L., Pedersen, W. L., Cober, E. R., Graef, G. L., Steadman, J. R., Grau, C. R., Nelson, B. D., del Rio, L. E., Helms, T., Anderson, T., Poysa, V., Rajcan, I., & Stienstra, W. C. (2002). Selected Soybean Plant Introductions with Partial Resistance to Sclerotinia sclerotiorum. *Plant Disease*, *86*(9), 971-980. https://doi.org/10.1094/pdis.2002.86.9.971

Horbach, R., Navarro-Quesada, A. R., Knogge, W., & Deising, H. B. (2011). When and how to kill a plant cell: Infection strategies of plant pathogenic fungi. *Journal of Plant Physiology*, *168*(1), 51-62. https://doi.org/https://doi.org/10.1016/j.jplph.2010.06.014

Jain, M., Olsen, H. E., Paten, B., & Akeson, M. (2016). The Oxford Nanopore MinION: delivery of nanopore sequencing to the genomics community. *Genome Biology*, *17*(1), 239. https://doi.org/10.1186/s13059-016-1103-0

Joelle, A., Cuomo, C. A., van Kan, J. A. L., Viaud, M., Benito, E. P., Couloux, A., Coutinho, P. M., de Vries, R. P., Dyer, P. S., Fillinger, S., Fournier, E., Gout, L., Hahn, M., Kohn, L., Lapalu, N., Plummer, K. M., Pradier, J.-M., Quévillon, E., Sharon, A., . . . Dickman, M. (2011). Genomic Analysis of the Necrotrophic Fungal Pathogens Sclerotinia sclerotiorum and Botrytis cinerea. *PLOS Genetics*, *7*(8), e1002230. https://doi.org/10.1371/journal.pgen.1002230

Kabbage, M., Yarden, O., & Dickman, M. B. (2015). Pathogenic attributes of Sclerotinia sclerotiorum: Switching from a biotrophic to necrotrophic lifestyle. *Plant Science*, *233*, 53-60. https://doi.org/https://doi.org/10.1016/j.plantsci.2014.12.018

Karandeni Dewage, C. S., Cools, K., Stotz, H. U., Qi, A., Huang, Y. J., Wells, R., & Fitt, B. D. L. (2022). Quantitative Trait Locus Mapping for Resistance Against Pyrenopeziza brassicae Derived From a Brassica napus Secondary Gene Pool. *Front Plant Sci*, *13*, 786189. https://doi.org/10.3389/fpls.2022.786189

Kim, H. S., & Diers, B. W. (2000). Inheritance of Partial Resistance to Sclerotinia Stem Rot in Soybean. *Crop Science*, *40*(1), 55-61. https://doi.org/https://doi.org/10.2135/cropsci2000.40155x

King, J., Leong, S. Y., Alpos, M., Johnson, C., McLeod, S., Peng, M., Sutton, K., & Oey, I. (2024). Role of food processing and incorporating legumes in food products to increase protein intake and enhance satiety. *Trends in Food Science & Technology*, *147*, 104466. https://doi.org/https://doi.org/10.1016/j.tifs.2024.104466

Kohn, L. M., Carbone, I., & Anderson, J. B. (1990). Mycelial interactions inSclerotinia sclerotiorum. *Experimental Mycology*, *14*(3), 255-267. https://doi.org/https://doi.org/10.1016/0147-5975(90)90023-M

Kohn, L. M., Stasovski, E., Carbone, I., Royer, J., & Anderson, J. B. (1991). Mycelial incompatibility and molecular markers identify genetic variability in field populations of *Sclerotinia sclerotiorum. Phytopathology*, *81*, 480-485. https://doi.org/10.1094/Phyto-81-480.

Kolkman, J. M., & Kelly, J. D. (2002). Agronomic Traits Affecting Resistance to White Mold in Common Bean. *Crop Science*, *42*(3). https://doi.org/10.2135/cropsci2002.6930

Kronenberg, Z. N., Fiddes, I. T., Gordon, D., Murali, S., Cantsilieris, S., Meyerson, O. S., Underwood, J. G., Nelson, B. J., Chaisson, M. J. P., Dougherty, M. L., Munson, K. M., Hastie, A. R., Diekhans, M., Hormozdiari, F., Lorusso, N., Hoekzema, K., Qiu, R., Clark, K., Raja, A., . . . Eichler, E. E. (2018). High-resolution comparative analysis of great ape genomes. *Science*, *360*(6393). https://doi.org/10.1126/science.aar6343

Kumar, S., & Verma, S. (2019). Variability in Plant Pathogens and Tools for its Characterization. *International Journal of Current Microbiology and Applied Sciences*, *8*(2), 2887-2902. https://doi.org/https://doi.org/10.20546/ijcmas.2019.802.338

Langner, T., Harant, A., Gomez-Luciano, L. B., Shrestha, R. K., Malmgren, A., Latorre, S. M., Burbano, H. A., Win, J., & Kamoun, S. (2021). Genomic rearrangements generate hypervariable mini-chromosomes in host-specific isolates of the blast fungus. *PLoS Genet*, *17*(2), e1009386. https://doi.org/10.1371/journal.pgen.1009386

Lehner, M. S., Paula Júnior, T. J., Hora Júnior, B. T., Teixeira, H., Vieira, R. F., Carneiro, J. E. S., & Mizubuti, E. S. G. (2015). Low genetic variability in Sclerotinia sclerotiorum populations from common bean fields in Minas Gerais State, Brazil, at regional, local and micro-scales. *Plant Pathology*, *64*(4), 921-931. https://doi.org/https://doi.org/10.1111/ppa.12322

Liu, J., Meng, Q., Zhang, Y., Xiang, H., Li, Y., Shi, F., Ma, L., Liu, C., Liu, Y., Su, B., & Li, Z. (2018). Mycelial compatibility group and genetic variation of sunflower Sclerotinia sclerotiorum in Northeast China. *Physiological and Molecular Plant Pathology*, *102*, 185-192. https://doi.org/https://doi.org/10.1016/j.pmpp.2018.03.006

Mahmoud, M., Gobet, N., Cruz-Dávalos, D. I., Mounier, N., Dessimoz, C., & Sedlazeck, F. J. (2019). Structural variant calling: the long and the short of it. *Genome Biology*, *20*(1), 246. https://doi.org/10.1186/s13059-019-1828-7

Marx, V. (2023). Method of the year: long-read sequencing. *Nature Methods*, *20*(1), 6-11. https://doi.org/10.1038/s41592-022-01730-w

Mayer, A. M., Staples, R. C., & Gil-ad, N. L. (2001). Mechanisms of survival of necrotrophic fungal plant pathogens in hosts expressing the hypersensitive response. *Phytochemistry*, *58*(1), 33-41. https://doi.org/https://doi.org/10.1016/S0031-9422(01)00187-X

Mbengue, M., Navaud, O., Peyraud, R., Barascud, M., Badet, T., Vincent, R., Barbacci, A., & Raffaele, S. (2016). Emerging Trends in Molecular Interactions between Plants and the Broad Host Range Fungal Pathogens Botrytis cinerea and Sclerotinia sclerotiorum. *Frontiers in Plant Science*, *7*. https://doi.org/https://doi.org/10.3389/fpls.2016.00422

McCaghey, M., Willbur, J., Smith, D. L., & Kabbage, M. (2019). The complexity of the Sclerotinia sclerotiorum pathosystem in soybean: virulence factors, resistance mechanisms, and their exploitation to control Sclerotinia stem rot. *Tropical Plant Pathology*, *44*(1), 12-22. https://doi.org/10.1007/s40858-018-0259-4

McClintock, B. (1931). Cytological observations of deficiencies involving known genes, translocations, and an inversion in Zea mays. *Missouri Agricultural Experiment Station Research Bulletin.*, *160*, 1-30.

McClintock, B. (1950). The origin and behavior of mutable loci in maize. *Proceedings of the National Academy of Sciences*, *36*(6), 344-355. https://doi.org/10.1073/pnas.36.6.344

McDonald, B. A., & Linde, C. (2002). PATHOGEN POPULATION GENETICS, EVOLUTIONARY POTENTIAL, AND DURABLE RESISTANCE. *Annual Review of Phytopathology*, *40*(Volume 40, 2002), 349-379. https://doi.org/https://doi.org/10.1146/annurev.phyto.40.120501.101443

McDonald, M. R., & Boland, G. J. (2004). Forecasting diseases caused by Sclerotinia spp. in eastern Canada: fact or fiction? *Canadian Journal of Plant Pathology*, *26*(4), 480-488. https://doi.org/10.1080/07060660409507168

Miklas, P. N., Johnson, W. C., Delorme, R., & Gepts, P. (2001). QTL Conditioning Physiological Resistance and Avoidance to White Mold in Dry Bean. *Crop Science*, *41*(2), 309-315. https://doi.org/https://doi.org/10.2135/cropsci2001.412309x

Miklas, P. N., Kelly, J. D., Beebe, S. E., & Blair, M. W. (2006). Common bean breeding for resistance against biotic and abiotic stresses: From classical to MAS breeding. *Euphytica*, *147*(1), 105-131. https://doi.org/10.1007/s10681-006-4600-5

Miklas, P. N., Kelly, J. D., Steadman, J. R., & McCoy, S. (2014). Registration of Pinto Bean Germplasm Line USPT-WM-12 with Partial White Mold Resistance. *Journal of Plant Registrations*, *8*(2), 183-186. https://doi.org/https://doi.org/10.3198/jpr2013.06.0034crg

Miklas, P. N., Porter, L. D., Kelly, J. D., & Myers, J. R. (2013). Characterization of white mold disease avoidance in common bean. *European Journal pf Plant Pathology*, *135*(3), 525-543. https://doi.org/10.1007/s10658-012-0153-8

Möller, M., & Stukenbrock, E. H. (2017). Evolution and genome architecture in fungal plant pathogens. *Nat Rev Microbiol*, *15*(12), 756-771. https://doi.org/10.1038/nrmicro.2017.76

Mundt, C. C. (2014). Durable resistance: A key to sustainable management of pathogens and pests. *Infection, Genetics and Evolution*, *27*, 446-455. https://doi.org/https://doi.org/10.1016/j.meegid.2014.01.011

Myers, J. R., & Kmiecik, K. (2017). Common Bean: Economic Importance and Relevance to Biological Science Research. In M. Pérez de la Vega, M. Santalla, & F. Marsolais (Eds.), *The Common Bean Genome* (pp. 1-20). Springer International Publishing. https://doi.org/10.1007/978-3-319-63526-2_1

Nandi, M., Selin, C., Brawerman, G., Fernando, W. G. D., & de Kievit, T. (2017). Hydrogen cyanide, which contributes to Pseudomonas chlororaphis strain PA23 biocontrol, is upregulated in the presence of glycine. *Biological Control*, *108*, 47-54. https://doi.org/https://doi.org/10.1016/j.biocontrol.2017.02.008

Nchanji, E. B., & Ageyo, O. C. (2021). Do Common Beans (Phaseolus vulgaris L.) Promote Good Health in Humans? A Systematic Review and Meta-Analysis of Clinical and Randomized Controlled Trials. *Nutrients*, *13*(11), 3701. https://doi.org/10.3390/nu13113701

Nelson, R., Wiesner-Hanks, T., Wisser, R., & Balint-Kurti, P. (2018). Navigating complexity to breed disease-resistant crops. *Nature Reviews Genetics*, *19*(1), 21-33. https://doi.org/10.1038/nrg.2017.82

Niks, R. E., Qi, X., & Marcel, T. C. (2015). Quantitative Resistance to Biotrophic Filamentous Plant Pathogens: Concepts, Misconceptions, and Mechanisms. *Annual Review of Phytopathology*, *53*(Volume 53, 2015), 445-470. https://doi.org/https://doi.org/10.1146/annurev-phyto-080614-115928

O'Sullivan, C. A., Belt, K., & Thatcher, L. F. (2021). Tackling Control of a Cosmopolitan Phytopathogen: Sclerotinia. *Frontiers in Plant Science*, *12*. https://doi.org/https://doi.org/10.3389/fpls.2021.707509

Oliveira, M., & Azevedo, L. (2022). Molecular Markers: An Overview of Data Published for Fungi over the Last Ten Years. *J Fungi (Basel)*, *8*(8). https://doi.org/10.3390/jof8080803

Oliver, R. P., & Ipcho, S. V. S. (2004). Arabidopsis pathology breathes new life into the necrotrophs-vs.-biotrophs classification of fungal pathogens. *Molecular Plant Pathology*, *5*(4), 347-352. https://doi.org/https://doi.org/10.1111/j.1364-3703.2004.00228.x

Otto-Hanson, L., Steadman, J. R., Higgins, R., & Eskridge, K. M. (2011). Variation in Sclerotinia sclerotiorum Bean Isolates from Multisite Resistance Screening Locations. *Plant Dis*, *95*(11), 1370-1377. https://doi.org/10.1094/PDIS-11-10-0865

Pariaud, B., Ravigné, V., Halkett, F., Goyeau, H., Carlier, J., & Lannou, C. (2009). Aggressiveness and its role in the adaptation of plant pathogens. *Plant Pathology*, *58*(3), 409-424. https://doi.org/https://doi.org/10.1111/j.1365-3059.2009.02039.x

Petzoldt, R., & Dickson, M. H. (1996). Straw test for resistance to white mold in beans. *Annu. Rpt. Bean Improv. Coop.*, *39*, 142-143.

Pollard, M. O., Gurdasani, D., Mentzer, A. J., Porter, T., & Sandhu, M. S. (2018). Long reads: their purpose and place. *Hum Mol Genet*, *27*(R2), R234-R241. https://doi.org/10.1093/hmg/ddy177

Potgieter, L., Feurtey, A., Dutheil, J. Y., & Stukenbrock, E. H. (2020). On Variant Discovery in Genomes of Fungal Plant Pathogens. *Front Microbiol*, *11*, 626. https://doi.org/10.3389/fmicb.2020.00626

Puhalla, J. E. (1985). Classification of strains of Fusarium oxysporum on the basis of vegetative compatibility. *Canadian Journal of Botany*, *63*(2), 179-183. https://doi.org/10.1139/b85-020

Purdy, L. H. (1979). *Sclerotinia sclerotiorum*: History, Diseases and Symptomatology, Host Range, Geographic Distribution, and Impact. *The American Phytopathological Society*, *69*(8), 875-880.

Rathi, A. S., Jattan, M., Punia, R., Singh, S., Kumar, P., & Avtar, R. (2018). Morphological and molecular diversity of Sclerotinia sclerotiorum infecting Indian mustard. *Indian Phytopathology*, *71*(3), 407-413. https://doi.org/10.1007/s42360-018-0054-7

Reich, J., McLaren, D., Kim, Y., Wally, O., Yevtushenko, D., Hamelin, R., Balasubramanian, P., & Chatterton, S. (2023). Occurrence of Ascospores and White Mold Caused by *Sclerotinia sclerotiorum* in Dry Bean Fields in Alberta, Canada. . *Plant Diseases*, *107*(12), 3754-3762. https://doi.org/doi: 10.1094/PDIS-11-22-2529-RE

Riou, C., Freyssinet, G., & Fevre, M. (1991). Production of Cell Wall-Degrading Enzymes by the Phytopathogenic Fungus Sclerotinia sclerotiorum. *Applied and Environmental Microbiology*, *57*(5), 1478-1484. https://doi.org/10.1128/aem.57.5.1478-1484.1991

Rodríguez, L., Mendez, D., Montecino, H., Carrasco, B., Arevalo, B., Palomo, I., & Fuentes, E. (2022). Role of Phaseolus vulgaris L. in the Prevention of Cardiovascular Diseases—Cardioprotective Potential of Bioactive Compounds. *Plants*, *11*(2), 186. https://doi.org/10.3390/plants11020186

Rollins Jeffrey, A., & Dickman Martin, B. (2001). pH Signaling in Sclerotinia sclerotiorum: Identification of a pacC/RIM1 Homolog. *Applied and Environmental Microbiology*, *67*(1), 75-81. https://doi.org/10.1128/AEM.67.1.75-81.2001

Saharan, G. S., & Mehta, N. (2008). *Sclerotinia Diseases of Crop Plants: Biology, Ecology and Disease Management*. https://link.springer.com/book/10.1007/978-1-4020-8408-9

Sanchis-Juan, A., Stephens, J., French, C. E., Gleadall, N., Mégy, K., Penkett, C., Shamardina, O., Stirrups, K., Delon, I., Dewhurst, E., Dolling, H., Erwood, M., Grozeva, D., Stefanucci, L., Arno, G., Webster, A. R., Cole, T., Austin, T., Branco, R. G., . . . Carss, K. J. (2018). Complex structural variants in Mendelian disorders: identification and breakpoint resolution using short- and long-read genome sequencing. *Genome Medicine*, *10*(1), 95. https://doi.org/10.1186/s13073-018-0606-6

Santana, M. F., Silva, J. C. F., Mizubuti, E. S. G., Arajo, E. F., & Queiroz, M. V. (2014). Analysis of Tc1-Mariner elements in Sclerotinia sclerotiorum suggests recent activity and flexible transposases. *BMC Microbiology*, *14*(1), 256. https://doi.org/10.1186/s12866-014-0256-9

Sathe, S. K. (2002). Dry Bean Protein Functionality. *Critical Reviews in Biotechnology*, *22*(2), 175-223. https://doi.org/10.1080/07388550290789487

Schafer, M. R., & Kohn, L. M. (2006). An optimized method for mycelial compatibility testing in Sclerotinia sclerotiorum. *Mycologia*, *98*(4), 593-597. https://doi.org/10.1080/15572536.2006.11832662

Schwartz, H. F., & Singh, S. P. (2013). Breeding Common Bean for Resistance to White Mold: A Review. *Crop Science*, *53*(5), 1832-1844. https://doi.org/https://doi.org/10.2135/cropsci2013.02.0081

Shahoveisi, F., Riahi Manesh, M., & del Río Mendoza, L. E. (2022). Modeling risk of Sclerotinia sclerotiorum-induced disease development on canola and dry bean using machine learning algorithms. *Scientific Reports*, *12*(1), 864. https://doi.org/10.1038/s41598-021-04743-1

Sharma, P., Meena, P. D., Kumar, A., Kumar, V., & Singh, D. (2015). Forewarning models for Sclerotinia rot (Sclerotinia sclerotiorum) in Indian mustard (Brassica juncea L.). *Phytoparasitica*, *43*(4), 509-516. https://doi.org/10.1007/s12600-015-0463-4

Sharma, P., Samkumar, A., Rao, M., Singh, V. V., Prasad, L., Mishra, D. C., Bhattacharya, R., & Gupta, N. C. (2018). Genetic Diversity Studies Based on Morphological Variability, Pathogenicity and Molecular Phylogeny of the Sclerotinia sclerotiorum Population From Indian Mustard (Brassica juncea). *Frontiers in Microbiology*, *9*. https://doi.org/10.3389/fmicb.2018.01169

Simpson, J. T., & Pop, M. (2015). The Theory and Practice of Genome Sequence Assembly. *Annual Review of Genomics and Human Genetics*, *16*(Volume 16, 2015), 153-172. https://doi.org/https://doi.org/10.1146/annurev-genom-090314-050032

Singh, S., & Schwartz, H. (2010). Review: Breeding common bean for resistance to insect pests and nematodes. *Canadian Journal of Plant Science*, *91*(2), 239-250. https://doi.org/10.4141/CJPS10002

Sirjusingh, C., & Kohn, L. M. (2001). Characterization of microsatellites in the fungal plant pathogen, Sclerotinia sclerotiorum. *Molecular Ecology Notes*, *1*(4), 267-269. https://doi.org/https://doi.org/10.1046/j.1471-8278.2001.00102.x

Smith, M. E., Henkel, T. W., & Rollins, J. A. (2015). How many fungi make sclerotia? *Fungal Ecology*, *13*, 211-220. https://doi.org/https://doi.org/10.1016/j.funeco.2014.08.010

Soule, M., Porter, L., Medina, J., Santana, G. P., Blair, M. W., & Miklas, P. N. (2011). Comparative QTL Map for White Mold Resistance in Common Bean, and Characterization of Partial Resistance in Dry Bean Lines VA19 and I9365-3. *Crop Science*, *51*(1), 123-139. https://doi.org/https://doi.org/10.2135/cropsci2010.06.0356

Steadman, J. R. (1983). White mold -- a serious yield-limiting disease of bean. *Plant Disease*, *67*(4), 346–350.

Sturtevant, A. H. (1913). The linear arrangement of six sex-linked factors in Drosophila, as shown by their mode of association. *Journal of Experimental Zoology*, *14*(1), 43-59. https://doi.org/https://doi.org/10.1002/jez.1400140104

Tok, F. M., Derviş, S., & Arslan, M. (2016). Analysis of genetic diversity of Sclerotinia sclerotiorum from eggplant by mycelial compatibility, random amplification of polymorphic DNA (RAPD) and simple sequence repeat (SSR) analyses. *Biotechnology &*

Biotechnological Equipment, *30*(5), 921-928. https://doi.org/10.1080/13102818.2016.1208059

Townsend, B. B., & Willetts, H. J. (1954). The development of sclerotia of certain fungi. *Transactions of the British Mycological Society*, *37*(3), 213-221. https://doi.org/https://doi.org/10.1016/S0007-1536(54)80003-9

Treangen, T. J., & Salzberg, S. L. (2011). Repetitive DNA and next-generation sequencing: computational challenges and solutions. *Nat Rev Genet*, *13*(1), 36-46. https://doi.org/10.1038/nrg3117

Van der Plank, J. E. (1984). *Disease resistance in plants / J. E. Vanderplank* (2nd ed.). Orlando, Fla. : Academic Press.

Vasconcellos, R. C. C., Oraguzie, O. B., Soler, A., Arkwazee, H., Myers, J. R., Ferreira, J. J., Song, Q., McClean, P., & Miklas, P. N. (2017). Meta-QTL for resistance to white mold in common bean. *PLOS ONE*, *12*(2), e0171685. https://doi.org/10.1371/journal.pone.0171685

Vinale, F., Manganiello, G., Nigro, M., Mazzei, P., Piccolo, A., Pascale, A., Ruocco, M., Marra, R., Lombardi, N., Lanzuise, S., Varlese, R., Cavallo, P., Lorito, M., & Woo, S. L. (2014). A Novel Fungal Metabolite with Beneficial Properties for Agricultural Applications. *Molecules*, *19*(7), 9760-9772.

Wang, A.-R., Zhang, C.-H., Zhang, L.-L., Lin, W.-W., Lin, D.-S., Lu, G.-D., Zhou, J., & Wang, Z.-H. (2009). Identification of Arabidopsis Mutants with Enhanced Resistance to Sclerotinia Stem Rot Disease from an Activation-tagged Library. *Journal of Phytopathology*, *157*(1), 63-69. https://doi.org/https://doi.org/10.1111/j.1439-0434.2008.01461.x

Wang, P., Meng, F., Moore, B. M., & Shiu, S. H. (2021). Impact of short-read sequencing on the misassembly of a plant genome. *BMC Genomics*, *22*(1), 99. https://doi.org/10.1186/s12864-021-07397-5

Wei, W., & Clough, S. J. (2016). Sclerotinia sclerotiorum: molecular aspects in plant pathogenic interactions. *Revisão Anual de Patologia de Plantas (RAPP).* , *24*, 174-189.

Wellenreuther, M., Mérot, C., Berdan, E., & Bernatchez, L. (2019). Going beyond SNPs: The role of structural genomic variants in adaptive evolution and species diversification. *Molecular Ecology*, *28*(6), 1203-1209. https://doi.org/https://doi.org/10.1111/mec.15066

Willbur, J. F., Ding, S., Marks, M. E., Lucas, H., Grau, C. R., Groves, L., Kabbage, M., & Smith, D. L. (2017). Comprehensive Sclerotinia Stem Rot Screening of Soybean Germplasm Requires Multiple of *Sclerotinia sclerotiorum*. *The American Phytopathological Society*, *101*(2), 272-394. https://doi.org/https://doi.org/10.1094/pdis-07-16-1055-re

Willetts, H. J., Wong, J. A. L., & Kirst, G. D. (1980). The Biology of Sclerotinia sclerotiorum, S. trifoliorum, and S. minor with Emphasis on Specific Nomenclature. *Botanical Review*, *46*(2), 101-165. http://www.jstor.org.proxy3.library.mcgill.ca/stable/4353966

Xia, Y., Liu, Y., Deng, M., & Xi, R. (2017). Pysim-sv: a package for simulating structural variation data with GC-biases. *BMC Bioinformatics*, *18*(3), 53. https://doi.org/10.1186/s12859-017-1464-8

Zaccaron, A. Z., & Stergiopoulos, I. (2024). Analysis of five near-complete genome assemblies of the tomato pathogen Cladosporium fulvum uncovers additional accessory chromosomes and structural variations induced by transposable elements effecting the loss of avirulence genes. *BMC Biology*, *22*(1). https://doi.org/10.1186/s12915-024-01818-z

CHAPTER 2: *Sclerotinia sclerotiorum* L. de Bary IN CANADA: PHENOTYPING TRAITS FOR EPIDEMIOLOGICAL INSIGHTS.

Esquivel García, Laura[1]; Chatterton, Syama[2]; Cadler, Brad[2]. Derbyshire, Mark[3]; Newman, Toby[3]; Hoyos-Villegas, Valerio[1*]

[1]Pulse Breeding and Genetics Laboratory, Department of Plant Science, McGill University,

[2]Lethbridge Research and Development Centre, AAFC, and

[3]Curtin University, Perth, Australia, Centre for Crop and Disease Management (CCDM).

*Corresponding author: valerio.hoyos-villegas@mcgill.ca

ABSTRACT:

Sclerotinia sclerotiorum L. de Bary (*Ss*) is one of the most destructive pathogens in Canada and around the world. It affects over 500 species of plants, including the economically important common bean. In Canada, its impact is pronounced, necessitating a comprehensive exploration of its genetic diversity and aggressiveness.

This study aimed to elucidate the genetic diversity and aggressiveness of *Ss* isolates collected from commercial fields in three Canadian provinces. Through a dual phenotypic trait analysis of Mycelial Compatibility Groups (MCGs) and aggressiveness determination, we investigated 39 *Ss* isolates from an interprovincial set and 30 samples from adjacent fields referred to as the proximal subset. In detail, the interprovincial set of 39 *Ss* of samples alone, was used to: a) classify *Ss* isolates by their mycelial compatibility and investigate *Ss* aggressiveness levels by stem inoculation *in planta* on the susceptible cultivar Beryl, b) Assess disease progression of *Ss* isolates when inoculated into two germplasms with different susceptibility to *Ss*, and the extent to which the cultivar-isolate interaction influenced their disease progression

Our investigation of Mycelial Compatibility Groups (MCGs) revealed the presence of 18 distinct MCGs in the interprovincial set, suggesting a population with high genetic diversity. Conversely, proximal fields exhibited a more clonal population, characterized by only two MCGs. A novel classification system for MCGs based on geographical dispersal and isolate frequency was proposed, delineating Core, Regional, and Endemic MCGs.

Aggressiveness testing identified that 82.35% of isolates displayed aggressive responses. In contrast, 17.65 % showed mildly aggressive isolates shedding light on the threat that *Ss* pose to

current commercial fields by displaying predominantly aggressive behavior among the isolates in the population of study.

Our analysis showed that the choice of cultivar influences the disease display with disease progress that differs depending on the cultivar's susceptibility. Our results provide valuable information on how *Ss* interact with its host contributing into the efforts towards selection of isolates for screening for resistance.

These phenotypic analyses highlight the complex interactions between *Ss* isolates and common bean cultivars, providing valuable information for understanding the pathogen's behavior. The observed disparity in genetic diversity between interprovincial and proximal fields hints at varied evolutionary pressures, possibly influenced by geographic isolation and agricultural practices.

In unraveling the complexities of *Ss* genetic diversity and aggressiveness, this study not only advances our comprehension of host-pathogen interaction but also paves the way for development of targeted control aiming at reducing the harmful effects of the pathogen on agricultural productivity. Our results are headed to provide farmers with the knowledge requisite for informed decision-making, thus strengthening the resilience of agroecosystems against the attack of adverse threats such as *Ss*.

Key message: This study outlines MCG and aggressiveness reactions of *Ss* isolates. Proposed classification system for MCGs enables comparative studies. High genetic diversity in *Ss* isolates from three Canadian Provinces categorized in 18 MCGs.

2.1. INTRODUCTION

Sclerotinia sclerotiorum L. de Bary (*Ss)* is the causal pathogen of white mold disease. *Ss* is a devastating fungus responsible for substantial yield and quality losses in common bean (*Phaseolus vulgaris* L.) (Gerard et al., 2011; McDonald & Boland, 2004). The disease is endemic and widespread in North and South American countries, observed during seasonally cooler and more humid environmental conditions (Miklas et al., 2013). Under favorable weather conditions, losses due to white mold can be as high as 100% in susceptible cultivars (Schwartz & Singh, 2013). Although control measures of white mold exist on several scales, maintaining a broad base of genetic resistance against a range of pathogen genotypes remains among the most effective management strategies for tailored disease management (Joelle et al., 2011). Improvement efforts focused on bean resistance to this disease have been performed. However, these efforts have helped to achieve partial levels of resistance, leaving room for improvement in the fight of this important pulse crop against this pathogen (Miklas et al., 2014). The multifaceted nature of *Ss* is widely acknowledged as the primary challenge in breeding programs. This has sparked an interest in providing as much information as possible about this evolving pathogen. This includes performing phenotyping of certain pathogen traits that can provide insights for effective plant breeding. This entails a more detailed description of the epidemiology of *Ss* and phenotypic characterization of white mold. However, finding an association between *Ss* phenotypic features and their underlying genomic counterparts remains a challenge due to the pathogen's genetic complexity, environmental influence on traits, and the intricate interactions between multiple genes and genotypes.

Reports of phenotypic variation commonly focus on the morphological features of the pathogen itself, such as mycelial growth characteristics, sclerotial formation and the use of Mycelial Compatibility Groups (MCG). Studies rarely conduct association analysis of phenotypic markers and phenotypic traits such as aggressiveness (Michael et al., 2020). In such studies, conflicting results on associations of phenotypic traits were observed, indicating that there is still room to understand the responses of phenotypic traits in *Ss*.

MCG testing has been a widely used phenotypic marker to characterize the ability of the pathogen to anastomose (fuse) with compatible isolates, forming a single colony (Kohn et al., 1991). This phenotypic marker has been largely used as a macroscopical marker for the identification of genetically similar isolates as initially described by Kohn et al. (1991), and most recently by Liu et al. (2018). On the other hand, testing the pathogen’s disease progression over time helps identify its

varying aggressiveness levels, which is beneficial for developing resistant varieties tailored to specific threats.

By combining data from diverse phenotypic responses, such as MCG reactions and a pathogen's aggressiveness, it is possible to gain insights into the dynamics of disease development. This approach helps in understanding the composition of pathogen populations and the influence this composition has on disease display. To our knowledge, only a few studies have combined MCG testing with detailed aggressiveness assessments to understand the complex interactions and evolutionary pressures shaping pathogen populations (Hambleton et al., 2002). More recent studies, such as the one by Denton-Giles et al. (2018), also followed this approach in canola. In their study they incorporated the study of MCGs, and Intergenic Spacer (IGS) region haplotype as well as chose highly aggressive and genetically diverse *Ss* isolates in screening for resistance providing a more contemporary understanding of the diversity and behavior of *Ss*. This highlights the need to keep up with the evolution in research methods to provide a more accurate representation of *Ss* diversity.

The purposes of this study were to: 1) Create a *Ss* collection from infected commercial fields across Canada; 2) Classify isolates into MCGs; 3) Compare the mycelial compatibility reactions in a proximal vs a more dispersed set of samples; 4) Build a dataset of isolate aggressiveness in Common bean (*Phaseolus vulgaris* L.) and 5) Establish the relationship between MCGs and aggressiveness for 39 isolates within Canadian provinces.

2.2. MATERIALS AND METHODS

2.2.1. Isolate collection

A total of 39 isolates were collected in three Canadian provinces between 2021 and 2022 through the Canadian Sclerotinia Initiative (*Canadian Sclerotinia Initiative*, 2021). The Canadian Sclerotinia Initiative, funded by Agriculture and AgriFood Canada (AAFC), aims to understand the epidemiology and genomics of *Ss*. By performing comparative phenotypic and genomic analyses of collected isolates, the initiative seeks to uncover resistance mechanisms in crops, helping manage and mitigate the impact of this widespread pathogen.

With the aim of comparing the mycelial reactions of samples from diverse geography in Canada vs a set with closer proximity, two sets of samples were collected:

- Interprovincial set: This was a set of 39 samples. Of the n=37, n=16 were collected from Quebec (QC), n=16 from Alberta (AB) and n=5 from Ontario (ON), n= 2 were added to this set from the proximal subset (10F, 1F). The interprovincial set was collected mainly in commercial fields of soybean (*Glycine max*) and common bean (*Phaseolus vulgaris* L.) (**Appendix A**).
- Proximal subset: Comparison group n= 30 samples from a single site located in Saint Apollinaire QC, collected from different crops e.g. common bean, soybean, sunflower, lettuce, ornamentals (**Appendix B**).

Samples in the interprovincial set were assigned a two-letter code representing their province of origin (e.g., O = Ontario, Q = Quebec, and A = Alberta), followed by a numeric identifier based on the order of collection, such as "Q1" for the first sample that was collected in Quebec. (**Appendix A**). Similarly, samples from the proximal subset were named based on the order of collection followed by an (F) identifier, indicating collection from a farm, such as "1F" for the first farm-collected samples (**Appendix B**). The approximate locations of the isolates are displayed in Figure 4.

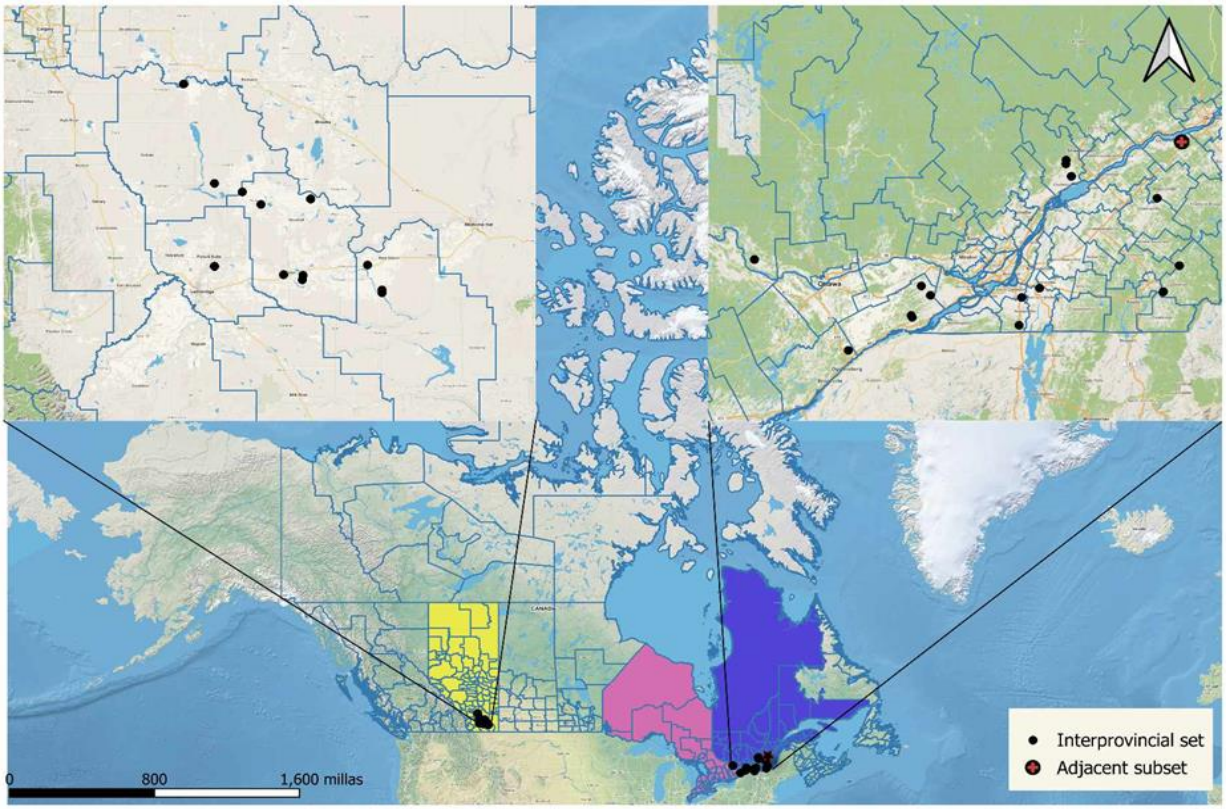

Figure 4. Geographical distribution of sample collection. The dark circles depict GPS based geographic location of the Interprovincial set composed by 39 isolates distributed across three Canadian provinces (Alberta, Ontario and Quebec) (coordinates in Appendix A), while the Proximal subset composed of 30 isolates from Quebec, is depicted by a cross-shaped icon (coordinates in Appendix B).

2.2.2. Sample handling and disinfection.

Isolates were obtained as sclerotia and stored in Petri dishes (100 x 15mm Sigma Aldrich) at 4°C until ready for experimentation. Stored sclerotia were surface disinfected in 10% (vol/vol) bleach for 1 min followed by 95% ethanol for 1 min, rinsed in double distilled water, dried on sterile filter paper, and each isolate was cultured onto potato dextrose agar (PDA; BD DifcoTM) in Petri dishes (100 x 15 mm). Active mycelia from the leading edge of colonies were then used for further analysis as recommended by Willbur et al. (2017).

2.2.3. Mycelial Compatibility Group testing.

Only 34 out 39 isolates from the interprovincial set underwent aggressiveness testing. Isolate A34 was discarded after MCG testing revealed that it was incompatible with all other *Ss* isolates in addition to displaying a phenotype dissimilar to *Ss*, suggesting it might be a different species. The remaining four isolates that were not tested for aggressiveness had culture issues at the time of testing (Q3, Q14, Q15 and A30) therefore, their aggressiveness remains unknown.

The experiment aimed to characterize the compatibility relationships among *Ss* isolates. Mycelial Compatibility Group testing (MCG) was performed in two sets of isolates, according to the methodology suggested by Schafer and Kohn (2006). Small mycelial plugs (3mm approx.) were taken from the edge of 3 to 4-day-old colonies growing on PDA at 23°C in darkness. All isolates were challenged against each other in an isolate-by-isolate pairing matrix ensuring confrontation in non-self-combination as well as self-to-self-confrontation as a control for compatibility. Plugs were placed at approximately 3.5 cm distance on opposite sides of 100 x 15 mm standard Petri dishes on PDA amended with 100 µL/L of McCormick's red food coloring as suggested by Schafer and Kohn (2006) to enhance visibility of the incompatible reaction. Isolates confronted against each other were incubated at 23°C for a week. A rating system for compatibility reactions was based on absence or presence of a red barrier between colonies, color conferred by usage of red food coloring to enhance visibility (Kohn et al., 1990; Leslie, 1993; Otto-Hanson et al., 2011). An evident barrage zone or a red dividing line was indicative of incompatibility, whilst no reaction line and the ability to grow together indicated compatibility. Pairings were evaluated seven days after inoculation by two different raters. The experiment was repeated after which MCGs were defined by confirming the results, which in both cases resulted in the same outcomes for all pairings. A scheme of the procedure to perform MCG testing can be seen in Figure 5.

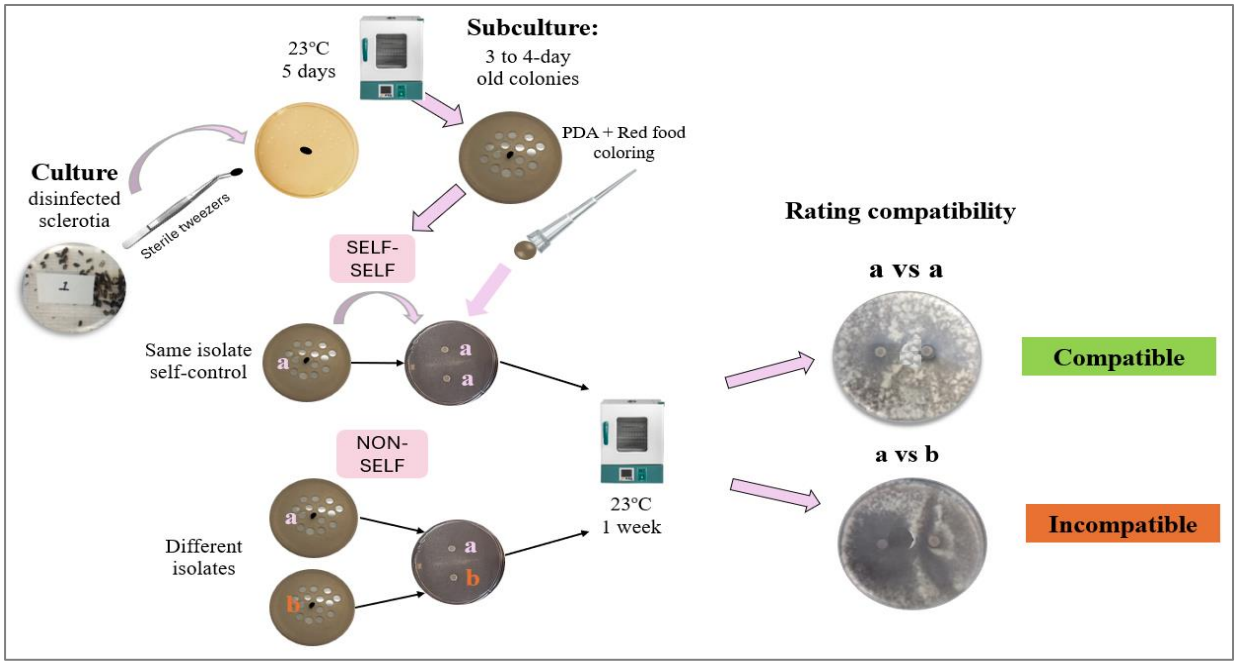

Figure 5. Schematic representation of MCG testing. The methodology for testing mycelial compatibility reactions consisted of culturing previously disinfected sclerotia in potato dextrose agar (PDA) plates, followed by incubation at 23ºC for 5 days. Then, 3 to 4 days old mycelia plugs were subcultured using sterile pipette tips to transfer them into PDA media amended with red food-coloring using self-to-self combinations as control for compatibility and pairing of all isolates against each other in non-self combinations. All paired isolates were incubated for 1 week after which their compatibility was rated.

2.2.4. Plant Materials

Two common bean cultivars were utilized to conduct aggressiveness evaluations: The first was the Andean landrace G122 'Jatu Rong' (Cranberry market class) from India (Miklas et al., 2001). G122 'Jatu Rong' has large seeds with red mottling, the plant exhibits determinate growth with upright architecture and resistance to oxalic acid (Kolkman & Kelly, 2000), which makes it a promising source of physiological resistance against *Ss* genotypes (Chung et al., 2008; Kolkman & Kelly, 2002). The susceptible cultivar 'Beryl' belongs to one of the major market classes produced worldwide (Great northern market class). Beryl plants have an indeterminate growth habit, are prone to lodging, and are often used as a susceptible check in screening for resistance (Otto-Hanson et al., 2011).

2.2.5. Isolate Aggressiveness Testing

To evaluate aggressiveness, inoculation *in planta* was conducted only for the interprovincial set. Common bean seeds of both cultivars were sown in 10 cm pots in moist all-purpose potting mix (Fafard Agro Mix G6) and then placed on benches under controlled greenhouse environment

conditions with temperatures ranging from 23 to 25 ºC. Seeds were watered daily and fertilized at the beginning of emergence with all-purpose fertilizing mix N-P-K 12-4-8 Miracle-Gro®. Agar plugs were taken from the edges of 3 to 5 days old actively growing mycelia to inoculate 20 to 28 days (about 4 weeks) old common bean plants using the straw test technique previously described by Petzoldt and Dickson (1996) with slight modifications by replacing straws for sterile 100µL pipette tips to collect agar plugs. After the third/fourth trifoliate, the main stem was excised, leaving approximately 2.5 cm of the remaining main stem. Pipette tips containing the inoculum were placed over excised main stems, and plants were placed in growth chambers with a light intensity of 600 µmoles/m2/s and were provided with misting humidifiers that provided constant relative humidity (RH) above 80%. Disease progression (lesion length) was recorded daily at five timepoints (3, 9, 12 and 15 days after inoculation) using a tape measure. Inoculated plants were placed in a Complete Randomized Design (CRD) with 6 replicates. Figure 6 illustrates the procedure used for inoculation in *Ss* aggressiveness determination assays.

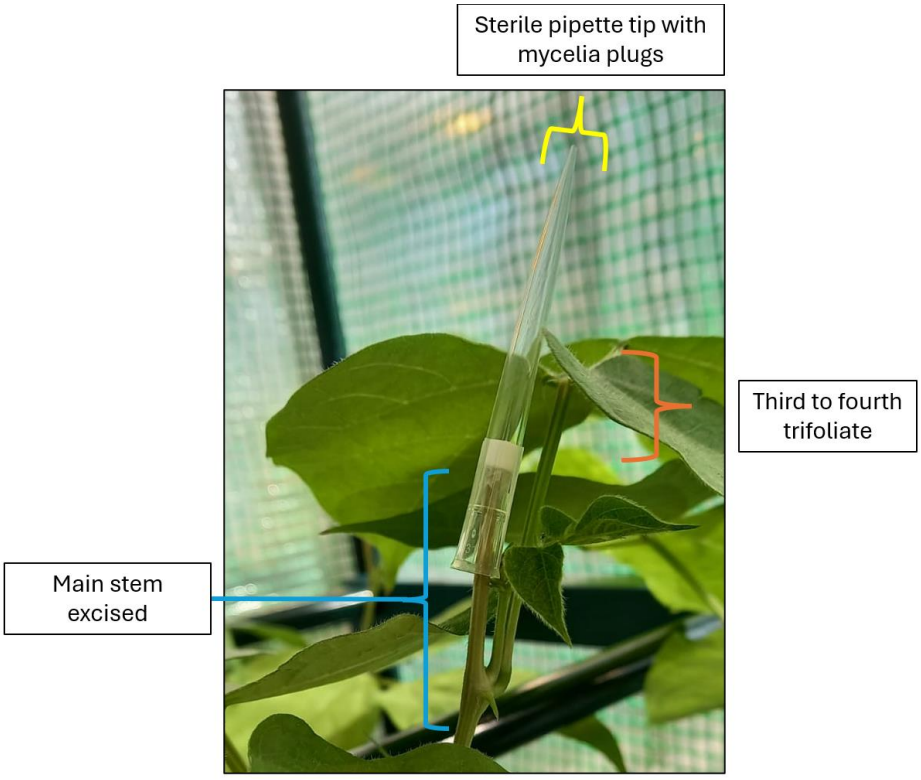

Figure 6. *In planta* inoculation of *Sclerotinia sclerotiorum* isolates for aggressiveness determination. The cut-stem inoculation technique involved excising the main stem after the third or fourth trifoliate leaf and applying a mycelial plug using a sterile 100µL pipette tip to the exposed tissue.

2.2.6. Data analyses

ANOVA was conducted with a General Linear Model (GLM) to analyze the data:

$$Y_{ijk} = \mu + cultivar_i + isolate_j + cultivar_i * isolate_j + error$$

The statistical analyses were conducted using IBM SPSS Statistics 29.0.1.1.

Post hoc Analysis:

Following a significant ANOVA result, Fisher's LSD test was performed to identify: 1) specific differences between isolates based on their mean STAUDPC values, 2) assessing whether the effect of isolates differed between cultivars, and 3) if their interaction significantly influenced disease progression.

As replicate numbers varied, an additional LSD value was calculated using the average number of replicates to determine a minimum difference required for statistically significant differences between isolate means. This facilitated pairwise comparisons, which were then used to classify isolates into aggressiveness groups based on disease severity, as measured by the STAUDPC. The classification of aggressiveness was carried out on the susceptible cultivar, following the criteria outlined by Willbur et al. (2017). In this approach, isolates were classified as "aggressive" and "mildly aggressive" where: "Aggressive" (A) = isolates whose STAUDPC values were not statistically different from the isolate with the highest STAUDPC, and significantly different from the isolate with the lowest STAUDPC. "Mildly Aggressive" (MA) = isolates with STAUDPC values greater than 0.00 but not significantly different from the lowest STAUDPC value.

2.3. RESULTS.

2.3.1. Mycelial Compatibility Group Testing.

Our research into the mycelial compatibility reactions among *Ss* collected in Canada helped to establish the mycelial compatibility relationships for 2 *Ss* sample subsets: the Proximal subset and

the Interprovincial set. By subjecting these subsets to compatibility testing independently, we aimed to elucidate the patterns of interaction within each subset and uncover any differences in compatibility between samples collected from proximal sites in contrast to those collected from geographically distant collection sites.

2.3.1.1. Mycelial Compatibility Group testing for Proximal Subset.

Our analysis of the mycelial compatibility reactions within the Proximal subset revealed interactions among samples collected from closely situated sites. Each isolate exhibited clear compatibility or incompatibility reactions in every pairing. Isolates were separated into two distinct MCGs based on their response, following a transitive approach for establishing MCGs. The MCGs were labeled as follows:

1. "Farm MCG A" (MCG1F) consisting of 20 isolates: 1F, 3F, 4F, 5F, 7F, 9F, 10F, 11F, 12F, 13F, 14F, 15F, 19F, 20F, 21F, 23F, 24F, 25F, 27F, 29F.
2. "Farm MCG B" (MCG2F) comprising 10 isolates 2F, 6F, 8F, 16F, 17F, 18F, 22F, 26F, 28F, 30F). The pairing matrix leading to these results can be visualized in Appendix C.

2.3.1.2. MCGs for Interprovincial set.

In contrast with the Proximal subset, assessing compatibility dynamics among samples collected from three Canadian provinces resulted in the establishment of 18 MCGs among 39 isolates tested. This subset originally included 37 samples, with two additional samples (1F and 10F) randomly selected from the Proximal subset.

Three key approaches were employed in establishing MCGs within the Interprovincial subset: i) identifying unique compatibility or incompatibility patterns among isolates, ii) identifying isolates that exhibited compatibility with two or more established MCGs and iii) classifying isolates as a unique MCG consisting of a single isolate if they exhibited incompatibility with all others. The dispersion of isolates among groups is represented in Figure 7. The geographic distribution of MCGs is displayed in Figure 8 with color tags assigned to each group. The pairing matrices that led to these results can be consulted in Appendix D.

Overall, after assessing self-pairing controls that were compatible in 100% of the cases, we identified that 21 % of isolates (n=8) were incompatible with others, and hence, they were assigned to independent MCGs (MCGs 10-17, Figure 6). The remaining isolates were distributed among 10

MCGs. Isolate distribution in these 10 MCGs resulted in the following: First, 58% of the isolates (n=22) were distributed among the established MCGs with a pattern of unique compatibility within the groups to which they were assigned (MCG1-MCG9 and MCG18). Second, 21% of isolates (n=8) exhibited compatibility with two or more established MCGs. In this study, we refer to this phenomenon as mixed compatibility (isolates Q14, Q15, Q18, A23, A25, A29, A31, A32), the majority of which came from AB and the rest from QC. None of the isolates from ON displayed compatibility across several MCGs nor were they assigned to a same MCG. The isolates with the broadest compatibility across MCGs were isolates A25 and A29 from AB, presenting compatibility with isolates of 9 and 8 out of 18 MCGs, respectively.

Out of the 18 established MCGs, three (MCG1, MCG5, and MCG7) formed the largest groups with 6, 3, and 3 isolates, respectively, showing unique compatibility despite having isolates with compatibility across more than one MCG. Additionally, these MCGs each contained at least one isolate from each province. MCG18, which consisted of two isolates from the Proximal subset (1F and 10F), displayed incompatibility reactions when challenged against all other established MCGs.

2.3.1.2.1. Classification system in MCGs.

A classification system is suggested based on the number and geographical distribution of isolates assigned to each MCG in this specific population. Three classes of MCGs are suggested based on patterns of frequency and geographic dispersal:

- **Class A: Core MCGs.**

MCGs that displayed high frequency and broad geographical distribution representing predominant *Ss* genotypes in the population of study. Within this class, we found MCG1, MCG5, and MCG7 (Figure 7). These MCGs contained the highest number of isolates with unique (MCG1: n=6, Q1, Q5, O11, Q12, Q13, A24; MCG5: n=3, Q6, O9, Q22; MCG7: n=3, O10, Q16, A33) and mixed compatibility (MCG1: n=4, Q14, A29, A31, A25; MCG5: n=5, Q14, A23, A29, A25, A32). Moreover, these MCGs contained at least one isolate from each province.

- **Class B: Regional MCGs.**

Isolates classified within the regional class of MCGs showed moderate frequency and moderate geographic dispersal. They contained lower number of isolates in comparison with MCGs in Class A. Potentially, MCGs classified within this class indicated regional variations in *Ss*. MCGs in this class in the population of study were MCG2, MCG3 and MCG18 (Figure 7). The distribution of isolates in this MCGs contained isolates with unique (MCG2: n=2, Q2, O8; MCG3: n=2, Q3, A30; MCG18: n=2, 1F and 10F) and mixed compatibility (MCG2; n=1, A29; MCG3; n=4, Q15, Q18, A29, A25). These MCGs did not contain isolates from all provinces.

- **Class C: Endemic MCGs.**

MCGs that displayed the lowest frequency and specific geographic distribution. Interestingly, the Interprovincial set displayed a significant presence of isolates categorized within this class. Within this class we found n=12 groups including MCG4, MCG6, MCG8-MCG17. Out of n=12 groups within this category only n=4 contained both, isolates with unique (MCG4: n=1, Q4; MCG6: n=1, O7; MCG8: n=1, Q17; MCG9: n=1, Q19) and mixed compatibility (MCG4: n=4, A29, A31, A25, A32; MCG6: n=3, Q18, A29, A25; MCG8: n=2, A29, A25; MCG9: n=2, A29, A25). The rest (n=9) represented MCGs composed of isolates incompatible with the rest of isolates within the population of study.

Overall, we identified that isolates with mixed compatibility (Q14, Q15, Q18, A23, A25, A29, A31, A32) transcend MCG classification system, as they are compatible across MCG classes. Although not class-less we recommend further analysis using genomic tools to better understand the phenomenon of mixed compatibility when isolates are classified in more than one class.

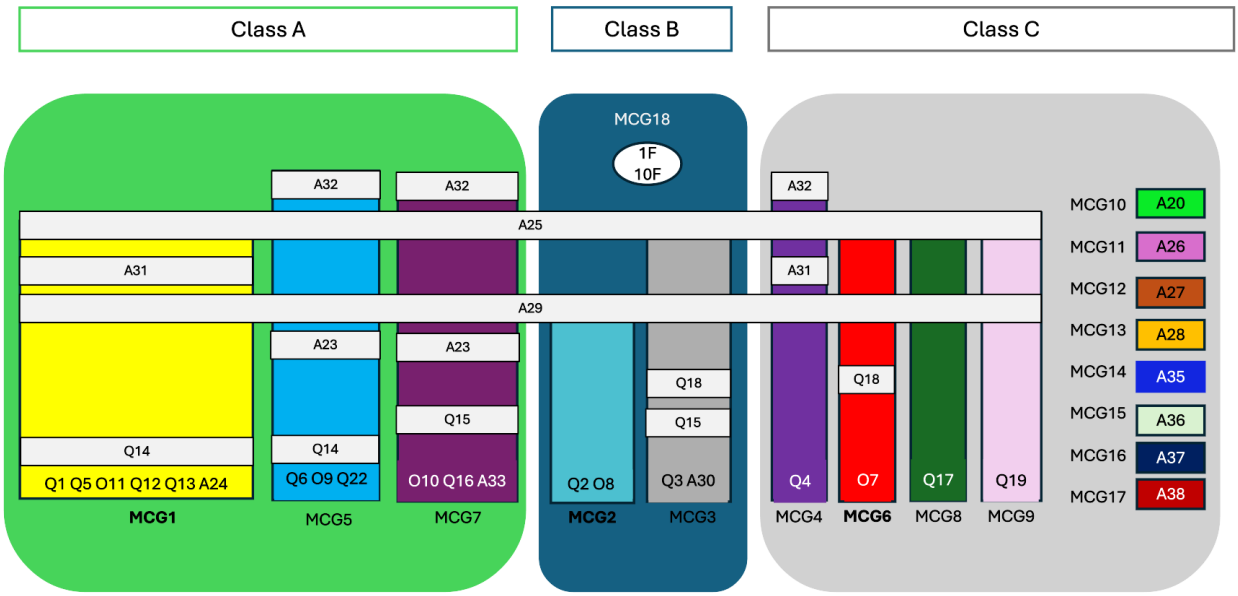

Figure 7. Established Mycelial Compatibility Groups (MCGs) of *Sclerotinia sclerotiorum* are depicted in colored charts (MCG1-MC17), showing isolates with unique compatibility. Light grey labels indicate isolates with mixed compatibility (Q14, Q15, Q18, A23, A25, A29, A31, A32) and the corresponding MCGs they are compatible with. Isolates within the circle (1F and 10F) represent a unique MCG (MCG18) from the proximal subset. MCGs are organized according to their geographical dispersal and frequency into three classes, each represented by different colors: Class A – Core MCGs (green); Class B – Regional MCGs (blue), and Class C – Endemic MCGs (grey). Isolate IDs are displayed in accordance with the province of provenance (A= Alberta, O= Ontario, Q= Quebec) followed by a number that was assigned to each sample according to their order of collection.

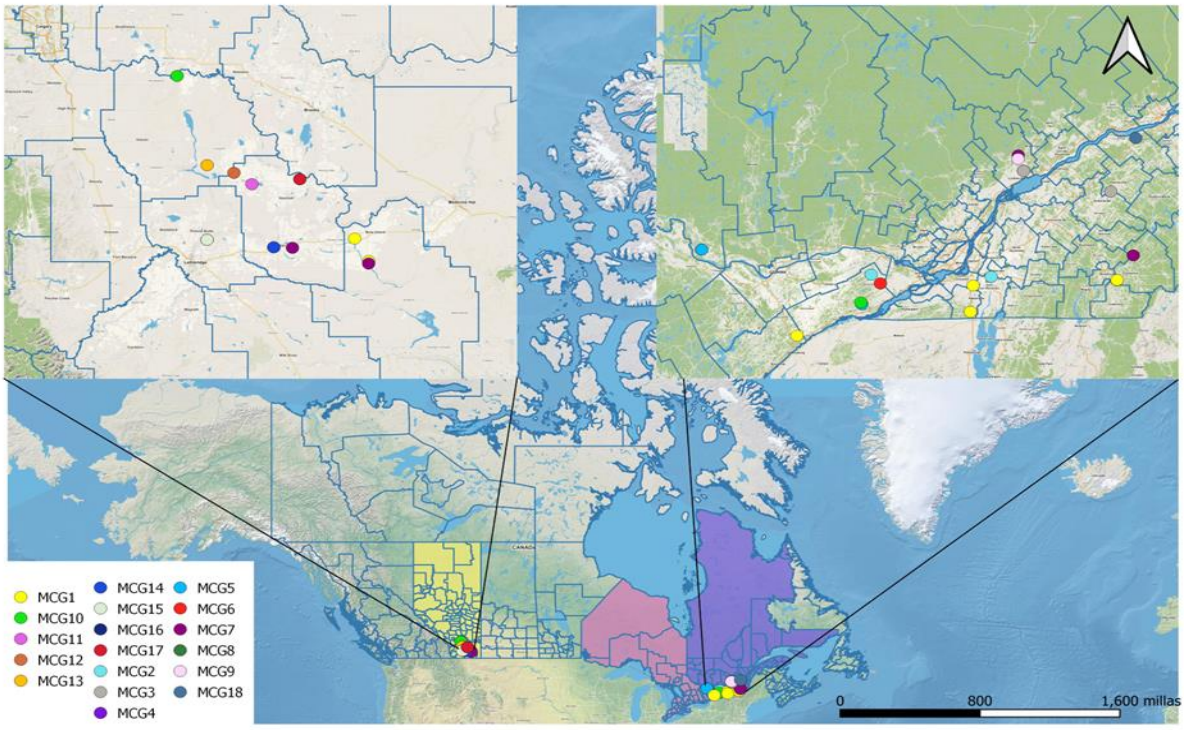

Figure 8. Geographical distribution of 18 established Mycelial Compatibility Groups (MCGs) of *Sclerotinia sclerotiorum* from three Canadian Provinces (Alberta, Quebec and Ontario). MCG1 displayed the highest frequency and was widely distributed by including at least one sample of each province.

2.3.2. Summary of inoculation results.

The artificial inoculation of all isolates resulted in development of stem lesions in both germplasms.

Given that the Interprovincial set stood out for its responses in relation to the MCG assays, further exploration of its isolate aggressiveness was performed. Aggressiveness experiments were conducted by inoculating two common bean germplasms: cultivar Beryl (Susceptible) and landrace G122 (Moderately Resistant).

After measuring disease progression and analyzing the STAUDPC values with a GLM, the ANOVA results revealed statistical differences between i) isolates ($p > 0.001$), iii) cultivars ($p > 0.001$) as well as a significant interaction effect between iii) isolate and cultivar ($p > 0.001$) as indicated in Table 1.

Table 1. ANOVA results from the univariate general linear model testing the effects of two common bean cultivars with different susceptibility to *Sclerotinia sclerotiourm*, effect of *Sclerotinia sclerotiorum* isolate range, and the effect of their interaction on disease severity (measured by STAUDPC).

Source of variation	Sum of Squares (SS)	Degrees of Freedom (df)	Mean Square (MS)	F-value	P-value	Partial Eta Squared
Model	49,693.223[a]	68	730.738	683.848	< 0.001	0.992
Cultivar	1,751.397	1	1,751.397	1,638.913	< 0.001	0.819
Isolate	134.568	33	4.078	3.816	< 0.001	0.259
Cultivar * Isolate	80.733	33	2.446	2.289	< 0.001	0.173
Error	385.777	361	1.069			
Total	50,078.999	429				

a. R Squared = 0.992 (Adjusted R Squared = 0.991).

2.3.2.1. Isolate aggressiveness determination.

We determined aggressiveness of the isolates. This assessment was based on Fisher's LSD ($\alpha = 0.05$) results observed in the susceptible cultivar Beryl, following the methodology outlined by Willbur et al. (2017). The aggressiveness designations are illustrated in the graph presented in Figure 9.

Overall, STAUDPC mean values illustrated varying disease progression responses in the susceptible cultivar Beryl, with some isolates exhibiting the highest (Isolate Q19, 14.353) and lowest (Isolate A26, 10.77) STAUDPC mean values.

Notably, isolate Q19 exhibited the highest STAUDPC value. A total of 28 isolates, including Q19, were categorized as 'aggressive', with STAUDPC values that were not statistically different from the highest STAUDPC value but significantly different ($p < 0.001$) from the lowest (n=28). These aggressive isolates represent 82.35% of the total tested population (IDs: Q19, O9, Q12, Q5, Q17, A23, A28, A24, A20, A36, A32, Q16, A35, A33, Q6, 10F, O7, Q4, O8, Q2, 1F, O11, A31,

Q13, A25, Q18, Q1, and O10). In contrast, 6 isolates (17.65%) were classified as 'mildly aggressive', showing STAUDPC values greater than 0.00 but not statistically different from the lowest STAUDPC value (n=6; IDs: A26, A27, A22, A38, A29, and A37).

The pairwise comparison results that led us to this classification is observed in **Appendix F**.

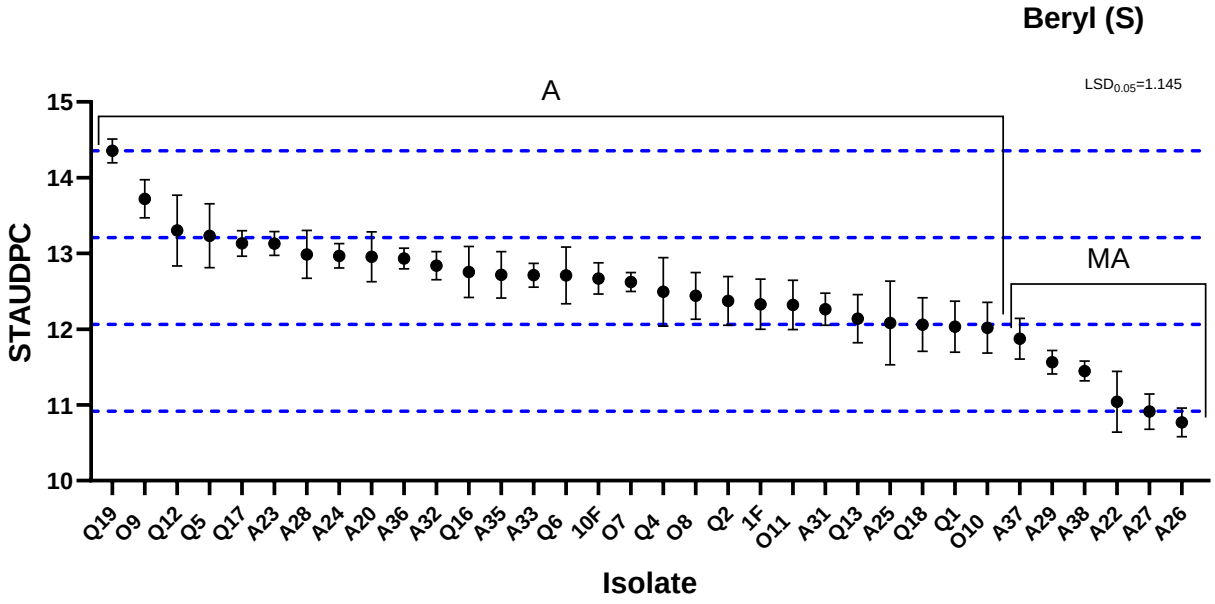

Figure 9. Aggressiveness responses of *Sclerotinia sclerotiorum* isolates from Interprovincial set determined upon analysis of the STAUDPC mean values resulting from measurements in susceptible (S) common bean cultivar 'Beryl'. The mean standardized areas under the disease progress curves (STAUDPC) are shown. Error bars represent the standard errors of the mean values. Aggressive isolates, defined as those whose STAUDPC values were not statistically different from the isolate with the highest STAUDPC and significantly different from the isolate with the lowest STAUDPC, are depicted by the letter A. 'Mildly Aggressive' isolates, with STAUDPC values greater than 0.00 but not significantly different from the lowest STAUDPC, are clustered and depicted with MA letters. The dotted blue grid lines indicate the LSD thresholds, starting with the first line based on the highest mean value (Q19 = 14.353). Subsequent lines were drawn consecutively to mark the statistical cutoffs based on LSD values.

2.3.2.2. Disease progression across cultivars and their interaction.

After determining isolate aggressiveness in the susceptible cultivar Beryl, we shifted our focus to evaluating how the range of *Ss* isolates influenced disease progression across both cultivars. Our analysis revealed significant variation in disease responses between the two cultivars ($p < 0.001$).

Between the two, the susceptible cultivar Beryl displayed the highest STAUDPC values, with an overall STAUDPC mean value of 12.47 ± 0.75 indicating greater disease severity. In contrast, the moderately resistant landrace G122, exhibited lower disease severity, with an overall

STAUDPC mean value of 8.33 ± 0.72. Pairwise comparisons confirmed that infection levels were consistently higher in Beryl compared to G122. **Appendix F**.

STAUDPC values in moderately resistant G122 landrace illustrated differences in disease progression as per the calculated STAUDPC. Figure 10 illustrates responses of *Ss* isolates from the Interprovincial set when inoculated into the moderately resistant landrace G122.

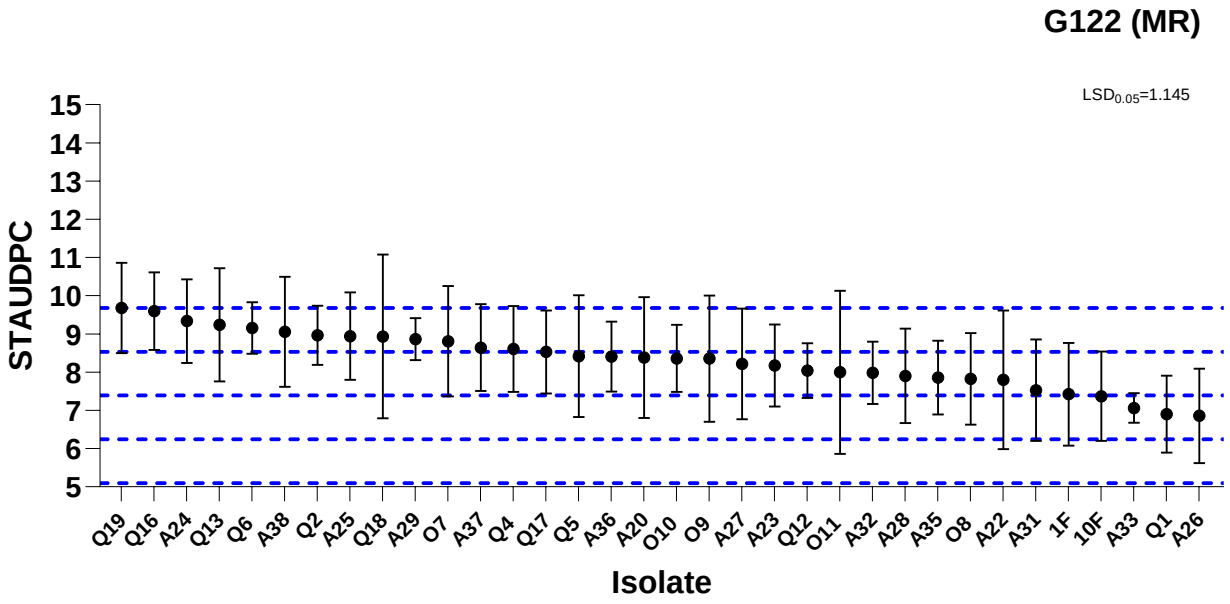

Figure 10. Disease progress responses determined upon analysis of the STAUDPC mean values of *Sclerotinia sclerotiorum* isolates from the Interprovincial set resulting from measurements in the moderately resistant (MR) landrace G122. STAUDPC responses. The mean standardized areas under the disease progress curves (STAUDPC) are shown. Error bars represent the standard errors of the mean values. The dotted blue grid lines indicate the LSD thresholds, starting with the first line based on the highest mean value (Q19 = 9.678). Subsequent lines were drawn consecutively to mark the statistical cutoffs based on LSD values."

The results display variability in disease response between cultivars, despite this variability some isolates consistently showed extreme STAUDPC values across both cultivars, with Q19 having the highest and A26 the lowest.

The ANOVA results (Table 1) indicate that cultivar susceptibility (susceptible vs. moderately resistant) was the primary driver of disease outcomes, modulating the impact of the isolates. Isolates also influenced disease severity ($p < 0.001$), thought to a lesser extent than cultivar susceptibility. The significant interaction between isolate and cultivar ($p < 0.001$) suggests that influence of each *Ss* isolate on disease severity was not uniform across cultivars, demonstrating that disease progression was dependent on the specific isolate-cultivar combination.

2.3.2.3. Description of qualitative observations in cultivar G122.

Qualitative observations revealed distinct responses to the pathogens' invasion: Firstly, upon inoculation with *Ss,* the moderately resistant landrace G122 exhibited self-pruning of infected zones at approximately three days after inoculation (usually when reaching the first node), often accompanied by the formation of callus tissue at the lesion site. Additionally, when the plant did not self-prune the infection zone, lesions often displayed a rust-colored appearance after the third day of inoculation.

2.3.3. Summary of phenotypic characterization.

After analyzing the Interprovincial set of samples. A complete description of their aggressiveness and the distribution of samples on different MCGs was conducted. Figure 10 summarizes our findings and include the classification of each MCG in our study, with the suggested MCG classes.

Two isolates, A25 and A29 which were broadly compatible across MCGs within classes A, B and C from our classification, displayed aggressive and mildly aggressiveness respectively. Despite their compatibility across different MCGs, A29 did not show the same statistical aggressiveness display as all isolates within those MCGs (intra-group).

Moreover, out of a total of 6 isolates with mild aggressiveness n=4 (66.66%) represented isolates classified within endemic groups (A26, MCG11; A27, MCG12; A37, MCG16 and A38, MCG17), from the remaining isolates with mild aggressiveness (A29) representing the 16.67% represented an isolate with mixed compatibility across MCG classes, and the remaining isolate Q22 (16.67%) was the only isolate that displayed mild aggressiveness and was located in the Core class of MCGs as per our classification.

Both the isolate with highest (Q19) and lowest (A26) STAUDPC mean values were assigned to endemic MCGs as per our classification.

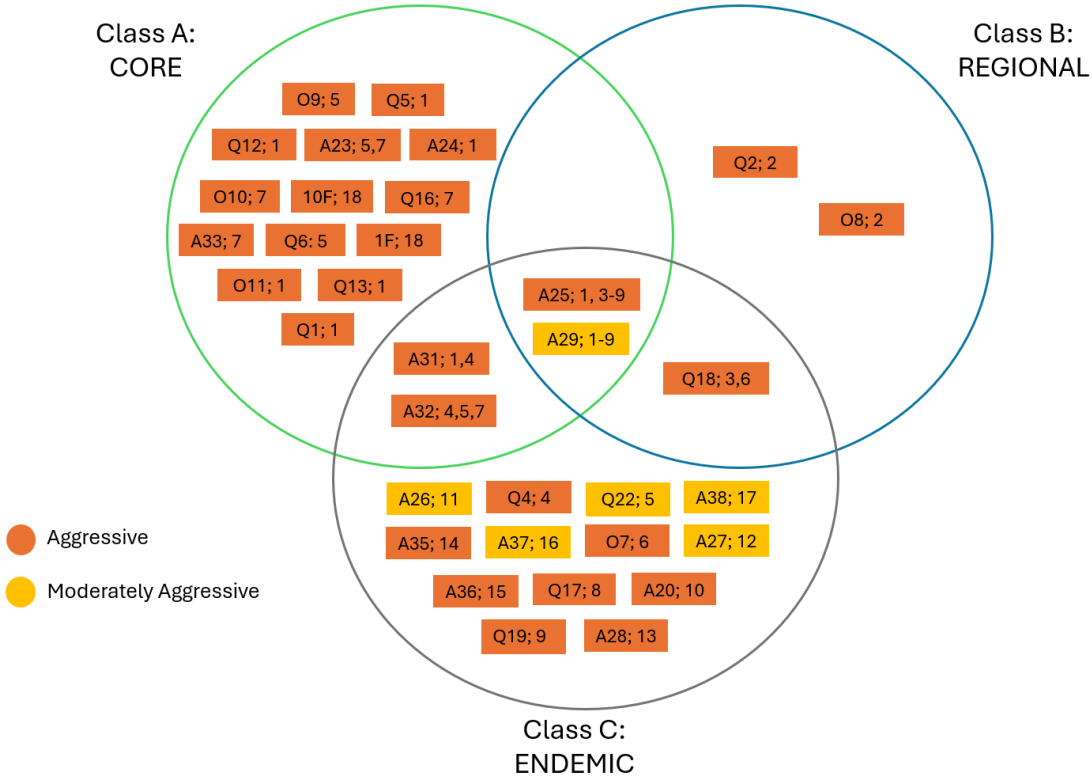

Figure 11. Venn Diagram illustrating the Mycelial Compatibility Groups (MCGs)and aggressiveness classes of *Sclerotinia sclerotiorum* isolates. Isolates were categorized based on geographic location and frequency, as proposed in this study and they were displayed in colored circles according to the class where they were categorized (green= Class A, Blue=Class A, and Grey= Class C). Two color tags represent the level of aggressiveness for each isolate. Each colored section contains the isolate ID, which includes the first letter of the corresponding province (Q = Quebec, O = Ontario, A = Alberta) and a numerical identifier based on the order of collection, followed by the MCG classification of each isolate.

2.4. DISCUSSION

The purpose of this study was to investigate the compatibility dynamics among *Ss* isolates from two diverse sets of samples collected in Canada. The Interprovincial set and the Proximal subset. Additionally, the study aimed at determining their differential responses in aggressiveness when inoculating a susceptible cultivar and a moderately resistant landrace with quantitative physiological resistance against this pathogen. Understanding the diversity of mycelial compatibility groups (MCGs) and aggressiveness is crucial to developing effective disease management strategies, including the deployment of resistant cultivars.

Our findings revealed how isolates from sites with geographic proximity (Proximal subset) led to the establishment of two MCGs (MC1F and MCG2F). In contrast, isolates from a more dispersed geographic area (Interprovincial set) revealed a more diverse population of *Ss*, with 18 distinct MCGs established out of 39 isolates tested.

It is suggested that the isolates from the Proximal subset may correspond to a more clonal population structure within this geographic region. There are literature reports on similar research with "local" sets of samples, where a clonal population was also observed (Kohn, 1995; Kull et al., 2004; Yatika, 1997). The explanation for a predominance of clones on proximal sites might be because ascospores disperse locally, spreading certain clonal lineages over a relatively short distance (Derbyshire & Denton-Giles, 2016; Rieux et al., 2014) This means that within a confined geographic area, such as the proximal subset in our study, a few clones can dominate the population. This clonal spread is facilitated by the wind-borne nature of the ascospores leading to a higher frequency of genetically identical or very similar isolates within that area (Cubeta et al., 1997; Kohn, 1995; Kull et al., 2004; McDonald & Linde, 2002).

Other studies reporting these types of "micro-geographical" populations suggest that a predominant clonality in *Ss* populations could arise from selective pressures such as environmental factors and agricultural practices favoring the presence of certain genotypes of limited gene flow between proximal populations (McDonald & Linde, 2002).

There might be diverse factors contributing to population structure in *Ss*, however, and it is also necessary to understand that although MCGs are routinely used to determine clonal lineages based on a self-recognition system, contemporary research suggests that vegetative compatibility is not always indicative of clonality as there might be events of recombination between strains without losing vegetative compatibility. Indeed, vegetative compatibility is a trait controlled by a small

number of polymorphic loci, allowing for recombination without losing compatibility (Kamvar, 2019). This means that strains within the same MCG may not be genetically identical clones but may exhibit genetic diversity due to recombination events. This is particularly interesting in our research as it highlights the need to keep exploring the complexities in *Ss* diversity by describing different phenotypic traits intra-MCG.

Reporting our observations about relationships encountered on isolates collected in proximity was crucial. These observations showed how these small, proximal populations displayed compatibility relationships. This is typical of a pathogen with predominant asexual reproduction behavior (Cubeta et al., 1997; Kohli et al., 1995; Kohli & Kohn, 1998; Yatika, 1997). Despite adjacent geographic dispersal, it also maintains some degree of variation which may be attributed to both its asexual reproduction (myceliogenic germination) and sexual reproduction of ascospores (via carpogenic germination) (Willetts et al., 1980) Therefore, those events leading to incompatibility still occur and the events influencing their genetic population structure are unknown and require further exploration. An important consideration is that the isolates from the proximal subset were collected in a field under an organic farming system. Organic farming systems often involve small-scale operations with crops grown in proximity (FAO, 2024; Jouzi et al., 2017), which may facilitate the spread of clonal lineages, leading to a higher prevalence of genetically similar isolates(Kamvar & Everhart, 2019). When facing a population with predominantly compatible reactions when performing MCG testing, researchers often use a transitive approach when dealing with large number of isolates. This involves grouping successive isolates into clusters based on their mutual compatibility relationships. For example, if isolate A is compatible with isolate B, and isolate is compatible with isolate C, then isolate A, B and C are grouped together, even if isolate A is not directly tested or compatible with isolate C. This method has been effectively applied in studies of MCGs in *Ss* (Schafer and Kohn, 2006), however, complementing MCG testing with genotyping techniques that more accurately reflect the specifics of mycelial compatibility at the molecular level by looking into the compatibility genes and loci involved in compatibility (Kamvar & Everhart, 2019).

The importance of understanding the dynamics of a proximal subset of samples also allows comparison to a population with broader geographic distribution, such as the interprovincial set analyzed in this study. Results from the interprovincial set showed differences in mycelial compatibility patterns that led us to establish 18 MCGs.

The percentage of samples allocated to MCGs composed of one isolate suggests that the interprovincial set of *Ss* collected in three Canadian provinces is a small population with high genetic diversity. Our results are supported by literature reports suggesting that the expectation for highly recombinant populations is that each collected isolate has one of two behaviors: a) it is incompatible with all others, or b) is part of an intransitive MCG (Schafer & Kohn, 2006). Both behaviors are observed in our set of samples. Firstly, 21% of samples allocated in MCGs with a single isolate incompatible with all others tested (MCG10 – MCG17). Secondly, the total number of isolates (n=8) that displayed compatibility with multiple MCGs (Q14, Q15, Q18, A23, A25, A29, A31, A32) is also evidence of meeting the description of isolates following their definition of "intransitive" MCGs as previously suggested. Moreover, the total number of established MCGs (n=8) with unique compatibility (MCG10-MCG17) might further suggest a high diversity. Despite the high diversity found in this small population, the significant number of isolates assigned to each MCG suggests the presence of a predominant group of clones responsible for the spread of *Ss* isolates. However, this diversity is likely also influenced by other non-clonal modes of reproduction. Similar patterns have been frequently reported in samples collected from wide geographical areas (Hambleton et al., 2002; Kohn et al., 1991).

An interesting debate takes place regarding isolates reported to be part of an "intransitive" MCG or otherwise identified to have mixed compatibility with established MCGs, as observed in our research. On the one hand, MCG testing has been utilized to type what are believed to be genetically similar isolates, as was demonstrated by Kohn et al. (1991) and most recently by Liu et al. (2018). Discussions have centered on the association of MCGs with unique DNA fingerprints in clonal populations, where each isolate typically exhibits a unique fingerprint associated with more than one MCG or sometimes a single MCG (Schafer & Kohn, 2006).

However, evidence suggests frequent outcrossing among *Ss* strains even within isolates classified within the same MCG, challenging the notion of sole clonality within MCGs (Attanayake et al., 2014; Buchwaldt et al., 2022; Derbyshire et al., 2019). Vegetative compatibility is controlled by a few polymorphic loci and is therefore inherited leading to mixed compatibility in offspring (Kamvar & Everhart, 2019). Outcrossing of isolates within the same MCG can lead to the emergence of new phenotypic traits in the offspring while conserving vegetative compatibility inherited from their parents, resulting in events of mixed compatibility. This explains the intriguing variability in

phenotypic traits among isolates within the same MCG often reported in infection to common bean (Kamvar et al., 2017; Rather et al., 2022)

An important contribution of our research is the finding of a pattern for classifying the associations in relationship of the frequency and geographical distribution of isolates into the established MCGs. When it comes to MCGs, there is not a universal system to cluster their relationships. Several MCG classification systems with diverse criteria have been used. The most common methods often involve classification with macroscopic traits such as Vegetative Compatibility (VC) which constitutes the basis for its wide usage presently (Glass & Kuldau, 1992; Leslie, 1993).

The classification system that we suggested keeps in mind that: a) *Ss* is a pathogen with a mixed reproduction system, b) their distribution is found over wide geographical areas, and c) increasingly displays events leading to apparent isolates with endemic distribution.

To that extent, our classification system comprised 3 MCG classes: Core MCGs comprised isolates that showed high frequency and dispersal, and regardless of the population size, *Ss* populations form MCGs that display high frequency and dispersal over a wide distribution. In studies where MCGs classification is included, isolates with a high frequency located in MCGs from more than 50% of the sites of collection will be considered in this class. Furthermore, a small number of Core MCGs with a high frequency of isolates within each will incline towards a population with a more clonal mode of reproduction. A second class: Regional MCGs will be composed of isolates with a moderate frequency and dispersal. It will contain fewer isolates, coming from less than 50% of collection sites, which will be lower than what will be expected in Core MCGs but always higher than the third class. The third class will constitute Endemic MCGs, which will show a low and localized frequency and might be associated with localized outbreaks or unique environmental conditions. It will almost follow a pattern of one isolate-specific MCG, translating into region-specific isolates. This class could switch from Class C to Class A or B if more samples are added to the study and if their geographic distribution increased. Otherwise, it will remain as endemic isolates. Although this is the first report of such a classification, most *Ss* MCG studies showed similar results in the patterns to the classification after establishing MCGs, which indicates transferability to our classification system.

Some limitations to our system of classification are likely to rise. For example, adding more isolates to a population might move a certain MCG from one class to another, but our classification method will still mostly be a useful tool to help plant pathologists and breeders select isolates that require further exploration based on their frequency and distribution. Current common bean breeding programs screening for resistance against white mold rely on randomly selected isolates without prior MCG identification. Some people consider MCG assays unreliable and outdated (Kamvar & Everhart, 2019). Our study highlights the value of complementing *Ss* population studies with prior MCG establishment. We suggest that this approach aids in discriminating and selectively exploring phenomena within a population, preventing costly genotyping efforts that may reveal ineffective sample selection retrospectively. In the worst-case scenario, random selection will lead to finding out that the isolate collection is constituted mostly by clones with wide distribution, which might not be suited to their research question.

Our results regarding the interprovincial set highlight the need to include a fair representation of isolates from adjacent areas in the study of bigger populations. The reasoning for this is supported by our observation on the proximal subset when it was tested independently, finding only 2 MCGs. However, when including two random isolates from a proximal subset into a more geographically dispersed group of isolates both isolates that previously were compatible with each other were incompatible with all other established MCGs from the interprovincial set. This compatibility issue reinforces the potential of classifying MCGs into three different classes, where the representation of them is not widely distributed over long distances but rather localized suggesting divergence of clones from potential events giving place to mutation (environmental, fungicides, etc.), or sexual reproduction (Buchwaldt et al., 2022; Derbyshire et al., 2019). However, further genetic studies are necessary to confirm this and refute the possibility that their occurrence might be attributed to anthropogenic activities including the diverse cultural practices than that of a pathogen reporting clonality.

The investigation into the aggressiveness of isolates yielded the aggressiveness classification of isolates tested. Several studies have addressed the aggressiveness of *Ss* from different geographic regions often demonstrating that the aggressiveness of isolates varies in a population (Yu et al., 2020). Pinpointing the isolates with the highest levels of aggressiveness is one of the foremost needs in plant breeding programs since this allows for adequate utilization of isolates in screening for new sources of genetic diversity (Taylor et al., 2014). Isolate Q19 displayed the highest STAUDPC value,

and it was classified as aggressive in our population sample. Determining aggressiveness may allow prioritization of isolates whose frequency in populations might be responsible for devastating outbreaks. Although breeders commonly prefer to use a single isolate, it is always a good idea to include screening with other isolates with different aggressiveness levels as demonstrated by Willbur et al. (2017), where multi-isolate assays accounted for the overall diversity of *Ss* isolates found in an infected field/population.

Challenging susceptible and current cultivars with moderate resistance against *Ss* highlights the need for integrated approaches to understand the current levels of aggressiveness of isolates across different cultivars. This understanding is crucial for predicting isolate behaviour and inform breeding programs about the mechanism regulating plant-pathogen interactions. In different crops, including common bean, the aggressiveness of *Ss* is often determined by inoculating susceptible cultivars to determine the relative pathogenicity of different isolates. Our study expanded on this approach by including a susceptible cultivar and a moderately resistant common bean landrace, each inoculated with the same isolates. This allowed us to investigate the effects of isolates causing current outbreaks and the interaction with the host they infect. Our results emphasize the importance of considering both cultivar susceptibility and isolate aggressiveness, as their combined influence shapes the overall disease response. This evidence is important as it shows that aggressiveness in *Ss* can vary based on the host genotype. This draws our attention to the initial definition of aggressiveness by Van der Plank (1963). In accordance with the author's earliest definition of aggressiveness, in a quantitative trait such as aggressiveness, it is more common to find a significant effect due to isolates but rarely due to the interaction of isolates and its host. However, this has proven to be different as pathogens evolve and our results demonstrate that for *Ss,* disease display varies depending on the isolate and the host susceptibility. This emphasizes the need to prioritize multi-isolate testing when exploring potential sources of germplasm resistance to avoid overlooking of resistance sources, which is agreement with the observations made by Willbur et al. (2017) in soybean and Denton-Giles et al. (2018) in canola.

An additional part in our study included some qualitative observations of the resistance mechanisms used by the moderately resistant landrace in the form of phenotypic responses to disease infection when tested against the *Ss* isolates. Inoculating current genetic resistant sources with isolates producing current outbreaks in commercial fields yielded intriguing findings. These results may

guide the screening for physiological resistance and assess the effectiveness of current sources of genetic resistance against *Ss* current isolates (Taylor et al., 2014).

Firstly, upon inoculation with *Ss* isolates, the moderately resistant landrace exhibited abscission of the infected zone at approximately three days after inoculation, accompanied by the formation of callus tissue at the lesion site. Additionally, when the plant did not produce abscission of the infection zone, lesions often displayed a rust-colored appearance after the third day of inoculation. Moreover, disease progression often stopped when it reached the plant's first node.

A common practice when screening for resistance often involves the utilization of the straw test inoculation method and rating system for resistance against *Ss* in common bean cultivars (Petzoldt & Dickson, 1996). This has been a useful tool leading to find sources of genetic resistance against *Ss*. However, the fast approach discriminates the mechanisms that might lead to biases and missing important sources of physiological mechanisms in response to disease infection. Despite the wide use of the straw test technique, raters might inadvertently overlook important symptoms related to the plant's defense mechanisms like discriminating qualitative data of plants that do not clearly show a site of infection on the rating day (usually day 7 after inoculation). The rater might think inoculation unsuccessful due to the absence of an infection site, missing the defense mechanism of a cultivar with the potential of detaching the stem at early infection. Detachment of stems can be viewed as a host defense mechanism aimed at limiting pathogen spread and promoting plant survival. When *Ss* infects a plant, it induces programmed cell death (PCD) in the infected tissue as part of its virulence strategy (Westrick et al., 2019; Williams et al., 2011). Although induction of cell death in infected tissues is a mechanism that necrotrophic fungi use to defeat the plant (Shlezinger et al., 2011), in certain cases, plants may be the ones who initiate the processes leading to the detachment of infected tissue as a survival mechanism to help isolating the infection, reduce the pathogen infection, trigger systemic resistance, and help enhance the recovery of the plant. Overall, common bean landrace G122 showed a self-pruning mechanism that is helping to minimize the impact of *Ss* isolates with a diverse range of aggressiveness levels. The self-pruning mechanisms that G122 may utilize might have helped to fight *Ss* isolates. This mechanism is often reported in the literature as "abscission" (Bleecker & Patterson, 1997; Olsson & Butenko, 2018). The phenomenon of abscission, in response to pathogen attack has been observed in various plant species including common bean, it involves detachment of organs, such as flowers, fruits, leaves and stems

in response to certain signals produced by biotic stresses (Gulfishan et al., 2019). This process has been studied during *Botrytis cinerea* infection of lettuce (De Cremer et al., 2013) and *Arabidopsis* (Breeze et al., 2011).

Callus formation and a brown appearance were also observed. These responses may be part of the defense mechanism that G122 has acquired through its breeding history. There is evidence that plants employ various defense mechanisms against pathogen infection, such as callus formation. Under laboratory conditions different balances in auxin and cytokinin influence callus formation (Ikeuchi et al., 2013). Evidence suggests that down-regulating of auxins signaling is used by plants as a defense mechanism (Spaepen & Vanderleyden, 2011). However, the mechanisms underlying the formation of callus enhancing defense mechanisms needs to further be explored. The rust-colored appearance in the stems might be due to the prolonged stress caused by *Ss* and may also indicate the pathogen's ability to overcome existing sources of genetic resistance. Our research suggests that screening for resistance against *Ss* could benefit from including both quantitative and qualitative observations to accurately represent sources of genetic resistance when screening with *Ss* isolates.

After classifying the isolates according to the phenotypic traits analysed in our study (MCGs and aggressiveness), we observed interesting relationships between these traits. Isolates that displayed broad compatibility across MCGs (A25 and A29) displayed aggressive and mild aggressiveness respectively, which varied from intra-group responses. We suggest that this broad geographic compatibility with established MCGs might be related to genetic divergence of these isolates. While clonal populations are typically characterized by low genetic diversity, some studies, such as Abreu et al. (2022), have suggested that higher than expected genetic diversity can occur in such populations. However, further studies are needed to corroborate this. Additionally, there is potential for horizontal gene transfer (HGT) occurring within the context of heterokaryons. Potentially there is a genetic exchange in the hyphal zone where the contact of the isolates tested is occurring, leading to acquisition of genes associated with compatibility or virulence, which is enabling its ability to interact with a broader number of host plants and *Ss* genotypes, leading to a higher genetic diversity (Soanes & Richards, 2014).

With complete data of isolate pathogenicity and characteristics, more tailored approaches to resolve different research questions can be done. For example, the inclination to use isolates such as A25 and A29 might be suggested when the interest is to explore sources of genetic diversity and mechanisms underlying the plasticity of isolates to display compatibility with intransitive MCGs. Choosing aggressive isolates with mixed compatibility (A23), and distribution across MCGs classes (A32) might be more appealing when dealing with examining aggressiveness. These targeted approaches to isolate selection might enable the focus of efforts on fighting the most concerning outbreaks in terms of genetic diversity and aggressiveness in localized areas.

Finally, the phenotypic response of the isolates studied, are a result of cultural practices and the environmental conditions under which *Ss* isolates are producing white mold disease in common bean across regions.

Most of the isolates assigned to endemic groups were collected from common beans in AB, a region with increased fungicide utilization. Globally, the most utilized fungicides to control *Ss* globally include fungicides in classes like anilinopyrimidines, methyl benzimidazole carbamates (MBCs), demethylation inhibitors (DMIs), quinone outside inhibitors (Qols) and succinate dehydrogenase (SDHIs).These fungicides can induce mutation in *Ss* and therefore contribute to genetic diversity (O'Sullivan et al., 2021). As previously stated, we suggest that the isolates in endemic groups represent novel sources of genetic diversity, likely arising from mutations that lead to the emergence of new genotypes as an evolutionary adaptation to environmental pressures. The presence of a majority of mildly aggressive isolates within these endemic groups raises questions about whether *Ss* may evolve its aggressiveness levels in response environmental pressures over time, facilitating adaptation.

Our research suggests that studying the combination of phenotypic traits serves as a foundation for determining research directions in *Ss* populations studies. However, focusing *Ss* populations studies solely on phenotypic traits lacks information about the underlying genetic mechanisms driving these traits. We suggest that molecular studies will represent an ideal source to uncover the genetic basis of MCGs and aggressiveness. The dual-reproduction system in *Ss* (clonal and sexual) confers this fungal pathogen with genetic attributes that the sole study of phenotypic traits, such as MCGs, may not fully capture. This can mask the specific distinction between clonal

lineages and recombinant populations, leading to an incomplete understanding of the pathogen's population structure. Therefore, we recommend adopting holistic approaches that integrate both phenotypic and molecular data to achieve a deeper understanding of *Ss* complexities.

2.5 CONCLUSIONS

- Among isolates collected from closely situated sites, each isolate exhibited clear compatibility or incompatibility reactions in every pairing, reflecting the straightforward nature of their responses.
- Geographical proximity among samples in the interprovincial subset did not translate into clustering of samples within the same MCGs despite their geographical closeness. This might be due to different environmental and cultural practices.
- Current studies in phenotypic traits described the mycelial compatibility as another phenotypic marker to describe genetically compatible isolates within a population. However, there is not a standardized classification system to denote the potential dynamics occurring in this macroscopic test. In this study we are suggesting a classification system based on frequency and geographic dispersal of the isolates.
- It was observed that the majority of samples in our study displayed aggressive behaviour which confirms that *Ss* poses a threat to food production. The levels of aggressiveness among isolates represent the current scenario in *Ss* genotypes across three Canadian provinces as their collection was done in accordance with farmers reports of the presence of the isolates in their crops.
- The importance of performing studies that include more than one phenotypic trait to characterize *Ss*, allows taking steps ahead in areas where is most required like accurate selection of isolates for screening for resistance.
- Identifying and utilizing diverse genetic sources of genetic resistance is effective because it provides broader-spectrum resistance to a wider range of pathogen aggressiveness. This approach enhances the ability to combat diverse isolates, ensuring that resistance is stable and reliable under varying conditions. However, incorporation of genetic sources of resistance requires evaluation against prevalent regional isolates and is crucial to optimize resistance.

2.6. REFERENCES

Abreu, M. J. d., Leite, M. E., Ferreira, A. N., Pereira, F. A., & Souza, E. A. d. (2022). Resistance of common bean lines to *Sclerotinia sclerotiorum* isolates under different environmental conditions. . *Pesquisa Agropecuária Brasileira*, *57*. https://doi.org/ https://doi.org/10.1590/S1678-3921

Attanayake, R. N., Tennekoon, V., Johnson, D. A., Porter, L. D., del Río-Mendoza, L., Jiang, D., & Chen, W. (2014). Inferring outcrossing in the homothallic fungus Sclerotinia sclerotiorum using linkage disequilibrium decay. *Heredity*, *113*(4), 353-363. https://doi.org/10.1038/hdy.2014.37

Bleecker, A. B., & Patterson, S. E. (1997). Last exit: senescence, abscission, and meristem arrest in Arabidopsis. *The Plant Cell*, *9*(7), 1169-1179. https://doi.org/10.1105/tpc.9.7.1169

Breeze, E., Harrison, E., McHattie, S., Hughes, L., Hickman, R., Hill, C., Kiddle, S., Kim, Y.-s., Penfold, C. A., Jenkins, D., Zhang, C., Morris, K., Jenner, C., Jackson, S., Thomas, B., Tabrett, A., Legaie, R., Moore, J. D., Wild, D. L., . . . Buchanan-Wollaston, V. (2011). High-Resolution Temporal Profiling of Transcripts during Arabidopsis Leaf Senescence Reveals a Distinct Chronology of Processes and Regulation *The Plant Cell*, *23*(3), 873-894. https://doi.org/10.1105/tpc.111.083345

Buchwaldt, L., Garg, H., Puri, K. D., Durkin, J., Adam, J., Harrington, M., Liabeuf, D., Davies, A., Hegedus, D. D., Sharpe, A. G., & Gali, K. K. (2022). Sources of genomic diversity in the self-fertile plant pathogen, Sclerotinia sclerotiorum, and consequences for resistance breeding. *PLOS ONE*, *17*(2), e0262891. https://doi.org/10.1371/journal.pone.0262891

Canadian Sclerotinia Initiative. (2021). https://www.pulsebreeding.ca/research/canadian-sclerotinia-initiative

Chung, Y. S., Sass, M. E., & Nienhuis, J. (2008). Validation of RAPD Markers for White Mold Resistance in Two Snap Bean Populations Based on Field and Greenhouse Evaluations. *Crop Science*, *48*(6), 2265-2273. https://doi.org/https://doi.org/10.2135/cropsci2007.12.0689

Cubeta, M. A., Cody, B. R., Kohli, Y., & Kohn, L. M. (1997). Clonality in Sclerotinia sclerotiorum on Infected Cabbage in Eastern North Carolina. *Phytopathology®*, *87*(10), 1000-1004. https://doi.org/10.1094/phyto.1997.87.10.1000

De Cremer, K., Mathys, J., Vos, C., Froenicke, L., Michelmore, R. W., Cammue, B. P. A., & De Coninck, B. (2013). RNAseq-based transcriptome analysis of Lactuca sativa infected by the fungal necrotroph Botrytis cinerea. *Plant, Cell & Environment*, *36*(11), 1992-2007. https://doi.org/https://doi.org/10.1111/pce.12106

Denton-Giles, M., Derbyshire, M. C., Khentry, Y., Buchwaldt, L., & Kamphuis, L. G. (2018). Partial stem resistance in Brassica napus to highly aggressive and genetically diverse Sclerotinia sclerotiorum isolates from Australia. *Canadian Journal of Plant Pathology*, *40*(4), 551-561. https://doi.org/10.1080/07060661.2018.1516699

Derbyshire, M. C., & Denton-Giles, M. (2016). The control of sclerotinia stem rot on oilseed rape (Brassica napus): current practices and future opportunities. *Plant Pathology*, *65*(6), 859-877. https://doi.org/https://doi.org/10.1111/ppa.12517

Derbyshire, M. C., Denton-Giles, M., Hane, J. K., Chang, S., Mousavi-Derazmahalleh, M., Raffaele, S., Buchwaldt, L., & Kamphuis, L. G. (2019). A whole genome scan of SNP data suggests a lack of abundant hard selective sweeps in the genome of the broad host range plant pathogenic fungus Sclerotinia sclerotiorum. *PLOS ONE*, *14*(3), e0214201. https://doi.org/10.1371/journal.pone.0214201

FAO. (2024). Organic Agriculture. https://www.fao.org/organicag/oa-faq/oa-faq1/en/

Gerard, P., Peter, S., Darren, R., & Chris, G. (2011). The interaction of annual weed and white mold management systems for dry bean production in Canada. *Canadian Journal of Plant Science*, *91*(3), 587-598. https://doi.org/10.4141/cjps10127

Glass, N. L., & Kuldau, G. A. (1992). Mating type and vegetative incompatibility in filamentous ascomycetes. *Annu Rev Phytopathol*, *30*, 201-224. https://doi.org/10.1146/annurev.py.30.090192.001221

Gulfishan, M., Jahan, A., Bhat, T. A., & Sahab, D. (2019). Chapter 16 - Plant Senescence and Organ Abscission. In M. Sarwat & N. Tuteja (Eds.), *Senescence Signalling and Control in Plants* (pp. 255-272). Academic Press. https://doi.org/https://doi.org/10.1016/B978-0-12-813187-9.00016-0

Hambleton, S., Walker, C., & Kohn, L. M. (2002). Clonal lineages of Sclerotinia sclerotiorum previously known from other crops predominate in 1999-2000 samples from Ontario and Quebec soybean. *Canadian Journal of Plant Pathology*, *24*(3), 309-315. https://doi.org/10.1080/07060660209507014

Ikeuchi, M., Sugimoto, K., & Iwase, A. (2013). Plant callus: mechanisms of induction and repression. *Plant Cell*, *25*(9), 3159-3173. https://doi.org/10.1105/tpc.113.116053

Joelle, A., Cuomo, C. A., van Kan, J. A. L., Viaud, M., Benito, E. P., Couloux, A., Coutinho, P. M., de Vries, R. P., Dyer, P. S., Fillinger, S., Fournier, E., Gout, L., Hahn, M., Kohn, L., Lapalu, N., Plummer, K. M., Pradier, J.-M., Quévillon, E., Sharon, A., . . . Dickman, M. (2011). Genomic Analysis of the Necrotrophic Fungal Pathogens Sclerotinia sclerotiorum and Botrytis cinerea. *PLOS Genetics*, *7*(8), e1002230. https://doi.org/10.1371/journal.pgen.1002230

Jouzi, Z., Azadi, H., Taheri, F., Zarafshani, K., Gebrehiwot, K., Van Passel, S., & Lebailly, P. (2017). Organic Farming and Small-Scale Farmers: Main Opportunities and Challenges. *Ecological Economics*, *132*, 144-154. https://doi.org/https://doi.org/10.1016/j.ecolecon.2016.10.016

Kamvar, Z. N., Amaradasa, B. S., Jhala, R., McCoy, S., Steadman, J. R., & Everhart, S. E. (2017). Population structure and phenotypic variation ofSclerotinia sclerotiorumfrom dry bean (Phaseolus vulgaris) in the United States. *PeerJ*, *5*, e4152. https://doi.org/10.7717/peerj.4152

Kamvar, Z. N., & Everhart, S. E. (2019). Something in the agar does not compute: on the discriminatory power of mycelial compatibility in Sclerotinia sclerotiorum. *Tropical Plant Pathology*, *44*(1), 32-40. https://doi.org/10.1007/s40858-018-0263-8

Kohli, Y., Brunner, L. J., Yoell, H., Milgroom, M. G., Anderson, J. B., Morrall, R. A. A., & Kohn, L. M. (1995). Clonal dispersal and spatial mixing in populations of the plant pathogenic fungus, Sclerotinia sclerotiorum. *Molecular Ecology*, *4*(1), 69-77. https://doi.org/https://doi.org/10.1111/j.1365-294X.1995.tb00193.x

Kohli, Y., & Kohn, L. M. (1998). Random association among alleles in clonal populations of Sclerotinia sclerotiorum. *Fungal Genet Biol*, *23*(2), 139-149. https://doi.org/10.1006/fgbi.1997.1026

Kohn, L. M. (1995). The clonal dynamic in wild and agricultural plant–pathogen populations. *Canadian Journal of Botany*, *73*(S1), 1231-1240. https://doi.org/10.1139/b95-383

Kohn, L. M., Carbone, I., & Anderson, J. B. (1990). Mycelial interactions inSclerotinia sclerotiorum. *Experimental Mycology*, *14*(3), 255-267. https://doi.org/https://doi.org/10.1016/0147-5975(90)90023-M

Kohn, L. M., Stasovski, E., Carbone, I., Royer, J., & Anderson, J. B. (1991). Mycelial incompatibility and molecular markers identify genetic variability in field populations of

Sclerotinia sclerotiorum. Phytopathology, *81*, 480-485. https://doi.org/10.1094/Phyto-81-480.

Kolkman, J. M., & Kelly, J. D. (2000). An indirect test using oxalate to determine physiological resistance to white mold in common bean. *Crop Science*, *40*(1), 281-285. https://doi.org/https://doi.org/10.2135/cropsci2000.401281x

Kolkman, J. M., & Kelly, J. D. (2002). Agronomic Traits Affecting Resistance to White Mold in Common Bean. *Crop Science*, *42*(3). https://doi.org/10.2135/cropsci2002.6930

Kull, L. S., Pedersen, W. L., Palmquist, D., & Hartman, G. L. (2004). Mycelial Compatibility Grouping and Aggressiveness of Sclerotinia sclerotiorum. *Plant Dis*, *88*(4), 325-332. https://doi.org/10.1094/PDIS.2004.88.4.325

Leslie, J. F. (1993). Fungal vegetative compatibility. *Annu Rev Phytopathol*, *31*, 127-150. https://doi.org/10.1146/annurev.py.31.090193.001015

Liu, J., Meng, Q., Zhang, Y., Xiang, H., Li, Y., Shi, F., Ma, L., Liu, C., Liu, Y., Su, B., & Li, Z. (2018). Mycelial compatibility group and genetic variation of sunflower Sclerotinia sclerotiorum in Northeast China. *Physiological and Molecular Plant Pathology*, *102*, 185-192. https://doi.org/https://doi.org/10.1016/j.pmpp.2018.03.006

McDonald, B. A., & Linde, C. (2002). PATHOGEN POPULATION GENETICS, EVOLUTIONARY POTENTIAL, AND DURABLE RESISTANCE. *Annual Review of Phytopathology*, *40*(Volume 40, 2002), 349-379. https://doi.org/https://doi.org/10.1146/annurev.phyto.40.120501.101443

McDonald, M. R., & Boland, G. J. (2004). Forecasting diseases caused by Sclerotinia spp. in eastern Canada: fact or fiction? *Canadian Journal of Plant Pathology*, *26*(4), 480-488. https://doi.org/10.1080/07060660409507168

Michael, J. P., Lui, K. Y., Thomson, L. L., Lamichhane, A. R., & Bennett, S. J. (2020). Impact of Preconditioning Temperature and Duration Period on Carpogenic Germination of Diverse Sclerotinia sclerotiorum Populations in Southwestern Australia. *Plant Disease*, *105*(6), 1798-1805. https://doi.org/10.1094/PDIS-09-20-1957-RE

Miklas, P. N., Johnson, W. C., Delorme, R., & Gepts, P. (2001). QTL Conditioning Physiological Resistance and Avoidance to White Mold in Dry Bean. *Crop Science*, *41*(2), 309-315. https://doi.org/https://doi.org/10.2135/cropsci2001.412309x

Miklas, P. N., Kelly, J. D., Steadman, J. R., & McCoy, S. (2014). Registration of Pinto Bean Germplasm Line USPT-WM-12 with Partial White Mold Resistance. *Journal of Plant Registrations*, *8*(2), 183-186. https://doi.org/https://doi.org/10.3198/jpr2013.06.0034crg

Miklas, P. N., Porter, L. D., Kelly, J. D., & Myers, J. R. (2013). Characterization of white mold disease avoidance in common bean. *European Journal pf Plant Pathology*, *135*(3), 525-543. https://doi.org/10.1007/s10658-012-0153-8

O'Sullivan, C. A., Belt, K., & Thatcher, L. F. (2021). Tackling Control of a Cosmopolitan Phytopathogen: Sclerotinia. *Frontiers in Plant Science*, *12*. https://doi.org/https://doi.org/10.3389/fpls.2021.707509

Olsson, V., & Butenko, M. A. (2018). Abscission in plants. *Current Biology*, *28*(8), PR338-R339. https://doi.org/https://doi.org/10.1016/j.cub.2018.02.069

Otto-Hanson, L., Steadman, J. R., Higgins, R., & Eskridge, K. M. (2011). Variation in Sclerotinia sclerotiorum Bean Isolates from Multisite Resistance Screening Locations. *Plant Dis*, *95*(11), 1370-1377. https://doi.org/10.1094/PDIS-11-10-0865

Petzoldt, R., & Dickson, M. H. (1996). Straw test for resistance to white mold in beans. *Annu. Rpt. Bean Improv. Coop.*, *39*, 142-143.

Rather, R. A., Ahanger, F. A., Ahanger, S. A., Basu, U., Wani, M. A., Rashid, Z., Sofi, P. A., Singh, V., Javeed, K., Baazeem, A., Alotaibi, S. S., Wani, O. A., Khanday, J. A., Dar, S. A., & Mushtaq, M. (2022). Morpho-Cultural and Pathogenic Variability of Sclerotinia sclerotiorum Causing White Mold of Common Beans in Temperate Climate. *Journal of Fungi*, *8*(7).

Rieux, A., Soubeyrand, S., Bonnot, F., Klein, E. K., Ngando, J. E., Mehl, A., Ravigne, V., Carlier, J., & De Lapeyre De Bellaire, L. (2014). Long-Distance Wind-Dispersal of Spores in a Fungal Plant Pathogen: Estimation of Anisotropic Dispersal Kernels from an Extensive Field Experiment. *PLOS ONE*, *9*(8), e103225. https://doi.org/10.1371/journal.pone.0103225

Schafer, M. R., & Kohn, L. M. (2006). An optimized method for mycelial compatibility testing in Sclerotinia sclerotiorum. *Mycologia*, *98*(4), 593-597. https://doi.org/10.1080/15572536.2006.11832662

Schwartz, H. F., & Singh, S. P. (2013). Breeding Common Bean for Resistance to White Mold: A Review. *Crop Science*, *53*(5), 1832-1844. https://doi.org/https://doi.org/10.2135/cropsci2013.02.0081

Shlezinger, N., Minz, A., Gur, Y., Hatam, I., Dagdas, Y. F., Talbot, N. J., & Sharon, A. (2011). Anti-Apoptotic Machinery Protects the Necrotrophic Fungus Botrytis cinerea from Host-Induced Apoptotic-Like Cell Death during Plant Infection. *PLOS Pathogens*, *7*(8), e1002185. https://doi.org/10.1371/journal.ppat.1002185

Soanes, D., & Richards, T. A. (2014). Horizontal gene transfer in eukaryotic plant pathogens. *Annu Rev Phytopathol*, *52*, 583-614. https://doi.org/10.1146/annurev-phyto-102313-050127

Spaepen, S., & Vanderleyden, J. (2011). Auxin and plant-microbe interactions. *Cold Spring Harb Perspect Biol*, *3*(4). https://doi.org/10.1101/cshperspect.a001438

Taylor, A., Coventry, E., Jones, J. E., & Clarkson, J. P. (2014). Resistance to a highly aggressive isolate of Sclerotinia sclerotiorum in a Brassica napus diversity set. *Plant Pathology*, *64*(4), 932-940. https://doi.org/https://doi.org/10.1111/ppa.12327

Van der Plank, J. E. (1963). Plant Diseases: Epidemics and Control. *Academic Press*, 349. https://doi.org/https://doi.org/10.1016/C2013-0-11642-X

Westrick, N. M., Ranjan, A., Jain, S., Grau, C. R., Smith, D. L., & Kabbage, M. (2019). Gene regulation of Sclerotinia sclerotiorum during infection of Glycine max: on the road to pathogenesis. *BMC Genomics*, *20*(1), 157. https://doi.org/10.1186/s12864-019-5517-4

Willbur, J. F., Ding, S., Marks, M. E., Lucas, H., Grau, C. R., Groves, L., Kabbage, M., & Smith, D. L. (2017). Comprehensive Sclerotinia Stem Rot Screening of Soybean Germplasm Requires Multiple of *Sclerotinia sclerotiorum*. *The American Phytopathological Society*, *101*(2), 272-394. https://doi.org/https://doi.org/10.1094/pdis-07-16-1055-re

Willetts, H. J., Wong, J. A. L., & Kirst, G. D. (1980). The Biology of Sclerotinia sclerotiorum, S. trifoliorum, and S. minor with Emphasis on Specific Nomenclature. *Botanical Review*, *46*(2), 101-165. http://www.jstor.org/stable/4353966

Williams, B., Kabbage, M., Kim, H. J., Britt, R., & Dickman, M. B. (2011). Tipping the balance: Sclerotinia sclerotiorum secreted oxalic acid suppresses host defenses by manipulating the host redox environment. *PLoS Pathog*, *7*(6), e1002107. https://doi.org/10.1371/journal.ppat.1002107

Yatika, K. (1997). *Clonality in field populations of Sclerotinia sclerotiorum* University of Toronto]. TSpace. https://tspace.library.utoronto.ca/handle/1807/10764

Yu, Y., Cai, J., Ma, L., Huang, Z., Wang, Y., Fang, A., Yang, Y., Qing, L., & Bi, C. (2020). Population Structure and Aggressiveness of Sclerotinia sclerotiorum From Rapeseed (Brassica napus)

in Chongqing City. *Plant Disease*, *104*(4), 1201-1206. https://doi.org/10.1094/PDIS-07-19-1401-RE

BRIDGING TEXT BETWEEN CHAPTERS:

The study of *Sclerotinia sclerotiorum (Ss),* a fungal pathogen affecting various crops in Canada, requires a multi-faceted approach to understand its complex biology and epidemiology. In this thesis, two distinct yet complementary chapters provided a complementary view of *Ss* by integrating phenotypic characterization and advanced genotyping. The first chapter, "*Sclerotinia sclerotiorum* L. de Bary in Canada: Phenotyping Traits for Epidemiological Insights" offers a detailed analysis of Mycelial Compatibility Groups (MCGs) and aggressiveness variations among *Ss* isolates. The second chapter, "Characterization of Structural Variants in *Sclerotinia sclerotiorum* L. de Bary with Nanopore Whole-Genome Sequencing," delves into the genomic underpinnings of *Ss*, highlighting the usefulness of long-read sequencing technology to study structural variants and genomic diversity.

Linking Phenotypic and Genotypic Insights

The research in phenotypic analysis of *Ss* isolates, particularly focusing on MCGs and their aggressiveness, provides the bases to understanding the pathogen's behavior and its interaction with its hosts. As described in detailed in the first chapter, significant variations were revealed in aggressiveness levels among isolates. This variability is critical for breeding programs aimed at developing resistant cultivars and for tailoring management practices to specific pathogen populations.

Headed to the second chapter of the thesis, the identification of high genetic diversity within small populations, as highlighted in the chapter, centers the attention to the complexity of *Ss* reproduction dynamics. This finding aligns with the genomic insights presented in the second chapter, where long-read sequencing helped in identifying structural variants (SVs) that would otherwise be difficult to detect with short reads. The presence of SVs, especially in non-coding regions, suggests a potential mechanism of adaptation mediated by regulatory elements in the genome. Intergenic regions can play important roles in controlling gene expression, chromatin structure, and the special organization of the genome, all of which could contribute to the pathogen's adaptability. While the specific biological significance of these SVs remains to be fully elucidated, our research indicates that linking phenotypic traits with genomic data improves our understanding of how genetic variations contribute to the overall genomic architecture and provides insights into their influence on traits that support the pathogen's wide adaptability.

Overall, there are certain steps toward developing disease managements strategies where the first is deciphering the pathogens populations dynamics to which we are contributing by phenotyping and are further complementing with genotyping with long reads.

The advancements in genomic characterization, particularly through Nanopore whole-genome sequencing, offer insights into the genome architecture of *Ss* as well as the potential implications of genomic variation such as structural variants (SVs) that can be achieved with high-quality genome assemblies as we demonstrate in the second chapter of this work.

The identification of structural variants and their potential impact on gene regulation and pathogen adaptability provides new avenues for research. Understanding these genetic variations allows researchers to identify targets for genetic interventions and develop strategies to mitigate the impact of *Ss* on crop production.

The integration of phenotypic and genomic analyses in this thesis follows a standardized approach for *Ss* research, emphasizing the importance of a complementary study of traits in plant pathogens.

By bridging the gap between phenotypic characterization and advanced genomic techniques, this thesis contributes to a deeper understanding of *Ss* and its complex biology. The findings are relevant and contribute to continued research and innovation in the field of plant pathology, highlighting the potential for integrated approaches to address the challenges posed by phytopathogenic fungi such as *Ss*.

CHAPTER 3: CHARACTERIZATION OF STRUCTURAL VARIANTS IN *Sclerotinia sclerotiorum* L. de Bary WITH NANOPORE WHOLE-GENOME SEQUENCING.

Esquivel García, Laura[1]; Derbyshire, Mark[2]; Hoyos-Villegas, Valerio[1*]

[1]Pulse Breeding and Genetics Laboratory, Department of Plant Science, McGill University,

[2]Centre for Crop and Disease Management, Curtin University, Perth, Australia

*Corresponding author: valerio.hoyos-villegas@mcgill.ca

ABSTRACT

Sclerotinia sclerotiorum L. de Bary (*Ss*) is a phytopathogenic fungus that is widespread across the globe, posing significant challenges to crop production due to its cosmopolitan behavior. This pathogen's extensive genetic diversity and high adaptability enable it to infect a wide range of host plants, leading to severe yield losses. Understanding its genetic diversity is crucial for developing effective plant breeding strategies to enhance crop resistance. However, traditional methods for genomic analysis have been hindered by the lack of standardized genetic markers and the limitations of short-read sequencing technologies, which often fail to capture the full extent of genomic variation and structural variants (SVs).

The objective of this study was to employ advanced sequencing techniques to overcome these limitations and provide a more comprehensive understanding of the genomic architecture of *Ss*. Specifically, we aimed to generate high-quality genome assemblies of two *Ss* isolates to identify genomic variation due to large structural variants.

To achieve this, we employed Nanopore whole-genome sequencing with the single Molecule Real-Time (SMRT) portable sequencer Mk1C. By applying this approach, we identified large structural variants (SVs) (> 2.5 Kb) predominantly located in non-coding regions.

Our analysis involved a whole-genome alignment approach using the variant caller Sniffles2, which resulted in the identification of 106 SVs. These SVs were analyzed to understand their potential impact on the genome architecture of isolates. The findings from this study highlight the usefulness of long-read sequencing in identifying large SVs that contribute to genomic variation, particularly in intergenic regions. These intergenic regions are known to have significant roles in

regulating gene expression, contributing to chromatin remodelling, and influencing spatial genome organization, which shape phenotypic traits that enhance the pathogen's adaptation to diverse ecological niches. Our findings add to the growing body of research on the impacts of genomic variation mediated by regulatory elements, highlighting the importance of non-coding sequences in the evolution and adaptability of *Ss to* diverse niches offering valuable information for breeding programs aimed at developing resistant crop varieties.

Our study demonstrates that long-read sequencing technologies, such as those provided by Nanopore sequencing, are essential tools for accurately characterizing the genomic diversity of *Ss.*

The ability to generate high-quality genome assemblies and identify large structural variants provides a deeper understanding of the genomic architecture of the genomes analyzed heading towards an understanding of its influence in overall genomic architecture This knowledge is critical for the development of effective plant breeding strategies to combat widespread and economically damaging impacts of *Ss* on global crop production.

Key messages: Nanopore whole-genome sequencing enabled accurate genomic characterization of *Ss* genotypes with distinct pathogenic profiles. High-quality assemblies of *Ss* enables exploration of SVs with rapid variant caller approach. SVs shape the genomic architecture of *Sclerotinia sclerotiorum* and might influence pathogenicity.

3.1. INTRODUCTION.

Sclerotinia sclerotiorum L. de Bary *(Ss)* is a devastating pathogen, which can cause severe epidemics in some important staple crops (Shahoveisi et al., 2022). In pulse crops, such as common bean (*Phaseolus vulgaris* L.), *Ss* has been reported to be among the top pathogens threatening its production (Bag, 2000; Miklas et al., 2006; Robison et al., 2018). It causes white mold, a disease characterized by white, cottony mycelial growth on infected plants, from which the disease derives its name (Saharan & Mehta, 2008). *Ss* has been particularly challenging due to its broad host range and ability to cause significant yield losses (Derbyshire et al., 2022). While resistant cultivars are preferred for disease control, there is a lack of data characterizing genomic variation driving mechanisms involved in the expression of white mold disease in common bean. Genomic variation in the context of fungal pathogens refers to the genetic differences observed among individuals or strains of the same fungal species at the genomic level (Dolatabadian & Fernando, 2022). Understanding the genomic variation of *Ss* is crucial for several reasons. Genomic studies of other plant pathogens, such as *Magnaporthe grisea* (rice blast fungus) (Dean et al., 2005) and *Phytophtora infestans* (potato late blight), have shown that understanding genetic diversity within pathogen populations can reveal mechanisms of pathogenicity, adaptation, and resistance evolution (Dean et al., 2005; Haas et al., 2009). These insights are vital for developing durable disease management strategies and resistant crop varieties.

Genomic variation in fungal pathogens encompasses a spectrum of genetic changes, ranging from single nucleotide variants (SNVs) to larger structural variants (SVs), such as insertions, deletions, and translocations (Feuk et al., 2006). In the past, SVs were believed to comprise 1000 base pairs. However, with the incorporation of novel sequencing techniques, the definition has been shaped and now recognizes SVs as spanning to genomic variation over 50 base pairs (Mahmoud et al., 2019). Traditionally, the study of genomic variation has placed more emphasis on single nucleotide variants (SNVs), offering valuable insights into the genetic makeup of several organisms. However, the advent of novel sequencing technologies has brought increasing attention to SVs due to their potential impact on some important fitness traits such as pathogenicity (Wold et al., 2021).

SVs can alter gene expression, influence virulence factors, and contribute to the pathogens' ability to overcome host defences (Hartmann, 2022). In the broader context of plant pathogens' genomes, SVs have shown that they can influence the pathogen's adaptation to plant defense mechanisms. For example, Zhou et al. (2022) demonstrated that different sources of genetic diversity, including SVs, play a crucial role in heritability and influence adaptation outcomes. Furthermore, Durak and Ozkilinc (2023) emphasized how differences in SVs dynamics between two *Molininia* species contributed to genome evolution and pathogenicity, with each species exhibiting unique SVs patterns correlating with their specific ecological niches and host interactions.

Recent studies reinforce the importance of SVs in pathogen evolution. Research on *Zymoseptoria tritici* by Amezrou et al. (2024) that SVs contribute to the emergence of virulent strains by enabling adaptation to host defenses and environmental changes. Similarly, in the tomato pathogen *Cladosporium fulvum*, SVs have been linked to variations in effector gene clusters, preventing recognition by tomato R-gene receptors and impacting the plant's ability to fend off infections (Zaccaron & Stergiopoulos, 2024). Despite these advancements, the study of SNVs has traditionally dominated genomic research, often overshadowing the equally critical role of structural variants.

This focus on SNVs has primarily relied on the use of high-throughput sequencing technologies that generate short reads, typically of about 150-300 bp in length. However, the use of short reads for SNV detection can result in bias. Short reads cannot be used to assemble or call variants in repetitive regions due to repeats being shorter than read length resulting in the need for long reads to improve the resolution of repetitive regions. Repetitive regions are often most important for rapid adaptation and coevolution with the host (Mahmoud et al., 2019; Potgieter et al., 2020). Given the critical role of structural variants in plant-pathogen interactions and the limitation of traditional sequencing methods, it is essential to explore these variants further.

This study highlights the importance of employing long-read sequencing techniques for comprehensive genomic analysis, providing valuable insight into the genetic diversity of *Ss* isolates. By elucidating genomic differences influencing genomic structure, this research was conducted to achieve the following objectives: a) Generate long reads with portable Mk1C sequencer, b) Generate High-Quality Genome Assemblies of representative *Ss* isolates, c) Build a

bioinformatic pipeline to identify structural variants, and d) Describe unique signatures of genomic architecture conferred by SVs in two *Ss* isolates.

3.2. MATERIALS AND METHODS

3.2.1. Methodology

3.2.1.1. Fungal material.

The fungal material employed in this study consisted of *Ss* isolates, from infected soybean (*Glycine max*) and common bean (*Phaseolus vulgaris* L.) field samples. Collection of isolates was done in Fall 2021. Isolates were previously phenotyped for Mycelial Compatibility Group (MCG) by challenging isolates against each other to establish mycelial compatibility, and aggressiveness through *in planta* inoculation of isolates into two common bean germplasms with different susceptibility levels (Susceptible – Beryl, and Moderately Resistant – G122) as indicated in Chapter 2. Following phenotyping for aggressiveness and MCGs, two samples were selected based on their sequencing performance, specifically considering the genome coverage achieved (>20X). Isolate information is shown in Table 2.

Table 2 displays the phenotypic characteristics of two *Ss* isolates, selected as models for investigating genomic architecture shaped by SVs.

Table 2. Sample identification, geographical, temporal and phenotypic information of *Sclerotinia sclerotiorum* isolates used for SV identification.

Sample ID	Province	Year of collection	Mycelial Compatibility Group	Aggressiveness designation
O7	Ontario	2021	6	Aggressive
Q12	Quebec	2021	1	Aggressive

3.2.1.2. Mycelial growth.

Ss inoculum for this study was started from previously disinfected sclerotia structures that were stored at 4°C. Each isolate was first cultured onto Potato Dextrose Agar, (PDA; BD Difco TM) in Petri dishes (100 x 15 mm) for three days. Active mycelia from the leading edge of colonies were transferred to Petri dishes (100 x 15 mm) containing half-strength liquid potato dextrose medium (P6685 – Sigma) for 5 days and placed in the incubator in the dark and a temperature of 25°C. Cultures were filtered with sterile cheesecloth, and further rinsed with double distilled water to remove excess media. The resulting tissue was then chopped into small chunks that were immediately transferred to sterile 2 mL microcentrifuge tubes in proportions of 1 g approximately, they were then stored at -80°C until DNA extraction.

3.2.1.3. High Molecular Weight gDNA extraction.

Three stainless ball bearing beads Cal. 4.5 mm (Artclaim) were added to each 2 mL microcentrifuge tubes containing the sample. Samples were then dipped into Liquid Nitrogen. Tissue was ground at a rate of 1400 per 30 s at the HG-600 Geno/Grinder® 2010, this step was repeated three times or until a fine powder was obtained with subsequent dipping in liquid Nitrogen as each grinding cycle was completed. High Molecular Weight gDNA was then extracted with the CTAB-based protocol suggested by Xin and Chen (2012).

3.2.1.4. Determination of DNA purity and metrics.

For each extraction, DNA yield was quantified on a Qubit™ 3 Fluorometer (Thermo Fisher Scientific), using the dsDNA HS (high sensitivity, 0.2 to 100 ng) Assay kit (Thermo Fisher Scientific) according to the Manufacturer´s protocols. A sample of 1 µl was added to 199 µl of a Qubit working solution. The purity of the extracted nucleic acids was assessed with the A260/280 and A260/230 absorbance ratios using a Nanodrop™ spectrophotometer (Thermo Scientific), aiming for a purity of no less than 1.8 for the OD 260/280 ratio and 2.0 to 2.2 for the OD 260/230 ratio, as recommended by Nanopore Technologies. The DNA fragment size distribution was assessed by electrophoresis (120V for 40 min) of genomic DNA on a 1% (w/v) agarose gel followed by staining with Sybr safe (brand) and UV light visualization.

3.2.1.5. Optimization with light DNA shearing

Genomic DNA (gDNA) was light sheared to a target size of 8Kb fragments using g-TUBES SKU: COV-520079 (DMark Biosciences). This process was performed according to the tailored Nanopore protocol "Shearing genomic DNA using the Covaris g-TUBE™" published at the Documentation section in the Nanopore community (https://community.nanoporetech.com/extraction_methods/covaris-g-tube), which suggest that input gDNA material of about 100-1000 ng diluted in 49 µL fragments in the same way than what the g-TUBE^{TM} official documentation suggests. The settings used to perform fragmentation to our desired target DNA fragment size were done considering an input of up to =< 4 µg gDNA of. It was centrifuged for 60 s at 7,200 RPM. The decision to add light shearing for sample processing was made as a part of an optimization process, where it was observed that a high abundance of gDNA molecules of desirable size optimized the pore occupancy and minimized the pore blockage. Including light shearing with g-TUBES generally yielded adequate genome coverage (>20X) and N50 to produce the genome assemblies. Sheared gDNA was then quality checked (QC'd) using gel electrophoresis to assess for fragment size distribution, purity, and to confirm successful shearing of samples post g-TUBE utilization. Statistical data, including genome coverage for both samples and N50 values are displayed in Chart 3.

3.2.1.6. Library Preparation and Sequencing

Library preparation was performed by using Nanopore's ligation sequencing kit specified for dSDNA (gDNA) - native barcoding (SQK - NBD112.96) according to manufacturer's instructions with slight modifications, consisting of increasing input gDNA to 500 ng = (96 fmol). End repair, dA-tailing, and adapter ligation were performed according to the manufacturer's instructions. The prepared libraries were then loaded into an Mk1C Nanopore device, using R.9.4.1 Flow cells (FLO-MIN 106D). For reference, the Mk1C device used for sequencing operated with the following software: MinKNOW (v23.04.5), Bream (v7.5.9), Config (v5.5.13), Guppy (v6.5.7), MinKNOW Core (v5.5.3). Sequencing was set to run for up to 24 hours. One flowcell washing step was performed to improve the flowcell pore occupancy and pore availability throughout the sequencing with Flow Cell Wash kit (EXP-WSH004) and obtain more sequence data. The settings for whole genome sequencing were chosen with a 200 bp minimum read.

3.2.1.7. Nanopore Data Analysis

The reference genome of isolate '1980 UF-70' (NCBI Bioproject ID: PRNJA348385) https://www.ncbi.nlm.nih.gov/bioproject/PRJNA348385/ was included for scaffolding, mapping, completeness assessment and variant calling. The complete bioinformatic pipeline is displayed in Figure 12.

Nanopore data analysis involved a multi-step approach described as follows:

1. Fast5 files containing the raw electrical signals from Nanopore sequencer were converted to pod5 files to facilitate the overall downstream analysis, conversion was done with the Python package POD5 v0.2.4 (https://github.com/nanoporetech/pod5-file-format).
2. Raw reads in pod5 format were converted into DNA sequences by basecalling with Guppy v.6.5.7 v6.5.7 (Guppy_v6.5.7), using the dna_r9.4.1_e8.1 super accurate (SUP) model, for accurate conversion. Options for barcode trimming and read splitting were enabled alongside basecalling.
3. Following basecalling, clean reads underwent quality control with Nanoplot v1.42.0 to generate summary statistics (De Coster & Rademakers, 2023) https://github.com/wdecoster/NanoPlot.
4. Clean reads were assembled into contiguous sequences with Flye v2.9.3 producing draft assemblies (Kolmogorov et al., 2019) https://github.com/fenderglass/Flye
5. Draft assemblies were then self-polished with Medaka v1.11.3 & v1.8.1 (https://github.com/nanoporetech/medaka).
6. RagTag software v.2.26 was used with settings for improving the assemblies and scaffold the genomes, utilizing the reference genome of isolate '1980 UF-70' (NCBI Bioproject ID: PRNJA348385) (Alonge et al., 2022; Alonge et al., 2019) (https://github.com/malonge/RagTag).
7. The improved and scaffolded assemblies were then assessed for completeness and quality by benchmarking universal single-copy orthologs (BUSCO) v.5.5.0 analysis (Manni et al., 2021; Simão et al., 2015).

3.2.1.8. Bioinformatics analysis for structural variant calling.

Aligned sequenced reads from *Ss* isolates O7 and Q12 were aligned to the reference genome strain 1980 UF-70 with Sniffles2 v.2.2 (Smolka et al., 2024) to identify structural variants. Sniffles2 v.2.2. was used in its population mode, which operates following a two-step process: 1) SV candidates were identified for each individual isolate. This involved aligning the reads from each sample to the reference genome and then generating a .snf file for each sample, 2) individual .snf files were combined for multi-sample SV calling. This approach allowed for the identification of SVs among different isolates (https://github.com/fritzsedlazeck/Sniffles)

Low-quality SVs were removed and only those with quality values n > 5 were retained. Finally, the Ensembl Variant Effect Predictor (VEP) tool was utilised to determine the effect of the variants found (McLaren et al., 2016) https://useast.ensembl.org/info/docs/tools/vep/index.html. Geneious software v2023.2.1 (https://www.geneious.com) was used to corroborate the results provided by VEP. Annotations from GenBank under Bioproject number PRJNA348385 were downloaded to enable the comparison of the VCF file containing the SVs of both genomes.

Individual inspection of each SV was performed with Geneious software v2023.2.1 Additionally, their protein domains were cross-referenced with Interpro (https://www.uniprot.org/help/uniparc) and displayed in Appendix G and Appendix H.

The complete bioinformatic pipeline is displayed in Figure 13.

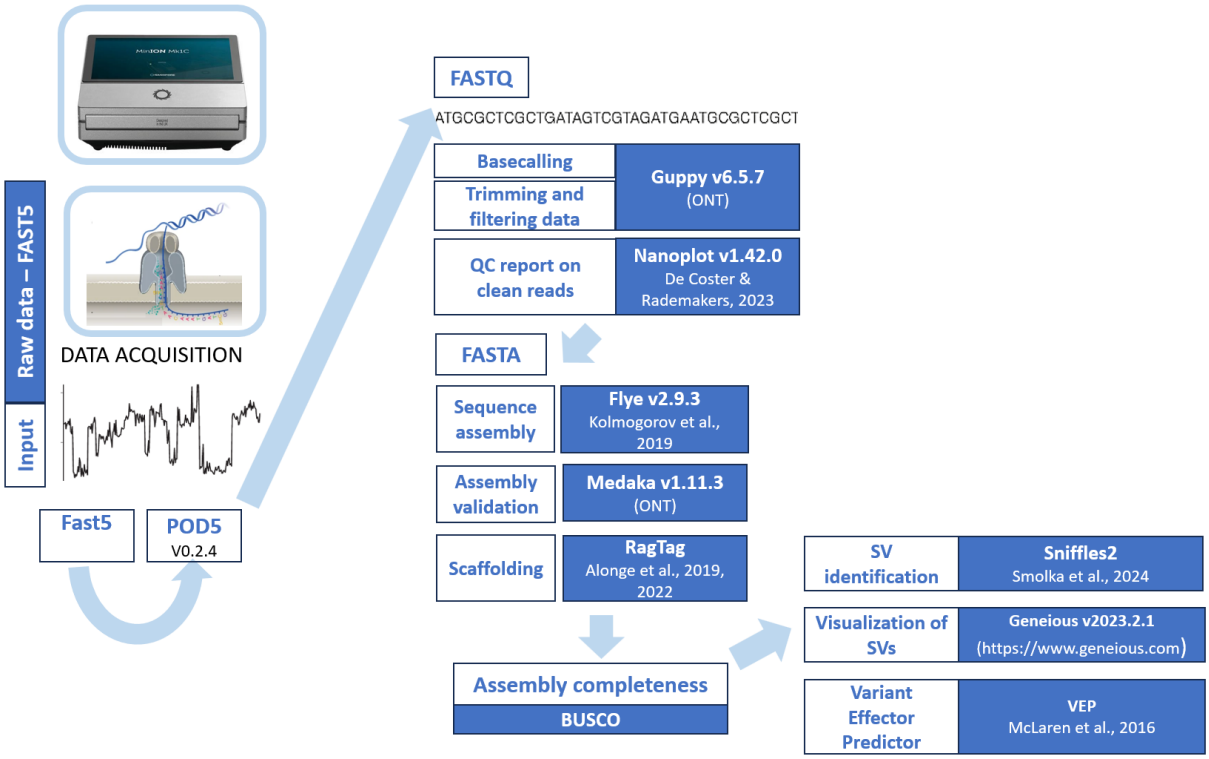

Figure 12. Bioinformatic pipeline to generate high-quality assemblies and structural variant identification with long read sequencing data in two *Sclerotinia sclerotiorum* genomes

All bioinformatics analyses were performed on the following computing platforms:

- Pawsey Supercomputing Research Centre. 2023. Setonix Supercomputer. Perth, Western Australia. https://doi.org/10.48569/18sb-8s43
- Pawsey Supercomputing Research Centre. 2023. Nimbus Research Cloud. Perth, Western Australia. https://doi.org/10.48569/v0j3-qd51
- Cedar cluster of the Digital Research Alliance of Canada (https://alliancecan.ca/en).

3.3. RESULTS

3.3.1. Overview of sequencing data with Nanopore reads

Whole Genome Sequencing (WGS) using long reads from Oxford Nanopore Technologies (ONT) was conducted on two *Ss* isolates: Isolate O7 (MCG6, Aggressive) and Q12 (MCG1, Aggressive). These isolates were selected based on genome coverage and were previously phenotyped for MCG and aggressiveness as described in Chapter 2.

Nanopore Sequencing generated 1,021.36 Mb and 965.69 Mb of raw sequencing data for Isolate O7 and Q12, respectively. After base-calling, filtering, and adapter trimming, 982.46 Mb and 925.71 Mb of clean data were retained with mean read lengths of 1,708.7 bp and 1,280.6 bp, respectively. The analysis revealed Fragment N50 values of 1,876,650 bp and 1,087,223 bp, with 78 and 133 contigs for the two isolates, indicating high contiguity in the assembled genomes.

In terms of sequencing depth, for isolate O7 an average genome coverage of 24.56x was achieved, covering 98.3% of the reference genome. Similarly, isolate Q12 exhibited an average genome coverage of 23.14x, covering 98.8% of the reference genome (Derbyshire et al., 2017).

Both genomes sequenced displayed similar assembly size to the previously reported complete *Ss* genome reported by Derbyshire et al. (2017), (38.80Mb), with approximately 38.7 to 38.50 Mb for isolate O7 and isolate Q12 respectively.

Table 3. Summary of *Sclerotinia sclerotiorum* genome assemblies and comparison with reference genome strain 1980 UF-70

Genome features	O7	Q12	1980 UF-70
Sequencing Platform	ONT	ONT	PacBio
Coverage (x)	24.56	23.14	36
Assembly size	38,731,900	38,531,848	38,806,497
GC content (%)	41.6	41.6	41.6
N50 length (bp)	1,876,650	1,087,223	2,387,400
BUSCO completeness (%)	98.3	98.8	97.78
Number of contigs	78	133	17
References	This study	This study	Derbyshire et al., 2017.

Table 3 presents summary statistics of the isolates analyzed in our study, along with the corresponding values obtained from the latest reference genome of strain 1980 UF-70 reported by (Derbyshire et al., 2017), which served as the basis for comparison in our analysis.

3.3.2. Structural Variants

3.3.2.1. Types of SVs identified

After conducting SV calling in two *Ss* genomes with Sniffles2, results indicated the predominant presence of insertion type structural variants. When delving into the specifics, our analysis revealed some disparities between isolate O7 and Q12.

3.3.2.2. Frequency and size range of SVs.

Isolate O7 showed a total of 91 insertions while isolate Q12 slightly fewer with 85 insertions. The SV calling, revealed a total of 106 SVs. Within this mosaic, 70 insertions were common to both genotypes. Further exploration revealed 21 unique SVs in isolate O7 and 15 in isolate Q12.

Delving deeper into the nature of these variants, we found that insertions exhibited an important diversity in length, ranging from 2.5 Kb to over 5 Kb, with half exceeding the latter threshold. Interestingly, SVs were dispersed across all 16 chromosomes.

3.2.2.3. Distribution of Structural Variants across the genome.

Our examination extended to individual chromosomes, unveiling variability in SV distribution. Chromosome 15 was an SV hotspot with n=12 shared and n=3 unique SVs in each genotype. Despite the prominence of shared SVs, Chromosome 15 stood out in displaying the highest count of SVs per genotype, n=5 for isolate O7 and n=5 for isolate Q12. Chromosome 12 exhibited a different profile among the 16 chromosomes displaying the chromosome with the least number of SVs n=1 shared/conserved isolate genomic location 1,768,205 bp; length 6,074 bp. Moreover, our analysis showed that SVs occurred in the same genomic location but differed in length. Table 4, describes the details of unique SVs with varying sizes:

Table 4. Structural Variants identified at the same genomic positions in two *Sclerotinia sclerotiorum* genomes, exhibiting variability in size length.

Chromosome number	**Position of Structural Variant (SV) (bp)**	**Size of unique SV (bp)**		**Total reduction (R); or increase (I) in size**
		Isolate O7	**Isolate Q12**	
1	2,503,508	4,925	3,561	R = 1,364 bp
2	2,740,295	5,888	4,201	R = 1,687 bp
2	3,048,966	6,302	5,080	R = 1,222 bp
7	1,385,843	5,854	4,549	R = 1,305 bp
8	1,887,397	2,954	9,056	I = 6,102 bp
15	1,705,938	13,024	8,651	R = 4,373 bp

We observed that in general unique SVs were variations in size but located in the same genomic position and tend to be shorter in isolate Q12. However, exceptions to this trend were observed in Chromosome 8, where the SV size in the isolate Q12 was larger than in isolate Q12.

To visually illustrate the genomic locations of the SVs found, we have included a detailed diagram below (Figure 14).

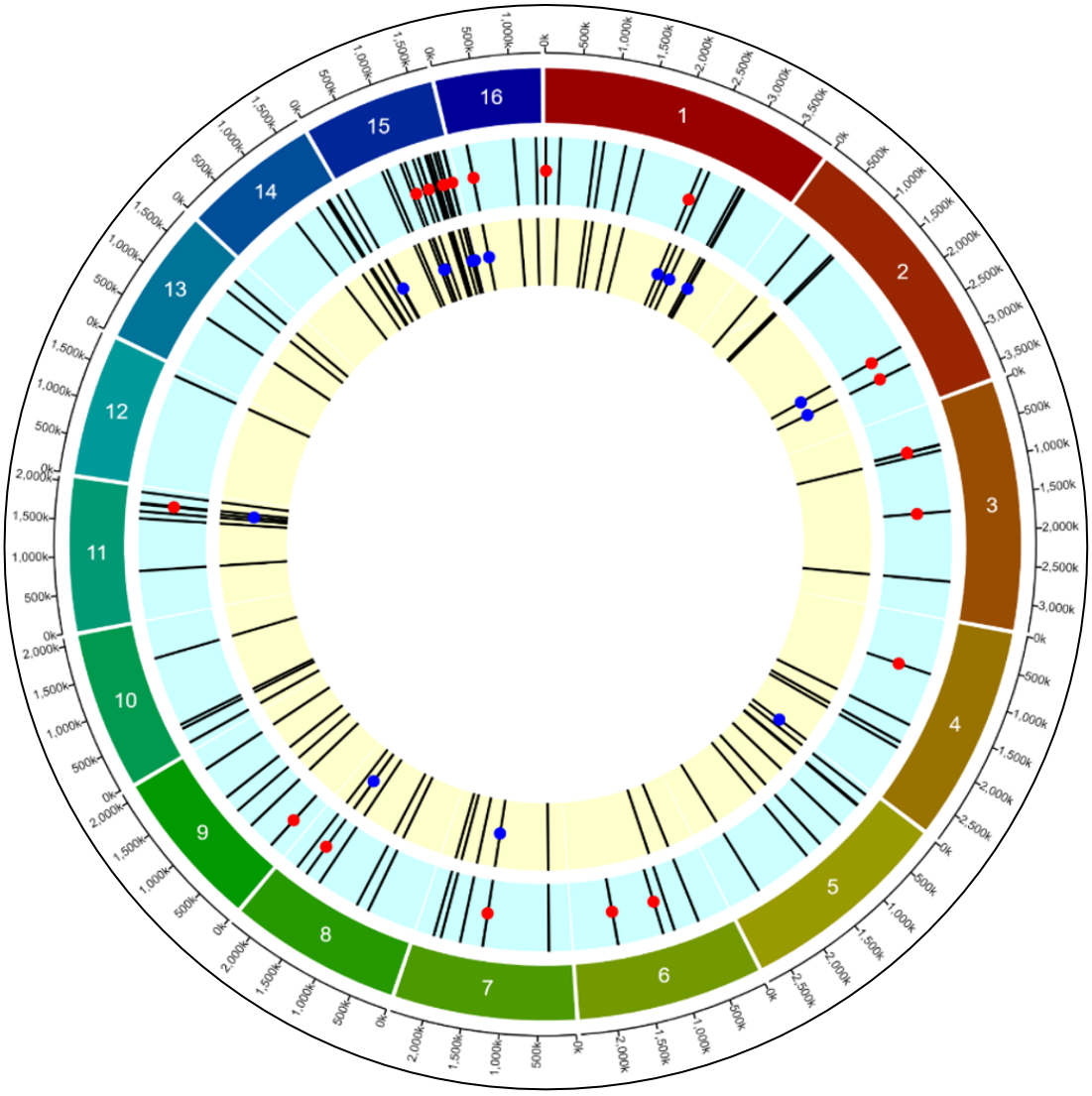

Figure 13. Circular plot depicting the genomic location of structural variants (SVs), identified by Sniffles2 across two *Sclerotinia sclerotiorum* genomes. The outermost circular sequence represents the '1980 UF-70' reference genome, with the 16 chromosomes color-coded to illustrate the genomic architecture of *Sclerotinia sclerotiorum*. The middle circular sequence corresponds to the genome of isolate O7, while the innermost sequence represents isolate Q12. Dark lines denote SVs insertions. Red colored circles highlight unique SVs specific to isolate O7, while blue-colored circles correspond to isolate Q12.

3.2.2.4. Variant Effect Prediction.

Variant effect prediction analysis performed in Ensembl revealed that 105 of SVs representing 99% of the total count were located in intergenic regions (IGRs) while only 1 SV (1%) was found overlapping a gene.

Since our interest was to describe the differences between genomic information from the two isolates, a deeper examination was conducted into unique SVs to each genotype.

Manual recording of neighboring genes in IGRs where SVs were found was done for reference (Table 5 and 6). This manual identification gave insights into the genes in proximity to each occurring SV and their genomic distance to them.

Individual visualization of each SV led to confirmation of their respective location in intergenic regions, except for SV on Chromosome 4 in isolate O7, where an SV of 2,619 bp in size was located at position 859,107 bp, overlapping with gene sscle_04g034550. This gene has a corresponding transcript ID APA08684 and is cross-referenced in UniParC as UPI0008DB91BC encoding a DUF676 domain-containing protein, which is implicated in lipid metabolic processes.

Overall, occurrence of unique SVs in isolate O7 was observed as follows: 7 SVs (33%) were under 5 Kb in size, 13 SVs (62%) were over 5 Kb, and 1 SV (5%) overlapped with a gene. In contrast,isolate Q12 exhibited 5 SVs (45%) under 5 Kb and 6 SVs (55%) over 5 Kb, with no SVs overlapping any genes.

Table 5. Summary of unique Structural Variants in *Sclerotinia sclerotiorum* isolate O7.

Chromosome	End (bp)	SV size (bp)	Gene(s) in hotspot	
1	13,362	5,363		sscle_01g000060
1	2,503,508	4,925	sscle_01g007290	sscle_01g0007300
2	2,740,295	5,888	sscle_02g019610	sscle_011810
2	3,048,966	6,302	sscle_02g020510	sscle_02g020520
3	639,862	6,301	sscle_03g024140	sscle_03g024150
3	647,229	5,303	sscle_03g024150	sscle_03g024160
3	1,692,051	6,025	sscle_03g027280	sscle_03g027290
4	859,107	2,619	sscle_04g034550 (in gene)	
6	1,077,780	5,752	sscle_06g051490	sscle_06g051500
6	1,801,698	5,725	sscle_06g053550	sscle_06g053560
6	1,802,888	4,505	sscle_06g053550	sscle_06g053560
7	1,385,843	5,854	sscle_07g059030	sscle_07g059040
8	1,887,397	2,954	sscle_08g067510	sscle_08g067520
9	242,070	6,679	sscle_09g069200	sscle_09g069210
11	1,798,365	5,289	sscle_11g085960	sscle_11g085970
15	1,066,586	4,024	sscle_15g105250	sscle_15g105260
15	1,291,052	11,810	sscle_15g105870	sscle_15g105880
15	1,545,048	3,739	sscle_15g106640	sscle_15g106650
15	1,558,203	4,972	sscle_15g106680	sscle_15g106690
15	1,705,938	13,024	sscle_15g107120	sscle_15g107130
16	253,340	9,419	sscle_16g108040	sscle_16g108050

Table 6. Summary of unique Structural Variants in *Sclerotinia sclerotiorum* isolate Q12.

Chromosome	End (bp)	SV size (bp)	Gene(s) in hotspot	
1	2,503,508	3,561	sscle_01g007290	sscle_01g007300
1	2,782,279	5,458	sscle_01g008110	sscle_01g008120
1	3,225,096	5,289	sscle_01g009420	sscle_01g009430
2	2,740,295	4,201	sscle_02g019610	sscle_011810
2	3,048,966	5,080	sscle_02g020510	sscle_02g020520
4	2,869,111	3,644	sscle_04g040280	
7	1,385,860	4,549	sscle_07g059030	sscle_07g059040
8	1,887,393	9,056	sscle_08g067510	sscle_08g067520
11	1,748,257	5,814	sscle_11g085800	sscle_012570
15	85,462	2,726	sscle_15g102500	sscle_15g102510
15	1,066,586	5,219	sscle_15g105250	sscle_15g105260
15	1,086,292	7,125	sscle_15g105290	sscle_15g105300
15	1,705,938	8,651	sscle_15g107120	sscle_15g107130
15	1,763,214	5,536	sscle_15g107310	
16	253,340	6,103	sscle_16g108040	sscle_16g108050

Table 4 and 5 summarize the SVs unique to each genome. SVs were characterized by a diverse mix of sizes ranging from 2.5 to > 5 Kb. Some of the SVs found are located in the same genomic location. For example, in Chromosome 15 SVs located at 1,705,938 bp, and the size of each SV is 13,024 bp and 8,651 bp for isolate O7 and isolate Q12, respectively.

3.4. DISCUSSION

Our study delved into the genomic landscape of two *Ss* isolates collected in Canada, uncovering SVs distributed across the genome. The identification of SVs was possible by generating in-house whole-genome sequencing reads with the portable Nanopore device Mk1C and producing high-quality assemblies of two *Sclerotinia sclerotiorum* isolates.

Regarding the creation of genome assemblies of *Ss* genomes in our study, we reported the construction of assemblies with high contiguity utilizing bioinformatics tools tailored for long reads. Our findings align with previous studies demonstrating the efficacy of long-read sequencing technologies in generating high-quality genome assemblies for *Ss.* For instance, the last complete genome of *Ss*, reported by Derbyshire et al. (2017), was also generated with long reads from PacBio, demonstrating the advantages of long reads in recovering gaps in the *Ss* genome. Regarding assembly size, our results are consistent with previous reports of the complete genome size (~38.80 Mb) (Amselem et al., 2011; Derbyshire et al., 2017). Both isolate O7 and Q12 exhibited comparable sizes (~38.70; ~38.50), indicating a high degree of conservation in genome size among different isolates. This observation aligns with the overall genomic stability observed in this pathogen across various studies (Amselem et al., 2011; Derbyshire et al., 2017; Zhang et al., 2021).

While our research yielded assemblies of good quality, they revealed notable discrepancies in contig numbers compared to the reference genome, which can be attributed to the lower genome coverage achieved in our samples. For instance, a study conducted by researchers in China reported a genome coverage of 166x, resulting in 28 contigs (Zhang et al., 2021). The reference genome on the other hand was assembled with 36x genome coverage and displayed 17 contigs, nearly the total number of Chromosomes in *Ss* (n=16) (Derbyshire et al., 2017). In contrast, our samples with 24.56x and 23.14x coverage resulted in 78 and 133 contigs, respectively. This aligns with the observation that high coverage and longer reads typically results in fewer contigs, indicating more complete and contiguous assemblies (Hotaling et al., 2023)

Additionally, it is crucial to acknowledge that the observed discrepancies may also stem from differences in the sequencing technologies utilised, each with its own unique constraints and limitations (error rate, chemistries, optimization methods etc.) (Amarasinghe et al., 2020)

Despite the noted discrepancy in contig numbers our assemblies remain a valuable resource for deriving genomic insights with reliability, establishing a foundation for further optimization. It is crucial to recognize that the assessment of assemblies should extend beyond their continuity encompassing their structural correctness (Howe et al., 2021).

Moreover, our research highlights the utility of long reads in constructing pipelines for identifying SVs that may be overlooked when using short reads. Long reads facilitate some of the most reliable approaches to detecting genomic variation, particularly through whole-genome assembly. Additionally, this study focused on identifying unique SVs with the potential of shaping the genomic architecture of two *Ss* isolates.

After obtaining high-quality genome assemblies through a pipeline for long-nanopore reads, and performing SV calling with Sniffles2, our results revealed the presence of SVs within the genomes analyzed. The genotypes shared 70 SVs, while 21 were unique to isolate O7 and 15 SVs were unique to isolate Q12. Most SVs were located in IGRs, except for one SV on Chromosome 4 of isolate O7, which overlaps with the gene sscle_04g034550, encoding a DUF676 domain-containing protein which is involved in lipid metabolic processes, a crucial pathway in cellular homeostasis and pathogen-host interactions (Derbyshire et al., 2017).

The fact that most of the SVs are located in IGRs raises questions about their potential regulatory roles, such as influencing the expression of neighboring genes. Although SVs might be considered neutral, their proximity to genes could impact the expression of nearby genes, chromatin structure, or even long-range interactions between regulatory elements and coding regions, however, the limited number of genomes analyzed also limits our ability to draw conclusions as per which of these genomic variations are genotype-specific, or population-specific.

Therefore, we limit our observations to their influence in genomic architecture as per how the SVs found in this study shape the differences in genome architecture between both genomes. Additionally, both genomes were previously characterized and were described to belong to a genetically diverse population, as indicated by the high number of established MCGs found in Chapter 2. Since both isolates were selected based on their genome coverage and it was determined that they belonged to different MCG it was suggested that this might indicate signatures of genetically distinct genomes as suggested by Kohn et al. (1991) and more recently by Liu et al. (2018). Our results on SV identification further supported this reasoning by the differences in the

genomic architecture in the form of distinct SVs spread throughout the genome in each analyzed genotype. The observation of differences in the number of unique SVs between the isolates underscore the dynamic nature of genomic variation within this fungal species (Gupta et al., 2022).

The unique structural variants found in each isolate are designated as accessories because they are not present in both individuals. In some cases, particular accessory segments are important for virulence (Eschenbrenner et al., 2020), they may result from mutations, insertions, deletions, or other structural changes occurring independently in each genotype over time (Hartmann, 2022; Langner et al., 2021). They may also be associated with adaptive traits or environmental pressures unique to each genotype, contributing to differences in host interactions, geographic distribution, or environmental niches (Badet et al., 2021)

Understanding the genomic nature of the location of SVs is crucial for disease management. In recent studies by Depotter and Doehlemann (2020) the potential of conserved SVs residing in core genomic regions was considered, proposing that they may hold indispensable virulence functions. In that sense when thinking of conserved SVs and plant breeding, the focus must be on targeting resistance genes that directly target conserved genomic regions resulting from a variety of adaptation pressures.

In our study, despite the limited number of samples, it is possible to suggest that some of the observed distinct accessory SVs may correspond to accessory “compartments”, a concept described by Möller and Stukenbrock (2017). These compartments are thought to arise from large-scale structural rearrangements spanning hundreds of kilobases and may harbor virulence determinants. It is worth noting that repeat-rich genomic regions in plant pathogens are often hotspots for structural variations, copy-number variations, or sequence polymorphisms. These dynamic compartments, previously referred to as fast-evolving regions, are subject to mutation accumulation due to relaxed selection pressure, as outlined by Frantzeskakis et al. (2019).

At a broad genomic level, SVs might be balanced or unbalanced in nature. This designation is dependent on the ability of SVs to alter the total amount of DNA. The former mainly involves DNA translocations or inversions in which the physical organization is altered. The latter on the other hand involves large deletions or insertions in which the physical organization of the DNA sequences results in altered DNA abundance (Gorkovskiy & Verstrepen, 2021). In that sense, the SVs insertions that we found which ranged from 2.5 to > 5 Kb located in IGRs of both *Ss* genomes

are believed to alter the DNA abundance and hence are unbalanced SVs. The occurrence of long insertions and other SVs are now gaining special attention due to its arguably large effect on genomic and phenotypic traits (Ho et al., 2020).

What causes presence of SVs has also been described by Huang et al. (2023). Various factors interplay contributing to the occurrence of large SV insertions, including the activity of Transposable Elements (TEs) within the genome (Santana et al., 2014), repair processes following DNA damage such as non-homologous end joining (NHEJ) or microhomology-mediated end joining (MMEJ) (Chiruvella et al., 2013; Stinson & Loparo, 2021).

The high prevalence of SVs, particularly polymorphisms of the insertion type, observed in both analyzed genomes suggests a dynamic genomic landscape undergoing ongoing evolutionary processes and genomic plasticity. This aligns with previous findings by Hartmann (2022) who discussed the implications of novel SVs on fungal pathogen adaptation to selection pressure. SVs have been linked to various fitness-relevant phenotypic traits, such as fungicide resistance, enhanced virulence, and evasion of host resistance mechanisms, highlighting their importance in pathogen fitness and survival, therefore, understanding the specifics on the functional implications of the SVs in the genotypes that we study is a field that requires further exploration (Wold et al., 2021). In the wheat pathogen *Zymoseptoria tritici*, a genomic variation modeling study was carried out by Badet et al. (2021). The authors found that phenotypic trait variation was significantly explained by SVs, supporting the need to continue their exploration for applications in plant breeding and biotechnology. Furthermore, the number of SVs found, highlighted the genomic plasticity exhibited by *Ss* genomes and reshuffling, despite the typical genome stability of this pathogen (Amaradasa & Everhart, 2016). This emphasizes the need to explore the mechanisms driving genetic variation and adaptation in *Ss*. The functional significance of the SVs might be a subject of future interest for further exploration on novel trait emergence and adaptation.

The distribution of insertions across all 16 chromosomes highlights the widespread nature of genomic alterations in *Ss*. Chromosomes with a high frequency of SVs suggest potential genomic hotspots for structural variation. Although the extent and specific functions affected by the large insertions were not captured in our analysis, further analysis may reveal the effect of such genomic variations, whose specifics will be crucial as they may affect important functions such as pathogenicity (Badet et al., 2020).

In our research, certain chromosomes exhibited higher levels of genomic variation; this was the case on chromosome 15, suggesting the presence of genomic hotspots predisposed to structural alterations. The abundance of SVs within this chromosome indicates a heightened propensity for genetic alterations and rearrangements, possibly driven by specific evolutionary pressures or genomic features inherent to this region. This finding aligns with previous research by Badet et al. (2021) highlighting the uneven distribution of SVs across chromosomes and underscoring the importance of understanding chromosomal architecture in shaping genomic diversity.

The clustering of SVs on chromosome 15 highlights its significance in contributing to the overall genomic diversity of *Ss* populations. Further investigation into the underlying mechanisms shaping this hotspot chromosome, such as recombination rates, repetitive elements, or environmental selection pressures, may elucidate the drivers of genomic variation in this region and their implications for fungal biology and pathogenicity.

In addition to noting chromosome hotspots for SVs, when analyzing their specific genomic location, we identified unique isolates that vary in size in both genomes. This analysis revealed an interesting pattern suggesting that SVs might be adapting to become more streamlined. Specifically, we observed a reduction in size in SVs located at the same genomic locations, identified as unique/accessory, with notable differences in size.

These findings may indicate that SV size reduction in isolates could be associated with a more compact and more efficient genome organization that enhances *Ss* adaptability. In their research, O'Malley et al. (2016) discussed how simplification, including genome reduction, can be a successful evolutionary strategy that can result in increased efficiency.

The genome reduction phenomenon observed in isolate Q12 in our research aligns with the “Streamlining theory” that has been extensively studied in bacterial genomes (Giovannoni et al., 2014; Murray et al., 2021; Sela et al., 2016) and suggest simplification of genomes enhancing fitness traits or adaptation to diverse ecological niches. In fact, the “Streamlining theory” principles are applicable to other organisms including fungal plant pathogens.

The most important evidence of drastic genome reduction is exemplified in the unicellular fungi-like organism Microsporidia, in which genome size reduction has been beneficial to

eliminate unnecessary metabolic pathways, allowing the microsporidia to rely on the host for many cellular functions (Jespersen et al., 2022).

Therefore, the observed reduction in size of accessory SVs in the isolates may suggest a streamlined genomic process similar to that seen in microsporidia. This reduction might indicate that *Ss* isolates might be shedding non-essential genomic baggage leading to a more advantageous lifestyle. This finding aligns with the theory of selective retention and expansion of virulence-related genes in *Magnaporte orizae*, further supporting our reasoning towards streamlining of SVs in *Ss* (Chiapello et al., 2015).

Conversely, the larger SVs in certain chromosomes may highlight regions where additional genetic material provides a selective advantage. Further research is needed to understand the functional impact of these SVs.

The functional significance of the SVs found in both genomes is beyond the span of our study, however, there is some evidence describing the effects of some of them. In some cases, the presence of novel SVs may reflect transposable element (TEs) proliferation or suppression. TEs in *Ss* are crucial for genomic evolution by increasing genomic diversity and genome plasticity (Beare Paul et al., 2009). An example highlighting the suppression of TE insertions in *Ss* was reported by Gambhir et al. (2020) where they described how the exposure to sublethal dosages of fungicide repressed TE insertions in all genomic backgrounds studied, while some strains of a certain genomic background showed increased frequency of INDELS, which sheds light on some of the factors that may influence genomic variation frequency, type, and distribution.

The discovery of SVs in IGRs of *Ss* genomes in our study sheds light on the significance of non-coding regions in genomic variation, further emphasizing the prevalence of structural variation in these regulatory genomic spaces. Traditionally regarded as genomic "blank spaces," intergenic regions are now acknowledged as pivotal for regulatory elements governing gene expression and contributing to genome plasticity (Sun et al., 2020). The effects of large insertions vary and may parallel those caused by single-base variations, such as altering receptor recognition, virulence, or gene expression (Jones et al., 2021).

Our findings underscore the importance of investigating non-coding regions in understanding the adaptive potential and evolutionary dynamics of fungal pathogens for their

potential involvement in shaping gene regulatory networks and influencing phenotypic traits, in addition to contributing to genomic diversity. SVs played an important role in genomic variation in the genomes analysed in our study. Similarly, in a recent report on fungal plant pathogen *A. fumigatus* Brown et al. (2022) described that non-coding regions exhibited higher levels of sequence variation compared to their corresponding protein-coding regions. The significance of SVs in IGRs warrants further exploration, as they may play pivotal roles in mediating fungal adaptation, pathogenicity, and host interactions.

Our results provide a foundation for studying differences in genomic architecture by identifying SVs in intergenic regions using long-read sequencing. However, it is essential to emphasize that the interpretation of these results is limited by the small number of genomes analyzed.

Previous studies, such as those by Derbyshire et al. (2019) in *Ss* are an example of how analyzing a larger number of genomes helps at gaining a more comprehensive understanding of genomic variations and the presence or absence of genomic features. Their analysis of 25 genomes revealed a scarcity of significant hard selective sweeps in the *Ss* genome, indicating that selective pressures may not be as influential as previously assumed in shaping its genetic diversity.

Despite the limitations, our findings pave the way for future research aimed at understanding the significance of SVs located in intergenic regions and their impact on overall genomic variation.

While our study focused solely on the identification of SVs, we provided insight into the genomic context of these variants by referencing neighboring genes and their functional domain. This approach offers a preliminary glimpse into the potential functional implications of SVs, laying the groundwork for future studies to explore their specific effects on gene expression and phenotype.

In addition to delving into the genomic repertoire of *Ss*, particularly in identifying SVs, our study underlines the significance of employing long-read sequencing technology, such as Oxford Nanopore, in genomic analyses of fungal pathogens like *Ss*. Long-read sequencing offers several advantages over traditional short-read sequencing methods, particularly in resolving complex genomic regions, such as repetitive sequences and SVs. The longer reads generated by Oxford

Nanopore sequencing provide more contiguous and accurate genome assemblies, enabling precise identification and characterization of SVs with enhanced sensitivity and resolution (Jones et al., 2021). Our study underscores the importance of utilizing advanced sequencing technologies to unravel the complexities of fungal genomes and their implications in pathogenicity and adaptation.

3.5. CONCLUSIONS

- Even though the scope of our research was limited by the lack of more genomes to analyze if the accessory SVs are fixed among isolates with different phenotypic traits. With our research we uncovered common and unique structural variants shaping the genome architecture of the studied isolates. Not much information can be provided regarding the specific significance of the location of SVs in each intergenic region. However, further investigation is needed to elucidate the specific impact of SV insertions on each *Ss* genotype.

- Investigating the functional significance and evolutionary origins of the unique SVs found in our research can provide valuable insights into the genetic basis of phenotypic differences between the two genotypes and enhance our understanding of their adaptation to diverse environments and hosts. Further studies incorporating additional genomic data from other isolates would strengthen our understanding of *Ss* biology, ecology, and evolution.
- Intergenic region observation prompts intriguing questions regarding the propensity of large SVs to accumulate in intergenic regions. Are these regions particularly susceptible to genomic alterations, driving the evolutionary trajectory of fungal genomes? Further exploration into the functional consequences of SVs in intergenic regions is warranted to elucidate their role in shaping fungal biology, pathogenicity, and host interactions.
- Overall, our findings shed light on the genomic dynamics of *Ss* and highlight the importance of structural variation in driving genomic diversity within this pathogenic fungus.

3.6. REFERENCES

Alonge, M., Lebeigle, L., Kirsche, M., Jenike, K., Ou, S., Aganezov, S., Wang, X., Lippman, Z. B., Schatz, M. C., & Soyk, S. (2022). Automated assembly scaffolding using RagTag elevates a new tomato system for high-throughput genome editing. *Genome Biology*, *23*(1), 258. https://doi.org/10.1186/s13059-022-02823-7

Alonge, M., Soyk, S., Ramakrishnan, S., Wang, X., Goodwin, S., Sedlazeck, F. J., Lippman, Z. B., & Schatz, M. C. (2019). RaGOO: fast and accurate reference-guided scaffolding of draft genomes. *Genome Biology*, *20*(1). https://doi.org/10.1186/s13059-019-1829-6

Amaradasa, B. S., & Everhart, S. E. (2016). Effects of Sublethal Fungicides on Mutation Rates and Genomic Variation in Fungal Plant Pathogen, Sclerotinia sclerotiorum. *PLOS ONE*, *11*(12), e0168079. https://doi.org/10.1371/journal.pone.0168079

Amarasinghe, S. L., Su, S., Dong, X., Zappia, L., Ritchie, M. E., & Gouil, Q. (2020). Opportunities and challenges in long-read sequencing data analysis. *Genome Biol*, *21*(1), 30. https://doi.org/10.1186/s13059-020-1935-5

Amezrou, R., Ducasse, A., Compain, J., Lapalu, N., Pitarch, A., Dupont, L., Confais, J., Goyeau, H., Kema, G. H. J., Croll, D., Amselem, J., Sanchez-Vallet, A., & Marcel, T. C. (2024). Quantitative pathogenicity and host adaptation in a fungal plant pathogen revealed by whole-genome sequencing. *Nature Communications*, *15*(1), 1933. https://doi.org/10.1038/s41467-024-46191-1

Amselem, J., Cuomo, C. A., van Kan, J. A., Viaud, M., Benito, E. P., Couloux, A., Coutinho, P. M., de Vries, R. P., Dyer, P. S., Fillinger, S., Fournier, E., Gout, L., Hahn, M., Kohn, L., Lapalu, N., Plummer, K. M., Pradier, J. M., Quevillon, E., Sharon, A., . . . Dickman, M. (2011). Genomic analysis of the necrotrophic fungal pathogens Sclerotinia sclerotiorum and Botrytis cinerea. *PLoS Genet*, *7*(8), e1002230. https://doi.org/10.1371/journal.pgen.1002230

Badet, T., Fouché, S., Hartmann, F. E., Zala, M., & Croll, D. (2021). Machine-learning predicts genomic determinants of meiosis-driven structural variation in a eukaryotic pathogen. *Nature Communications*, *12*(1), 3551. https://doi.org/10.1038/s41467-021-23862-x

Badet, T., Oggenfuss, U., Abraham, L., McDonald, B. A., & Croll, D. (2020). A 19-isolate reference-quality global pangenome for the fungal wheat pathogen Zymoseptoria tritici. *BMC Biology*, *18*(1), 12. https://doi.org/10.1186/s12915-020-0744-3

Bag, T. K. (2000). An outbreak of watery pod rot of French bean in the hills of Arunachal Pradesh. *Journal of Mycology and Plant Pathology*, *30*(1), 130-131.

Beare Paul, A., Unsworth, N., Andoh, M., Voth Daniel, E., Omsland, A., Gilk Stacey, D., Williams Kelly, P., Sobral Bruno, W., Kupko John, J., Porcella Stephen, F., Samuel James, E., & Heinzen Robert, A. (2009). Comparative Genomics Reveal Extensive Transposon-Mediated Genomic Plasticity and Diversity among Potential Effector Proteins within the Genus Coxiella. *Infection and Immunity*, *77*(2), 642-656. https://doi.org/10.1128/iai.01141-08

Brown, A., Mead, M. E., Steenwyk, J. L., Goldman, G. H., & Rokas, A. (2022). Extensive Non-Coding Sequence Divergence Between the Major Human Pathogen Aspergillus fumigatus and its Relatives. *Frontiers in Fungal Biology*, *3*. https://doi.org/10.3389/ffunb.2022.802494

Chiapello, H., Mallet, L., Guérin, C., Aguileta, G., Amselem, J., Kroj, T., Ortega-Abboud, E., Lebrun, M.-H., Henrissat, B., Gendrault, A., Rodolphe, F., Tharreau, D., & Fournier, E. (2015). Deciphering Genome Content and Evolutionary Relationships of Isolates from the

Fungus Magnaporthe oryzae Attacking Different Host Plants. *Genome Biology and Evolution*, *7*(10), 2896-2912. https://doi.org/10.1093/gbe/evv187

Chiruvella, K. K., Liang, Z., & Wilson, T. E. (2013). Repair of double-strand breaks by end joining. *Cold Spring Harb Perspect Biol*, *5*(5), a012757. https://doi.org/10.1101/cshperspect.a012757

De Coster, W., & Rademakers, R. (2023). NanoPack2: population-scale evaluation of long-read sequencing data. *Bioinformatics*, *39*(5), btad311. https://doi.org/10.1093/bioinformatics/btad311

Dean, R. A., Talbot, N. J., Ebbole, D. J., Farman, M. L., Mitchell, T. K., Orbach, M. J., Thon, M., Kulkarni, R., Xu, J.-R., Pan, H., Read, N. D., Lee, Y.-H., Carbone, I., Brown, D., Oh, Y. Y., Donofrio, N., Jeong, J. S., Soanes, D. M., Djonovic, S., . . . Birren, B. W. (2005). The genome sequence of the rice blast fungus Magnaporthe grisea. *Nature*, *434*(7036), 980-986. https://doi.org/10.1038/nature03449

Depotter, J. R. L., & Doehlemann, G. (2020). Target the core: durable plant resistance against filamentous plant pathogens through effector recognition. *Pest Management Science*, *76*(2), 426-431. https://doi.org/https://doi.org/10.1002/ps.5677

Derbyshire, M., Denton-Giles, M., Hegedus, D., Seifbarghy, S., Rollins, J., van Kan, J., Seidl, M. F., Faino, L., Mbengue, M., Navaud, O., Raffaele, S., Hammond-Kosack, K., Heard, S., & Oliver, R. (2017). The complete genome sequence of the phytopathogenic fungus Sclerotinia sclerotiorum reveals insights into the genome architecture of broad host range pathogens. *Genome Biol Evol*, *9*(3), 593-618. https://doi.org/10.1093/gbe/evx030

Derbyshire, M. C., Denton-Giles, M., Hane, J. K., Chang, S., Mousavi-Derazmahalleh, M., Raffaele, S., Buchwaldt, L., & Kamphuis, L. G. (2019). A whole genome scan of SNP data suggests a lack of abundant hard selective sweeps in the genome of the broad host range plant pathogenic fungus Sclerotinia sclerotiorum. *PLOS ONE*, *14*(3), e0214201. https://doi.org/10.1371/journal.pone.0214201

Derbyshire, M. C., Newman, T. E., Khentry, Y., & Owolabi Taiwo, A. (2022). The evolutionary and molecular features of the broad-host-range plant pathogen Sclerotinia sclerotiorum. *Molecular Plant Pathology*, *23*(8), 1075-1090. https://doi.org/https://doi.org/10.1111/mpp.13221

Dolatabadian, A., & Fernando, W. G. (2022). Genomic Variations and Mutational Events Associated with Plant–Pathogen Interactions. *Biology*, *11*(3).

Durak, M. R., & Ozkilinc, H. (2023). Genome-Wide Discovery of Structural Variants Reveals Distinct Variant Dynamics for Two Closely Related Monilinia Species. *Genome Biology and Evolution*, *15*(6), evad085. https://doi.org/10.1093/gbe/evad085

Eschenbrenner, C. J., Feurtey, A., & Stukenbrock, E. H. (2020). Population Genomics of Fungal Plant Pathogens and the Analyses of Rapidly Evolving Genome Compartments. In J. Y. Dutheil (Ed.), *Statistical Population Genomics* (pp. 337-355). Springer US. https://doi.org/10.1007/978-1-0716-0199-0_14

Feuk, L., Marshall, C. R., Wintle, R. F., & Scherer, S. W. (2006). Structural variants: changing the landscape of chromosomes and design of disease studies. *Hum Mol Genet*, *15 Spec No 1*, R57-66. https://doi.org/10.1093/hmg/ddl057

Frantzeskakis, L., Kusch, S., & Panstruga, R. (2019). The need for speed: compartmentalized genome evolution in filamentous phytopathogens. *Molecular Plant Pathology*, *20*(1), 3-7. https://doi.org/https://doi.org/10.1111/mpp.12738

Gambhir, N., Kamvar, Z. N., Higgins, R., Amaradasa, B. S., & Everhart, S. E. (2020). Spontaneous and Fungicide-Induced Genomic Variation in Sclerotinia sclerotiorum. *Phytopathology®*, *111*(1), 160-169. https://doi.org/10.1094/PHYTO-10-20-0471-FI

Giovannoni, S. J., Cameron Thrash, J., & Temperton, B. (2014). Implications of streamlining theory for microbial ecology. *The ISME Journal*, *8*(8), 1553-1565. https://doi.org/10.1038/ismej.2014.60

Gorkovskiy, A., & Verstrepen, K. J. (2021). The Role of Structural Variation in Adaptation and Evolution of Yeast and Other Fungi. *Genes (Basel)*, *12*(5). https://doi.org/10.3390/genes12050699

Guo, N., Wang, S., Gao, L., Liu, Y., Wang, X., Lai, E., Duan, M., Wang, G., Li, J., Yang, M., Zong, M., Han, S., Pei, Y., Borm, T., Sun, H., Miao, L., Liu, D., Yu, F., Zhang, W., . . . Liu, F. (2021). Genome sequencing sheds light on the contribution of structural variants to Brassica oleracea diversification. *BMC Biol*, *19*(1), 93. https://doi.org/10.1186/s12915-021-01031-2

Gupta, N. C., Yadav, S., Arora, S., Mishra, D. C., Budhlakoti, N., Gaikwad, K., Rao, M., Prasad, L., Rai, P. K., & Sharma, P. (2022). Draft genome sequencing and secretome profiling of Sclerotinia sclerotiorum revealed effector repertoire diversity and allied broad-host range necrotrophy. *Scientific Reports*, *12*(1), 21855. https://doi.org/10.1038/s41598-022-22028-z

Haas, B. J., Kamoun, S., Zody, M. C., Jiang, R. H., Handsaker, R. E., Cano, L. M., Grabherr, M., Kodira, C. D., Raffaele, S., Torto-Alalibo, T., Bozkurt, T. O., Ah-Fong, A. M., Alvarado, L., Anderson, V. L., Armstrong, M. R., Avrova, A., Baxter, L., Beynon, J., Boevink, P. C., . . . Nusbaum, C. (2009). Genome sequence and analysis of the Irish potato famine pathogen Phytophthora infestans. *Nature*, *461*(7262), 393-398. https://doi.org/10.1038/nature08358

Hamim, I., Sekine, K.-T., & Komatsu, K. (2022). How do emerging long-read sequencing technologies function in transforming the plant pathology research landscape? *Plant Molecular Biology*, *110*(6), 469-484. https://doi.org/10.1007/s11103-022-01305-5

Hartmann, F. E. (2022). Using structural variants to understand the ecological and evolutionary dynamics of fungal plant pathogens. *New Phytologist*, *234*(1), 43-49. https://doi.org/https://doi.org/10.1111/nph.17907

Ho, S. S., Urban, A. E., & Mills, R. E. (2020). Structural variation in the sequencing era. *Nat Rev Genet*, *21*(3), 171-189. https://doi.org/10.1038/s41576-019-0180-9

Hotaling, S., Wilcox, E. R., Heckenhauer, J., Stewart, R. J., & Frandsen, P. B. (2023). Highly accurate long reads are crucial for realizing the potential of biodiversity genomics. *BMC Genomics*, *24*(1), 117. https://doi.org/10.1186/s12864-023-09193-9

Howe, K., Chow, W., Collins, J., Pelan, S., Pointon, D.-L., Sims, Y., Torrance, J., Tracey, A., & Wood, J. (2021). Significantly improving the quality of genome assemblies through curation. *GigaScience*, *10*(1), giaa153. https://doi.org/10.1093/gigascience/giaa153

Huang, J., Liu, S., & Cook, D. E. (2023). Dynamic Genomes - Mechanisms and consequences of genomic diversity impacting plant-fungal interactions. *Physiological and Molecular Plant Pathology*, *125*, 102006. https://doi.org/https://doi.org/10.1016/j.pmpp.2023.102006

Jespersen, N., Monrroy, L., & Barandun, J. (2022). Impact of Genome Reduction in Microsporidia. In L. M. Weiss & A. W. Reinke (Eds.), *Microsporidia: Current Advances in Biology* (pp. 1-42). Springer International Publishing. https://doi.org/10.1007/978-3-030-93306-7_1

Jones, D. A. B., Rozano, L., Debler, J. W., Mancera, R. L., Moolhuijzen, P. M., & Hane, J. K. (2021). An automated and combinative method for the predictive ranking of candidate

effector proteins of fungal plant pathogens. *Scientific Reports*, *11*(1), 19731. https://doi.org/10.1038/s41598-021-99363-0

Kohn, L. M., Stasovski, E., Carbone, I., Royer, J., & Anderson, J. B. (1991). Mycelial incompatibility and molecular markers identify genetic variability in field populations of *Sclerotinia sclerotiorum. Phytopathology*, *81*, 480-485. https://doi.org/10.1094/Phyto-81-480.

Kolmogorov, M., Yuan, J., Lin, Y., & Pevzner, P. A. (2019). Assembly of long, error-prone reads using repeat graphs. *Nature Biotechnology*, *37*(5), 540-546. https://doi.org/10.1038/s41587-019-0072-8

Langner, T., Harant, A., Gomez-Luciano, L. B., Shrestha, R. K., Malmgren, A., Latorre, S. M., Burbano, H. A., Win, J., & Kamoun, S. (2021). Genomic rearrangements generate hypervariable mini-chromosomes in host-specific isolates of the blast fungus. *PLoS Genet*, *17*(2), e1009386. https://doi.org/10.1371/journal.pgen.1009386

Liu, J., Meng, Q., Zhang, Y., Xiang, H., Li, Y., Shi, F., Ma, L., Liu, C., Liu, Y., Su, B., & Li, Z. (2018). Mycelial compatibility group and genetic variation of sunflower Sclerotinia sclerotiorum in Northeast China. *Physiological and Molecular Plant Pathology*, *102*, 185-192. https://doi.org/https://doi.org/10.1016/j.pmpp.2018.03.006

Mahmoud, M., Gobet, N., Cruz-Dávalos, D. I., Mounier, N., Dessimoz, C., & Sedlazeck, F. J. (2019). Structural variant calling: the long and the short of it. *Genome Biology*, *20*(1), 246. https://doi.org/10.1186/s13059-019-1828-7

Manni, M., Berkeley, M. R., Seppey, M., Simão, F. A., & Zdobnov, E. M. (2021). BUSCO Update: Novel and Streamlined Workflows along with Broader and Deeper Phylogenetic Coverage for Scoring of Eukaryotic, Prokaryotic, and Viral Genomes. *Molecular Biology and Evolution*, *38*(10), 4647-4654. https://doi.org/10.1093/molbev/msab199

McLaren, W., Gil, L., Hunt, S. E., Riat, H. S., Ritchie, G. R. S., Thormann, A., Flicek, P., & Cunningham, F. (2016). The Ensembl Variant Effect Predictor. *Genome Biology*, *17*(1), 122. https://doi.org/10.1186/s13059-016-0974-4

Miklas, P. N., Kelly, J. D., Beebe, S. E., & Blair, M. W. (2006). Common bean breeding for resistance against biotic and abiotic stresses: From classical to MAS breeding. *Euphytica*, *147*(1), 105-131. https://doi.org/10.1007/s10681-006-4600-5

Möller, M., & Stukenbrock, E. H. (2017). Evolution and genome architecture in fungal plant pathogens. *Nat Rev Microbiol*, *15*(12), 756-771. https://doi.org/10.1038/nrmicro.2017.76

Murray, G. G. R., Charlesworth, J., Miller, E. L., Casey, M. J., Lloyd, C. T., Gottschalk, M., Tucker, A. W., Welch, J. J., & Weinert, L. A. (2021). Genome Reduction Is Associated with Bacterial Pathogenicity across Different Scales of Temporal and Ecological Divergence. *Molecular Biology and Evolution*, *38*(4), 1570-1579. https://doi.org/10.1093/molbev/msaa323

O'Malley, M. A., Wideman, J. G., & Ruiz-Trillo, I. (2016). Losing Complexity: The Role of Simplification in Macroevolution. *Trends Ecol Evol*, *31*(8), 608-621. https://doi.org/10.1016/j.tree.2016.04.004

Potgieter, L., Feurtey, A., Dutheil, J. Y., & Stukenbrock, E. H. (2020). On Variant Discovery in Genomes of Fungal Plant Pathogens. *Front Microbiol*, *11*, 626. https://doi.org/10.3389/fmicb.2020.00626

Robison, F. M., Turner, M. F., Jahn, C. E., Schwartz, H. F., Prenni, J. E., Brick, M. A., & Heuberger, A. L. (2018). Common bean varieties demonstrate differential physiological and metabolic

responses to the pathogenic fungus Sclerotinia sclerotiorum. *Plant Cell Environ*, *41*(9), 2141-2154. https://doi.org/10.1111/pce.13176

Saharan, G. S., & Mehta, N. (2008). *Sclerotinia Diseases of Crop Plants: Biology, Ecology and Disease Management*. https://link.springer.com/book/10.1007/978-1-4020-8408-9

Santana, M. F., Silva, J. C. F., Mizubuti, E. S. G., Arajo, E. F., & Queiroz, M. V. (2014). Analysis of Tc1-Mariner elements in Sclerotinia sclerotiorum suggests recent activity and flexible transposases. *BMC Microbiology*, *14*(1), 256. https://doi.org/10.1186/s12866-014-0256-9

Sela, I., Wolf, Y. I., & Koonin, E. V. (2016). Theory of prokaryotic genome evolution. *Proceedings of the National Academy of Sciences*, *113*(41), 11399-11407. https://doi.org/10.1073/pnas.1614083113

Shahoveisi, F., Riahi Manesh, M., & del Río Mendoza, L. E. (2022). Modeling risk of Sclerotinia sclerotiorum-induced disease development on canola and dry bean using machine learning algorithms. *Scientific Reports*, *12*(1), 864. https://doi.org/10.1038/s41598-021-04743-1

Simão, F. A., Waterhouse, R. M., Ioannidis, P., Kriventseva, E. V., & Zdobnov, E. M. (2015). BUSCO: assessing genome assembly and annotation completeness with single-copy orthologs. *Bioinformatics*, *31*(19), 3210-3212. https://doi.org/10.1093/bioinformatics/btv351

Smolka, M., Paulin, L. F., Grochowski, C. M., Horner, D. W., Mahmoud, M., Behera, S., Kalef-Ezra, E., Gandhi, M., Hong, K., Pehlivan, D., Scholz, S. W., Carvalho, C. M. B., Proukakis, C., & Sedlazeck, F. J. (2024). Detection of mosaic and population-level structural variants with Sniffles2. *Nature Biotechnology*. https://doi.org/10.1038/s41587-023-02024-y

Stinson, B. M., & Loparo, J. J. (2021). Repair of DNA Double-Strand Breaks by the Nonhomologous End Joining Pathway. *Annual Review of Biochemistry*, *90*(Volume 90, 2021), 137-164. https://doi.org/https://doi.org/10.1146/annurev-biochem-080320-110356

Sun, S., Hoy, M. J., & Heitman, J. (2020). Fungal pathogens. *Current Biology*, *30*(19), R1163-R1169. https://doi.org/https://doi.org/10.1016/j.cub.2020.07.032

van Dijk, E. L., Naquin, D., Gorrichon, K., Jaszczyszyn, Y., Ouazahrou, R., Thermes, C., & Hernandez, C. (2023). Genomics in the long-read sequencing era. *Trends Genet*, *39*(9), 649-671. https://doi.org/10.1016/j.tig.2023.04.006

Wold, J., Koepfli, K.-P., Galla, S. J., Eccles, D., Hogg, C. J., ., M. F. L. L., Guhlin, J., Santure, A. W., & Steeves, T. E. (2021). Expanding the conservation genomics toolbox: Incorporating structural variants to enhance genomic studies for species of conservation concern. *Molecular Ecology*, *30*(23), 5949-5965. https://doi.org/https://doi.org/10.1111/mec.16141

Xin, Z., & Chen, J. (2012). A high throughput DNA extraction method with high yield and quality. *Plant Methods*, *8*(1), 26. https://doi.org/10.1186/1746-4811-8-26

Zaccaron, A. Z., & Stergiopoulos, I. (2024). Analysis of five near-complete genome assemblies of the tomato pathogen Cladosporium fulvum uncovers additional accessory chromosomes and structural variations induced by transposable elements effecting the loss of avirulence genes. *BMC Biology*, *22*(1). https://doi.org/10.1186/s12915-024-01818-z

Zhang, X., Cheng, X., Liu, L., & Liu, S. (2021). Genome Sequence Resource for the Plant Pathogen Sclerotinia sclerotiorum WH6 Isolated in China. *Plant Disease*, *105*(11), 3720-3722. https://doi.org/10.1094/PDIS-01-21-0146-A

Zhou, Y., Zhang, Z., Bao, Z., Li, H., Lyu, Y., Zan, Y., Wu, Y., Cheng, L., Fang, Y., Wu, K., Zhang, J., Lyu, H., Lin, T., Gao, Q., Saha, S., Mueller, L., Fei, Z., Städler, T., Xu, S., . . . Huang, S. (2022). Graph pangenome captures missing heritability and empowers tomato breeding. *Nature*, *606*(7914), 527-534. https://doi.org/10.1038/s41586-022-04808-9

3. GENERAL DISCUSSIONS.

In the battle against fungal pathogens, disease management strategies prioritized should be environmentally friendly, cost-effective, durable, and widely accepted among common bean producers (Davies et al., 2021; El-Baky & Amara, 2021; Thambugala et al., 2020). These strategies are essential for sustainable agriculture and ensuring long-term crop health and productivity.

The cornerstone of disease control lies in understanding the disease through factors influencing genetic diversity determinants of population composition (Atallah & Subbarao, 2012). Understanding these factors allows for the implementation of preventive measures and the selection of methods with both short and long-term effectiveness. Over time, disease prevention and control have been achieved through the development of resistant cultivars. However, their development is challenged by the low heritability, inefficient breeding methods, and the constant struggle to keep up with the phenotypic and genomic characterization of isolates that provide a more integrated representation of current threats in commercial fields. Thus, a constant description of population composition and sampling that represents the current genetic diversity in commercial fields is essential for effective disease management (Ender & Kelly, 2005; Kolkman & Kelly, 2000).

By studying both phenotypic traits and genomic characterization, breeders can contribute complementary approaches for improved disease management. Phenotypic characterization, such as assessing MCGs and aggressiveness, provides a deeper understanding of some crucial characteristics that shape the pathogens' dynamics. In our study, classifying samples into diverse MCGs confirmed the relevance of using phenotypic macroscopic markers like MCGs to explore the genetic composition of a population. While some authors approach this cautiously, its inclusion

in genetic studies greatly benefits decision-making in research directions (Kamvar & Everhart, 2019). This strategy captured the complexity of MCGs characterizing the isolates, allowing for a more comprehensive understanding of the compatibility landscape among isolates collected in proximity compared with samples collected at more dispersed points.

Studies combining phenotypic and genomic characterization similar to ours aimed at understanding *Ss* and its relationship with different hosts, combining different phenotypic characteristics such as morphology, oxalic acid production, physiology, and more (Aldrich-Wolfe et al., 2015).

Our study of aggressiveness and MCGs highlighted the relationships and raises some hypotheses on the population dynamics. It not only revealed a high genetic diversity in the population with clonal events but also showcased variability in aggressiveness even among samples with presumed predominantly clonal nature. Similar findings have been observed in other fungal plant pathogens like *Podosphaera leucotricha*. In their study, Ganan-Betancur et al. (2021) suggested that the high genetic diversity in *P. leucotricha* was explained by an independent evolution of local populations under the effect of geographical barriers and limited long-distance conidial dispersal. Similar to *P. leucotricha*, *Ss* faces geographical barriers which results in localized epidemics that may lead to endemic groups as shown in our research. Nevertheless, we suggest that population dynamics in *Ss* have yet room for further exploration, as those geographical barriers do not seem to affect some isolates as those in our study with compatibility with several MCGs and across distant locations. It further highlights that *Ss* is a pathogen that keeps on evolving leading to its adaptability over geographical barriers and diverse cultural cropping practices.

The extent in which geographical barriers influence genetic diversity in *Ss* is constantly updated. Although geographical barriers do contribute to the population structure, more important

is to consider the pathogens' mode of infection resulting from ascospores dispersal whose air-borne nature allows the pathogen to localize over a broad geographical range (Derbyshire & Denton-Giles, 2016).

Studying the levels of aggressiveness, highlights the need for maintaining datasets of current aggressive genotypes that pose the greatest threat to the crop which is a field that needs constant updating to capture the actual threat that each isolate pose to current commercial fields. With the creation of datasets of current isolates affecting commercial fields the options of timely reports of aggressiveness are enabled. Additionally, it stresses the need for incorporating isolates that more reliably represent the current strains affecting commercial fields. Determination of isolates aggressiveness enhances the reliability on screening and selection of potential sources of resistance in common bean breeding programs. Similarly to our study, other researchers have performed a few studies to characterize the aggressiveness of *Ss* isolates on other crops like canola (Denton-Giles et al., 2018), demonstrating that incorporating aggressiveness characterization facilitates a reliable choice of resistant germplasms when the isolates used account for tailored representation of field populations rather than randomly selecting isolates without prior phenotypic characterization. Although we performed a phenotypic characterization of aggressiveness in isolates, the genetic basis of aggressiveness in *Ss* remains insufficiently understood and requires further exploration. Characterizing these genetics factors would provide valuable insights into the mechanisms driving pathogenicity and could help in identifying genetic markers for aggressiveness (Pariaud et al., 2009).

In our study, we used the most widely adopted inoculation method for *Ss* in common bean, which is stem inoculation (Petzoldt & Dickson, 1996), due to its reproducibility. However, it is crucial to consider that utilizing a broader range of inoculation techniques may capture valuable

insights into unexplored defense mechanisms in common bean. These methods, which aim to produce infection through rapid, reliable, non-contact approaches, contrast with traditional contact methods such as the one employed in our study and were recently reported to successfully produce basal infection in canola, lupin and lettuce, for example positioning the agar plugs below the soil surface or a second one consisting in mixing the dry inoculum in the form of a powder (Han et al., 2024). Exploring these alternative techniques could provide interesting insights and is worth investigating in common bean research to compare current approaches and consider their incorporation as a tool for *Ss* aggressiveness characterization. This would enable to contrast isolates variability in relationship with the inoculation method tested in our research. Incorporating new reproducible inoculation techniques would allow common bean breeding research to keep up with the new approaches for screening disease-resistant germplasms while accounting for the successfulness of the traits considered as aggressiveness to see how they fit in common bean aggressiveness studies (Pariaud et al., 2009).

Studying the complexities of *Ss* benefits from phenotypic characterization as it provides essential insights into the pathogen's behavior including aggressiveness, population structure and host range. Such phenotypic data are crucial to understand how different isolates interact with their hosts, which helps in identifying factors that contribute to epidemic outbreaks. Moreover, characterizing phenotypic offers valuable data on the observable traits that influence infection patterns, survival, and spread in different ecological settings. However, the study of phenotypic traits alone is just a small component of a bigger picture. To fully understand *Ss* complexities, effective characterization of the pathogen should also include genotyping techniques to reveal genetic diversity and potential correlations between genetic and phenotypic traits. Combining

phenotypic and genotypic data enhances our understanding of how Ss adapts to diverse conditions, aiding in predicting and managing its spread.

The integration of genomic characterization into disease management practices offers substantial benefits. Genomic studies provide detailed insights into the genetic makeup and variability of fungal pathogens (Hartmann, 2022). By combining phenotypic data with genomic data, researchers can develop more robust and effective disease management strategies.

One of the main constraints of different genotyping studies is that they often employ different methodologies, making the results difficult to compare. The lack of standardization due to the use of diverse molecular markers across studies, further complicates the development of a unified understanding of genetic variations. Our research aimed to address this issue by contributing to the standardization of genomic studies with whole genome sequencing to capture the full extent of genomic variation in the isolates of study. We suggest that utilizing advanced sequencing technologies, such as long-read sequencing, to achieve more consistent and comparable results. By utilizing these technologies, we can generate more comprehensive genomic data that facilitate better cross-study comparisons.

In our research, the methodology employed to perform in-house sequencing was described in the second chapter. Although the optimization for in-house sequencing itself is not one of the main objectives of our research, the general discussion section provides ample opportunity to expand on some of our observations and thoughts regarding this process.

When we think about in-house sequencing with the most advanced techniques, such as high-throughput DNA sequencing technologies, we often assume the process is straightforward. However, optimizing in-house sequencing, especially for fungal pathogens, presents several

specific challenges. These challenges include technical limitations, resource constraints, the need to tailor techniques to the specific organism, and the requirement for specialized expertise (Aragona et al., 2022).

With adequate training and guidance, results from in-house sequencing can be obtained in a timely manner. This discussion allows us to highlight some of the main challenges in long-read sequencing. One significant issue is the high standard required for DNA quality. There is pressing need for development and dissemination of faster kits or alternatives that can reduce preparation time. Long-read sequencing technologies, like those provided by nanopore platforms, benefit genomic exploration by avoiding biases introduced by PCR when sequencing native DNA. However, they still demand high-quality DNA (Carter & Hussain, 2017).

When obtaining good quality assemblies, the full extent of genomic variation may be explored. However, the high error rate continues to be an issue of major concern among researchers. Despite the advantages of long-read sequencing, such as providing more comprehensive genomic data, these methods still face high error rates around 5-6%, even with ongoing efforts to reduce them further. To solve this problem, researchers are using hybrid pipelines incorporating short-read data along with long-read sequencing offering reliable results with popular software assemblers like Canu (Koren et al., 2017). However, this often affects the timely processing of data as it requires further expertise and high computing resources.

Maintaining up-to-date base of tools, reagents, and the latest technological chemistries is essential. Although nanopore sequencing (the sequencing platform that we used in our research) is improving and getting closer to achieving error rates similar to those of short-read technologies, this remains an ongoing challenge (Delahaye & Nicolas, 2021; Sahlin & Medvedev, 2021). Moreover, the lack of optimized methods and kits specifically tailored for fungal pathogens has

been a significant hurdle in our research, stressing on the need for continued innovation and customization in sequencing techniques in fungal plant pathogens.

In spite of the challenges, our research highlights that genomic characterization is possible and does not have to be a bottleneck but an opportunity to create a more collaborative research environment where innovation sets up as the top priority.

Overall, the results obtained in the sequencing component of our research provided assemblies of good quality to undergo exploration of the genomic composition with a pipeline that enabled the identification of SVs, but it is important to acknowledge that they present a certain degree of fragmentation. As time and research evolves, the incorporation of better optimization methods for DNA extraction, library preparation combined with sequencing training will yield better results addressing this difficulties, switching to methods that may produce improved assemblies which is possible as demonstrated in the *Ss* reference genome getting a contig number close to the number of chromosomes (Derbyshire et al., 2017).

Talking about the hurdles faced by in house sequencing also leads us to acknowledging the most important advantages of utilizing this approach. For example, by conducting in-house sequencing, costs are significantly reduced. The expense associated with outsourcing sequencing projects to external facilities can limit delivery of research results, especially for large-scale studies.

Additionally, time is optimized with real-time data generation, offering up-to-date information and maintaining quality control throughout the sequencing process. This immediacy is critical for making timely decisions and adjustments in experimental designs. The time saved

can be redirected towards bioinformatics analysis and further experimental validation, enhancing the overall efficiency of research projects.

Previous attempts to characterize genomic diversity had limitations, exploring only certain regions of the genome. However, with the advent of in-house sequencing, compete information is now readily available, allowing researchers to explore all sources of genomic variation (Atallah & Subbarao, 2012).

More time and high-quality assemblies, like the ones generated in our study, have the potential to undergo further exploration with pipelines for the creation of graph pangenomes. These pipelines offer reliable and accurate methods for capturing the full spectrum of genomic variation (Hickey et al., 2024). However, constructing high-quality pangenome graphs requires significant time and computational resources, posing constraints for many research projects. Additionally, the complexity of pangenome graphs can make them challenging to interpret, demanding advanced bioinformatics expertise.

Our study lays the groundwork to standardized and more representative studies at a cost-effective price with long read sequencing.

Rapid approaches, such as the rapid identification of SVs used in this study, lead to fast data generation and provide valuable preliminary insights (Smolka et al., 2024). While these methods are beneficial for quickly exploring genetic variations, they are often limited in accuracy and comprehensiveness compared to more exhaustive techniques. Rapid methods may miss subtle or rare variations and can produce higher rates of false positives or negatives, demanding for further validation and refinement. This remains a possibility for future research as the duration of the program only enabled for what is presented in this work.

Ultimately, integrating both phenotypic and genomic data in the study of fungal pathogens enhances our ability to develop effective disease management strategies. By utilizing advanced sequencing technologies and comprehensive data analysis, we can achieve a deeper understanding of pathogen diversity and dynamics, leading to more sustainable and resilient agricultural practices.

4.1 REFERENCES

Aldrich-Wolfe, L., Travers, S., & Nelson, B. J. (2015). Genetic Variation of *Sclerotinia sclerotiorum* from Multiple Crops in the North Central United States. *PLOS ONE*, *10*(9). https://doi.org/https://doi.org/10.1371/journal.pone.0139188

Aragona, M., Haegi, A., Valente, M. T., Riccioni, L., Orzali, L., Vitale, S., Luongo, L., & Infantino, A. (2022). New-Generation Sequencing Technology in Diagnosis of Fungal Plant Pathogens: A Dream Comes True? *Journal of Fungi*, *8*(7), 737. https://doi.org/10.3390/jof8070737

Atallah, Z. K., & Subbarao, K. V. (2012). Population biology of fungal plant pathogens. *Methods Mol Biol*, *835*, 333-363. https://doi.org/10.1007/978-1-61779-501-5_20

Carter, J. M., & Hussain, S. (2017). Robust long-read native DNA sequencing using the ONT CsgG Nanopore system. *Wellcome Open Res*, *2*, 23. https://doi.org/10.12688/wellcomeopenres.11246.3

Davies, C. R., Wohlgemuth, F., Young, T., Violet, J., Dickinson, M., Sanders, J.-W., Vallieres, C., & Avery, S. V. (2021). Evolving challenges and strategies for fungal control in the food supply chain. *Fungal Biology Reviews*, *36*, 15-26. https://doi.org/https://doi.org/10.1016/j.fbr.2021.01.003

Delahaye, C., & Nicolas, J. (2021). Sequencing DNA with nanopores: Troubles and biases. *PLOS ONE*, *16*(10), e0257521. https://doi.org/10.1371/journal.pone.0257521

Denton-Giles, M., Derbyshire, M. C., Khentry, Y., Buchwaldt, L., & Kamphuis, L. G. (2018). Partial stem resistance in Brassica napus to highly aggressive and genetically diverse Sclerotinia sclerotiorum isolates from Australia. *Canadian Journal of Plant Pathology*, *40*(4), 551-561. https://doi.org/10.1080/07060661.2018.1516699

Derbyshire, M., Denton-Giles, M., Hegedus, D., Seifbarghy, S., Rollins, J., van Kan, J., Seidl, M. F., Faino, L., Mbengue, M., Navaud, O., Raffaele, S., Hammond-Kosack, K., Heard, S., & Oliver, R. (2017). The complete genome sequence of the phytopathogenic fungus Sclerotinia sclerotiorum reveals insights into the genome architecture of broad host range pathogens. *Genome Biol Evol*, *9*(3), 593-618. https://doi.org/10.1093/gbe/evx030

Derbyshire, M. C., & Denton-Giles, M. (2016). The control of sclerotinia stem rot on oilseed rape (Brassica napus): current practices and future opportunities. *Plant Pathology*, *65*(6), 859-877. https://doi.org/https://doi.org/10.1111/ppa.12517

El-Baky, N. A., & Amara, A. A. A. F. (2021). Recent Approaches towards Control of Fungal Diseases in Plants: An Updated Review. *Journal of Fungi*, *7*(11), 900. https://doi.org/10.3390/jof7110900

Ender, M., & Kelly, J. D. (2005). Identification of QTL Associated with White Mold Resistance in Common Bean. *Crop Science*, *45*(6), 2482-2490. https://doi.org/https://doi.org/10.2135/cropsci2005.0064

Ganan-Betancur, L., Peever, T. L., Evans, K., & Amiri, A. (2021). High Genetic Diversity in Predominantly Clonal Populations of the Powdery Mildew Fungus Podosphaera leucotricha from U.S. Apple Orchards. *Appl Environ Microbiol*, *87*(15), e0046921. https://doi.org/10.1128/AEM.00469-21

Han, V.-C., Michael, P. J., Crockett, R., Swift, B., & Bennett, S. J. (2024). Effective, consistent, and rapid non-contact application methods for seedling basal stem infection by Sclerotinia sclerotiorum. *Plant Disease*. https://doi.org/10.1094/PDIS-11-23-2412-SC

Hartmann, F. E. (2022). Using structural variants to understand the ecological and evolutionary dynamics of fungal plant pathogens. *New Phytologist*, *234*(1), 43-49. https://doi.org/https://doi.org/10.1111/nph.17907

Hickey, G., Monlong, J., Ebler, J., Novak, A. M., Eizenga, J. M., Gao, Y., Abel, H. J., Antonacci-Fulton, L. L., Asri, M., Baid, G., Baker, C. A., Belyaeva, A., Billis, K., Bourque, G., Buonaiuto, S., Carroll, A., Chaisson, M. J. P., Chang, P.-C., Chang, X. H., . . . Human Pangenome Reference, C. (2024). Pangenome graph construction from genome alignments with Minigraph-Cactus. *Nature Biotechnology*, *42*(4), 663-673. https://doi.org/10.1038/s41587-023-01793-w

Kamvar, Z. N., & Everhart, S. E. (2019). Something in the agar does not compute: on the discriminatory power of mycelial compatibility in Sclerotinia sclerotiorum. *Tropical Plant Pathology*, *44*(1), 32-40. https://doi.org/10.1007/s40858-018-0263-8

Kolkman, J. M., & Kelly, J. D. (2000). An indirect test using oxalate to determine physiological resistance to white mold in common bean. *Crop Science*, *40*(1), 281-285. https://doi.org/https://doi.org/10.2135/cropsci2000.401281x

Koren, S., Walenz, B. P., Berlin, K., Miller, J. R., Bergman, N. H., & Phillippy, A. M. (2017). Canu: scalable and accurate long-read assembly via adaptive k-mer weighting and repeat separation. *Genome Res*, *27*(5), 722-736. https://doi.org/10.1101/gr.215087.116

Pariaud, B., Ravigné, V., Halkett, F., Goyeau, H., Carlier, J., & Lannou, C. (2009). Aggressiveness and its role in the adaptation of plant pathogens. *Plant Pathology*, *58*(3), 409-424. https://doi.org/https://doi.org/10.1111/j.1365-3059.2009.02039.x

Petzoldt, R., & Dickson, M. H. (1996). Straw test for resistance to white mold in beans. *Annu. Rpt. Bean Improv. Coop.*, *39*, 142-143.

Sahlin, K., & Medvedev, P. (2021). Error correction enables use of Oxford Nanopore technology for reference-free transcriptome analysis. *Nature Communications*, *12*(1), 2. https://doi.org/10.1038/s41467-020-20340-8

Smolka, M., Paulin, L. F., Grochowski, C. M., Horner, D. W., Mahmoud, M., Behera, S., Kalef-Ezra, E., Gandhi, M., Hong, K., Pehlivan, D., Scholz, S. W., Carvalho, C. M. B., Proukakis, C., & Sedlazeck, F. J. (2024). Detection of mosaic and population-level structural variants with Sniffles2. *Nature Biotechnology*. https://doi.org/10.1038/s41587-023-02024-y

Thambugala, K. M., Daranagama, D. A., Phillips, A. J. L., Kannangara, S. D., & Promputtha, I. (2020). Fungi vs. Fungi in Biocontrol: An Overview of Fungal Antagonists Applied Against Fungal Plant Pathogens. *Frontiers in Cellular and Infection Microbiology*, *10*. https://doi.org/10.3389/fcimb.2020.604923

5. CONCLUDING REMARKS

- *Ss* is variable in phenotypic and genomic characteristics. The incorporation of integrated approaches to describe the pathogens' diversity are crucial.
- Mycelial Compatibility Group testing continue to be a useful tool in *Ss* population studies, as long as the basis of mycelial compatibility are understood. We provided novel insights into a classification system based on frequency and geographic dispersal of MCGs.
- Adopting novel sequencing technologies that capture large genomic variations as SVs is advised and encouraged.

FUTURE PERSPECTIVES

Overall, our research studied the intricacies of samples that displayed mixed compatibility on the MCGs assays across geographic barriers. While we have laid the groundwork for understanding the dynamics of isolate compatibility across both proximal and distant locations in Canada, further study guaranties explanation of the complexity of these relationships. Our hypotheses, though foundational remains constrained by the limited scope of our initial investigations.

To overcome these limitations, we propose whole genomic characterizations of all samples of interest. This will involve selecting key isolates that exemplify the phenomena we aim to explain. For example, isolates displaying mixed compatibility may harbor significant genomic variations that contribute to their plasticity. Therefore, it will be crucial to validate these findings through microscopic analysis of the events occurring at the fusion area, combined with whole genome sequencing of representative isolates from each MCGs. Particular emphasis should be placed on isolates exhibiting the highest degree of mixed compatibility.

Moreover, expanding the diversity of our samples will allow for a broader representation of geographic regions and isolate types. This expanded diversity will enhance our understanding of the genetic underpinnings and environmental interactions that drive mixed compatibility, ultimately contributing to more comprehensive and robust conclusions.

To utilize the most aggressive isolates, evaluated in our research as they offer a promising source to incorporate in multi-isolate evaluation of potential sources of resistance germplasm in common bean and other pulses. This approach will ensure that the screening process accounts for the real threat posed by *Ss* isolates in commercial fields. Currently in our lab, a diverse set of common bean varieties with known and unknown resistance traits are being screened. We propose adopting isolates with high aggressiveness levels for genomic analysis and QTL mapping to identify genetic markers linked to resistance.

Incorporating more isolates for a broader representation in genomic variation studies will yield more comprehensive and interesting results like understanding specific sources of genomic variations driving phenotypic traits such as pathogenicity. In this study, our genomic evaluation included only two isolates with various levels of aggressiveness, we propose expanding our study

to include a larger number of isolates. This will ensure a more accurate representations of the genetic diversity and evolutionary dynamics of the pathogen, enhancing our understanding of resistance mechanisms and improving the reliability of our findings.

FINAL ACKNOWLEDGMENTS

I would like to extend a final heartfelt appreciation to my dear friend Jérôme Gélinas Bélanger for listening patiently to my struggles and offering me his time by sitting on explaining some questions that I had in my final chapter, where he contributed helping me with the Circa plot to summarize my results. I really appreciate his time and experience.

6. APPENDICES

APPENDIX A

Table A. Displays detailed information on all *Ss* samples used in this research, collected from three Canadian provinces. Each sample ID consists of a letter representing the province (Alberta=A, Quebec=Q, Ontario=O) and a numerical identifier indicating the collection order. Additional data, including host, year of collection, collector, and GPS coordinates, are also provided for comprehensive insight.

Table F. Interprovincial set of *Ss* samples.

ID	Location	Host	Year of collection	GPS coordinates
Q1	Sherbrooke, QC.	*Glycine max*	Fall 2021	45.34930 -71.79073
Q2	Saint-Jean-sur-Richelieu, QC.	*Glycine max*	Fall 2021	45.382366 -73.235753
Q3	Princeville, QC	*Glycine max*	Fall 2021	46.14131217 -71.8609087
Q4	Shawville, QC.	*Glycine max*	Fall 2021	45.624639-76.566528
Q5	Shawville, QC.	*Glycine max*	Fall 2021	45.625517-76.566533
Q6	Shawville, QC.	*Glycine max*	Fall 2021	45.624783-76.565169
O7	South Glengarry, ON	*Glycine max*	Fall 2021	45.3216667-74.510556
O8	Alexandria, ON	*Glycine max*	Fall 2021	45.401111-74.616111
O9	Martintown, ON	*Glycine max*	Fall 2021	45.134167-74.723611
O10	South Glengarry, ON	*Glycine max*	Fall 2021	45.150556-74.734722
O11	Edwardsburgh/Cardinal, ON	*Glycine max*	Fall 2021	44.850833-75.47
Q12	Saint Jaques le Mineur, QC	*Glycine max*	Fall 2021	45.302917, -73.443456
Q13	Saint Bernard de Lacolle, QC	*Glycine max*	Fall 2021	45.066429, -73.474604
Q14	Cookshire-Eaton, QC	*Glycine max*	Fall 2022	45.3528437, -71.7888578
Q15	Dudswel, QC	*Glycine max*	Fall 2022	45.5733291, -71.6011245
Q16	Charette, QC	*P. vulgaris*	Fall 2022	46.46, -72.924444
Q17	La Grande-Acadie, QC	*P. vulgaris*	Fall 2022	46.325, -72.863889
Q18	La Grande-Acadie, QC	*P. vulgaris*	Fall 2022	46.324167, -72.864167
Q19	Charette, QC	*P. vulgaris*	Fall 2022	46.428611, -72.926389
Q20	Lethbrigde, AB	*P. vulgaris*	Unknown	Estimate location assigned
Q22	LODS McGill, QC	*P. vulgaris*	Fall 2021	45.4225, -73.946944
A23	Taber, AB	*P. vulgaris*	Fall 2020	49.778851, -112.048622
A24	Bow Island, AB	*P. vulgaris*	Fall 2020	49.702367, -111.432732
A25	Bow Island, AB	*P. vulgaris*	Fall 2020	49.83279, -111.545617
A26	Enchant, AB	*P. vulgaris*	Fall 2020	50.146297, -112.376104
A27	Enchant, AB	*P. vulgaris*	Fall 2020	50.21172, -112.521637
A28	Enchant, AB	*P. vulgaris*	Fall 2020	50.25553, -112.599189
A29	Lethbrigde, AB	*P. vulgaris*	Fall 2020	49.825403, -112.738694

A30	Lethbridge **	*P. vulgaris*	Fall 2021	49.825403, -112.738694
A31	Vauxhall	*P. vulgaris*	Fall 2021	50.175, -111.989
A32	Taber	*P. vulgaris*	Fall 2021	49.782, -112.2
A33	Bow Island	*P. vulgaris*	Fall 2021	49.687673, -111.432713
A34	Taber	*P. vulgaris*	Fall 2021	49.775, -112.054
A35	Taber	*P. vulgaris*	Fall 2021	49.782, -112.2
A36	Lethbrigde	*P. vulgaris*	Fall 2021	49.825403, -112.738694
A37	Vauxhall	*P. vulgaris*	Fall 2021	50.175, -111.989
A38	Vauxhall	*P. vulgaris*	Fall 2021	50.175, -111.989

APPENDIX B.

Table B. Contains the details on *Ss* samples from the Proximal subset, characterized for its collection in adjacent crops in an organic farm in Quebec, they were utilized to contrast its responses to the responses of the Interprovincial subset in the MCG testing. Each sample's ID consists of a numerical identifier followed by the "F" letter representing its provenance from a farm. Similar to the Interprovincial set, additional data such as host, year of collection, collector, and GPS coordinates, are also provided.

Table G. Proximal subset of *Ss* samples.

ID	Location	Host	Year of collection	GPS coordinates
1F	Saint Apolinaire, QC.	*Nicotiana silvestris*	Fall 2021	46.611346 -71.572284
2F	Saint Apolinaire, QC.	*Cosmos bipinnatus*	Fall 2021	46.611060 -71.572051
3F	Saint Apolinaire, QC.	*Zinnia elegans*	Fall 2021	46.609450 -71.574243
4F	Saint Apolinaire, QC.	*Digitalis purpurea*	Fall 2021	Isaac and Catherine
5F	Saint Apolinaire, QC.	*Echium vulgare*	Fall 2021	46.610914 -71.572830
6F	Saint Apolinaire, QC.	*P. vulgaris*	Fall 2021	46.611164 -71.572887
7F	Saint Apolinaire, QC.	*P. vulgaris*	Fall 2021	46.610608 -71.573887
8F	Saint Apolinaire, QC.	*Zinnia elegans*	Fall 2021	46.611262 -71.572238
9F	Saint Apolinaire, QC.	*P. vulgaris*	Fall 2021	46.609797 -71.574261
10F	Saint Apolinaire, QC.	*Lactuca sativa*	Fall 2021	46.611299 -71.572468
11F	Saint Apolinaire, QC.	*P. vulgaris*	Fall 2021	46.613148 -71.573363
12F	Saint Apolinaire, QC.	*Lactuca sativa*	Fall 2021	46.611113 -71.572763
13F	Saint Apolinaire, QC.	*Helianthus annus*	Fall 2021	46.611357 -71.572256
14F	Saint Apolinaire, QC.	*Lactuca sativa*	Fall 2021	46.610869 -71.572519
15F	Saint Apolinaire, QC.	*Lactuca sativa*	Fall 2021	46.610848 -71.573754
16F	Saint Apolinaire, QC.	*P. vulgaris*	Fall 2021	46.609303 -71.574168
17F	Saint Apolinaire, QC.	*Lactuca sativa*	Fall 2021	46.610544 -71.573836
18F	Saint Apolinaire, QC.	*Lactuca sativa*	Fall 2021	46.611117 -71.572084
19F	Saint Apolinaire, QC.	*Brassica oleracea*	Fall 2021	46.610730 -71.573959
20F	Saint Apolinaire, QC.	*Lactuca sativa*	Fall 2021	46.611551 -71.573300
21F	Saint Apolinaire, QC.	*P. vulgaris*	Fall 2021	46.610379 -71.573423

22F	Saint Apolinaire, QC.	*P. vulgaris*	Fall 2021	46.615792 -71.554180
23F	Saint Apolinaire, QC.	*P. vulgaris*	Fall 2021	46.611416 -71.572495
24F	Saint Apolinaire, QC.	*P. vulgaris*	Fall 2021	46.609860 -71.571286
25F	Saint Apolinaire, QC.	*Zinnia elegans*	Fall 2021	46.610909 -71.572678
26F	Saint Apolinaire, QC.	*P. vulgaris*	Fall 2021	46.610803 -71.572386
27F	Saint Apolinaire, QC.	*Cosmos bipinnatus*	Fall 2021	46.609620 -71.574524
28F	Saint Apolinaire, QC.	*Cosmos sulphureus*	Fall 2021	46.613205 -71.573318
29F	Saint Apolinaire, QC.	*Lactuca sativa*	Fall 2021	46.613205 -71.573318
30F	Saint Apolinaire, QC.	*P. vulgaris*	Fall 2021	46.611116 -71.572072

APPENDIX C.

Figure C. Pairing-matrix for the Interprovincial set showing the combinations in which all *Ss* isolates were challenged against each other in an isolate-by-isolate pairing matrix. This ensures confrontation in non-self-combination as well as self-to-self-confrontation as a control for compatibility. All reactions were recorded to establish distinct Mycelia Compatibility Groups (MCGs). In the matrix, 'C' indicates compatible pairings (colored green), and 'I' indicates incompatible reactions (colored yellow) for clearer visualization.

Figure C. Pairing-matrix for Interprovincial set

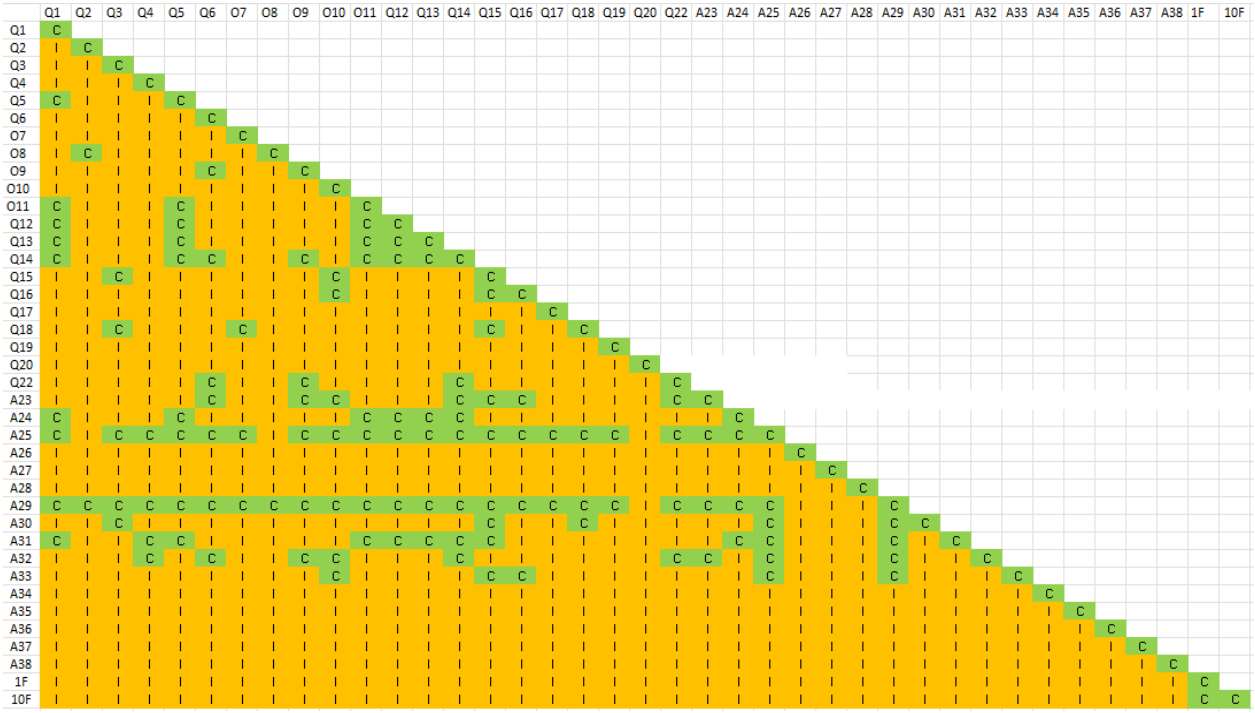

APPENDIX D.

Figure D. Displays pairing-matrix for the proximal subset showing the combinations in which all *Ss* isolates collected in a farm proximal location were challenged against each other in an isolate-by-isolate pairing matrix. All reactions are displayed with a 'C' indicating compatible pairings (colored green), and 'I' indicating incompatible reactions (colored yellow).

Figure D.1. Pairing-matrix for Proximal subset

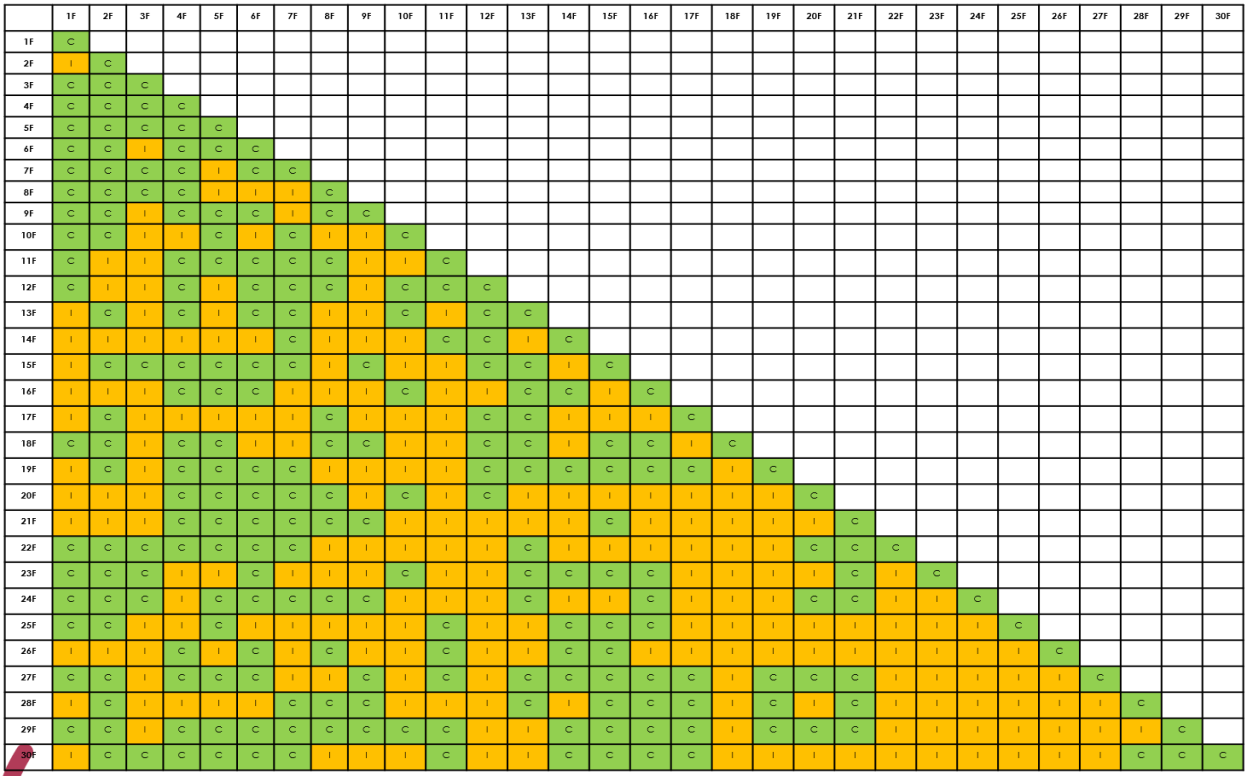

APPENDIX E.

Table E. Descriptive Statistics. The table provides a summary of the STAUDPC mean values for 34 *Sclerotinia sclerotiorum* isolates, along with the standard error, when inoculated into susceptible cultivar Beryl and moderately resistant landrace G122.

Estimates

Dependent Variable: STAUDPC

				95% Confidence Interval	
Cultivar	Isolate	Mean	Std. Error	Lower Bound	Upper Bound
Beryl	Q1	12.033	.365	11.314	12.751
	Q2	12.371	.391	11.603	13.140
	Q4	12.497	.422	11.667	13.327
	Q5	13.234	.365	12.515	13.952
	Q6	12.710	.345	12.032	13.388
	O7	12.622	.422	11.792	13.452
	O8	12.439	.391	11.670	13.207
	O9	13.720	.391	12.952	14.488
	O10	12.020	.422	11.190	12.850
	O11	12.320	.391	11.552	13.088
	Q12	13.304	.391	12.536	14.073
	Q13	12.137	.391	11.369	12.906
	Q16	12.756	.365	12.038	13.475
	Q17	13.134	.391	12.366	13.903
	Q18	12.063	.517	11.046	13.079
	Q19	14.354	.391	13.586	15.123
	A20	12.959	.391	12.190	13.727
	Q22	11.044	.462	10.135	11.953
	A23	13.132	.422	12.302	13.962
	A24	12.967	.391	12.199	13.736
	A25	12.082	.462	11.173	12.991
	A26	10.766	.462	9.857	11.675
	A27	10.912	.462	10.003	11.821
	A28	12.986	.391	12.217	13.754
	A29	11.563	.517	10.546	12.579
	A31	12.262	.345	11.585	12.940
	A32	12.837	.345	12.159	13.514
	A33	12.715	.422	11.885	13.545

	A35	12.718	.422	11.888	13.548
	A36	12.931	.345	12.253	13.609
	A37	11.874	.365	11.155	12.592
	A38	11.448	.462	10.539	12.357
	1F	12.328	.462	11.419	13.237
	10F	12.668	.462	11.759	13.577
G122	Q1	6.903	.422	6.073	7.733
	Q2	8.966	.391	8.197	9.734
	Q4	8.603	.345	7.926	9.281
	Q5	8.418	.462	7.509	9.327
	Q6	9.152	.517	8.136	10.169
	O7	8.811	.391	8.043	9.580
	O8	7.825	.422	6.995	8.655
	O9	8.354	.391	7.586	9.123
	O10	8.361	.391	7.593	9.130
	O11	7.994	.462	7.085	8.903
	Q12	8.038	.422	7.208	8.868
	Q13	9.240	.365	8.521	9.959
	Q16	9.592	.422	8.762	10.422
	Q17	8.530	.462	7.621	9.439
	Q18	8.934	.462	8.025	9.843
	Q19	9.678	.517	8.661	10.694
	A20	8.383	.422	7.553	9.213
	Q22	7.801	.391	7.033	8.570
	A23	8.171	.391	7.403	8.940
	A24	9.340	.422	8.510	10.170
	A25	8.943	.391	8.174	9.711
	A26	6.857	.422	6.027	7.687
	A27	8.215	.517	7.199	9.231
	A28	7.902	.462	6.993	8.811
	A29	8.866	.462	7.957	9.775
	A31	7.529	.365	6.810	8.247
	A32	7.980	.365	7.261	8.699
	A33	7.064	.462	6.155	7.973
	A35	7.860	.462	6.951	8.769
	A36	8.403	.391	7.634	9.171
	A37	8.640	.462	7.731	9.549
	A38	9.054	.391	8.286	9.823
	1F	7.422	.462	6.513	8.331
	10F	7.366	.462	6.457	8.275

APPENDIX F.

Table F. Pairwise comparisons. This table presents the results of Fisher's Least Significant Difference (LSD) post hoc analysis for the mean STAUDPC of 34 *Sclerotinia sclerotiorum* on the susceptible cultivar Beryl and moderately resistant landrace G122. The table includes mean differences between isolates, along with their significance levels.

Estimates

Dependent Variable: STAUDPC

Cultivar	Isolate	Mean difference	Std. Error	Sig.[b]	95% Confidence Interval	
					Lower Bound	Upper Bound
Beryl	Q1vs.Q2	-0.339	0.535	0.527	-1.391	0.713
	Q1vs.Q4	-0.464	0.558	0.406	-1.562	0.634
	Q1vs.Q5	-1.201*	0.517	0.021	-2.218	-0.185
	Q1vs.Q6	-0.678	0.502	0.178	-1.665	0.31
	Q1vs.O7	-0.589	0.558	0.292	-1.687	0.509
	Q1vs.O8	-0.406	0.535	0.448	-1.458	0.646
	Q1vs.O9	-1.688*	0.535	0.002	-2.74	-0.635
	Q1vs.O10	0.012	0.558	0.982	-1.085	1.11
	Q1vs.O11	-0.288	0.535	0.591	-1.34	0.765
	Q1vs.Q12	-1.272*	0.535	0.018	-2.324	-0.22
	Q1vs.Q13	-0.105	0.535	0.845	-1.157	0.947
	Q1vs.Q16	-0.724	0.517	0.162	-1.74	0.293
	Q1vs.Q17	-1.102*	0.535	0.04	-2.154	-0.05
	Q1vs.Q18	-0.03	0.633	0.962	-1.275	1.215
	Q1vs.Q19	-2.322*	0.535	0	-3.374	-1.27
	Q1vs.A20	-0.926	0.535	0.084	-1.978	0.126
	Q1vs.A22	0.988	0.589	0.094	-0.17	2.147
	Q1vs.A23	-1.099*	0.558	0.05	-2.197	-0.001
	Q1vs.A24	-0.935	0.535	0.081	-1.987	0.117
	Q1vs.A25	-0.05	0.589	0.933	-1.208	1.109
	Q1vs.A26	1.266*	0.589	0.032	0.108	2.425
	Q1vs.A27	1.121	0.589	0.058	-0.038	2.279
	Q1vs.A28	-0.953	0.535	0.076	-2.005	0.099
	Q1vs.A29	0.47	0.633	0.458	-0.775	1.715
	Q1vs.A31	-0.23	0.502	0.648	-1.218	0.758
	Q1vs.A32	-0.804	0.502	0.11	-1.792	0.184
	Q1vs.A33	-0.683	0.558	0.222	-1.78	0.415
	Q1vs.A35	-0.686	0.558	0.22	-1.784	0.412
	Q1vs.A36	-0.899	0.502	0.074	-1.886	0.089
	Q1vs.A37	0.159	0.517	0.759	-0.858	1.175
	Q1vs.A38	0.584	0.589	0.322	-0.574	1.743

	Q1vs.1F	-0.296	0.589	0.616	-1.454	0.863
	Q1vs.10F	-0.635	0.589	0.282	-1.794	0.523
	Q2vs.Q1	0.339	0.535	0.527	-0.713	1.391
	Q2vs.Q4	-0.125	0.575	0.828	-1.256	1.006
	Q2vs.Q5	-0.862	0.535	0.108	-1.914	0.19
	Q2vs.Q6	-0.339	0.521	0.516	-1.363	0.686
	Q2vs.O7	-0.25	0.575	0.664	-1.381	0.881
	Q2vs.O8	-0.067	0.553	0.903	-1.154	1.02
	Q2vs.O9	-1.349*	0.553	0.015	-2.435	-0.262
	Q2vs.O10	0.351	0.575	0.542	-0.78	1.482
	Q2vs.O11	0.051	0.553	0.926	-1.035	1.138
	Q2vs.Q12	-0.933	0.553	0.092	-2.02	0.154
	Q2vs.Q13	0.234	0.553	0.672	-0.852	1.321
	Q2vs.Q16	-0.385	0.535	0.472	-1.437	0.667
	Q2vs.Q17	-0.763	0.553	0.168	-1.85	0.324
	Q2vs.Q18	0.309	0.648	0.634	-0.965	1.583
	Q2vs.Q19	-1.983*	0.553	0	-3.07	-0.896
	Q2vs.A20	-0.587	0.553	0.289	-1.674	0.5
Beryl	Q2vs.Q22	1.327*	0.605	0.029	0.137	2.518
	Q2vs.A23	-0.76	0.575	0.187	-1.891	0.371
	Q2vs.A24	-0.596	0.553	0.282	-1.682	0.491
	Q2vs.A25	0.289	0.605	0.633	-0.901	1.48
	Q2vs.A26	1.605*	0.605	0.008	0.415	2.796
	Q2vs.A27	1.459*	0.605	0.016	0.269	2.65
	Q2vs.A28	-0.614	0.553	0.267	-1.701	0.472
	Q2vs.A29	0.809	0.648	0.213	-0.465	2.083
	Q2vs.A31	0.109	0.521	0.834	-0.915	1.134
	Q2vs.A32	-0.465	0.521	0.372	-1.49	0.559
	Q2vs.A33	-0.344	0.575	0.551	-1.475	0.787
	Q2vs.A35	-0.347	0.575	0.547	-1.478	0.784
	Q2vs.A36	-0.56	0.521	0.283	-1.584	0.465
	Q2vs.A37	0.498	0.535	0.353	-0.554	1.55
	Q2vs.A38	0.923	0.605	0.128	-0.267	2.114
	Q2vs.1F	0.043	0.605	0.943	-1.147	1.234
	Q2vs.10F	-0.297	0.605	0.624	-1.487	0.894
	Q4vs.Q1	0.464	0.558	0.406	-0.634	1.562
	Q4vs.Q2	0.125	0.575	0.828	-1.006	1.256
	Q4vs.Q5	-0.737	0.558	0.188	-1.835	0.361
Beryl	Q4vs.Q6	-0.213	0.545	0.696	-1.285	0.858
	Q4vs.O7	-0.125	0.597	0.834	-1.299	1.049
	Q4vs.O8	0.058	0.575	0.92	-1.073	1.189
	Q4vs.O9	-1.223*	0.575	0.034	-2.354	-0.092

	Q4vs.O10	0.477	0.597	0.425	-0.697	1.65
	Q4vs.O11	0.177	0.575	0.759	-0.954	1.308
	Q4vs.Q12	-0.808	0.575	0.161	-1.939	0.323
	Q4vs.Q13	0.36	0.575	0.532	-0.771	1.491
	Q4vs.Q16	-0.26	0.558	0.642	-1.357	0.838
	Q4vs.Q17	-0.638	0.575	0.268	-1.769	0.493
	Q4vs.Q18	0.434	0.667	0.516	-0.878	1.746
	Q4vs.Q19	-1.858*	0.575	0.001	-2.989	-0.727
	Q4vs.A20	-0.462	0.575	0.422	-1.593	0.669
	Q4vs.Q22	1.453*	0.626	0.021	0.222	2.684
	Q4vs.A23	-0.635	0.597	0.288	-1.809	0.539
	Q4vs.A24	-0.47	0.575	0.414	-1.601	0.661
	Q4vs.A25	0.415	0.626	0.508	-0.816	1.646
	Q4vs.A26	1.731*	0.626	0.006	0.5	2.962
	Q4vs.A27	1.585*	0.626	0.012	0.354	2.816
	Q4vs.A28	-0.489	0.575	0.396	-1.62	0.642
	Q4vs.A29	0.934	0.667	0.162	-0.378	2.246
	Q4vs.A31	0.234	0.545	0.667	-0.837	1.306
	Q4vs.A32	-0.34	0.545	0.533	-1.411	0.731
	Q4vs.A33	-0.218	0.597	0.715	-1.392	0.955
	Q4vs.A35	-0.222	0.597	0.711	-1.395	0.952
	Q4vs.A36	-0.434	0.545	0.426	-1.506	0.637
	Q4vs.A37	0.623	0.558	0.265	-0.475	1.721
	Q4vs.A38	1.049	0.626	0.095	-0.182	2.28
	Q4vs.1F	0.169	0.626	0.788	-1.062	1.4
	Q4vs.10F	-0.171	0.626	0.784	-1.402	1.06
Beryl	Q5vs.Q1	1.201*	0.517	0.021	0.185	2.218
	Q5vs.Q2	0.862	0.535	0.108	-0.19	1.914
	Q5vs.Q4	0.737	0.558	0.188	-0.361	1.835
	Q5vs.Q6	0.524	0.502	0.298	-0.464	1.512
	Q5vs.O7	0.612	0.558	0.274	-0.486	1.71
	Q5vs.O8	0.795	0.535	0.138	-0.257	1.847
	Q5vs.O9	-0.486	0.535	0.364	-1.538	0.566
	Q5vs.O10	1.214*	0.558	0.03	0.116	2.312
	Q5vs.O11	0.914	0.535	0.089	-0.138	1.966
	Q5vs.Q12	-0.071	0.535	0.895	-1.123	0.982
	Q5vs.Q13	1.097*	0.535	0.041	0.044	2.149
	Q5vs.Q16	0.477	0.517	0.356	-0.539	1.494
	Q5vs.Q17	0.099	0.535	0.853	-0.953	1.152
	Q5vs.Q18	1.171	0.633	0.065	-0.074	2.416
	Q5vs.Q19	-1.121*	0.535	0.037	-2.173	-0.068
	Q5vs.A20	0.275	0.535	0.607	-0.777	1.327

	Q5vs.Q22	2.190*	0.589	0	1.031	3.349
	Q5vs.A23	0.102	0.558	0.855	-0.996	1.2
	Q5vs.A24	0.267	0.535	0.619	-0.786	1.319
	Q5vs.A25	1.152	0.589	0.051	-0.007	2.311
	Q5vs.A26	2.468*	0.589	0	1.309	3.627
	Q5vs.A27	2.322*	0.589	0	1.163	3.481
	Q5vs.A28	0.248	0.535	0.643	-0.804	1.3
	Q5vs.A29	1.671*	0.633	0.009	0.426	2.916
	Q5vs.A31	0.972	0.502	0.054	-0.016	1.959
	Q5vs.A32	0.397	0.502	0.43	-0.591	1.385
	Q5vs.A33	0.519	0.558	0.353	-0.579	1.617
	Q5vs.A35	0.515	0.558	0.357	-0.582	1.613
	Q5vs.A36	0.303	0.502	0.547	-0.685	1.29
	Q5vs.A37	1.360*	0.517	0.009	0.344	2.376
	Q5vs.A38	1.786*	0.589	0.003	0.627	2.945
	Q5vs.1F	0.906	0.589	0.125	-0.253	2.065
	Q5vs.10F	0.566	0.589	0.338	-0.593	1.725
Beryl	Q6vs.Q1	0.678	0.502	0.178	-0.31	1.665
	Q6vs.Q2	0.339	0.521	0.516	-0.686	1.363
	Q6vs.Q4	0.213	0.545	0.696	-0.858	1.285
	Q6vs.Q5	-0.524	0.502	0.298	-1.512	0.464
	Q6vs.O7	0.088	0.545	0.871	-0.983	1.16
	Q6vs.O8	0.271	0.521	0.603	-0.753	1.296
	Q6vs.O9	-1.01	0.521	0.053	-2.034	0.014
	Q6vs.O10	0.69	0.545	0.206	-0.381	1.761
	Q6vs.O11	0.39	0.521	0.455	-0.634	1.414
	Q6vs.Q12	-0.594	0.521	0.255	-1.619	0.43
	Q6vs.Q13	0.573	0.521	0.272	-0.452	1.597
	Q6vs.Q16	-0.046	0.502	0.927	-1.034	0.942
	Q6vs.Q17	-0.424	0.521	0.416	-1.449	0.6
	Q6vs.Q18	0.648	0.621	0.298	-0.574	1.869
	Q6vs.Q19	-1.644*	0.521	0.002	-2.669	-0.62
	Q6vs.A20	-0.249	0.521	0.634	-1.273	0.776
	Q6vs.Q22	1.666*	0.577	0.004	0.532	2.8
	Q6vs.A23	-0.422	0.545	0.439	-1.493	0.65
	Q6vs.A24	-0.257	0.521	0.622	-1.282	0.767
	Q6vs.A25	0.628	0.577	0.277	-0.506	1.762
	Q6vs.A26	1.944*	0.577	0.001	0.81	3.078
	Q6vs.A27	1.798*	0.577	0.002	0.664	2.932
	Q6vs.A28	-0.276	0.521	0.597	-1.3	0.749
	Q6vs.A29	1.148	0.621	0.066	-0.074	2.369
	Q6vs.A31	0.448	0.487	0.359	-0.511	1.406

	Q6vs.A32	-0.127	0.487	0.795	-1.085	0.832
	Q6vs.A33	-0.005	0.545	0.993	-1.076	1.066
	Q6vs.A35	-0.008	0.545	0.988	-1.08	1.063
	Q6vs.A36	-0.221	0.487	0.65	-1.179	0.737
	Q6vs.A37	0.836	0.502	0.097	-0.152	1.824
	Q6vs.A38	1.262*	0.577	0.029	0.128	2.396
	Q6vs.1F	0.382	0.577	0.508	-0.752	1.516
	Q6vs.10F	0.042	0.577	0.942	-1.092	1.176
	O7vs.Q1	0.589	0.558	0.292	-0.509	1.687
	O7vs.Q2	0.25	0.575	0.664	-0.881	1.381
	O7s.Q4	0.125	0.597	0.834	-1.049	1.299
	O7vs.Q5	-0.612	0.558	0.274	-1.71	0.486
	O7vs.O6	-0.088	0.545	0.871	-1.16	0.983
	O7vs.O8	0.183	0.575	0.75	-0.948	1.314
	O7vs.O9	-1.098	0.575	0.057	-2.229	0.033
	O7vs.O10	0.602	0.597	0.314	-0.572	1.775
	O7vs.O11	0.302	0.575	0.6	-0.829	1.433
	O7vs.Q12	-0.683	0.575	0.236	-1.814	0.448
	O7vs.Q13	0.485	0.575	0.4	-0.646	1.616
	O7vs.Q16	-0.135	0.558	0.81	-1.232	0.963
	O7vs.Q17	-0.513	0.575	0.373	-1.644	0.618
	O7vs.Q18	0.559	0.667	0.403	-0.753	1.871
	O7vs.Q19	-1.733*	0.575	0.003	-2.864	-0.602
	O7vs.A20	-0.337	0.575	0.558	-1.468	0.794
Beryl	O7vs.Q22	1.578*	0.626	0.012	0.347	2.809
	O7vs.A23	-0.51	0.597	0.393	-1.684	0.664
	O7vs.A24	-0.345	0.575	0.548	-1.476	0.786
	O7vs.A25	0.54	0.626	0.389	-0.691	1.771
	O7vs.A26	1.856*	0.626	0.003	0.625	3.087
	O7vs.A27	1.710*	0.626	0.007	0.479	2.941
	O7vs.A28	-0.364	0.575	0.527	-1.495	0.767
	O7vs.A29	1.059	0.667	0.113	-0.253	2.371
	O7vs.A31	0.359	0.545	0.51	-0.712	1.431
	O7vs.A32	-0.215	0.545	0.693	-1.286	0.856
	O7vs.A33	-0.093	0.597	0.876	-1.267	1.08
	O7vs.A35	-0.097	0.597	0.871	-1.27	1.077
	O7vsA36	-0.309	0.545	0.57	-1.381	0.762
	O7vs.A37	0.748	0.558	0.181	-0.35	1.846
	O7vs.A38	1.174	0.626	0.062	-0.057	2.405
	O7vs.1F	0.294	0.626	0.639	-0.937	1.525
	O7vs.10F	-0.046	0.626	0.941	-1.277	1.185
Beryl	O8vs.Q1	0.406	0.535	0.448	-0.646	1.458

	O8vs.Q2	0.067	0.553	0.903	-1.02	1.154
	O8s.Q4	-0.058	0.575	0.92	-1.189	1.073
	O8vs.Q5	-0.795	0.535	0.138	-1.847	0.257
	O8vs.O6	-0.271	0.521	0.603	-1.296	0.753
	O8vs.O7	-0.183	0.575	0.75	-1.314	0.948
	O8vs.O9	-1.281*	0.553	0.021	-2.368	-0.195
	O8vs.O10	0.419	0.575	0.467	-0.712	1.55
	O8vs.O11	0.119	0.553	0.83	-0.968	1.205
	O8vs.Q12	-0.866	0.553	0.118	-1.952	0.221
	O8vs.Q13	0.301	0.553	0.586	-0.785	1.388
	O8vs.Q16	-0.318	0.535	0.553	-1.37	0.734
	O8vs.Q17	-0.696	0.553	0.209	-1.782	0.391
	O8vs.Q18	0.376	0.648	0.562	-0.898	1.65
	O8vs.Q19	-1.916*	0.553	0.001	-3.002	-0.829
	O8vs.A20	-0.52	0.553	0.347	-1.607	0.567
	O8vs.Q22	1.395*	0.605	0.022	0.204	2.585
	O8vs.A23	-0.693	0.575	0.229	-1.824	0.438
	O8vs.A24	-0.529	0.553	0.339	-1.615	0.558
	O8vs.A25	0.357	0.605	0.556	-0.834	1.547
	O8vs.A26	1.673*	0.605	0.006	0.482	2.863
	O8vs.A27	1.527*	0.605	0.012	0.336	2.717
	O8vs.A28	-0.547	0.553	0.323	-1.634	0.54
	O8vs.A29	0.876	0.648	0.177	-0.398	2.15
	O8vs.A31	0.176	0.521	0.735	-0.848	1.201
	O8vs.A32	-0.398	0.521	0.445	-1.423	0.626
	O8vs.A33	-0.276	0.575	0.631	-1.407	0.855
	O8vs.A35	-0.28	0.575	0.627	-1.411	0.851
	O8vsA36	-0.493	0.521	0.345	-1.517	0.532
	O8vs.A37	0.565	0.535	0.292	-0.487	1.617
	O8vs.A38	0.991	0.605	0.103	-0.2	2.181
	O8vs.1F	0.111	0.605	0.855	-1.08	1.301
	O8vs.10F	-0.229	0.605	0.705	-1.42	0.961
Beryl	O9vs.Q1	1.688*	0.535	0.002	0.635	2.74
	O9vs.Q2	1.349*	0.553	0.015	0.262	2.435
	O9vs.Q4	1.223*	0.575	0.034	0.092	2.354
	O9vs.Q5	0.486	0.535	0.364	-0.566	1.538
	O9vs.O6	1.01	0.521	0.053	-0.014	2.034
	O9vs.O7	1.098	0.575	0.057	-0.033	2.229
	O9vs.O8	1.281*	0.553	0.021	0.195	2.368
	O9vs.O10	1.700*	0.575	0.003	0.569	2.831
	O9vs.O11	1.400*	0.553	0.012	0.313	2.487

	O9vs.Q12	0.416	0.553	0.452	-0.671	1.502
	O9vs.Q13	1.583*	0.553	0.004	0.496	2.67
	O9vs.Q16	0.964	0.535	0.072	-0.088	2.016
	O9vs.Q17	0.586	0.553	0.29	-0.501	1.672
	O9vs.Q18	1.657*	0.648	0.011	0.383	2.932
	O9vs.Q19	-0.634	0.553	0.252	-1.721	0.452
	O9vs.A20	0.761	0.553	0.169	-0.325	1.848
	O9vs.Q22	2.676*	0.605	0	1.486	3.866
	O9vs.A23	0.588	0.575	0.307	-0.543	1.719
	O9vs.A24	0.753	0.553	0.174	-0.334	1.84
	O9vs.A25	1.638*	0.605	0.007	0.448	2.828
	O9vs.A26	2.954*	0.605	0	1.764	4.144
	O9vs.A27	2.808*	0.605	0	1.618	3.998
	O9vs.A28	0.734	0.553	0.185	-0.352	1.821
	O9vs.A29	2.158*	0.648	0.001	0.883	3.432
	O9vs.A31	1.458*	0.521	0.005	0.433	2.482
	O9vs.A32	0.883	0.521	0.091	-0.141	1.908
	O9vs.A33	1.005	0.575	0.081	-0.126	2.136
	O9vs.A35	1.002	0.575	0.082	-0.129	2.133
	O9vsA36	0.789	0.521	0.131	-0.236	1.813
	O9vs.A37	1.846*	0.535	0.001	0.794	2.898
	O9vs.A38	2.272*	0.605	0	1.082	3.462
	O9vs.1F	1.392*	0.605	0.022	0.202	2.582
	O9vs.10F	1.052	0.605	0.083	-0.138	2.242
	O10vs.Q1	-0.012	0.558	0.982	-1.11	1.085
	O10vs.Q2	-0.351	0.575	0.542	-1.482	0.78
	O10vs.Q4	-0.477	0.597	0.425	-1.65	0.697
	O10vs.Q5	-1.214*	0.558	0.03	-2.312	-0.116
	O10vs.O6	-0.69	0.545	0.206	-1.761	0.381
	O10vs.O7	-0.602	0.597	0.314	-1.775	0.572
	O10vs.O8	-0.419	0.575	0.467	-1.55	0.712
	O10vs.O9	-1.700*	0.575	0.003	-2.831	-0.569
Beryl	O10vs.O11	-0.3	0.575	0.602	-1.431	0.831
	O10vs.Q12	-1.284*	0.575	0.026	-2.415	-0.153
	O10vs.Q13	-0.117	0.575	0.839	-1.248	1.014
	O10vs.Q16	-0.736	0.558	0.188	-1.834	0.362
	O10vs.Q17	-1.114	0.575	0.053	-2.245	0.017
	O10vs.Q18	-0.042	0.667	0.949	-1.355	1.27
	O10vs.Q19	-2.334*	0.575	0	-3.465	-1.203
	O10vs.A20	-0.939	0.575	0.104	-2.07	0.192
	O10vs.Q22	0.976	0.626	0.12	-0.255	2.207

	O10vs.A23	-1.112	0.597	0.063	-2.285	0.062
	O10vs.A24	-0.947	0.575	0.1	-2.078	0.184
	O10vs.A25	-0.062	0.626	0.921	-1.293	1.169
	O10vs.A26	1.254*	0.626	0.046	0.023	2.485
	O10vs.A27	1.108	0.626	0.078	-0.123	2.339
	O10vs.A28	-0.966	0.575	0.094	-2.097	0.165
	O10vs.A29	0.458	0.667	0.493	-0.855	1.77
	O10vs.A31	-0.242	0.545	0.657	-1.314	0.829
	O10vs.A32	-0.817	0.545	0.135	-1.888	0.255
	O10vs.A33	-0.695	0.597	0.245	-1.869	0.479
	O10vs.A35	-0.698	0.597	0.243	-1.872	0.475
	O10vsA36	-0.911	0.545	0.095	-1.983	0.16
	O10vs.A37	0.146	0.558	0.794	-0.952	1.244
	O10vs.A38	0.572	0.626	0.361	-0.659	1.803
	O10vs.1F	-0.308	0.626	0.623	-1.539	0.923
	O10vs.10F	-0.648	0.626	0.301	-1.879	0.583
Beryl	O11vs.Q1	0.288	0.535	0.591	-0.765	1.34
	O11vs.Q2	-0.051	0.553	0.926	-1.138	1.035
	O11vs.Q4	-0.177	0.575	0.759	-1.308	0.954
	O11vs.Q5	-0.914	0.535	0.089	-1.966	0.138
	O11vs.O6	-0.39	0.521	0.455	-1.414	0.634
	O11vs.O7	-0.302	0.575	0.6	-1.433	0.829
	O11vs.O8	-0.119	0.553	0.83	-1.205	0.968
	O11vs.O9	-1.400*	0.553	0.012	-2.487	-0.313
	O11vs.O10	0.3	0.575	0.602	-0.831	1.431
	O11vs.Q12	-0.984	0.553	0.076	-2.071	0.102
	O11vs.Q13	0.183	0.553	0.741	-0.904	1.27
	O11vs.Q16	-0.436	0.535	0.415	-1.488	0.616
	O11vs.Q17	-0.814	0.553	0.141	-1.901	0.272
	O11vs.Q18	0.257	0.648	0.691	-1.017	1.532
	O11vs.Q19	-2.034*	0.553	0	-3.121	-0.948
	O11vs.A20	-0.639	0.553	0.249	-1.725	0.448
	O11vs.Q22	1.276*	0.605	0.036	0.086	2.466
	O11vs.A23	-0.812	0.575	0.159	-1.943	0.319
	O11vs.A24	-0.647	0.553	0.242	-1.734	0.44
	O11vs.A25	0.238	0.605	0.694	-0.952	1.428
	O11vs.A26	1.554*	0.605	0.011	0.364	2.744
	O11vs.A27	1.408*	0.605	0.021	0.218	2.598
	O11vs.A28	-0.666	0.553	0.229	-1.752	0.421
	O11vs.A29	0.758	0.648	0.243	-0.517	2.032
	O11vs.A31	0.058	0.521	0.912	-0.967	1.082
	O11vs.A32	-0.517	0.521	0.322	-1.541	0.508

	O11vs.A33	-0.395	0.575	0.493	-1.526	0.736
	O11vs.A35	-0.398	0.575	0.489	-1.529	0.733
	O11vsA36	-0.611	0.521	0.242	-1.636	0.413
	O11vs.A37	0.446	0.535	0.405	-0.606	1.498
	O11vs.A38	0.872	0.605	0.151	-0.318	2.062
	O11vs.1F	-0.008	0.605	0.989	-1.198	1.182
	O11vs.10F	-0.348	0.605	0.566	-1.538	0.842
	Q12vs.Q1	1.272*	0.535	0.018	0.22	2.324
	Q12vs.Q2	0.933	0.553	0.092	-0.154	2.02
	Q12vs.Q4	0.808	0.575	0.161	-0.323	1.939
	Q12vs.Q5	0.071	0.535	0.895	-0.982	1.123
	Q12vs.O6	0.594	0.521	0.255	-0.43	1.619
	Q12vs.O7	0.683	0.575	0.236	-0.448	1.814
	Q12vs.O8	0.866	0.553	0.118	-0.221	1.952
	Q12vs.O9	-0.416	0.553	0.452	-1.502	0.671
	Q12vs.O10	1.284*	0.575	0.026	0.153	2.415
	Q12vs.O11	0.984	0.553	0.076	-0.102	2.071
	Q12vs.Q13	1.167*	0.553	0.035	0.08	2.254
	Q12vs.Q16	0.548	0.535	0.306	-0.504	1.6
	Q12vs.Q17	0.17	0.553	0.759	-0.917	1.257
	Q12vs.Q18	1.242	0.648	0.056	-0.032	2.516
	Q12vs.Q19	-1.05	0.553	0.058	-2.137	0.037
	Q12vs.A20	0.346	0.553	0.532	-0.741	1.432
Beryl	Q12vs.Q22	2.260*	0.605	0	1.07	3.451
	Q12vs.A23	0.173	0.575	0.764	-0.958	1.304
	Q12vs.A24	0.337	0.553	0.542	-0.75	1.424
	Q12vs.A25	1.222*	0.605	0.044	0.032	2.413
	Q12vs.A26	2.538*	0.605	0	1.348	3.729
	Q12vs.A27	2.392*	0.605	0	1.202	3.583
	Q12vs.A28	0.319	0.553	0.565	-0.768	1.405
	Q12vs.A29	1.742*	0.648	0.008	0.468	3.016
	Q12vs.A31	1.042*	0.521	0.046	0.018	2.067
	Q12vs.A32	0.468	0.521	0.37	-0.557	1.492
	Q12vs.A33	0.589	0.575	0.306	-0.542	1.72
	Q12vs.A35	0.586	0.575	0.309	-0.545	1.717
	Q12vsA36	0.373	0.521	0.474	-0.651	1.398
	Q12vs.A37	1.431*	0.535	0.008	0.378	2.483
	Q12vs.A38	1.856*	0.605	0.002	0.666	3.047
	Q12vs.1F	0.976	0.605	0.108	-0.214	2.167
	Q12vs.10F	0.636	0.605	0.294	-0.554	1.827
Beryl	Q13vs.Q1	0.105	0.535	0.845	-0.947	1.157

	Q13vs.Q2	-0.234	0.553	0.672	-1.321	0.852
	Q13vs.Q4	-0.36	0.575	0.532	-1.491	0.771
	Q13vs.Q5	-1.097*	0.535	0.041	-2.149	-0.044
	Q13vs.O6	-0.573	0.521	0.272	-1.597	0.452
	Q13vs.O7	-0.485	0.575	0.4	-1.616	0.646
	Q13vs.O8	-0.301	0.553	0.586	-1.388	0.785
	Q13vs.O9	-1.583*	0.553	0.004	-2.67	-0.496
	Q13vs.O10	0.117	0.575	0.839	-1.014	1.248
	Q13vs.O11	-0.183	0.553	0.741	-1.27	0.904
	Q13vs.Q12	-1.167*	0.553	0.035	-2.254	-0.08
	Q13vs.Q16	-0.619	0.535	0.248	-1.671	0.433
	Q13vs.Q17	-0.997	0.553	0.072	-2.084	0.09
	Q13vs.Q18	0.075	0.648	0.908	-1.2	1.349
	Q13vs.Q19	-2.217*	0.553	0	-3.304	-1.13
	Q13vs.A20	-0.821	0.553	0.138	-1.908	0.265
	Q13vs.Q22	1.093	0.605	0.072	-0.097	2.284
	Q13vs.A23	-0.995	0.575	0.085	-2.126	0.136
	Q13vs.A24	-0.83	0.553	0.134	-1.917	0.257
	Q13vs.A25	0.055	0.605	0.927	-1.135	1.246
	Q13vs.A26	1.371*	0.605	0.024	0.181	2.562
	Q13vs.A27	1.225*	0.605	0.044	0.035	2.416
	Q13vs.A28	-0.849	0.553	0.125	-1.935	0.238
	Q13vs.A29	0.575	0.648	0.376	-0.7	1.849
	Q13vs.A31	-0.125	0.521	0.81	-1.15	0.899
	Q13vs.A32	-0.7	0.521	0.18	-1.724	0.325
	Q13vs.A33	-0.578	0.575	0.316	-1.709	0.553
	Q13vs.A35	-0.581	0.575	0.313	-1.712	0.55
	Q13vsA36	-0.794	0.521	0.128	-1.818	0.231
	Q13vs.A37	0.263	0.535	0.623	-0.789	1.316
	Q13vs.A38	0.689	0.605	0.256	-0.501	1.88
	Q13vs.1F	-0.191	0.605	0.753	-1.381	1
	Q13vs.10F	-0.531	0.605	0.381	-1.721	0.66
Beryl	Q16vs.Q1	0.724	0.517	0.162	-0.293	1.74
	Q16vs.Q2	0.385	0.535	0.472	-0.667	1.437
	Q16vs.Q4	0.26	0.558	0.642	-0.838	1.357
	Q16vs.Q5	-0.477	0.517	0.356	-1.494	0.539
	Q16vs.O6	0.046	0.502	0.927	-0.942	1.034
	Q16vs.O7	0.135	0.558	0.81	-0.963	1.232
	Q16vs.O8	0.318	0.535	0.553	-0.734	1.37
	Q16vs.O9	-0.964	0.535	0.072	-2.016	0.088
	Q16vs.O10	0.736	0.558	0.188	-0.362	1.834
	Q16vs.O11	0.436	0.535	0.415	-0.616	1.488

	Q16vs.Q12	-0.548	0.535	0.306	-1.6	0.504
	Q16vs.Q13	0.619	0.535	0.248	-0.433	1.671
	Q16vs.Q17	-0.378	0.535	0.48	-1.43	0.674
	Q16vs.Q18	0.694	0.633	0.274	-0.551	1.939
	Q16vs.Q19	-1.598*	0.535	0.003	-2.65	-0.546
	Q16vs.A20	-0.202	0.535	0.706	-1.254	0.85
	Q16vs.Q22	1.712*	0.589	0.004	0.553	2.871
	Q16vs.A23	-0.375	0.558	0.502	-1.473	0.722
	Q16vs.A24	-0.211	0.535	0.694	-1.263	0.841
	Q16vs.A25	0.674	0.589	0.253	-0.485	1.833
	Q16vs.A26	1.990*	0.589	0.001	0.831	3.149
	Q16vs.A27	1.844*	0.589	0.002	0.685	3.003
	Q16vs.A28	-0.229	0.535	0.668	-1.282	0.823
	Q16vs.A29	1.194	0.633	0.06	-0.051	2.439
	Q16vs.A31	0.494	0.502	0.326	-0.494	1.482
	Q16vs.A32	-0.08	0.502	0.873	-1.068	0.907
	Q16vs.A33	0.041	0.558	0.941	-1.057	1.139
	Q16vs.A35	0.038	0.558	0.946	-1.06	1.136
	Q16vsA36	-0.175	0.502	0.728	-1.163	0.813
	Q16vs.A37	0.883	0.517	0.089	-0.134	1.899
	Q16vs.A38	1.308*	0.589	0.027	0.149	2.467
	Q16vs.1F	0.428	0.589	0.468	-0.731	1.587
	Q16vs.10F	0.088	0.589	0.881	-1.071	1.247
Beryl	Q17vs.Q1	1.102*	0.535	0.04	0.05	2.154
	Q17vs.Q2	0.763	0.553	0.168	-0.324	1.85
	Q17vs.Q4	0.638	0.575	0.268	-0.493	1.769
	Q17vs.Q5	-0.099	0.535	0.853	-1.152	0.953
	Q17vs.O6	0.424	0.521	0.416	-0.6	1.449
	Q17vs.O7	0.513	0.575	0.373	-0.618	1.644
	Q17vs.O8	0.696	0.553	0.209	-0.391	1.782
	Q17vs.O9	-0.586	0.553	0.29	-1.672	0.501
	Q17vs.O10	1.114	0.575	0.053	-0.017	2.245
	Q17vs.O11	0.814	0.553	0.141	-0.272	1.901
	Q17vs.Q12	-0.17	0.553	0.759	-1.257	0.917
	Q17vs.Q13	0.997	0.553	0.072	-0.09	2.084
	Q17vs.Q16	0.378	0.535	0.48	-0.674	1.43
	Q17vs.Q18	1.072	0.648	0.099	-0.202	2.346
	Q17vs.Q19	-1.220*	0.553	0.028	-2.307	-0.133
	Q17vs.A20	0.176	0.553	0.751	-0.911	1.262
	Q17vs.Q22	2.090*	0.605	0.001	0.9	3.281
	Q17vs.A23	0.003	0.575	0.996	-1.128	1.134
	Q17vs.A24	0.167	0.553	0.762	-0.92	1.254

	Q17vs.A25	1.052	0.605	0.083	-0.138	2.243
	Q17vs.A26	2.368*	0.605	0	1.178	3.559
	Q17vs.A27	2.222*	0.605	0	1.032	3.413
	Q17vs.A28	0.149	0.553	0.788	-0.938	1.235
	Q17vs.A29	1.572*	0.648	0.016	0.298	2.846
	Q17vs.A31	0.872	0.521	0.095	-0.152	1.897
	Q17vs.A32	0.298	0.521	0.568	-0.727	1.322
	Q17vs.A33	0.419	0.575	0.466	-0.712	1.55
	Q17vs.A35	0.416	0.575	0.47	-0.715	1.547
	Q17vsA36	0.203	0.521	0.697	-0.821	1.228
	Q17vs.A37	1.261*	0.535	0.019	0.208	2.313
	Q17vs.A38	1.686*	0.605	0.006	0.496	2.877
	Q17vs.1F	0.806	0.605	0.184	-0.384	1.997
	Q17vs.10F	0.466	0.605	0.442	-0.724	1.657
Beryl	Q18vs.Q1	0.03	0.633	0.962	-1.215	1.275
	Q18vs.Q2	-0.309	0.648	0.634	-1.583	0.965
	Q18vs.Q4	-0.434	0.667	0.516	-1.746	0.878
	Q18vs.Q5	-1.171	0.633	0.065	-2.416	0.074
	Q18vs.O6	-0.648	0.621	0.298	-1.869	0.574
	Q18vs.O7	-0.559	0.667	0.403	-1.871	0.753
	Q18vs.O8	-0.376	0.648	0.562	-1.65	0.898
	Q18vs.O9	-1.657*	0.648	0.011	-2.932	-0.383
	Q18vs.O10	0.042	0.667	0.949	-1.27	1.355
	Q18vs.O11	-0.257	0.648	0.691	-1.532	1.017
	Q18vs.Q12	-1.242	0.648	0.056	-2.516	0.032
	Q18vs.Q13	-0.075	0.648	0.908	-1.349	1.2
	Q18vs.Q16	-0.694	0.633	0.274	-1.939	0.551
	Q18vs.Q17	-1.072	0.648	0.099	-2.346	0.202
	Q18vs.Q19	-2.292*	0.648	0	-3.566	-1.018
	Q18vs.A20	-0.896	0.648	0.168	-2.17	0.378
	Q18vs.Q22	1.019	0.693	0.143	-0.345	2.382
	Q18vs.A23	-1.069	0.667	0.11	-2.381	0.243
	Q18vs.A24	-0.905	0.648	0.164	-2.179	0.37
	Q18vs.A25	-0.02	0.693	0.978	-1.383	1.344
	Q18vs.A26	1.297	0.693	0.062	-0.067	2.66
	Q18vs.A27	1.151	0.693	0.098	-0.213	2.514
	Q18vs.A28	-0.923	0.648	0.155	-2.197	0.351
	Q18vs.A29	0.5	0.731	0.494	-0.937	1.937
	Q18vs.A31	-0.2	0.621	0.748	-1.421	1.022
	Q18vs.A32	-0.774	0.621	0.213	-1.996	0.447
	Q18vs.A33	-0.652	0.667	0.329	-1.965	0.66
	Q18vs.A35	-0.656	0.667	0.326	-1.968	0.656

	Q18vsA36	-0.869	0.621	0.163	-2.09	0.353
	Q18vs.A37	0.189	0.633	0.766	-1.056	1.434
	Q18vs.A38	0.614	0.693	0.376	-0.749	1.978
	Q18vs.1F	-0.265	0.693	0.702	-1.629	1.098
	Q18vs.10F	-0.605	0.693	0.383	-1.969	0.758
Beryl	Q19vs.Q1	2.322*	0.535	0	1.27	3.374
	Q19vs.Q2	1.983*	0.553	0	0.896	3.07
	Q19vs.Q4	1.858*	0.575	0.001	0.727	2.989
	Q19vs.Q5	1.121*	0.535	0.037	0.068	2.173
	Q19vs.O6	1.644*	0.521	0.002	0.62	2.669
	Q19vs.O7	1.733*	0.575	0.003	0.602	2.864
	Q19vs.O8	1.916*	0.553	0.001	0.829	3.002
	Q19vs.O9	0.634	0.553	0.252	-0.452	1.721
	Q19vs.O10	2.334*	0.575	0	1.203	3.465
	Q19vs.O11	2.034*	0.553	0	0.948	3.121
	Q19vs.Q12	1.05	0.553	0.058	-0.037	2.137
	Q19vs.Q13	2.217*	0.553	0	1.13	3.304
	Q19vs.Q16	1.598*	0.535	0.003	0.546	2.65
	Q19vs.Q17	1.220*	0.553	0.028	0.133	2.307
	Q19vs.Q18	2.292*	0.648	0	1.018	3.566
	Q19vs.A20	1.396*	0.553	0.012	0.309	2.482
	Q19vs.Q22	3.310*	0.605	0	2.12	4.501
	Q19vs.A23	1.223*	0.575	0.034	0.092	2.354
	Q19vs.A24	1.387*	0.553	0.012	0.3	2.474
	Q19vs.A25	2.272*	0.605	0	1.082	3.463
	Q19vs.A26	3.588*	0.605	0	2.398	4.779
	Q19vs.A27	3.442*	0.605	0	2.252	4.633
	Q19vs.A28	1.369*	0.553	0.014	0.282	2.455
	Q19vs.A29	2.792*	0.648	0	1.518	4.066
	Q19vs.A31	2.092*	0.521	0	1.068	3.117
	Q19vs.A32	1.518*	0.521	0.004	0.493	2.542
	Q19vs.A33	1.639*	0.575	0.005	0.508	2.77
	Q19vs.A35	1.636*	0.575	0.005	0.505	2.767
	Q19vsA36	1.423*	0.521	0.007	0.399	2.448
	Q19vs.A37	2.481*	0.535	0	1.428	3.533
	Q19vs.A38	2.906*	0.605	0	1.716	4.097
	Q19vs.1F	2.026*	0.605	0.001	0.836	3.217
	Q19vs.10F	1.686*	0.605	0.006	0.496	2.877

Beryl	A20vs.Q1	0.926	0.535	0.084	-0.126	1.978
	A20vs.Q2	0.587	0.553	0.289	-0.5	1.674
	A20vs.Q4	0.462	0.575	0.422	-0.669	1.593
	A20vs.Q5	-0.275	0.535	0.607	-1.327	0.777
	A20vs.O6	0.249	0.521	0.634	-0.776	1.273
	A20vs.O7	0.337	0.575	0.558	-0.794	1.468
	A20vs.O8	0.52	0.553	0.347	-0.567	1.607
	A20vs.O9	-0.761	0.553	0.169	-1.848	0.325
	A20vs.O10	0.939	0.575	0.104	-0.192	2.07
	A20vs.O11	0.639	0.553	0.249	-0.448	1.725
	A20vs.Q12	-0.346	0.553	0.532	-1.432	0.741
	A20vs.Q13	0.821	0.553	0.138	-0.265	1.908
	A20vs.Q16	0.202	0.535	0.706	-0.85	1.254
	A20vs.Q17	-0.176	0.553	0.751	-1.262	0.911
	A20vs.Q18	0.896	0.648	0.168	-0.378	2.17
	A20vs.Q19	-1.396*	0.553	0.012	-2.482	-0.309
	A20vs.Q22	1.915*	0.605	0.002	0.724	3.105
	A20vs.A23	-0.173	0.575	0.764	-1.304	0.958
	A20vs.A24	-0.009	0.553	0.988	-1.095	1.078
	A20vs.A25	0.877	0.605	0.148	-0.314	2.067
	A20vs.A26	2.193*	0.605	0	1.002	3.383
	A20vs.A27	2.047*	0.605	0.001	0.856	3.237
	A20vs.A28	-0.027	0.553	0.961	-1.114	1.06
	A20vs.A29	1.396*	0.648	0.032	0.122	2.67
	A20vs.A31	0.696	0.521	0.182	-0.328	1.721
	A20vs.A32	0.122	0.521	0.815	-0.903	1.146
	A20vs.A33	0.244	0.575	0.672	-0.887	1.375
	A20vs.A35	0.24	0.575	0.676	-0.891	1.371
	A20vsA36	0.027	0.521	0.958	-0.997	1.052
	A20vs.A37	1.085*	0.535	0.043	0.033	2.137
	A20vs.A38	1.511*	0.605	0.013	0.32	2.701
	A20vs.1F	0.631	0.605	0.298	-0.56	1.821
	A20vs.10F	0.291	0.605	0.631	-0.9	1.481
Beryl	A22vs.Q1	-0.988	0.589	0.094	-2.147	0.17
	A22vs.Q2	-1.327*	0.605	0.029	-2.518	-0.137
	A22vs.Q4	-1.453*	0.626	0.021	-2.684	-0.222
	A22vs.Q5	-2.190*	0.589	0	-3.349	-1.031
	A22vs.O6	-1.666*	0.577	0.004	-2.8	-0.532
	A22vs.O7	-1.578*	0.626	0.012	-2.809	-0.347
	A22vs.O8	-1.395*	0.605	0.022	-2.585	-0.204
	A22vs.O9	-2.676*	0.605	0	-3.866	-1.486

	A22vs.O10	-0.976	0.626	0.12	-2.207	0.255
	A22vs.O11	-1.276*	0.605	0.036	-2.466	-0.086
	A22vs.Q12	-2.260*	0.605	0	-3.451	-1.07
	A22vs.Q13	-1.093	0.605	0.072	-2.284	0.097
	A22vs.Q16	-1.712*	0.589	0.004	-2.871	-0.553
	A22vs.Q17	-2.090*	0.605	0.001	-3.281	-0.9
	A22vs.Q18	-1.019	0.693	0.143	-2.382	0.345
	A22vs.Q19	-3.310*	0.605	0	-4.501	-2.12
	A22vs.A20	-1.915*	0.605	0.002	-3.105	-0.724
	A22vs.A23	-2.088*	0.626	0.001	-3.319	-0.857
	A22vs.A24	-1.923*	0.605	0.002	-3.114	-0.733
	A22vs.A25	-1.038	0.654	0.113	-2.324	0.248
	A22vs.A26	0.278	0.654	0.671	-1.008	1.564
	A22vs.A27	0.132	0.654	0.84	-1.154	1.418
	A22vs.A28	-1.942*	0.605	0.001	-3.132	-0.751
	A22vs.A29	-0.518	0.693	0.455	-1.882	0.845
	A22vs.A31	-1.218*	0.577	0.035	-2.352	-0.084
	A22vs.A32	-1.793*	0.577	0.002	-2.927	-0.659
	A22vs.A33	-1.671*	0.626	0.008	-2.902	-0.44
	A22vs.A35	-1.674*	0.626	0.008	-2.905	-0.443
	A22vsA36	-1.887*	0.577	0.001	-3.021	-0.753
	A22vs.A37	-0.83	0.589	0.16	-1.989	0.329
	A22vs.A38	-0.404	0.654	0.537	-1.69	0.882
	A22vs.1F	-1.284	0.654	0.05	-2.57	0.002
	A22vs.10F	-1.624*	0.654	0.013	-2.91	-0.338
Beryl	A23vs.Q1	1.099*	0.558	0.05	0.001	2.197
	A23vs.Q2	0.76	0.575	0.187	-0.371	1.891
	A23vs.Q4	0.635	0.597	0.288	-0.539	1.809
	A23vs.Q5	-0.102	0.558	0.855	-1.2	0.996
	A23vs.O6	0.422	0.545	0.439	-0.65	1.493
	A23vs.O7	0.51	0.597	0.393	-0.664	1.684
	A23vs.O8	0.693	0.575	0.229	-0.438	1.824
	A23vs.O9	-0.588	0.575	0.307	-1.719	0.543
	A23vs.O10	1.112	0.597	0.063	-0.062	2.285
	A23vs.O11	0.812	0.575	0.159	-0.319	1.943
	A23vs.Q12	-0.173	0.575	0.764	-1.304	0.958
	A23vs.Q13	0.995	0.575	0.085	-0.136	2.126
	A23vs.Q16	0.375	0.558	0.502	-0.722	1.473
	A23vs.Q17	-0.003	0.575	0.996	-1.134	1.128
	A23vs.Q18	1.069	0.667	0.11	-0.243	2.381

	A23vs.Q19	-1.223*	0.575	0.034	-2.354	-0.092
	A23vs.A20	0.173	0.575	0.764	-0.958	1.304
	A23vs.A22	2.088*	0.626	0.001	0.857	3.319
	A23vs.A24	0.165	0.575	0.775	-0.966	1.296
	A23vs.A25	1.05	0.626	0.094	-0.181	2.281
	A23vs.A26	2.366*	0.626	0	1.135	3.597
	A23vs.A27	2.220*	0.626	0	0.989	3.451
	A23vs.A28	0.146	0.575	0.8	-0.985	1.277
	A23vs.A29	1.569*	0.667	0.019	0.257	2.881
	A23vs.A31	0.869	0.545	0.111	-0.202	1.941
	A23vs.A32	0.295	0.545	0.589	-0.776	1.366
	A23vs.A33	0.417	0.597	0.486	-0.757	1.59
	A23vs.A35	0.413	0.597	0.489	-0.76	1.587
	A23vsA36	0.201	0.545	0.713	-0.871	1.272
	A23vs.A37	1.258*	0.558	0.025	0.16	2.356
	A23vs.A38	1.684*	0.626	0.007	0.453	2.915
	A23vs.1F	0.804	0.626	0.2	-0.427	2.035
	A23vs.10F	0.464	0.626	0.459	-0.767	1.695
Beryl	A24vs.Q1	0.935	0.535	0.081	-0.117	1.987
	A24vs.Q2	0.596	0.553	0.282	-0.491	1.682
	A24vs.Q4	0.47	0.575	0.414	-0.661	1.601
	A24vs.Q5	-0.267	0.535	0.619	-1.319	0.786
	A24vs.O6	0.257	0.521	0.622	-0.767	1.282
	A24vs.O7	0.345	0.575	0.548	-0.786	1.476
	A24vs.O8	0.529	0.553	0.339	-0.558	1.615
	A24vs.O9	-0.753	0.553	0.174	-1.84	0.334
	A24vs.O10	0.947	0.575	0.1	-0.184	2.078
	A24vs.O11	0.647	0.553	0.242	-0.44	1.734
	A24vs.Q12	-0.337	0.553	0.542	-1.424	0.75
	A24vs.Q13	0.83	0.553	0.134	-0.257	1.917
	A24vs.Q16	0.211	0.535	0.694	-0.841	1.263
	A24vs.Q17	-0.167	0.553	0.762	-1.254	0.92
	A24vs.Q18	0.905	0.648	0.164	-0.37	2.179
	A24vs.Q19	-1.387*	0.553	0.012	-2.474	-0.3
	A24vs.A20	0.009	0.553	0.988	-1.078	1.095
	A24vs.A22	1.923*	0.605	0.002	0.733	3.114
	A24vs.A23	-0.165	0.575	0.775	-1.296	0.966
	A24vs.A25	0.885	0.605	0.145	-0.305	2.076
	A24vs.A26	2.201*	0.605	0	1.011	3.392
	A24vs.A27	2.055*	0.605	0.001	0.865	3.246
	A24vs.A28	-0.019	0.553	0.973	-1.105	1.068

	A24vs.A29	1.405*	0.648	0.031	0.13	2.679
	A24vs.A31	0.705	0.521	0.177	-0.32	1.729
	A24vs.A32	0.13	0.521	0.802	-0.894	1.155
	A24vs.A33	0.252	0.575	0.661	-0.879	1.383
	A24vs.A35	0.249	0.575	0.666	-0.882	1.38
	A24vsA36	0.036	0.521	0.945	-0.988	1.061
	A24vs.A37	1.093*	0.535	0.042	0.041	2.146
	A24vs.A38	1.519*	0.605	0.013	0.329	2.71
	A24vs.1F	0.639	0.605	0.292	-0.551	1.83
	A24vs.10F	0.299	0.605	0.621	-0.891	1.49
Beryl	A25vs.Q1	0.05	0.589	0.933	-1.109	1.208
	A25vs.Q2	-0.289	0.605	0.633	-1.48	0.901
	A25vs.Q4	-0.415	0.626	0.508	-1.646	0.816
	A25vs.Q5	-1.152	0.589	0.051	-2.311	0.007
	A25vs.O6	-0.628	0.577	0.277	-1.762	0.506
	A25vs.O7	-0.54	0.626	0.389	-1.771	0.691
	A25vs.O8	-0.357	0.605	0.556	-1.547	0.834
	A25vs.O9	-1.638*	0.605	0.007	-2.828	-0.448
	A25vs.O10	0.062	0.626	0.921	-1.169	1.293
	A25vs.O11	-0.238	0.605	0.694	-1.428	0.952
	A25vs.Q12	-1.222*	0.605	0.044	-2.413	-0.032
	A25vs.Q13	-0.055	0.605	0.927	-1.246	1.135
	A25vs.Q16	-0.674	0.589	0.253	-1.833	0.485
	A25vs.Q17	-1.052	0.605	0.083	-2.243	0.138
	A25vs.Q18	0.02	0.693	0.978	-1.344	1.383
	A25vs.Q19	-2.272*	0.605	0	-3.463	-1.082
	A25vs.A20	-0.877	0.605	0.148	-2.067	0.314
	A25vs.A22	1.038	0.654	0.113	-0.248	2.324
	A25vs.A23	-1.05	0.626	0.094	-2.281	0.181
	A25vs.A24	-0.885	0.605	0.145	-2.076	0.305
	A25vs.A26	1.316*	0.654	0.045	0.03	2.602
	A25vs.A27	1.17	0.654	0.074	-0.116	2.456
	A25vs.A28	-0.904	0.605	0.136	-2.094	0.287
	A25vs.A29	0.52	0.693	0.454	-0.844	1.883
	A25vs.A31	-0.18	0.577	0.755	-1.314	0.954
	A25vs.A32	-0.755	0.577	0.191	-1.889	0.379
	A25vs.A33	-0.633	0.626	0.313	-1.864	0.598
	A25vs.A35	-0.636	0.626	0.31	-1.867	0.595
	A25vsA36	-0.849	0.577	0.142	-1.983	0.285
	A25vs.A37	0.208	0.589	0.724	-0.951	1.367
	A25vs.A38	0.634	0.654	0.333	-0.652	1.92
	A25vs.1F	-0.246	0.654	0.707	-1.532	1.04

	A25vs.10F	-0.586	0.654	0.371	-1.872	0.7
Beryl	A26vs.Q1	-1.266*	0.589	0.032	-2.425	-0.108
	A26vs.Q2	-1.605*	0.605	0.008	-2.796	-0.415
	A26vs.Q4	-1.731*	0.626	0.006	-2.962	-0.5
	A26vs.Q5	-2.468*	0.589	0	-3.627	-1.309
	A26vs.O6	-1.944*	0.577	0.001	-3.078	-0.81
	A26vs.O7	-1.856*	0.626	0.003	-3.087	-0.625
	A26vs.O8	-1.673*	0.605	0.006	-2.863	-0.482
	A26vs.O9	-2.954*	0.605	0	-4.144	-1.764
	A26vs.O10	-1.254*	0.626	0.046	-2.485	-0.023
	A26vs.O11	-1.554*	0.605	0.011	-2.744	-0.364
	A26vs.Q12	-2.538*	0.605	0	-3.729	-1.348
	A26vs.Q13	-1.371*	0.605	0.024	-2.562	-0.181
	A26vs.Q16	-1.990*	0.589	0.001	-3.149	-0.831
	A26vs.Q17	-2.368*	0.605	0	-3.559	-1.178
	A26vs.Q18	-1.297	0.693	0.062	-2.66	0.067
	A26vs.Q19	-3.588*	0.605	0	-4.779	-2.398
	A26vs.A20	-2.193*	0.605	0	-3.383	-1.002
	A26vs.A22	-0.278	0.654	0.671	-1.564	1.008
	A26vs.A23	-2.366*	0.626	0	-3.597	-1.135
	A26vs.A24	-2.201*	0.605	0	-3.392	-1.011
	A26vs.A25	-1.316*	0.654	0.045	-2.602	-0.03
	A26vs.A27	-0.146	0.654	0.823	-1.432	1.14
	A26vs.A28	-2.220*	0.605	0	-3.41	-1.029
	A26vs.A29	-0.796	0.693	0.251	-2.16	0.567
	A26vs.A31	-1.496*	0.577	0.01	-2.63	-0.362
	A26vs.A32	-2.071*	0.577	0	-3.205	-0.937
	A26vs.A33	-1.949*	0.626	0.002	-3.18	-0.718
	A26vs.A35	-1.952*	0.626	0.002	-3.183	-0.721
	A26vsA36	-2.165*	0.577	0	-3.299	-1.031
	A26vs.A37	-1.108	0.589	0.061	-2.267	0.051
	A26vs.A38	-0.682	0.654	0.298	-1.968	0.604
	A26vs.1F	-1.562*	0.654	0.017	-2.848	-0.276
	A26vs.10F	-1.902*	0.654	0.004	-3.188	-0.616
Beryl	A27vs.Q1	-1.121	0.589	0.058	-2.279	0.038
	A27vs.Q2	-1.459*	0.605	0.016	-2.65	-0.269
	A27vs.Q4	-1.585*	0.626	0.012	-2.816	-0.354
	A27vs.Q5	-2.322*	0.589	0	-3.481	-1.163

	A27vs.O6	-1.798*	0.577	0.002	-2.932	-0.664
	A27vs.O7	-1.710*	0.626	0.007	-2.941	-0.479
	A27vs.O8	-1.527*	0.605	0.012	-2.717	-0.336
	A27vs.O9	-2.808*	0.605	0	-3.998	-1.618
	A27vs.O10	-1.108	0.626	0.078	-2.339	0.123
	A27vs.O11	-1.408*	0.605	0.021	-2.598	-0.218
	A27vs.Q12	-2.392*	0.605	0	-3.583	-1.202
	A27vs.Q13	-1.225*	0.605	0.044	-2.416	-0.035
	A27vs.Q16	-1.844*	0.589	0.002	-3.003	-0.685
	A27vs.Q17	-2.222*	0.605	0	-3.413	-1.032
	A27vs.Q18	-1.151	0.693	0.098	-2.514	0.213
	A27vs.Q19	-3.442*	0.605	0	-4.633	-2.252
	A27vs.A20	-2.047*	0.605	0.001	-3.237	-0.856
	A27vs.A22	-0.132	0.654	0.84	-1.418	1.154
	A27vs.A23	-2.220*	0.626	0	-3.451	-0.989
	A27vs.A24	-2.055*	0.605	0.001	-3.246	-0.865
	A27vs.A25	-1.17	0.654	0.074	-2.456	0.116
	A27vs.A26	0.146	0.654	0.823	-1.14	1.432
	A27vs.A28	-2.074*	0.605	0.001	-3.264	-0.883
	A27vs.A29	-0.65	0.693	0.349	-2.014	0.713
	A27vs.A31	-1.350*	0.577	0.02	-2.484	-0.216
	A27vs.A32	-1.925*	0.577	0.001	-3.059	-0.791
	A27vs.A33	-1.803*	0.626	0.004	-3.034	-0.572
	A27vs.A35	-1.806*	0.626	0.004	-3.037	-0.575
	A27vsA36	-2.019*	0.577	0.001	-3.153	-0.885
	A27vs.A37	-0.962	0.589	0.104	-2.121	0.197
	A27vs.A38	-0.536	0.654	0.413	-1.822	0.75
	A27vs.1F	-1.416*	0.654	0.031	-2.702	-0.13
	A27vs.10F	-1.756*	0.654	0.008	-3.042	-0.47
Beryl	A28vs.Q1	0.953	0.535	0.076	-0.099	2.005
	A28vs.Q2	0.614	0.553	0.267	-0.472	1.701
	A28vs.Q4	0.489	0.575	0.396	-0.642	1.62
	A28vs.Q5	-0.248	0.535	0.643	-1.3	0.804
	A28vs.O6	0.276	0.521	0.597	-0.749	1.3
	A28vs.O7	0.364	0.575	0.527	-0.767	1.495
	A28vs.O8	0.547	0.553	0.323	-0.54	1.634
	A28vs.O9	-0.734	0.553	0.185	-1.821	0.352
	A28vs.O10	0.966	0.575	0.094	-0.165	2.097
	A28vs.O11	0.666	0.553	0.229	-0.421	1.752
	A28vs.Q12	-0.319	0.553	0.565	-1.405	0.768

	A28vs.Q13	0.849	0.553	0.125	-0.238	1.935
	A28vs.Q16	0.229	0.535	0.668	-0.823	1.282
	A28vs.Q17	-0.149	0.553	0.788	-1.235	0.938
	A28vs.Q18	0.923	0.648	0.155	-0.351	2.197
	A28vs.Q19	-1.369*	0.553	0.014	-2.455	-0.282
	A28vs.A20	0.027	0.553	0.961	-1.06	1.114
	A28vs.A22	1.942*	0.605	0.001	0.751	3.132
	A28vs.A23	-0.146	0.575	0.8	-1.277	0.985
	A28vs.A24	0.019	0.553	0.973	-1.068	1.105
	A28vs.A25	0.904	0.605	0.136	-0.287	2.094
	A28vs.A26	2.220*	0.605	0	1.029	3.41
	A28vs.A27	2.074*	0.605	0.001	0.883	3.264
	A28vs.A29	1.423*	0.648	0.029	0.149	2.697
	A28vs.A31	0.723	0.521	0.166	-0.301	1.748
	A28vs.A32	0.149	0.521	0.775	-0.875	1.174
	A28vs.A33	0.271	0.575	0.638	-0.86	1.402
	A28vs.A35	0.267	0.575	0.642	-0.864	1.398
	A28vsA36	0.055	0.521	0.917	-0.97	1.079
	A28vs.A37	1.112*	0.535	0.038	0.06	2.164
	A28vs.A38	1.538*	0.605	0.011	0.347	2.728
	A28vs.1F	0.658	0.605	0.278	-0.533	1.848
	A28vs.10F	0.318	0.605	0.6	-0.873	1.508
Beryl	A29vs.Q1	-0.47	0.633	0.458	-1.715	0.775
	A29vs.Q2	-0.809	0.648	0.213	-2.083	0.465
	A29vs.Q4	-0.934	0.667	0.162	-2.246	0.378
	A29vs.Q5	-1.671*	0.633	0.009	-2.916	-0.426
	A29vs.O6	-1.148	0.621	0.066	-2.369	0.074
	A29vs.O7	-1.059	0.667	0.113	-2.371	0.253
	A29vs.O8	-0.876	0.648	0.177	-2.15	0.398
	A29vs.O9	-2.158*	0.648	0.001	-3.432	-0.883
	A29vs.O10	-0.458	0.667	0.493	-1.77	0.855
	A29vs.O11	-0.758	0.648	0.243	-2.032	0.517
	A29vs.Q12	-1.742*	0.648	0.008	-3.016	-0.468
	A29vs.Q13	-0.575	0.648	0.376	-1.849	0.7
	A29vs.Q16	-1.194	0.633	0.06	-2.439	0.051
	A29vs.Q17	-1.572*	0.648	0.016	-2.846	-0.298
	A29vs.Q18	-0.5	0.731	0.494	-1.937	0.937
	A29vs.Q19	-2.792*	0.648	0	-4.066	-1.518
	A29vs.A20	-1.396*	0.648	0.032	-2.67	-0.122
	A29vs.A22	0.518	0.693	0.455	-0.845	1.882
	A29vs.A23	-1.569*	0.667	0.019	-2.881	-0.257

	A29vs.A24	-1.405*	0.648	0.031	-2.679	-0.13
	A29vs.A25	-0.52	0.693	0.454	-1.883	0.844
	A29vs.A26	0.796	0.693	0.251	-0.567	2.16
	A29vs.A27	0.65	0.693	0.349	-0.713	2.014
	A29vs.A28	-1.423*	0.648	0.029	-2.697	-0.149
	A29vs.A31	-0.7	0.621	0.261	-1.921	0.522
	A29vs.A32	-1.274*	0.621	0.041	-2.496	-0.053
	A29vs.A33	-1.153	0.667	0.085	-2.465	0.16
	A29vs.A35	-1.156	0.667	0.084	-2.468	0.156
	A29vsA36	-1.369*	0.621	0.028	-2.59	-0.147
	A29vs.A37	-0.311	0.633	0.623	-1.556	0.934
	A29vs.A38	0.114	0.693	0.869	-1.249	1.478
	A29vs.1F	-0.766	0.693	0.27	-2.129	0.598
	A29vs.10F	-1.105	0.693	0.112	-2.469	0.258
Beryl	A31vs.Q1	0.23	0.502	0.648	-0.758	1.218
	A31vs.Q2	-0.109	0.521	0.834	-1.134	0.915
	A31vs.Q4	-0.234	0.545	0.667	-1.306	0.837
	A31vs.Q5	-0.972	0.502	0.054	-1.959	0.016
	A31vs.O6	-0.448	0.487	0.359	-1.406	0.511
	A31vs.O7	-0.359	0.545	0.51	-1.431	0.712
	A31vs.O8	-0.176	0.521	0.735	-1.201	0.848
	A31vs.O9	-1.458*	0.521	0.005	-2.482	-0.433
	A31vs.O10	0.242	0.545	0.657	-0.829	1.314
	A31vs.O11	-0.058	0.521	0.912	-1.082	0.967
	A31vs.Q12	-1.042*	0.521	0.046	-2.067	-0.018
	A31vs.Q13	0.125	0.521	0.81	-0.899	1.15
	A31vs.Q16	-0.494	0.502	0.326	-1.482	0.494
	A31vs.Q17	-0.872	0.521	0.095	-1.897	0.152
	A31vs.Q18	0.2	0.621	0.748	-1.022	1.421
	A31vs.Q19	-2.092*	0.521	0	-3.117	-1.068
	A31vs.A20	-0.696	0.521	0.182	-1.721	0.328
	A31vs.A22	1.218*	0.577	0.035	0.084	2.352
	A31vs.A23	-0.869	0.545	0.111	-1.941	0.202
	A31vs.A24	-0.705	0.521	0.177	-1.729	0.32
	A31vs.A25	0.18	0.577	0.755	-0.954	1.314
	A31vs.A26	1.496*	0.577	0.01	0.362	2.63
	A31vs.A27	1.350*	0.577	0.02	0.216	2.484
	A31vs.A28	-0.723	0.521	0.166	-1.748	0.301
	A31vs.A29	0.7	0.621	0.261	-0.522	1.921
	A31vs.A32	-0.574	0.487	0.239	-1.533	0.384
	A31vs.A33	-0.453	0.545	0.407	-1.524	0.619
	A31vs.A35	-0.456	0.545	0.403	-1.528	0.615

	A31vsA36	-0.669	0.487	0.171	-1.627	0.289
	A31vs.A37	0.388	0.502	0.44	-0.599	1.376
	A31vs.A38	0.814	0.577	0.159	-0.32	1.948
	A31vs.1F	-0.066	0.577	0.909	-1.2	1.068
	A31vs.10F	-0.406	0.577	0.482	-1.54	0.728
Beryl	A32vs.Q1	0.804	0.502	0.11	-0.184	1.792
	A32vs.Q2	0.465	0.521	0.372	-0.559	1.49
	A32vs.Q4	0.34	0.545	0.533	-0.731	1.411
	A32vs.Q5	-0.397	0.502	0.43	-1.385	0.591
	A32vs.O6	0.127	0.487	0.795	-0.832	1.085
	A32vs.O7	0.215	0.545	0.693	-0.856	1.286
	A32vs.O8	0.398	0.521	0.445	-0.626	1.423
	A32vs.O9	-0.883	0.521	0.091	-1.908	0.141
	A32vs.O10	0.817	0.545	0.135	-0.255	1.888
	A32vs.O11	0.517	0.521	0.322	-0.508	1.541
	A32vs.Q12	-0.468	0.521	0.37	-1.492	0.557
	A32vs.Q13	0.7	0.521	0.18	-0.325	1.724
	A32vs.Q16	0.08	0.502	0.873	-0.907	1.068
	A32vs.Q17	-0.298	0.521	0.568	-1.322	0.727
	A32vs.Q18	0.774	0.621	0.213	-0.447	1.996
	A32vs.Q19	-1.518*	0.521	0.004	-2.542	-0.493
	A32vs.A20	-0.122	0.521	0.815	-1.146	0.903
	A32vs.A22	1.793*	0.577	0.002	0.659	2.927
	A32vs.A23	-0.295	0.545	0.589	-1.366	0.776
	A32vs.A24	-0.13	0.521	0.802	-1.155	0.894
	A32vs.A25	0.755	0.577	0.191	-0.379	1.889
	A32vs.A26	2.071*	0.577	0	0.937	3.205
	A32vs.A27	1.925*	0.577	0.001	0.791	3.059
	A32vs.A28	-0.149	0.521	0.775	-1.174	0.875
	A32vs.A29	1.274*	0.621	0.041	0.053	2.496
	A32vs.A31	0.574	0.487	0.239	-0.384	1.533
	A32vs.A33	0.122	0.545	0.823	-0.95	1.193
	A32vs.A35	0.118	0.545	0.828	-0.953	1.19
	A32vsA36	-0.094	0.487	0.846	-1.053	0.864
	A32vs.A37	0.963	0.502	0.056	-0.025	1.951
	A32vs.A38	1.389*	0.577	0.017	0.255	2.523
	A32vs.1F	0.509	0.577	0.378	-0.625	1.643
	A32vs.10F	0.169	0.577	0.77	-0.965	1.303
Beryl	A33vs.Q1	0.683	0.558	0.222	-0.415	1.78
	A33vs.Q2	0.344	0.575	0.551	-0.787	1.475
	A33vs.Q4	0.218	0.597	0.715	-0.955	1.392
	A33vs.Q5	-0.519	0.558	0.353	-1.617	0.579

	A33vs.O6	0.005	0.545	0.993	-1.066	1.076
	A33vs.O7	0.093	0.597	0.876	-1.08	1.267
	A33vs.O8	0.276	0.575	0.631	-0.855	1.407
	A33vs.O9	-1.005	0.575	0.081	-2.136	0.126
	A33vs.O10	0.695	0.597	0.245	-0.479	1.869
	A33vs.O11	0.395	0.575	0.493	-0.736	1.526
	A33vs.Q12	-0.589	0.575	0.306	-1.72	0.542
	A33vs.Q13	0.578	0.575	0.316	-0.553	1.709
	A33vs.Q16	-0.041	0.558	0.941	-1.139	1.057
	A33vs.Q17	-0.419	0.575	0.466	-1.55	0.712
	A33vs.Q18	0.652	0.667	0.329	-0.66	1.965
	A33vs.Q19	-1.639*	0.575	0.005	-2.77	-0.508
	A33vs.A20	-0.244	0.575	0.672	-1.375	0.887
	A33vs.A22	1.671*	0.626	0.008	0.44	2.902
	A33vs.A23	-0.417	0.597	0.486	-1.59	0.757
	A33vs.A24	-0.252	0.575	0.661	-1.383	0.879
	A33vs.A25	0.633	0.626	0.313	-0.598	1.864
	A33vs.A26	1.949*	0.626	0.002	0.718	3.18
	A33vs.A27	1.803*	0.626	0.004	0.572	3.034
	A33vs.A28	-0.271	0.575	0.638	-1.402	0.86
	A33vs.A29	1.153	0.667	0.085	-0.16	2.465
	A33vs.A31	0.453	0.545	0.407	-0.619	1.524
	A33vs.A32	-0.122	0.545	0.823	-1.193	0.95
	A33vs.A35	-0.003	0.597	0.996	-1.177	1.17
	A33vsA36	-0.216	0.545	0.692	-1.288	0.855
	A33vs.A37	0.841	0.558	0.133	-0.257	1.939
	A33vs.A38	1.267*	0.626	0.044	0.036	2.498
	A33vs.1F	0.387	0.626	0.537	-0.844	1.618
	A33vs.10F	0.047	0.626	0.94	-1.184	1.278
Beryl	A35vs.Q1	0.686	0.558	0.22	-0.412	1.784
	A35vs.Q2	0.347	0.575	0.547	-0.784	1.478
	A35vs.Q4	0.222	0.597	0.711	-0.952	1.395
	A35vs.Q5	-0.515	0.558	0.357	-1.613	0.582
	A35vs.O6	0.008	0.545	0.988	-1.063	1.08
	A35vs.O7	0.097	0.597	0.871	-1.077	1.27
	A35vs.O8	0.28	0.575	0.627	-0.851	1.411
	A35vs.O9	-1.002	0.575	0.082	-2.133	0.129
	A35vs.O10	0.698	0.597	0.243	-0.475	1.872
	A35vs.O11	0.398	0.575	0.489	-0.733	1.529
	A35vs.Q12	-0.586	0.575	0.309	-1.717	0.545
	A35vs.Q13	0.581	0.575	0.313	-0.55	1.712
	A35vs.Q16	-0.038	0.558	0.946	-1.136	1.06

	A35vs.Q17	-0.416	0.575	0.47	-1.547	0.715
	A35vs.Q18	0.656	0.667	0.326	-0.656	1.968
	A35vs.Q19	-1.636*	0.575	0.005	-2.767	-0.505
	A35vs.A20	-0.24	0.575	0.676	-1.371	0.891
	A35vs.A22	1.674*	0.626	0.008	0.443	2.905
	A35vs.A23	-0.413	0.597	0.489	-1.587	0.76
	A35vs.A24	-0.249	0.575	0.666	-1.38	0.882
	A35vs.A25	0.636	0.626	0.31	-0.595	1.867
	A35vs.A26	1.952*	0.626	0.002	0.721	3.183
	A35vs.A27	1.806*	0.626	0.004	0.575	3.037
	A35vs.A28	-0.267	0.575	0.642	-1.398	0.864
	A35vs.A29	1.156	0.667	0.084	-0.156	2.468
	A35vs.A31	0.456	0.545	0.403	-0.615	1.528
	A35vs.A32	-0.118	0.545	0.828	-1.19	0.953
	A35vs.A33	0.003	0.597	0.996	-1.17	1.177
	A35vsA36	-0.213	0.545	0.696	-1.284	0.859
	A35vs.A37	0.845	0.558	0.131	-0.253	1.942
	A35vs.A38	1.270*	0.626	0.043	0.039	2.501
	A35vs.1F	0.39	0.626	0.533	-0.841	1.621
	A35vs.10F	0.05	0.626	0.936	-1.181	1.281
Beryl	A36vs.Q1	0.899	0.502	0.074	-0.089	1.886
	A36vs.Q2	0.56	0.521	0.283	-0.465	1.584
	A36vs.Q4	0.434	0.545	0.426	-0.637	1.506
	A36vs.Q5	-0.303	0.502	0.547	-1.29	0.685
	A36vs.O6	0.221	0.487	0.65	-0.737	1.179
	A36vs.O7	0.309	0.545	0.57	-0.762	1.381
	A36vs.O8	0.493	0.521	0.345	-0.532	1.517
	A36vs.O9	-0.789	0.521	0.131	-1.813	0.236
	A36vs.O10	0.911	0.545	0.095	-0.16	1.983
	A36vs.O11	0.611	0.521	0.242	-0.413	1.636
	A36vs.Q12	-0.373	0.521	0.474	-1.398	0.651
	A36vs.Q13	0.794	0.521	0.128	-0.231	1.818
	A36vs.Q16	0.175	0.502	0.728	-0.813	1.163
	A36vs.Q17	-0.203	0.521	0.697	-1.228	0.821
	A36vs.Q18	0.869	0.621	0.163	-0.353	2.09
	A36vs.Q19	-1.423*	0.521	0.007	-2.448	-0.399
	A36vs.A20	-0.027	0.521	0.958	-1.052	0.997
	A36vs.A22	1.887*	0.577	0.001	0.753	3.021
	A36vs.A23	-0.201	0.545	0.713	-1.272	0.871
	A36vs.A24	-0.036	0.521	0.945	-1.061	0.988
	A36vs.A25	0.849	0.577	0.142	-0.285	1.983
	A36vs.A26	2.165*	0.577	0	1.031	3.299

	A36vs.A27	2.019*	0.577	0.001	0.885	3.153
	A36vs.A28	-0.055	0.521	0.917	-1.079	0.97
	A36vs.A29	1.369*	0.621	0.028	0.147	2.59
	A36vs.A31	0.669	0.487	0.171	-0.289	1.627
	A36vs.A32	0.094	0.487	0.846	-0.864	1.053
	A36vs.A33	0.216	0.545	0.692	-0.855	1.288
	A36vs.A35	0.213	0.545	0.696	-0.859	1.284
	A36vs.A37	1.057*	0.502	0.036	0.07	2.045
	A36vs.A38	1.483*	0.577	0.011	0.349	2.617
	A36vs.1F	0.603	0.577	0.296	-0.531	1.737
	A36vs.10F	0.263	0.577	0.648	-0.871	1.397
Beryl	A37vs.Q1	-0.159	0.517	0.759	-1.175	0.858
	A37vs.Q2	-0.498	0.535	0.353	-1.55	0.554
	A37vs.Q4	-0.623	0.558	0.265	-1.721	0.475
	A37vs.Q5	-1.360*	0.517	0.009	-2.376	-0.344
	A37vs.O6	-0.836	0.502	0.097	-1.824	0.152
	A37vs.O7	-0.748	0.558	0.181	-1.846	0.35
	A37vs.O8	-0.565	0.535	0.292	-1.617	0.487
	A37vs.O9	-1.846*	0.535	0.001	-2.898	-0.794
	A37vs.O10	-0.146	0.558	0.794	-1.244	0.952
	A37vs.O11	-0.446	0.535	0.405	-1.498	0.606
	A37vs.Q12	-1.431*	0.535	0.008	-2.483	-0.378
	A37vs.Q13	-0.263	0.535	0.623	-1.316	0.789
	A37vs.Q16	-0.883	0.517	0.089	-1.899	0.134
	A37vs.Q17	-1.261*	0.535	0.019	-2.313	-0.208
	A37vs.Q18	-0.189	0.633	0.766	-1.434	1.056
	A37vs.Q19	-2.481*	0.535	0	-3.533	-1.428
	A37vs.A20	-1.085*	0.535	0.043	-2.137	-0.033
	A37vs.A22	0.83	0.589	0.16	-0.329	1.989
	A37vs.A23	-1.258*	0.558	0.025	-2.356	-0.16
	A37vs.A24	-1.093*	0.535	0.042	-2.146	-0.041
	A37vs.A25	-0.208	0.589	0.724	-1.367	0.951
	A37vs.A26	1.108	0.589	0.061	-0.051	2.267
	A37vs.A27	0.962	0.589	0.104	-0.197	2.121
	A37vs.A28	-1.112*	0.535	0.038	-2.164	-0.06
	A37vs.A29	0.311	0.633	0.623	-0.934	1.556
	A37vs.A31	-0.388	0.502	0.44	-1.376	0.599
	A37vs.A32	-0.963	0.502	0.056	-1.951	0.025
	A37vs.A33	-0.841	0.558	0.133	-1.939	0.257
	A37vs.A35	-0.845	0.558	0.131	-1.942	0.253
	A37vs.A36	-1.057*	0.502	0.036	-2.045	-0.07

	A37vs.A38	0.426	0.589	0.47	-0.733	1.585
	A37vs.1F	-0.454	0.589	0.441	-1.613	0.705
	A37vs.10F	-0.794	0.589	0.179	-1.953	0.365
	A38vs.Q1	-0.584	0.589	0.322	-1.743	0.574
	A38vs.Q2	-0.923	0.605	0.128	-2.114	0.267
	A38vs.Q4	-1.049	0.626	0.095	-2.28	0.182
	A38vs.Q5	-1.786*	0.589	0.003	-2.945	-0.627
	A38vs.O6	-1.262*	0.577	0.029	-2.396	-0.128
	A38vs.O7	-1.174	0.626	0.062	-2.405	0.057
	A38vs.O8	-0.991	0.605	0.103	-2.181	0.2
	A38vs.O9	-2.272*	0.605	0	-3.462	-1.082
	A38vs.O10	-0.572	0.626	0.361	-1.803	0.659
	A38vs.O11	-0.872	0.605	0.151	-2.062	0.318
	A38vs.Q12	-1.856*	0.605	0.002	-3.047	-0.666
	A38vs.Q13	-0.689	0.605	0.256	-1.88	0.501
	A38vs.Q16	-1.308*	0.589	0.027	-2.467	-0.149
	A38vs.Q17	-1.686*	0.605	0.006	-2.877	-0.496
	A38vs.Q18	-0.614	0.693	0.376	-1.978	0.749
	A38vs.Q19	-2.906*	0.605	0	-4.097	-1.716
Beryl	A38vs.A20	-1.511*	0.605	0.013	-2.701	-0.32
	A38vs.A22	0.404	0.654	0.537	-0.882	1.69
	A38vs.A23	-1.684*	0.626	0.007	-2.915	-0.453
	A38vs.A24	-1.519*	0.605	0.013	-2.71	-0.329
	A38vs.A25	-0.634	0.654	0.333	-1.92	0.652
	A38vs.A26	0.682	0.654	0.298	-0.604	1.968
	A38vs.A27	0.536	0.654	0.413	-0.75	1.822
	A38vs.A28	-1.538*	0.605	0.011	-2.728	-0.347
	A38vs.A29	-0.114	0.693	0.869	-1.478	1.249
	A38vs.A31	-0.814	0.577	0.159	-1.948	0.32
	A38vs.A32	-1.389*	0.577	0.017	-2.523	-0.255
	A38vs.A33	-1.267*	0.626	0.044	-2.498	-0.036
	A38vs.A35	-1.270*	0.626	0.043	-2.501	-0.039
	A38vs.A36	-1.483*	0.577	0.011	-2.617	-0.349
	A38vs.A37	-0.426	0.589	0.47	-1.585	0.733
	A38vs.1F	-0.88	0.654	0.179	-2.166	0.406
	A38vs.10F	-1.22	0.654	0.063	-2.506	0.066
	1Fvs.Q1	0.296	0.589	0.616	-0.863	1.454
	1Fvs.Q2	-0.043	0.605	0.943	-1.234	1.147
Beryl	1Fvs.Q4	-0.169	0.626	0.788	-1.4	1.062
	1Fvs.Q5	-0.906	0.589	0.125	-2.065	0.253
	1Fvs.O6	-0.382	0.577	0.508	-1.516	0.752

	1Fvs.O7	-0.294	0.626	0.639	-1.525	0.937
	1Fvs.O8	-0.111	0.605	0.855	-1.301	1.08
	1Fvs.O9	-1.392*	0.605	0.022	-2.582	-0.202
	1Fvs.O10	0.308	0.626	0.623	-0.923	1.539
	1Fvs.O11	0.008	0.605	0.989	-1.182	1.198
	1Fvs.Q12	-0.976	0.605	0.108	-2.167	0.214
	1Fvs.Q13	0.191	0.605	0.753	-1	1.381
	1Fvs.Q16	-0.428	0.589	0.468	-1.587	0.731
	1Fvs.Q17	-0.806	0.605	0.184	-1.997	0.384
	1Fvs.Q18	0.265	0.693	0.702	-1.098	1.629
	1Fvs.Q19	-2.026*	0.605	0.001	-3.217	-0.836
	1Fvs.A20	-0.631	0.605	0.298	-1.821	0.56
	1Fvs.A22	1.284	0.654	0.05	-0.002	2.57
	1Fvs.A23	-0.804	0.626	0.2	-2.035	0.427
	1Fvs.A24	-0.639	0.605	0.292	-1.83	0.551
	1Fvs.A25	0.246	0.654	0.707	-1.04	1.532
	1Fvs.A26	1.562*	0.654	0.017	0.276	2.848
	1Fvs.A27	1.416*	0.654	0.031	0.13	2.702
	1Fvs.A28	-0.658	0.605	0.278	-1.848	0.533
	1Fvs.A29	0.766	0.693	0.27	-0.598	2.129
	1Fvs.A31	0.066	0.577	0.909	-1.068	1.2
	1Fvs.A32	-0.509	0.577	0.378	-1.643	0.625
	1Fvs.A33	-0.387	0.626	0.537	-1.618	0.844
	1Fvs.A35	-0.39	0.626	0.533	-1.621	0.841
	1Fvs.A36	-0.603	0.577	0.296	-1.737	0.531
	1Fvs.A37	0.454	0.589	0.441	-0.705	1.613
	1Fvs.A38	0.88	0.654	0.179	-0.406	2.166
	1Fvs.10F	-0.34	0.654	0.603	-1.626	0.946
Beryl	10Fvs.Q1	0.635	0.589	0.282	-0.523	1.794
	10Fvs.Q2	0.297	0.605	0.624	-0.894	1.487
	10Fvs.Q4	0.171	0.626	0.784	-1.06	1.402
	10Fvs.Q5	-0.566	0.589	0.338	-1.725	0.593
	10Fvs.O6	-0.042	0.577	0.942	-1.176	1.092
	10Fvs.O7	0.046	0.626	0.941	-1.185	1.277
	10Fvs.O8	0.229	0.605	0.705	-0.961	1.42
	10Fvs.O9	-1.052	0.605	0.083	-2.242	0.138
	10Fvs.O10	0.648	0.626	0.301	-0.583	1.879
	10Fvs.O11	0.348	0.605	0.566	-0.842	1.538
	10Fvs.Q12	-0.636	0.605	0.294	-1.827	0.554
	10Fvs.Q13	0.531	0.605	0.381	-0.66	1.721
	10Fvs.Q16	-0.088	0.589	0.881	-1.247	1.071
	10Fvs.Q17	-0.466	0.605	0.442	-1.657	0.724

	10Fvs.Q18	0.605	0.693	0.383	-0.758	1.969
	10Fvs.Q19	-1.686*	0.605	0.006	-2.877	-0.496
	10Fvs.A20	-0.291	0.605	0.631	-1.481	0.9
	10Fvs.A22	1.624*	0.654	0.013	0.338	2.91
	10Fvs.A23	-0.464	0.626	0.459	-1.695	0.767
	10Fvs.A24	-0.299	0.605	0.621	-1.49	0.891
	10Fvs.A25	0.586	0.654	0.371	-0.7	1.872
	10Fvs.A26	1.902*	0.654	0.004	0.616	3.188
	10Fvs.A27	1.756*	0.654	0.008	0.47	3.042
	10Fvs.A28	-0.318	0.605	0.6	-1.508	0.873
	10Fvs.A29	1.105	0.693	0.112	-0.258	2.469
	10Fvs.A31	0.406	0.577	0.482	-0.728	1.54
	10Fvs.A32	-0.169	0.577	0.77	-1.303	0.965
	10Fvs.A33	-0.047	0.626	0.94	-1.278	1.184
	10Fvs.A35	-0.05	0.626	0.936	-1.281	1.181
	10Fvs.A36	-0.263	0.577	0.648	-1.397	0.871
	10Fvs.A37	0.794	0.589	0.179	-0.365	1.953
	10Fvs.A39	1.22	0.654	0.063	-0.066	2.506
	10Fvs.1F	0.34	0.654	0.603	-0.946	1.626

Estimates

Dependent Variable: STAUDPC

Cultivar	Isolate	Mean difference	Std. Error	Sig.[b]	95% Confidence Interval	
					Lower Bound	Upper Bound
G122	Q1vs.Q2	-2.062*	0.575	0	-3.193	-0.931
	Q1vs.Q4	-1.700*	0.545	0.002	-2.771	-0.629
	Q1vs.Q5	-1.515*	0.626	0.016	-2.746	-0.284
	Q1vs.Q6	-2.249*	0.667	0.001	-3.561	-0.937
	Q1vs.O7	-1.908*	0.575	0.001	-3.039	-0.777
	Q1vs.O8	-0.922	0.597	0.123	-2.095	0.252
	Q1vs.O9	-1.451*	0.575	0.012	-2.582	-0.32
	Q1vs.O10	-1.458*	0.575	0.012	-2.589	-0.327
	Q1vs.O11	-1.091	0.626	0.082	-2.322	0.14
	Q1vs.Q12	-1.135	0.597	0.058	-2.309	0.039
	Q1vs.Q13	-2.337*	0.558	0	-3.435	-1.239
	Q1vs.Q16	-2.688*	0.597	0	-3.862	-1.515
	Q1vs.Q17	-1.627*	0.626	0.01	-2.858	-0.396
	Q1vs.Q18	-2.031*	0.626	0.001	-3.262	-0.8
	Q1vs.Q19	-2.774*	0.667	0	-4.086	-1.462

	Q1vs.A20	-1.480*	0.597	0.014	-2.654	-0.306
	Q1vs.A22	-0.898	0.575	0.119	-2.029	0.233
	Q1vs.A23	-1.268*	0.575	0.028	-2.399	-0.137
	Q1vs.A24	-2.437*	0.597	0	-3.61	-1.263
	Q1vs.A25	-2.040*	0.575	0	-3.171	-0.909
	Q1vs.A26	0.047	0.597	0.938	-1.127	1.22
	Q1vs.A27	-1.312	0.667	0.05	-2.624	0.001
	Q1vs.A28	-0.999	0.626	0.111	-2.23	0.232
	Q1vs.A29	-1.963*	0.626	0.002	-3.194	-0.732
	Q1vs.A31	-0.625	0.558	0.263	-1.723	0.472
	Q1vs.A32	-1.077	0.558	0.055	-2.175	0.021
	Q1vs.A33	-0.161	0.626	0.798	-1.392	1.07
	Q1vs.A35	-0.957	0.626	0.127	-2.188	0.274
	Q1vs.A36	-1.500*	0.575	0.01	-2.631	-0.369
	Q1vs.A37	-1.737*	0.626	0.006	-2.968	-0.506
	Q1vs.A38	-2.151*	0.575	0	-3.282	-1.02
	Q1vs.1F	-0.519	0.626	0.408	-1.75	0.712
	Q1vs.10F	-0.463	0.626	0.46	-1.694	0.768
	Q2vs.Q1	2.062*	0.575	0	0.931	3.193
	Q2vs.Q4	0.362	0.521	0.487	-0.662	1.387
	Q2vs.Q5	0.548	0.605	0.366	-0.643	1.738
	Q2vs.Q6	-0.187	0.648	0.773	-1.461	1.087
	Q2vs.O7	0.154	0.553	0.78	-0.932	1.241
	Q2vs.O8	1.141*	0.575	0.048	0.01	2.272
	Q2vs.O9	0.611	0.553	0.269	-0.475	1.698
	Q2vs.O10	0.604	0.553	0.275	-0.482	1.691
	Q2vs.O11	0.972	0.605	0.109	-0.219	2.162
	Q2vs.Q12	0.927	0.575	0.108	-0.204	2.058
	Q2vs.Q13	-0.274	0.535	0.608	-1.326	0.778
G122	Q2vs.Q16	-0.626	0.575	0.277	-1.757	0.505
	Q2vs.Q17	0.436	0.605	0.472	-0.755	1.626
	Q2vs.Q18	0.032	0.605	0.958	-1.159	1.222
	Q2vs.Q19	-0.712	0.648	0.273	-1.986	0.562
	Q2vs.A20	0.582	0.575	0.312	-0.549	1.713
	Q2vs.Q22	1.164*	0.553	0.036	0.078	2.251
	Q2vs.A23	0.794	0.553	0.151	-0.292	1.881
	Q2vs.A24	-0.374	0.575	0.516	-1.505	0.757
	Q2vs.A25	0.023	0.553	0.967	-1.064	1.11
	Q2vs.A26	2.109*	0.575	0	0.978	3.24
	Q2vs.A27	0.751	0.648	0.247	-0.523	2.025
	Q2vs.A28	1.064	0.605	0.08	-0.127	2.254

	Q2vs.A29	0.1	0.605	0.869	-1.091	1.29
	Q2vs.A31	1.437*	0.535	0.008	0.385	2.489
	Q2vs.A32	0.986	0.535	0.066	-0.066	2.038
	Q2vs.A33	1.902*	0.605	0.002	0.711	3.092
	Q2vs.A35	1.106	0.605	0.069	-0.085	2.296
	Q2vs.A36	0.563	0.553	0.309	-0.524	1.65
	Q2vs.A37	0.326	0.605	0.591	-0.865	1.516
	Q2vs.A38	-0.089	0.553	0.873	-1.175	0.998
	Q2vs.1F	1.544*	0.605	0.011	0.353	2.734
	Q2vs.10F	1.600*	0.605	0.009	0.409	2.79
G122	Q4vs.Q1	1.700*	0.545	0.002	0.629	2.771
	Q4vs.Q2	-0.362	0.521	0.487	-1.387	0.662
	Q4vs.Q5	0.185	0.577	0.748	-0.949	1.319
	Q4vs.Q6	-0.549	0.621	0.377	-1.771	0.672
	Q4vs.O7	-0.208	0.521	0.69	-1.233	0.816
	Q4vs.O8	0.778	0.545	0.154	-0.293	1.85
	Q4vs.O9	0.249	0.521	0.633	-0.775	1.274
	Q4vs.O10	0.242	0.521	0.643	-0.783	1.266
	Q4vs.O11	0.609	0.577	0.291	-0.525	1.743
	Q4vs.Q12	0.565	0.545	0.3	-0.506	1.636
	Q4vs.Q13	-0.637	0.502	0.206	-1.624	0.351
	Q4vs.Q16	-0.988	0.545	0.071	-2.06	0.083
	Q4vs.Q17	0.073	0.577	0.899	-1.061	1.207
	Q4vs.Q18	-0.331	0.577	0.567	-1.465	0.803
	Q4vs.Q19	-1.074	0.621	0.085	-2.296	0.147
	Q4vs.A20	0.22	0.545	0.687	-0.851	1.291
	Q4vs.Q22	0.802	0.521	0.125	-0.223	1.826
	Q4vs.A23	0.432	0.521	0.408	-0.593	1.456
	Q4vs.A24	-0.737	0.545	0.177	-1.808	0.335
	Q4vs.A25	-0.34	0.521	0.515	-1.364	0.685
	Q4vs.A26	1.747*	0.545	0.001	0.675	2.818
	Q4vs.A27	0.388	0.621	0.532	-0.833	1.61
	Q4vs.A28	0.701	0.577	0.225	-0.433	1.835
	Q4vs.A29	-0.263	0.577	0.649	-1.397	0.871
	Q4vs.A31	1.075*	0.502	0.033	0.087	2.062
	Q4vs.A32	0.623	0.502	0.215	-0.364	1.611
	Q4vs.A33	1.539*	0.577	0.008	0.405	2.673
	Q4vs.A35	0.743	0.577	0.198	-0.391	1.877
	Q4vs.A36	0.2	0.521	0.701	-0.824	1.225
	Q4vs.A37	-0.037	0.577	0.949	-1.171	1.097
	Q4vs.A38	-0.451	0.521	0.387	-1.475	0.574
	Q4vs.1F	1.181*	0.577	0.041	0.047	2.315

	Q4vs.10F	1.237*	0.577	0.033	0.103	2.371
G122	Q5vs.Q1	1.515*	0.626	0.016	0.284	2.746
	Q5vs.Q2	-0.548	0.605	0.366	-1.738	0.643
	Q5vs.Q4	-0.185	0.577	0.748	-1.319	0.949
	Q5vs.Q6	-0.734	0.693	0.29	-2.098	0.629
	Q5vs.O7	-0.393	0.605	0.516	-1.584	0.797
	Q5vs.O8	0.593	0.626	0.344	-0.638	1.824
	Q5vs.O9	0.064	0.605	0.916	-1.127	1.254
	Q5vs.O10	0.057	0.605	0.926	-1.134	1.247
	Q5vs.O11	0.424	0.654	0.517	-0.862	1.71
	Q5vs.Q12	0.38	0.626	0.545	-0.851	1.611
	Q5vs.Q13	-0.822	0.589	0.164	-1.981	0.337
	Q5vs.Q16	-1.174	0.626	0.062	-2.405	0.057
	Q5vs.Q17	-0.112	0.654	0.864	-1.398	1.174
	Q5vs.Q18	-0.516	0.654	0.43	-1.802	0.77
	Q5vs.Q19	-1.26	0.693	0.07	-2.623	0.104
	Q5vs.A20	0.035	0.626	0.956	-1.196	1.266
	Q5vs.Q22	0.617	0.605	0.309	-0.574	1.807
	Q5vs.A23	0.247	0.605	0.684	-0.944	1.437
	Q5vs.A24	-0.922	0.626	0.142	-2.153	0.309
	Q5vs.A25	-0.525	0.605	0.386	-1.715	0.666
	Q5vs.A26	1.561*	0.626	0.013	0.33	2.792
	Q5vs.A27	0.203	0.693	0.77	-1.161	1.567
	Q5vs.A28	0.516	0.654	0.43	-0.77	1.802
	Q5vs.A29	-0.448	0.654	0.494	-1.734	0.838
	Q5vs.A31	0.889	0.589	0.132	-0.27	2.048
	Q5vs.A32	0.438	0.589	0.458	-0.721	1.597
	Q5vs.A33	1.354*	0.654	0.039	0.068	2.64
	Q5vs.A35	0.558	0.654	0.394	-0.728	1.844
	Q5vs.A36	0.015	0.605	0.98	-1.175	1.206
	Q5vs.A37	-0.222	0.654	0.734	-1.508	1.064
	Q5vs.A38	-0.636	0.605	0.294	-1.827	0.554
	Q5vs.1F	0.996	0.654	0.129	-0.29	2.282
	Q5vs.10F	1.052	0.654	0.108	-0.234	2.338
G122	Q6vs.Q1	2.249*	0.667	0.001	0.937	3.561
	Q6vs.Q2	0.187	0.648	0.773	-1.087	1.461
	Q6vs.Q4	0.549	0.621	0.377	-0.672	1.771
	Q6vs.Q5	0.734	0.693	0.29	-0.629	2.098
	Q6vs.O7	0.341	0.648	0.599	-0.933	1.615
	Q6vs.O8	1.328*	0.667	0.047	0.015	2.64
	Q6vs.O9	0.798	0.648	0.219	-0.476	2.072
	Q6vs.O10	0.791	0.648	0.223	-0.483	2.065

	Q6vs.O11	1.159	0.693	0.096	-0.205	2.522
	Q6vs.Q12	1.114	0.667	0.096	-0.198	2.426
	Q6vs.Q13	-0.087	0.633	0.89	-1.332	1.157
	Q6vs.Q16	-0.439	0.667	0.511	-1.751	0.873
	Q6vs.Q17	0.622	0.693	0.37	-0.741	1.986
	Q6vs.Q18	0.219	0.693	0.753	-1.145	1.582
	Q6vs.Q19	-0.525	0.731	0.473	-1.962	0.912
	Q6vs.A20	0.769	0.667	0.25	-0.543	2.081
	Q6vs.Q22	1.351*	0.648	0.038	0.077	2.625
	Q6vs.A23	0.981	0.648	0.131	-0.293	2.255
	Q6vs.A24	-0.188	0.667	0.779	-1.5	1.125
	Q6vs.A25	0.21	0.648	0.746	-1.065	1.484
	Q6vs.A26	2.296*	0.667	0.001	0.984	3.608
	Q6vs.A27	0.938	0.731	0.2	-0.5	2.375
	Q6vs.A28	1.251	0.693	0.072	-0.113	2.614
	Q6vs.A29	0.286	0.693	0.68	-1.077	1.65
	Q6vs.A31	1.624*	0.633	0.011	0.379	2.869
	Q6vs.A32	1.173	0.633	0.065	-0.072	2.417
	Q6vs.A33	2.088*	0.693	0.003	0.725	3.452
	Q6vs.A35	1.293	0.693	0.063	-0.071	2.656
	Q6vs.A36	0.75	0.648	0.248	-0.525	2.024
	Q6vs.A37	0.513	0.693	0.46	-0.851	1.876
	Q6vs.A38	0.098	0.648	0.88	-1.176	1.372
	Q6vs.1F	1.730*	0.693	0.013	0.367	3.094
	Q6vs.10F	1.787*	0.693	0.01	0.423	3.15
G122	O7vs.Q1	1.908*	0.575	0.001	0.777	3.039
	O7vs.Q2	-0.154	0.553	0.78	-1.241	0.932
	O7s.Q4	0.208	0.521	0.69	-0.816	1.233
	O7vs.Q5	0.393	0.605	0.516	-0.797	1.584
	O7vs.O6	-0.341	0.648	0.599	-1.615	0.933
	O7vs.O8	0.986	0.575	0.087	-0.145	2.117
	O7vs.O9	0.457	0.553	0.409	-0.63	1.544
	O7vs.O10	0.45	0.553	0.416	-0.637	1.537
	O7vs.O11	0.817	0.605	0.178	-0.373	2.008
	O7vs.Q12	0.773	0.575	0.18	-0.358	1.904
	O7vs.Q13	-0.429	0.535	0.424	-1.481	0.624
	O7vs.Q16	-0.78	0.575	0.176	-1.911	0.351
	O7vs.Q17	0.281	0.605	0.642	-0.909	1.472
	O7vs.Q18	-0.123	0.605	0.84	-1.313	1.068
	O7vs.Q19	-0.866	0.648	0.182	-2.14	0.408
	O7vs.A20	0.428	0.575	0.457	-0.703	1.559
	O7vs.Q22	1.01	0.553	0.068	-0.077	2.097

	O7vs.A23	0.64	0.553	0.248	-0.447	1.727
	O7vs.A24	-0.529	0.575	0.359	-1.66	0.602
	O7vs.A25	-0.131	0.553	0.812	-1.218	0.955
	O7vs.A26	1.955*	0.575	0.001	0.824	3.086
	O7vs.A27	0.596	0.648	0.358	-0.678	1.871
	O7vs.A28	0.909	0.605	0.134	-0.281	2.1
	O7vs.A29	-0.055	0.605	0.928	-1.245	1.136
	O7vs.A31	1.283*	0.535	0.017	0.231	2.335
	O7vs.A32	0.831	0.535	0.121	-0.221	1.884
	O7vs.A33	1.747*	0.605	0.004	0.557	2.938
	O7vs.A35	0.951	0.605	0.117	-0.239	2.142
	O7vsA36	0.409	0.553	0.46	-0.678	1.495
	O7vs.A37	0.171	0.605	0.777	-1.019	1.362
	O7vs.A38	-0.243	0.553	0.661	-1.33	0.844
	O7vs.1F	1.389*	0.605	0.022	0.199	2.58
	O7vs.10F	1.445*	0.605	0.017	0.255	2.636
G122	O8vs.Q1	0.922	0.597	0.123	-0.252	2.095
	O8vs.Q2	-1.141*	0.575	0.048	-2.272	-0.010
	O8s.Q4	-0.778	0.545	0.154	-1.850	0.293
	O8vs.Q5	-0.593	0.626	0.344	-1.824	0.638
	O8vs.O6	-1.328*	0.667	0.047	-2.640	-0.015
	O8vs.O7	-0.986	0.575	0.087	-2.117	0.145
	O8vs.O9	-0.529	0.575	0.358	-1.660	0.602
	O8vs.O10	-0.536	0.575	0.352	-1.667	0.595
	O8vs.O11	-0.169	0.626	0.787	-1.400	1.062
	O8vs.Q12	-0.213	0.597	0.721	-1.387	0.960
	O8vs.Q13	-1.415*	0.558	0.012	-2.513	-0.317
	O8vs.Q16	-1.767*	0.597	0.003	-2.940	-0.593
	O8vs.Q17	-0.705	0.626	0.261	-1.936	0.526
	O8vs.Q18	-1.109	0.626	0.077	-2.340	0.122
	O8vs.Q19	-1.853*	0.667	0.006	-3.165	-0.540
	O8vs.A20	-0.558	0.597	0.350	-1.732	0.615
	O8vs.Q22	0.024	0.575	0.967	-1.107	1.155
	O8vs.A23	-0.346	0.575	0.547	-1.477	0.785
	O8vs.A24	-1.515*	0.597	0.012	-2.689	-0.341
	O8vs.A25	-1.118	0.575	0.053	-2.249	0.013
	O8vs.A26	0.968	0.597	0.106	-0.205	2.142
	O8vs.A27	-0.390	0.667	0.559	-1.702	0.922
	O8vs.A28	-0.077	0.626	0.902	-1.308	1.154
	O8vs.A29	-1.041	0.626	0.097	-2.272	0.190
	O8vs.A31	0.296	0.558	0.596	-0.802	1.394

	O8vs.A32	-0.155	0.558	0.781	-1.253	0.943
	O8vs.A33	0.761	0.626	0.225	-0.470	1.992
	O8vs.A35	-0.035	0.626	0.955	-1.266	1.196
	O8vsA36	-0.578	0.575	0.316	-1.709	0.553
	O8vs.A37	-0.815	0.626	0.194	-2.046	0.416
	O8vs.A38	-1.229*	0.575	0.033	-2.360	-0.098
	O8vs.1F	0.403	0.626	0.520	-0.828	1.634
	O8vs.10F	0.459	0.626	0.464	-0.772	1.690
	O9vs.Q1	1.451*	0.575	0.012	0.320	2.582
	O9vs.Q2	-0.611	0.553	0.269	-1.698	0.475
	O9vs.Q4	-0.249	0.521	0.633	-1.274	0.775
	O9vs.Q5	-0.064	0.605	0.916	-1.254	1.127
	O9vs.O6	-0.798	0.648	0.219	-2.072	0.476
	O9vs.O7	-0.457	0.553	0.409	-1.544	0.630
	O9vs.O8	0.529	0.575	0.358	-0.602	1.660
	O9vs.O10	-0.007	0.553	0.990	-1.094	1.080
	O9vs.O11	0.360	0.605	0.552	-0.830	1.551
	O9vs.Q12	0.316	0.575	0.583	-0.815	1.447
	O9vs.Q13	-0.886	0.535	0.099	-1.938	0.166
	O9vs.Q16	-1.237*	0.575	0.032	-2.368	-0.106
	O9vs.Q17	-0.176	0.605	0.772	-1.366	1.015
	O9vs.Q18	-0.580	0.605	0.339	-1.770	0.611
	O9vs.Q19	-1.323*	0.648	0.042	-2.597	-0.049
	O9vs.A20	-0.029	0.575	0.960	-1.160	1.102
G122	O9vs.Q22	0.553	0.553	0.318	-0.534	1.640
	O9vs.A23	0.183	0.553	0.741	-0.904	1.270
	O9vs.A24	-0.986	0.575	0.087	-2.117	0.145
	O9vs.A25	-0.589	0.553	0.288	-1.675	0.498
	O9vs.A26	1.498*	0.575	0.010	0.367	2.629
	O9vs.A27	0.139	0.648	0.830	-1.135	1.413
	O9vs.A28	0.452	0.605	0.455	-0.738	1.643
	O9vs.A29	-0.512	0.605	0.398	-1.702	0.679
	O9vs.A31	0.826	0.535	0.124	-0.227	1.878
	O9vs.A32	0.374	0.535	0.485	-0.678	1.426
	O9vs.A33	1.290*	0.605	0.034	0.100	2.481
	O9vs.A35	0.494	0.605	0.415	-0.696	1.685
	O9vsA36	-0.049	0.553	0.930	-1.135	1.038
	O9vs.A37	-0.286	0.605	0.637	-1.476	0.905
	O9vs.A38	-0.700	0.553	0.206	-1.787	0.387
	O9vs.1F	0.932	0.605	0.124	-0.258	2.123
	O9vs.10F	0.988	0.605	0.103	-0.202	2.179
G122	O10vs.Q1	1.458*	0.575	0.012	0.327	2.589

	O10vs.Q2	-0.604	0.553	0.275	-1.691	0.482
	O10vs.Q4	-0.242	0.521	0.643	-1.266	0.783
	O10vs.Q5	-0.057	0.605	0.926	-1.247	1.134
	O10vs.O6	-0.791	0.648	0.223	-2.065	0.483
	O10vs.O7	-0.450	0.553	0.416	-1.537	0.637
	O10vs.O8	0.536	0.575	0.352	-0.595	1.667
	O10vs.O9	0.007	0.553	0.990	-1.080	1.094
	O10vs.O11	0.367	0.605	0.544	-0.823	1.558
	O10vs.Q12	0.323	0.575	0.575	-0.808	1.454
	O10vs.Q13	-0.879	0.535	0.101	-1.931	0.174
	O10vs.Q16	-1.230*	0.575	0.033	-2.361	-0.099
	O10vs.Q17	-0.169	0.605	0.781	-1.359	1.022
	O10vs.Q18	-0.573	0.605	0.345	-1.763	0.618
	O10vs.Q19	-1.316*	0.648	0.043	-2.590	-0.042
	O10vs.A20	-0.022	0.575	0.970	-1.153	1.109
	O10vs.Q22	0.560	0.553	0.312	-0.527	1.647
	O10vs.A23	0.190	0.553	0.731	-0.897	1.277
	O10vs.A24	-0.979	0.575	0.090	-2.110	0.152
	O10vs.A25	-0.581	0.553	0.293	-1.668	0.505
	O10vs.A26	1.505*	0.575	0.009	0.374	2.636
	O10vs.A27	0.146	0.648	0.821	-1.128	1.421
	O10vs.A28	0.459	0.605	0.448	-0.731	1.650
	O10vs.A29	-0.505	0.605	0.405	-1.695	0.686
	O10vs.A31	0.833	0.535	0.120	-0.219	1.885
	O10vs.A32	0.381	0.535	0.476	-0.671	1.434
	O10vs.A33	1.297*	0.605	0.033	0.107	2.488
	O10vs.A35	0.501	0.605	0.408	-0.689	1.692
	O10vsA36	-0.041	0.553	0.940	-1.128	1.045
	O10vs.A37	-0.279	0.605	0.646	-1.469	0.912
	O10vs.A38	-0.693	0.553	0.211	-1.780	0.394
	O10vs.1F	0.939	0.605	0.122	-0.251	2.130
	O10vs.10F	0.995	0.605	0.101	-0.195	2.186
G122	O11vs.Q1	1.091	0.626	0.082	-0.140	2.322
	O11vs.Q2	-0.972	0.605	0.109	-2.162	0.219
	O11vs.Q4	-0.609	0.577	0.291	-1.743	0.525
	O11vs.Q5	-0.424	0.654	0.517	-1.710	0.862
	O11vs.O6	-1.159	0.693	0.096	-2.522	0.205
	O11vs.O7	-0.817	0.605	0.178	-2.008	0.373
	O11vs.O8	0.169	0.626	0.787	-1.062	1.400
	O11vs.O9	-0.360	0.605	0.552	-1.551	0.830
	O11vs.O10	-0.367	0.605	0.544	-1.558	0.823
	O11vs.Q12	-0.044	0.626	0.944	-1.275	1.187

	O11vs.Q13	-1.246*	0.589	0.035	-2.405	-0.087
	O11vs.Q16	-1.598*	0.626	0.011	-2.829	-0.367
	O11vs.Q17	-0.536	0.654	0.413	-1.822	0.750
	O11vs.Q18	-0.940	0.654	0.151	-2.226	0.346
	O11vs.Q19	-1.684*	0.693	0.016	-3.047	-0.320
	O11vs.A20	-0.389	0.626	0.534	-1.620	0.842
	O11vs.Q22	0.193	0.605	0.751	-0.998	1.383
	O11vs.A23	-0.177	0.605	0.770	-1.368	1.013
	O11vs.A24	-1.346*	0.626	0.032	-2.577	-0.115
	O11vs.A25	-0.949	0.605	0.118	-2.139	0.242
	O11vs.A26	1.137	0.626	0.070	-0.094	2.368
	O11vs.A27	-0.221	0.693	0.750	-1.585	1.143
	O11vs.A28	0.092	0.654	0.888	-1.194	1.378
	O11vs.A29	-0.872	0.654	0.183	-2.158	0.414
	O11vs.A31	0.465	0.589	0.430	-0.694	1.624
	O11vs.A32	0.014	0.589	0.981	-1.145	1.173
	O11vs.A33	0.930	0.654	0.156	-0.356	2.216
	O11vs.A35	0.134	0.654	0.838	-1.152	1.420
	O11vsA36	-0.409	0.605	0.500	-1.599	0.782
	O11vs.A37	-0.646	0.654	0.324	-1.932	0.640
	O11vs.A38	-1.060	0.605	0.081	-2.251	0.130
	O11vs.1F	0.572	0.654	0.382	-0.714	1.858
	O11vs.10F	0.628	0.654	0.337	-0.658	1.914
G122	Q12vs.Q1	1.135	0.597	0.058	-0.039	2.309
	Q12vs.Q2	-0.927	0.575	0.108	-2.058	0.204
	Q12vs.Q4	-0.565	0.545	0.300	-1.636	0.506
	Q12vs.Q5	-0.380	0.626	0.545	-1.611	0.851
	Q12vs.O6	-1.114	0.667	0.096	-2.426	0.198
	Q12vs.O7	-0.773	0.575	0.180	-1.904	0.358
	Q12vs.O8	0.213	0.597	0.721	-0.960	1.387
	Q12vs.O9	-0.316	0.575	0.583	-1.447	0.815
	Q12vs.O10	-0.323	0.575	0.575	-1.454	0.808
	Q12vs.O11	0.044	0.626	0.944	-1.187	1.275
	Q12vs.Q13	-1.202*	0.558	0.032	-2.300	-0.104
	Q12vs.Q16	-1.553*	0.597	0.010	-2.727	-0.380
	Q12vs.Q17	-0.492	0.626	0.433	-1.723	0.739
	Q12vs.Q18	-0.896	0.626	0.153	-2.127	0.335
	Q12vs.Q19	-1.639*	0.667	0.015	-2.951	-0.327
	Q12vs.A20	-0.345	0.597	0.564	-1.519	0.829
	Q12vs.Q22	0.237	0.575	0.681	-0.894	1.368
	Q12vs.A23	-0.133	0.575	0.817	-1.264	0.998
	Q12vs.A24	-1.302*	0.597	0.030	-2.475	-0.128

	Q12vs.A25	-0.905	0.575	0.117	-2.036	0.226
	Q12vs.A26	1.182*	0.597	0.048	0.008	2.355
	Q12vs.A27	-0.177	0.667	0.791	-1.489	1.136
	Q12vs.A28	0.136	0.626	0.828	-1.095	1.367
	Q12vs.A29	-0.828	0.626	0.187	-2.059	0.403
	Q12vs.A31	0.510	0.558	0.362	-0.588	1.607
	Q12vs.A32	0.058	0.558	0.917	-1.040	1.156
	Q12vs.A33	0.974	0.626	0.120	-0.257	2.205
	Q12vs.A35	0.178	0.626	0.776	-1.053	1.409
	Q12vsA36	-0.365	0.575	0.527	-1.496	0.766
	Q12vs.A37	-0.602	0.626	0.337	-1.833	0.629
	Q12vs.A38	-1.016	0.575	0.078	-2.147	0.115
	Q12vs.1F	0.616	0.626	0.325	-0.615	1.847
	Q12vs.10F	0.672	0.626	0.284	-0.559	1.903
G122	Q13vs.Q1	2.337*	0.558	0.000	1.239	3.435
	Q13vs.Q2	0.274	0.535	0.608	-0.778	1.326
	Q13vs.Q4	0.637	0.502	0.206	-0.351	1.624
	Q13vs.Q5	0.822	0.589	0.164	-0.337	1.981
	Q13vs.O6	0.087	0.633	0.890	-1.157	1.332
	Q13vs.O7	0.429	0.535	0.424	-0.624	1.481
	Q13vs.O8	1.415*	0.558	0.012	0.317	2.513
	Q13vs.O9	0.886	0.535	0.099	-0.166	1.938
	Q13vs.O10	0.879	0.535	0.101	-0.174	1.931
	Q13vs.O11	1.246*	0.589	0.035	0.087	2.405
	Q13vs.Q12	1.202*	0.558	0.032	0.104	2.300
	Q13vs.Q16	-0.352	0.558	0.529	-1.450	0.746
	Q13vs.Q17	0.710	0.589	0.229	-0.449	1.869
	Q13vs.Q18	0.306	0.589	0.604	-0.853	1.465
	Q13vs.Q19	-0.438	0.633	0.490	-1.682	0.807
	Q13vs.A20	0.857	0.558	0.126	-0.241	1.955
	Q13vs.Q22	1.439*	0.535	0.008	0.386	2.491
	Q13vs.A23	1.069*	0.535	0.047	0.016	2.121
	Q13vs.A24	-0.100	0.558	0.858	-1.198	0.998
	Q13vs.A25	0.297	0.535	0.579	-0.755	1.349
	Q13vs.A26	2.383*	0.558	0.000	1.285	3.481
	Q13vs.A27	1.025	0.633	0.106	-0.220	2.270
	Q13vs.A28	1.338*	0.589	0.024	0.179	2.497
	Q13vs.A29	0.374	0.589	0.526	-0.785	1.533
	Q13vs.A31	1.711*	0.517	0.001	0.695	2.728
	Q13vs.A32	1.260*	0.517	0.015	0.244	2.276
	Q13vs.A33	2.176*	0.589	0.000	1.017	3.335
	Q13vs.A35	1.380*	0.589	0.020	0.221	2.539

	Q13vsA36	0.837	0.535	0.119	-0.215	1.889
	Q13vs.A37	0.600	0.589	0.309	-0.559	1.759
	Q13vs.A38	0.186	0.535	0.729	-0.866	1.238
	Q13vs.1F	1.818*	0.589	0.002	0.659	2.977
	Q13vs.10F	1.874*	0.589	0.002	0.715	3.033
	Q16vs.Q1	2.688*	0.597	0.000	1.515	3.862
	Q16vs.Q2	0.626	0.575	0.277	-0.505	1.757
	Q16vs.Q4	0.988	0.545	0.071	-0.083	2.060
	Q16vs.Q5	1.174	0.626	0.062	-0.057	2.405
	Q16vs.O6	0.439	0.667	0.511	-0.873	1.751
	Q16vs.O7	0.780	0.575	0.176	-0.351	1.911
	Q16vs.O8	1.767*	0.597	0.003	0.593	2.940
	Q16vs.O9	1.237*	0.575	0.032	0.106	2.368
	Q16vs.O10	1.230*	0.575	0.033	0.099	2.361
	Q16vs.O11	1.598*	0.626	0.011	0.367	2.829
	Q16vs.Q12	1.553*	0.597	0.010	0.380	2.727
	Q16vs.Q13	0.352	0.558	0.529	-0.746	1.450
	Q16vs.Q17	1.062	0.626	0.091	-0.169	2.293
	Q16vs.Q18	0.658	0.626	0.294	-0.573	1.889
	Q16vs.Q19	-0.086	0.667	0.898	-1.398	1.226
	Q16vs.A20	1.208*	0.597	0.044	0.035	2.382
G122	Q16vs.Q22	1.790*	0.575	0.002	0.659	2.921
	Q16vs.A23	1.420*	0.575	0.014	0.289	2.551
	Q16vs.A24	0.252	0.597	0.674	-0.922	1.425
	Q16vs.A25	0.649	0.575	0.260	-0.482	1.780
	Q16vs.A26	2.735*	0.597	0.000	1.561	3.909
	Q16vs.A27	1.377*	0.667	0.040	0.064	2.689
	Q16vs.A28	1.690*	0.626	0.007	0.459	2.921
	Q16vs.A29	0.726	0.626	0.247	-0.505	1.957
	Q16vs.A31	2.063*	0.558	0.000	0.965	3.161
	Q16vs.A32	1.612*	0.558	0.004	0.514	2.710
	Q16vs.A33	2.528*	0.626	0.000	1.297	3.759
	Q16vs.A35	1.732*	0.626	0.006	0.501	2.963
	Q16vsA36	1.189*	0.575	0.039	0.058	2.320
	Q16vs.A37	0.952	0.626	0.129	-0.279	2.183
	Q16vs.A38	0.537	0.575	0.351	-0.594	1.668
	Q16vs.1F	2.170*	0.626	0.001	0.939	3.401
	Q16vs.10F	2.226*	0.626	0.000	0.995	3.457
	Q17vs.Q1	1.627*	0.626	0.010	0.396	2.858
G122	Q17vs.Q2	-0.436	0.605	0.472	-1.626	0.755
	Q17vs.Q4	-0.073	0.577	0.899	-1.207	1.061

	Q17vs.Q5	0.112	0.654	0.864	-1.174	1.398
	Q17vs.O6	-0.622	0.693	0.370	-1.986	0.741
	Q17vs.O7	-0.281	0.605	0.642	-1.472	0.909
	Q17vs.O8	0.705	0.626	0.261	-0.526	1.936
	Q17vs.O9	0.176	0.605	0.772	-1.015	1.366
	Q17vs.O10	0.169	0.605	0.781	-1.022	1.359
	Q17vs.O11	0.536	0.654	0.413	-0.750	1.822
	Q17vs.Q12	0.492	0.626	0.433	-0.739	1.723
	Q17vs.Q13	-0.710	0.589	0.229	-1.869	0.449
	Q17vs.Q16	-1.062	0.626	0.091	-2.293	0.169
	Q17vs.Q18	-0.404	0.654	0.537	-1.690	0.882
	Q17vs.Q19	-1.148	0.693	0.099	-2.511	0.216
	Q17vs.A20	0.147	0.626	0.815	-1.084	1.378
	Q17vs.Q22	0.729	0.605	0.230	-0.462	1.919
	Q17vs.A23	0.359	0.605	0.554	-0.832	1.549
	Q17vs.A24	-0.810	0.626	0.196	-2.041	0.421
	Q17vs.A25	-0.413	0.605	0.496	-1.603	0.778
	Q17vs.A26	1.673*	0.626	0.008	0.442	2.904
	Q17vs.A27	0.315	0.693	0.650	-1.049	1.679
	Q17vs.A28	0.628	0.654	0.337	-0.658	1.914
	Q17vs.A29	-0.336	0.654	0.608	-1.622	0.950
	Q17vs.A31	1.001	0.589	0.090	-0.158	2.160
	Q17vs.A32	0.550	0.589	0.351	-0.609	1.709
	Q17vs.A33	1.466*	0.654	0.026	0.180	2.752
	Q17vs.A35	0.670	0.654	0.306	-0.616	1.956
	Q17vsA36	0.127	0.605	0.834	-1.063	1.318
	Q17vs.A37	-0.110	0.654	0.866	-1.396	1.176
	Q17vs.A38	-0.524	0.605	0.387	-1.715	0.666
	Q17vs.1F	1.108	0.654	0.091	-0.178	2.394
	Q17vs.10F	1.164	0.654	0.076	-0.122	2.450
G122	Q18vs.Q1	2.031*	0.626	0.001	0.800	3.262
	Q18vs.Q2	-0.032	0.605	0.958	-1.222	1.159
	Q18vs.Q4	0.331	0.577	0.567	-0.803	1.465
	Q18vs.Q5	0.516	0.654	0.430	-0.770	1.802
	Q18vs.O6	-0.219	0.693	0.753	-1.582	1.145
	Q18vs.O7	0.123	0.605	0.840	-1.068	1.313
	Q18vs.O8	1.109	0.626	0.077	-0.122	2.340
	Q18vs.O9	0.580	0.605	0.339	-0.611	1.770
	Q18vs.O10	0.573	0.605	0.345	-0.618	1.763
	Q18vs.O11	0.940	0.654	0.151	-0.346	2.226
	Q18vs.Q12	0.896	0.626	0.153	-0.335	2.127
	Q18vs.Q13	-0.306	0.589	0.604	-1.465	0.853
	Q18vs.Q16	-0.658	0.626	0.294	-1.889	0.573

	Q18vs.Q17	0.404	0.654	0.537	-0.882	1.690
	Q18vs.Q19	-0.744	0.693	0.284	-2.107	0.620
	Q18vs.A20	0.551	0.626	0.380	-0.680	1.782
	Q18vs.Q22	1.133	0.605	0.062	-0.058	2.323
	Q18vs.A23	0.763	0.605	0.209	-0.428	1.953
	Q18vs.A24	-0.406	0.626	0.517	-1.637	0.825
	Q18vs.A25	-0.009	0.605	0.988	-1.199	1.182
	Q18vs.A26	2.077*	0.626	0.001	0.846	3.308
	Q18vs.A27	0.719	0.693	0.301	-0.645	2.083
	Q18vs.A28	1.032	0.654	0.115	-0.254	2.318
	Q18vs.A29	0.068	0.654	0.917	-1.218	1.354
	Q18vs.A31	1.405*	0.589	0.018	0.246	2.564
	Q18vs.A32	0.954	0.589	0.106	-0.205	2.113
	Q18vs.A33	1.870*	0.654	0.004	0.584	3.156
	Q18vs.A35	1.074	0.654	0.101	-0.212	2.360
	Q18vsA36	0.531	0.605	0.381	-0.659	1.722
	Q18vs.A37	0.294	0.654	0.653	-0.992	1.580
	Q18vs.A38	-0.120	0.605	0.843	-1.311	1.070
	Q18vs.1F	1.512*	0.654	0.021	0.226	2.798
	Q18vs.10F	1.568*	0.654	0.017	0.282	2.854
G122	Q19vs.Q1	2.774*	0.667	0.000	1.462	4.086
	Q19vs.Q2	0.712	0.648	0.273	-0.562	1.986
	Q19vs.Q4	1.074	0.621	0.085	-0.147	2.296
	Q19vs.Q5	1.260	0.693	0.070	-0.104	2.623
	Q19vs.O6	0.525	0.731	0.473	-0.912	1.962
	Q19vs.O7	0.866	0.648	0.182	-0.408	2.140
	Q19vs.O8	1.853*	0.667	0.006	0.540	3.165
	Q19vs.O9	1.323*	0.648	0.042	0.049	2.597
	Q19vs.O10	1.316*	0.648	0.043	0.042	2.590
	Q19vs.O11	1.684*	0.693	0.016	0.320	3.047
	Q19vs.Q12	1.639*	0.667	0.015	0.327	2.951
	Q19vs.Q13	0.438	0.633	0.490	-0.807	1.682
	Q19vs.Q16	0.086	0.667	0.898	-1.226	1.398
	Q19vs.Q17	1.148	0.693	0.099	-0.216	2.511
	Q19vs.Q18	0.744	0.693	0.284	-0.620	2.107
	Q19vs.A20	1.294	0.667	0.053	-0.018	2.606
	Q19vs.Q22	1.876*	0.648	0.004	0.602	3.150
	Q19vs.A23	1.506*	0.648	0.021	0.232	2.780
	Q19vs.A24	0.337	0.667	0.613	-0.975	1.650
	Q19vs.A25	0.735	0.648	0.258	-0.540	2.009
	Q19vs.A26	2.821*	0.667	0.000	1.509	4.133

	Q19vs.A27	1.463*	0.731	0.046	0.025	2.900
	Q19vs.A28	1.776*	0.693	0.011	0.412	3.139
	Q19vs.A29	0.812	0.693	0.243	-0.552	2.175
	Q19vs.A31	2.149*	0.633	0.001	0.904	3.394
	Q19vs.A32	1.698*	0.633	0.008	0.453	2.942
	Q19vs.A33	2.614*	0.693	0.000	1.250	3.977
	Q19vs.A35	1.818*	0.693	0.009	0.454	3.181
	Q19vsA36	1.275*	0.648	0.050	0.000	2.549
	Q19vs.A37	1.038	0.693	0.135	-0.326	2.401
	Q19vs.A38	0.623	0.648	0.337	-0.651	1.897
	Q19vs.1F	2.255*	0.693	0.001	0.892	3.619
	Q19vs.10F	2.312*	0.693	0.001	0.948	3.675
G122	A20vs.Q1	1.480*	0.597	0.014	0.306	2.654
	A20vs.Q2	-0.582	0.575	0.312	-1.713	0.549
	A20vs.Q4	-0.220	0.545	0.687	-1.291	0.851
	A20vs.Q5	-0.035	0.626	0.956	-1.266	1.196
	A20vs.O6	-0.769	0.667	0.250	-2.081	0.543
	A20vs.O7	-0.428	0.575	0.457	-1.559	0.703
	A20vs.O8	0.558	0.597	0.350	-0.615	1.732
	A20vs.O9	0.029	0.575	0.960	-1.102	1.160
	A20vs.O10	0.022	0.575	0.970	-1.109	1.153
	A20vs.O11	0.389	0.626	0.534	-0.842	1.620
	A20vs.Q12	0.345	0.597	0.564	-0.829	1.519
	A20vs.Q13	-0.857	0.558	0.126	-1.955	0.241
	A20vs.Q16	-1.208*	0.597	0.044	-2.382	-0.035
	A20vs.Q17	-0.147	0.626	0.815	-1.378	1.084
	A20vs.Q18	-0.551	0.626	0.380	-1.782	0.680
	A20vs.Q19	-1.294	0.667	0.053	-2.606	0.018
	A20vs.Q22	0.582	0.575	0.312	-0.549	1.713
	A20vs.A23	0.212	0.575	0.713	-0.919	1.343
	A20vs.A24	-0.957	0.597	0.110	-2.130	0.217
	A20vs.A25	-0.560	0.575	0.331	-1.691	0.571
	A20vs.A26	1.527*	0.597	0.011	0.353	2.700
	A20vs.A27	0.168	0.667	0.801	-1.144	1.481
	A20vs.A28	0.481	0.626	0.442	-0.750	1.712
	A20vs.A29	-0.483	0.626	0.441	-1.714	0.748
	A20vs.A31	0.855	0.558	0.127	-0.243	1.952
	A20vs.A32	0.403	0.558	0.470	-0.695	1.501
	A20vs.A33	1.319*	0.626	0.036	0.088	2.550
	A20vs.A35	0.523	0.626	0.404	-0.708	1.754
	A20vsA36	-0.020	0.575	0.973	-1.151	1.111

	A20vs.A37	-0.257	0.626	0.682	-1.488	0.974
	A20vs.A38	-0.671	0.575	0.244	-1.802	0.460
	A20vs.1F	0.961	0.626	0.125	-0.270	2.192
	A20vs.10F	1.017	0.626	0.105	-0.214	2.248
G122	A22vs.Q1	0.898	0.575	0.119	-0.233	2.029
	A22vs.Q2	-1.164*	0.553	0.036	-2.251	-0.078
	A22vs.Q4	-0.802	0.521	0.125	-1.826	0.223
	A22vs.Q5	-0.617	0.605	0.309	-1.807	0.574
	A22vs.O6	-1.351*	0.648	0.038	-2.625	-0.077
	A22vs.O7	-1.010	0.553	0.068	-2.097	0.077
	A22vs.O8	-0.024	0.575	0.967	-1.155	1.107
	A22vs.O9	-0.553	0.553	0.318	-1.640	0.534
	A22vs.O10	-0.560	0.553	0.312	-1.647	0.527
	A22vs.O11	-0.193	0.605	0.751	-1.383	0.998
	A22vs.Q12	-0.237	0.575	0.681	-1.368	0.894
	A22vs.Q13	-1.439*	0.535	0.008	-2.491	-0.386
	A22vs.Q16	-1.790*	0.575	0.002	-2.921	-0.659
	A22vs.Q17	-0.729	0.605	0.230	-1.919	0.462
	A22vs.Q18	-1.133	0.605	0.062	-2.323	0.058
	A22vs.Q19	-1.876*	0.648	0.004	-3.150	-0.602
	A22vs.A20	-0.582	0.575	0.312	-1.713	0.549
	A22vs.A23	-0.370	0.553	0.504	-1.457	0.717
	A22vs.A24	-1.539*	0.575	0.008	-2.670	-0.408
	A22vs.A25	-1.141*	0.553	0.040	-2.228	-0.055
	A22vs.A26	0.945	0.575	0.101	-0.186	2.076
	A22vs.A27	-0.414	0.648	0.524	-1.688	0.861
	A22vs.A28	-0.101	0.605	0.868	-1.291	1.090
	A22vs.A29	-1.065	0.605	0.079	-2.255	0.126
	A22vs.A31	0.273	0.535	0.611	-0.779	1.325
	A22vs.A32	-0.179	0.535	0.739	-1.231	0.874
	A22vs.A33	0.737	0.605	0.224	-0.453	1.928
	A22vs.A35	-0.059	0.605	0.923	-1.249	1.132
	A22vsA36	-0.601	0.553	0.277	-1.688	0.485
	A22vs.A37	-0.839	0.605	0.167	-2.029	0.352
	A22vs.A38	-1.253*	0.553	0.024	-2.340	-0.166
	A22vs.1F	0.379	0.605	0.531	-0.811	1.570
	A22vs.10F	0.435	0.605	0.472	-0.755	1.626
G122	A23vs.Q1	1.268*	0.575	0.028	0.137	2.399
	A23vs.Q2	-0.794	0.553	0.151	-1.881	0.292
	A23vs.Q4	-0.432	0.521	0.408	-1.456	0.593
	A23vs.Q5	-0.247	0.605	0.684	-1.437	0.944
	A23vs.O6	-0.981	0.648	0.131	-2.255	0.293

	A23vs.O7	-0.640	0.553	0.248	-1.727	0.447
	A23vs.O8	0.346	0.575	0.547	-0.785	1.477
	A23vs.O9	-0.183	0.553	0.741	-1.270	0.904
	A23vs.O10	-0.190	0.553	0.731	-1.277	0.897
	A23vs.O11	0.177	0.605	0.770	-1.013	1.368
	A23vs.Q12	0.133	0.575	0.817	-0.998	1.264
	A23vs.Q13	-1.069*	0.535	0.047	-2.121	-0.016
	A23vs.Q16	-1.420*	0.575	0.014	-2.551	-0.289
	A23vs.Q17	-0.359	0.605	0.554	-1.549	0.832
	A23vs.Q18	-0.763	0.605	0.209	-1.953	0.428
	A23vs.Q19	-1.506*	0.648	0.021	-2.780	-0.232
	A23vs.A20	-0.212	0.575	0.713	-1.343	0.919
	A23vs.A22	0.370	0.553	0.504	-0.717	1.457
	A23vs.A24	-1.169*	0.575	0.043	-2.300	-0.038
	A23vs.A25	-0.771	0.553	0.164	-1.858	0.315
	A23vs.A26	1.315*	0.575	0.023	0.184	2.446
	A23vs.A27	-0.044	0.648	0.946	-1.318	1.231
	A23vs.A28	0.269	0.605	0.657	-0.921	1.460
	A23vs.A29	-0.695	0.605	0.252	-1.885	0.496
	A23vs.A31	0.643	0.535	0.230	-0.409	1.695
	A23vs.A32	0.191	0.535	0.721	-0.861	1.244
	A23vs.A33	1.107	0.605	0.068	-0.083	2.298
	A23vs.A35	0.311	0.605	0.607	-0.879	1.502
	A23vsA36	-0.231	0.553	0.676	-1.318	0.855
	A23vs.A37	-0.469	0.605	0.439	-1.659	0.722
	A23vs.A38	-0.883	0.553	0.111	-1.970	0.204
	A23vs.1F	0.749	0.605	0.216	-0.441	1.940
	A23vs.10F	0.805	0.605	0.184	-0.385	1.996
G122	A24vs.Q1	2.437*	0.597	0.000	1.263	3.610
	A24vs.Q2	0.374	0.575	0.516	-0.757	1.505
	A24vs.Q4	0.737	0.545	0.177	-0.335	1.808
	A24vs.Q5	0.922	0.626	0.142	-0.309	2.153
	A24vs.O6	0.188	0.667	0.779	-1.125	1.500
	A24vs.O7	0.529	0.575	0.359	-0.602	1.660
	A24vs.O8	1.515*	0.597	0.012	0.341	2.689
	A24vs.O9	0.986	0.575	0.087	-0.145	2.117
	A24vs.O10	0.979	0.575	0.090	-0.152	2.110
	A24vs.O11	1.346*	0.626	0.032	0.115	2.577
	A24vs.Q12	1.302*	0.597	0.030	0.128	2.475
	A24vs.Q13	0.100	0.558	0.858	-0.998	1.198
	A24vs.Q16	-0.252	0.597	0.674	-1.425	0.922
	A24vs.Q17	0.810	0.626	0.196	-0.421	2.041

	A24vs.Q18	0.406	0.626	0.517	-0.825	1.637
	A24vs.Q19	-0.337	0.667	0.613	-1.650	0.975
	A24vs.A20	0.957	0.597	0.110	-0.217	2.130
	A24vs.A22	1.539*	0.575	0.008	0.408	2.670
	A24vs.A23	1.169*	0.575	0.043	0.038	2.300
	A24vs.A25	0.397	0.575	0.490	-0.734	1.528
	A24vs.A26	2.483*	0.597	0.000	1.310	3.657
	A24vs.A27	1.125	0.667	0.093	-0.187	2.437
	A24vs.A28	1.438*	0.626	0.022	0.207	2.669
	A24vs.A29	0.474	0.626	0.449	-0.757	1.705
	A24vs.A31	1.811*	0.558	0.001	0.713	2.909
	A24vs.A32	1.360*	0.558	0.015	0.262	2.458
	A24vs.A33	2.276*	0.626	0.000	1.045	3.507
	A24vs.A35	1.480*	0.626	0.019	0.249	2.711
	A24vsA36	0.937	0.575	0.104	-0.194	2.068
	A24vs.A37	0.700	0.626	0.264	-0.531	1.931
	A24vs.A38	0.286	0.575	0.620	-0.845	1.417
	A24vs.1F	1.918*	0.626	0.002	0.687	3.149
	A24vs.10F	1.974*	0.626	0.002	0.743	3.205
G122	A25vs.Q1	2.040*	0.575	0.000	0.909	3.171
	A25vs.Q2	-0.023	0.553	0.967	-1.110	1.064
	A25vs.Q4	0.340	0.521	0.515	-0.685	1.364
	A25vs.Q5	0.525	0.605	0.386	-0.666	1.715
	A25vs.O6	-0.210	0.648	0.746	-1.484	1.065
	A25vs.O7	0.131	0.553	0.812	-0.955	1.218
	A25vs.O8	1.118	0.575	0.053	-0.013	2.249
	A25vs.O9	0.589	0.553	0.288	-0.498	1.675
	A25vs.O10	0.581	0.553	0.293	-0.505	1.668
	A25vs.O11	0.949	0.605	0.118	-0.242	2.139
	A25vs.Q12	0.905	0.575	0.117	-0.226	2.036
	A25vs.Q13	-0.297	0.535	0.579	-1.349	0.755
	A25vs.Q16	-0.649	0.575	0.260	-1.780	0.482
	A25vs.Q17	0.413	0.605	0.496	-0.778	1.603
	A25vs.Q18	0.009	0.605	0.988	-1.182	1.199
	A25vs.Q19	-0.735	0.648	0.258	-2.009	0.540
	A25vs.A20	0.560	0.575	0.331	-0.571	1.691
	A25vs.A22	1.141*	0.553	0.040	0.055	2.228
	A25vs.A23	0.771	0.553	0.164	-0.315	1.858
	A25vs.A24	-0.397	0.575	0.490	-1.528	0.734
	A25vs.A26	2.086*	0.575	0.000	0.955	3.217
	A25vs.A27	0.728	0.648	0.262	-0.546	2.002

	A25vs.A28	1.041	0.605	0.086	-0.150	2.231
	A25vs.A29	0.077	0.605	0.899	-1.114	1.267
	A25vs.A31	1.414*	0.535	0.009	0.362	2.466
	A25vs.A32	0.963	0.535	0.073	-0.089	2.015
	A25vs.A33	1.879*	0.605	0.002	0.688	3.069
	A25vs.A35	1.083	0.605	0.074	-0.108	2.273
	A25vsA36	0.540	0.553	0.329	-0.547	1.627
	A25vs.A37	0.303	0.605	0.617	-0.888	1.493
	A25vs.A38	-0.111	0.553	0.840	-1.198	0.975
	A25vs.1F	1.521*	0.605	0.012	0.330	2.711
	A25vs.10F	1.577*	0.605	0.010	0.386	2.767
G122	A26vs.Q1	-0.047	0.597	0.938	-1.220	1.127
	A26vs.Q2	-2.109*	0.575	0.000	-3.240	-0.978
	A26vs.Q4	-1.747*	0.545	0.001	-2.818	-0.675
	A26vs.Q5	-1.561*	0.626	0.013	-2.792	-0.330
	A26vs.O6	-2.296*	0.667	0.001	-3.608	-0.984
	A26vs.O7	-1.955*	0.575	0.001	-3.086	-0.824
	A26vs.O8	-0.968	0.597	0.106	-2.142	0.205
	A26vs.O9	-1.498*	0.575	0.010	-2.629	-0.367
	A26vs.O10	-1.505*	0.575	0.009	-2.636	-0.374
	A26vs.O11	-1.137	0.626	0.070	-2.368	0.094
	A26vs.Q12	-1.182*	0.597	0.048	-2.355	-0.008
	A26vs.Q13	-2.383*	0.558	0.000	-3.481	-1.285
	A26vs.Q16	-2.735*	0.597	0.000	-3.909	-1.561
	A26vs.Q17	-1.673*	0.626	0.008	-2.904	-0.442
	A26vs.Q18	-2.077*	0.626	0.001	-3.308	-0.846
	A26vs.Q19	-2.821*	0.667	0.000	-4.133	-1.509
	A26vs.A20	-1.527*	0.597	0.011	-2.700	-0.353
	A26vs.A22	-0.945	0.575	0.101	-2.076	0.186
	A26vs.A23	-1.315*	0.575	0.023	-2.446	-0.184
	A26vs.A24	-2.483*	0.597	0.000	-3.657	-1.310
	A26vs.A25	-2.086*	0.575	0.000	-3.217	-0.955
	A26vs.A27	-1.358*	0.667	0.043	-2.671	-0.046
	A26vs.A28	-1.045	0.626	0.096	-2.276	0.186
	A26vs.A29	-2.009*	0.626	0.001	-3.240	-0.778
	A26vs.A31	-0.672	0.558	0.229	-1.770	0.426
	A26vs.A32	-1.123*	0.558	0.045	-2.221	-0.025
	A26vs.A33	-0.207	0.626	0.741	-1.438	1.024
	A26vs.A35	-1.003	0.626	0.110	-2.234	0.228

	A26vsA36	-1.546*	0.575	0.008	-2.677	-0.415
	A26vs.A37	-1.783*	0.626	0.005	-3.014	-0.552
	A26vs.A38	-2.198*	0.575	0.000	-3.329	-1.067
	A26vs.1F	-0.565	0.626	0.367	-1.796	0.666
	A26vs.10F	-0.509	0.626	0.416	-1.740	0.722
G122	A27vs.Q1	1.312	0.667	0.050	-0.001	2.624
	A27vs.Q2	-0.751	0.648	0.247	-2.025	0.523
	A27vs.Q4	-0.388	0.621	0.532	-1.610	0.833
	A27vs.Q5	-0.203	0.693	0.770	-1.567	1.161
	A27vs.O6	-0.938	0.731	0.200	-2.375	0.500
	A27vs.O7	-0.596	0.648	0.358	-1.871	0.678
	A27vs.O8	0.390	0.667	0.559	-0.922	1.702
	A27vs.O9	-0.139	0.648	0.830	-1.413	1.135
	A27vs.O10	-0.146	0.648	0.821	-1.421	1.128
	A27vs.O11	0.221	0.693	0.750	-1.143	1.585
	A27vs.Q12	0.177	0.667	0.791	-1.136	1.489
	A27vs.Q13	-1.025	0.633	0.106	-2.270	0.220
	A27vs.Q16	-1.377*	0.667	0.040	-2.689	-0.064
	A27vs.Q17	-0.315	0.693	0.650	-1.679	1.049
	A27vs.Q18	-0.719	0.693	0.301	-2.083	0.645
	A27vs.Q19	-1.463*	0.731	0.046	-2.900	-0.025
	A27vs.A20	-0.168	0.667	0.801	-1.481	1.144
	A27vs.A22	0.414	0.648	0.524	-0.861	1.688
	A27vs.A23	0.044	0.648	0.946	-1.231	1.318
	A27vs.A24	-1.125	0.667	0.093	-2.437	0.187
	A27vs.A25	-0.728	0.648	0.262	-2.002	0.546
	A27vs.A26	1.358*	0.667	0.043	0.046	2.671
	A27vs.A28	0.313	0.693	0.652	-1.051	1.677
	A27vs.A29	-0.651	0.693	0.348	-2.015	0.713
	A27vs.A31	0.686	0.633	0.279	-0.559	1.931
	A27vs.A32	0.235	0.633	0.711	-1.010	1.480
	A27vs.A33	1.151	0.693	0.098	-0.213	2.515
	A27vs.A35	0.355	0.693	0.609	-1.009	1.719
	A27vsA36	-0.188	0.648	0.772	-1.462	1.086
	A27vs.A37	-0.425	0.693	0.540	-1.789	0.939
	A27vs.A38	-0.839	0.648	0.196	-2.113	0.435
	A27vs.1F	0.793	0.693	0.254	-0.571	2.157
	A27vs.10F	0.849	0.693	0.222	-0.515	2.213
G122	A28vs.Q1	0.999	0.626	0.111	-0.232	2.230
	A28vs.Q2	-1.064	0.605	0.080	-2.254	0.127
	A28vs.Q4	-0.701	0.577	0.225	-1.835	0.433
	A28vs.Q5	-0.516	0.654	0.430	-1.802	0.770

	A28vs.O6	-1.251	0.693	0.072	-2.614	0.113
	A28vs.O7	-0.909	0.605	0.134	-2.100	0.281
	A28vs.O8	0.077	0.626	0.902	-1.154	1.308
	A28vs.O9	-0.452	0.605	0.455	-1.643	0.738
	A28vs.O10	-0.459	0.605	0.448	-1.650	0.731
	A28vs.O11	-0.092	0.654	0.888	-1.378	1.194
	A28vs.Q12	-0.136	0.626	0.828	-1.367	1.095
	A28vs.Q13	-1.338*	0.589	0.024	-2.497	-0.179
	A28vs.Q16	-1.690*	0.626	0.007	-2.921	-0.459
	A28vs.Q17	-0.628	0.654	0.337	-1.914	0.658
	A28vs.Q18	-1.032	0.654	0.115	-2.318	0.254
	A28vs.Q19	-1.776*	0.693	0.011	-3.139	-0.412
	A28vs.A20	-0.481	0.626	0.442	-1.712	0.750
	A28vs.A22	0.101	0.605	0.868	-1.090	1.291
	A28vs.A23	-0.269	0.605	0.657	-1.460	0.921
	A28vs.A24	-1.438*	0.626	0.022	-2.669	-0.207
	A28vs.A25	-1.041	0.605	0.086	-2.231	0.150
	A28vs.A26	1.045	0.626	0.096	-0.186	2.276
	A28vs.A27	-0.313	0.693	0.652	-1.677	1.051
	A28vs.A29	-0.964	0.654	0.141	-2.250	0.322
	A28vs.A31	0.373	0.589	0.527	-0.786	1.532
	A28vs.A32	-0.078	0.589	0.895	-1.237	1.081
	A28vs.A33	0.838	0.654	0.201	-0.448	2.124
	A28vs.A35	0.042	0.654	0.949	-1.244	1.328
	A28vsA36	-0.501	0.605	0.409	-1.691	0.690
	A28vs.A37	-0.738	0.654	0.260	-2.024	0.548
	A28vs.A38	-1.152	0.605	0.058	-2.343	0.038
	A28vs.1F	0.480	0.654	0.463	-0.806	1.766
	A28vs.10F	0.536	0.654	0.413	-0.750	1.822
G122	A29vs.Q1	1.963*	0.626	0.002	0.732	3.194
	A29vs.Q2	-0.100	0.605	0.869	-1.290	1.091
	A29vs.Q4	0.263	0.577	0.649	-0.871	1.397
	A29vs.Q5	0.448	0.654	0.494	-0.838	1.734
	A29vs.O6	-0.286	0.693	0.680	-1.650	1.077
	A29vs.O7	0.055	0.605	0.928	-1.136	1.245
	A29vs.O8	1.041	0.626	0.097	-0.190	2.272
	A29vs.O9	0.512	0.605	0.398	-0.679	1.702
	A29vs.O10	0.505	0.605	0.405	-0.686	1.695
	A29vs.O11	0.872	0.654	0.183	-0.414	2.158
	A29vs.Q12	0.828	0.626	0.187	-0.403	2.059
	A29vs.Q13	-0.374	0.589	0.526	-1.533	0.785
	A29vs.Q16	-0.726	0.626	0.247	-1.957	0.505

	A29vs.Q17	0.336	0.654	0.608	-0.950	1.622
	A29vs.Q18	-0.068	0.654	0.917	-1.354	1.218
	A29vs.Q19	-0.812	0.693	0.243	-2.175	0.552
	A29vs.A20	0.483	0.626	0.441	-0.748	1.714
	A29vs.A22	1.065	0.605	0.079	-0.126	2.255
	A29vs.A23	0.695	0.605	0.252	-0.496	1.885
	A29vs.A24	-0.474	0.626	0.449	-1.705	0.757
	A29vs.A25	-0.077	0.605	0.899	-1.267	1.114
	A29vs.A26	2.009*	0.626	0.001	0.778	3.240
	A29vs.A27	0.651	0.693	0.348	-0.713	2.015
	A29vs.A28	0.964	0.654	0.141	-0.322	2.250
	A29vs.A31	1.337*	0.589	0.024	0.178	2.496
	A29vs.A32	0.886	0.589	0.134	-0.273	2.045
	A29vs.A33	1.802*	0.654	0.006	0.516	3.088
	A29vs.A35	1.006	0.654	0.125	-0.280	2.292
	A29vsA36	0.463	0.605	0.445	-0.727	1.654
	A29vs.A37	0.226	0.654	0.730	-1.060	1.512
	A29vs.A38	-0.188	0.605	0.756	-1.379	1.002
	A29vs.1F	1.444*	0.654	0.028	0.158	2.730
	A29vs.10F	1.500*	0.654	0.022	0.214	2.786
G122	A31vs.Q1	0.625	0.558	0.263	-0.472	1.723
	A31vs.Q2	-1.437*	0.535	0.008	-2.489	-0.385
	A31vs.Q4	-1.075*	0.502	0.033	-2.062	-0.087
	A31vs.Q5	-0.889	0.589	0.132	-2.048	0.270
	A31vs.O6	-1.624*	0.633	0.011	-2.869	-0.379
	A31vs.O7	-1.283*	0.535	0.017	-2.335	-0.231
	A31vs.O8	-0.296	0.558	0.596	-1.394	0.802
	A31vs.O9	-0.826	0.535	0.124	-1.878	0.227
	A31vs.O10	-0.833	0.535	0.120	-1.885	0.219
	A31vs.O11	-0.465	0.589	0.430	-1.624	0.694
	A31vs.Q12	-0.510	0.558	0.362	-1.607	0.588
	A31vs.Q13	-1.711*	0.517	0.001	-2.728	-0.695
	A31vs.Q16	-2.063*	0.558	0.000	-3.161	-0.965
	A31vs.Q17	-1.001	0.589	0.090	-2.160	0.158
	A31vs.Q18	-1.405*	0.589	0.018	-2.564	-0.246
	A31vs.Q19	-2.149*	0.633	0.001	-3.394	-0.904
	A31vs.A20	-0.855	0.558	0.127	-1.952	0.243
	A31vs.A22	-0.273	0.535	0.611	-1.325	0.779
	A31vs.A23	-0.643	0.535	0.230	-1.695	0.409
	A31vs.A24	-1.811*	0.558	0.001	-2.909	-0.713
	A31vs.A25	-1.414*	0.535	0.009	-2.466	-0.362

	A31vs.A26	0.672	0.558	0.229	-0.426	1.770
	A31vs.A27	-0.686	0.633	0.279	-1.931	0.559
	A31vs.A28	-0.373	0.589	0.527	-1.532	0.786
	A31vs.A29	-1.337*	0.589	0.024	-2.496	-0.178
	A31vs.A32	-0.451	0.517	0.383	-1.468	0.565
	A31vs.A33	0.465	0.589	0.431	-0.694	1.624
	A31vs.A35	-0.331	0.589	0.574	-1.490	0.828
	A31vsA36	-0.874	0.535	0.103	-1.926	0.178
	A31vs.A37	-1.111	0.589	0.060	-2.270	0.048
	A31vs.A38	-1.526*	0.535	0.005	-2.578	-0.473
	A31vs.1F	0.107	0.589	0.856	-1.052	1.266
	A31vs.10F	0.163	0.589	0.783	-0.996	1.322
G122	A32vs.Q1	1.077	0.558	0.055	-0.021	2.175
	A32vs.Q2	-0.986	0.535	0.066	-2.038	0.066
	A32vs.Q4	-0.623	0.502	0.215	-1.611	0.364
	A32vs.Q5	-0.438	0.589	0.458	-1.597	0.721
	A32vs.O6	-1.173	0.633	0.065	-2.417	0.072
	A32vs.O7	-0.831	0.535	0.121	-1.884	0.221
	A32vs.O8	0.155	0.558	0.781	-0.943	1.253
	A32vs.O9	-0.374	0.535	0.485	-1.426	0.678
	A32vs.O10	-0.381	0.535	0.476	-1.434	0.671
	A32vs.O11	-0.014	0.589	0.981	-1.173	1.145
	A32vs.Q12	-0.058	0.558	0.917	-1.156	1.040
	A32vs.Q13	-1.260*	0.517	0.015	-2.276	-0.244
	A32vs.Q16	-1.612*	0.558	0.004	-2.710	-0.514
	A32vs.Q17	-0.550	0.589	0.351	-1.709	0.609
	A32vs.Q18	-0.954	0.589	0.106	-2.113	0.205
	A32vs.Q19	-1.698*	0.633	0.008	-2.942	-0.453
	A32vs.A20	-0.403	0.558	0.470	-1.501	0.695
	A32vs.A22	0.179	0.535	0.739	-0.874	1.231
	A32vs.A23	-0.191	0.535	0.721	-1.244	0.861
	A32vs.A24	-1.360*	0.558	0.015	-2.458	-0.262
	A32vs.A25	-0.963	0.535	0.073	-2.015	0.089
	A32vs.A26	1.123*	0.558	0.045	0.025	2.221
	A32vs.A27	-0.235	0.633	0.711	-1.480	1.010
	A32vs.A28	0.078	0.589	0.895	-1.081	1.237
	A32vs.A29	-0.886	0.589	0.134	-2.045	0.273
	A32vs.A31	0.451	0.517	0.383	-0.565	1.468
	A32vs.A33	0.916	0.589	0.121	-0.243	2.075
	A32vs.A35	0.120	0.589	0.839	-1.039	1.279
	A32vsA36	-0.423	0.535	0.430	-1.475	0.629
	A32vs.A37	-0.660	0.589	0.263	-1.819	0.499

	A32vs.A38	-1.074*	0.535	0.045	-2.126	-0.022
	A32vs.1F	0.558	0.589	0.344	-0.601	1.717
	A32vs.10F	0.614	0.589	0.298	-0.545	1.773
G122	A33vs.Q1	0.161	0.626	0.798	-1.070	1.392
	A33vs.Q2	-1.902*	0.605	0.002	-3.092	-0.711
	A33vs.Q4	-1.539*	0.577	0.008	-2.673	-0.405
	A33vs.Q5	-1.354*	0.654	0.039	-2.640	-0.068
	A33vs.O6	-2.088*	0.693	0.003	-3.452	-0.725
	A33vs.O7	-1.747*	0.605	0.004	-2.938	-0.557
	A33vs.O8	-0.761	0.626	0.225	-1.992	0.470
	A33vs.O9	-1.290*	0.605	0.034	-2.481	-0.100
	A33vs.O10	-1.297*	0.605	0.033	-2.488	-0.107
	A33vs.O11	-0.930	0.654	0.156	-2.216	0.356
	A33vs.Q12	-0.974	0.626	0.120	-2.205	0.257
	A33vs.Q13	-2.176*	0.589	0.000	-3.335	-1.017
	A33vs.Q16	-2.528*	0.626	0.000	-3.759	-1.297
	A33vs.Q17	-1.466*	0.654	0.026	-2.752	-0.180
	A33vs.Q18	-1.870*	0.654	0.004	-3.156	-0.584
	A33vs.Q19	-2.614*	0.693	0.000	-3.977	-1.250
	A33vs.A20	-1.319*	0.626	0.036	-2.550	-0.088
	A33vs.A22	-0.737	0.605	0.224	-1.928	0.453
	A33vs.A23	-1.107	0.605	0.068	-2.298	0.083
	A33vs.A24	-2.276*	0.626	0.000	-3.507	-1.045
	A33vs.A25	-1.879*	0.605	0.002	-3.069	-0.688
	A33vs.A26	0.207	0.626	0.741	-1.024	1.438
	A33vs.A27	-1.151	0.693	0.098	-2.515	0.213
	A33vs.A28	-0.838	0.654	0.201	-2.124	0.448
	A33vs.A29	-1.802*	0.654	0.006	-3.088	-0.516
	A33vs.A31	-0.465	0.589	0.431	-1.624	0.694
	A33vs.A32	-0.916	0.589	0.121	-2.075	0.243
	A33vs.A35	-0.796	0.654	0.224	-2.082	0.490
	A33vsA36	-1.339*	0.605	0.028	-2.529	-0.148
	A33vs.A37	-1.576*	0.654	0.016	-2.862	-0.290
	A33vs.A38	-1.990*	0.605	0.001	-3.181	-0.800
	A33vs.1F	-0.358	0.654	0.584	-1.644	0.928
	A33vs.10F	-0.302	0.654	0.644	-1.588	0.984
G122	A34vs.Q1	0.957	0.626	0.127	-0.274	2.188
	A35vs.Q2	-1.106	0.605	0.069	-2.296	0.085
	A35vs.Q4	-0.743	0.577	0.198	-1.877	0.391
	A35vs.Q5	-0.558	0.654	0.394	-1.844	0.728

	A35vs.O6	-1.293	0.693	0.063	-2.656	0.071
	A35vs.O7	-0.951	0.605	0.117	-2.142	0.239
	A35vs.O8	0.035	0.626	0.955	-1.196	1.266
	A35vs.O9	-0.494	0.605	0.415	-1.685	0.696
	A35vs.O10	-0.501	0.605	0.408	-1.692	0.689
	A35vs.O11	-0.134	0.654	0.838	-1.420	1.152
	A35vs.Q12	-0.178	0.626	0.776	-1.409	1.053
	A35vs.Q13	-1.380*	0.589	0.020	-2.539	-0.221
	A35vs.Q16	-1.732*	0.626	0.006	-2.963	-0.501
	A35vs.Q17	-0.670	0.654	0.306	-1.956	0.616
	A35vs.Q18	-1.074	0.654	0.101	-2.360	0.212
	A35vs.Q19	-1.818*	0.693	0.009	-3.181	-0.454
	A35vs.A20	-0.523	0.626	0.404	-1.754	0.708
	A35vs.A22	0.059	0.605	0.923	-1.132	1.249
	A35vs.A23	-0.311	0.605	0.607	-1.502	0.879
	A35vs.A24	-1.480*	0.626	0.019	-2.711	-0.249
	A35vs.A25	-1.083	0.605	0.074	-2.273	0.108
	A35vs.A26	1.003	0.626	0.110	-0.228	2.234
	A35vs.A27	-0.355	0.693	0.609	-1.719	1.009
	A35vs.A28	-0.042	0.654	0.949	-1.328	1.244
	A35vs.A29	-1.006	0.654	0.125	-2.292	0.280
	A35vs.A31	0.331	0.589	0.574	-0.828	1.490
	A35vs.A32	-0.120	0.589	0.839	-1.279	1.039
	A35vs.A33	0.796	0.654	0.224	-0.490	2.082
	A35vsA36	-0.543	0.605	0.370	-1.733	0.648
	A35vs.A37	-0.780	0.654	0.234	-2.066	0.506
	A35vs.A38	-1.194*	0.605	0.049	-2.385	-0.004
	A35vs.1F	0.438	0.654	0.503	-0.848	1.724
	A35vs.10F	0.494	0.654	0.450	-0.792	1.780
G122	A36vs.Q1	1.500*	0.575	0.010	0.369	2.631
	A36vs.Q2	-0.563	0.553	0.309	-1.650	0.524
	A36vs.Q4	-0.200	0.521	0.701	-1.225	0.824
	A36vs.Q5	-0.015	0.605	0.980	-1.206	1.175
	A36vs.O6	-0.750	0.648	0.248	-2.024	0.525
	A36vs.O7	-0.409	0.553	0.460	-1.495	0.678
	A36vs.O8	0.578	0.575	0.316	-0.553	1.709
	A36vs.O9	0.049	0.553	0.930	-1.038	1.135
	A36vs.O10	0.041	0.553	0.940	-1.045	1.128
	A36vs.O11	0.409	0.605	0.500	-0.782	1.599
	A36vs.Q12	0.365	0.575	0.527	-0.766	1.496
	A36vs.Q13	-0.837	0.535	0.119	-1.889	0.215
	A36vs.Q16	-1.189*	0.575	0.039	-2.320	-0.058

	A36vs.Q17	-0.127	0.605	0.834	-1.318	1.063
	A36vs.Q18	-0.531	0.605	0.381	-1.722	0.659
	A36vs.Q19	-1.275*	0.648	0.050	-2.549	0.000
	A36vs.A20	0.020	0.575	0.973	-1.111	1.151
	A36vs.A22	0.601	0.553	0.277	-0.485	1.688
	A36vs.A23	0.231	0.553	0.676	-0.855	1.318
	A36vs.A24	-0.937	0.575	0.104	-2.068	0.194
	A36vs.A25	-0.540	0.553	0.329	-1.627	0.547
	A36vs.A26	1.546*	0.575	0.008	0.415	2.677
	A36vs.A27	0.188	0.648	0.772	-1.086	1.462
	A36vs.A28	0.501	0.605	0.409	-0.690	1.691
	A36vs.A29	-0.463	0.605	0.445	-1.654	0.727
	A36vs.A31	0.874	0.535	0.103	-0.178	1.926
	A36vs.A32	0.423	0.535	0.430	-0.629	1.475
	A36vs.A33	1.339*	0.605	0.028	0.148	2.529
	A36vs.A35	0.543	0.605	0.370	-0.648	1.733
	A36vs.A37	-0.237	0.605	0.695	-1.428	0.953
	A36vs.A38	-0.651	0.553	0.239	-1.738	0.435
	A36vs.1F	0.981	0.605	0.106	-0.210	2.171
	A36vs.10F	1.037	0.605	0.088	-0.154	2.227
G122	A37vs.Q1	1.737*	0.626	0.006	0.506	2.968
	A37vs.Q2	-0.326	0.605	0.591	-1.516	0.865
	A37vs.Q4	0.037	0.577	0.949	-1.097	1.171
	A37vs.Q5	0.222	0.654	0.734	-1.064	1.508
	A37vs.O6	-0.513	0.693	0.460	-1.876	0.851
	A37vs.O7	-0.171	0.605	0.777	-1.362	1.019
	A37vs.O8	0.815	0.626	0.194	-0.416	2.046
	A37vs.O9	0.286	0.605	0.637	-0.905	1.476
	A37vs.O10	0.279	0.605	0.646	-0.912	1.469
	A37vs.O11	0.646	0.654	0.324	-0.640	1.932
	A37vs.Q12	0.602	0.626	0.337	-0.629	1.833
	A37vs.Q13	-0.600	0.589	0.309	-1.759	0.559
	A37vs.Q16	-0.952	0.626	0.129	-2.183	0.279
	A37vs.Q17	0.110	0.654	0.866	-1.176	1.396
	A37vs.Q18	-0.294	0.654	0.653	-1.580	0.992
	A37vs.Q19	-1.038	0.693	0.135	-2.401	0.326
	A37vs.A20	0.257	0.626	0.682	-0.974	1.488
	A37vs.A22	0.839	0.605	0.167	-0.352	2.029
	A37vs.A23	0.469	0.605	0.439	-0.722	1.659
	A37vs.A24	-0.700	0.626	0.264	-1.931	0.531
	A37vs.A25	-0.303	0.605	0.617	-1.493	0.888
	A37vs.A26	1.783*	0.626	0.005	0.552	3.014

	A37vs.A27	0.425	0.693	0.540	-0.939	1.789
	A37vs.A28	0.738	0.654	0.260	-0.548	2.024
	A37vs.A29	-0.226	0.654	0.730	-1.512	1.060
	A37vs.A31	1.111	0.589	0.060	-0.048	2.270
	A37vs.A32	0.660	0.589	0.263	-0.499	1.819
	A37vs.A33	1.576*	0.654	0.016	0.290	2.862
	A37vs.A35	0.780	0.654	0.234	-0.506	2.066
	A37vs.A36	0.237	0.605	0.695	-0.953	1.428
	A37vs.A38	-0.414	0.605	0.494	-1.605	0.776
	A37vs.1F	1.218	0.654	0.063	-0.068	2.504
	A37vs.10F	1.274	0.654	0.052	-0.012	2.560
G122	A38vs.Q1	2.151*	0.575	0.000	1.020	3.282
	A38vs.Q2	0.089	0.553	0.873	-0.998	1.175
	A38vs.Q4	0.451	0.521	0.387	-0.574	1.475
	A38vs.Q5	0.636	0.605	0.294	-0.554	1.827
	A38vs.O6	-0.098	0.648	0.880	-1.372	1.176
	A38vs.O7	0.243	0.553	0.661	-0.844	1.330
	A38vs.O8	1.229*	0.575	0.033	0.098	2.360
	A38vs.O9	0.700	0.553	0.206	-0.387	1.787
	A38vs.O10	0.693	0.553	0.211	-0.394	1.780
	A38vs.O11	1.060	0.605	0.081	-0.130	2.251
	A38vs.Q12	1.016	0.575	0.078	-0.115	2.147
	A38vs.Q13	-0.186	0.535	0.729	-1.238	0.866
	A38vs.Q16	-0.537	0.575	0.351	-1.668	0.594
	A38vs.Q17	0.524	0.605	0.387	-0.666	1.715
	A38vs.Q18	0.120	0.605	0.843	-1.070	1.311
	A38vs.Q19	-0.623	0.648	0.337	-1.897	0.651
	A38vs.A20	0.671	0.575	0.244	-0.460	1.802
	A38vs.A22	1.253*	0.553	0.024	0.166	2.340
	A38vs.A23	0.883	0.553	0.111	-0.204	1.970
	A38vs.A24	-0.286	0.575	0.620	-1.417	0.845
	A38vs.A25	0.111	0.553	0.840	-0.975	1.198
	A38vs.A26	2.198*	0.575	0.000	1.067	3.329
	A38vs.A27	0.839	0.648	0.196	-0.435	2.113
	A38vs.A28	1.152	0.605	0.058	-0.038	2.343
	A38vs.A29	0.188	0.605	0.756	-1.002	1.379
	A38vs.A31	1.526*	0.535	0.005	0.473	2.578
	A38vs.A32	1.074*	0.535	0.045	0.022	2.126
	A38vs.A33	1.990*	0.605	0.001	0.800	3.181
	A38vs.A35	1.194*	0.605	0.049	0.004	2.385
	A38vs.A36	0.651	0.553	0.239	-0.435	1.738
	A38vs.A37	0.414	0.605	0.494	-0.776	1.605

	A38vs.1F	1.632*	0.605	0.007	0.442	2.823
	A38vs.10F	1.688*	0.605	0.006	0.498	2.879
G122	1Fvs.Q1	0.519	0.626	0.408	-0.712	1.750
	1Fvs.Q2	-1.544*	0.605	0.011	-2.734	-0.353
	1Fvs.Q4	-1.181*	0.577	0.041	-2.315	-0.047
	1Fvs.Q5	-0.996	0.654	0.129	-2.282	0.290
	1Fvs.O6	-1.730*	0.693	0.013	-3.094	-0.367
	1Fvs.O7	-1.389*	0.605	0.022	-2.580	-0.199
	1Fvs.O8	-0.403	0.626	0.520	-1.634	0.828
	1Fvs.O9	-0.932	0.605	0.124	-2.123	0.258
	1Fvs.O10	-0.939	0.605	0.122	-2.130	0.251
	1Fvs.O11	-0.572	0.654	0.382	-1.858	0.714
	1Fvs.Q12	-0.616	0.626	0.325	-1.847	0.615
	1Fvs.Q13	-1.818*	0.589	0.002	-2.977	-0.659
	1Fvs.Q16	-2.170*	0.626	0.001	-3.401	-0.939
	1Fvs.Q17	-1.108	0.654	0.091	-2.394	0.178
	1Fvs.Q18	-1.512*	0.654	0.021	-2.798	-0.226
	1Fvs.Q19	-2.255*	0.693	0.001	-3.619	-0.892
	1Fvs.A20	-0.961	0.626	0.125	-2.192	0.270
	1Fvs.A22	-0.379	0.605	0.531	-1.570	0.811
	1Fvs.A23	-0.749	0.605	0.216	-1.940	0.441
	1Fvs.A24	-1.918*	0.626	0.002	-3.149	-0.687
	1Fvs.A25	-1.521*	0.605	0.012	-2.711	-0.330
	1Fvs.A26	0.565	0.626	0.367	-0.666	1.796
	1Fvs.A27	-0.793	0.693	0.254	-2.157	0.571
	1Fvs.A28	-0.480	0.654	0.463	-1.766	0.806
	1Fvs.A29	-1.444*	0.654	0.028	-2.730	-0.158
	1Fvs.A31	-0.107	0.589	0.856	-1.266	1.052
	1Fvs.A32	-0.558	0.589	0.344	-1.717	0.601
	1Fvs.A33	0.358	0.654	0.584	-0.928	1.644
	1Fvs.A35	-0.438	0.654	0.503	-1.724	0.848
	1Fvs.A36	-0.981	0.605	0.106	-2.171	0.210
	1Fvs.A37	-1.218	0.654	0.063	-2.504	0.068
	1Fvs.A38	-1.632*	0.605	0.007	-2.823	-0.442
	1Fvs.10F	0.056	0.654	0.932	-1.230	1.342
G122	10Fvs.Q1	0.463	0.626	0.460	-0.768	1.694
	10Fvs.Q2	-1.600*	0.605	0.009	-2.790	-0.409
	10Fvs.Q4	-1.237*	0.577	0.033	-2.371	-0.103
	10Fvs.Q5	-1.052	0.654	0.108	-2.338	0.234
	10Fvs.O6	-1.787*	0.693	0.010	-3.150	-0.423

	10Fvs.O7	-1.445*	0.605	0.017	-2.636	-0.255
	10Fvs.O8	-0.459	0.626	0.464	-1.690	0.772
	10Fvs.O9	-0.988	0.605	0.103	-2.179	0.202
	10Fvs.O10	-0.995	0.605	0.101	-2.186	0.195
	10Fvs.O11	-0.628	0.654	0.337	-1.914	0.658
	10Fvs.Q12	-0.672	0.626	0.284	-1.903	0.559
	10Fvs.Q13	-1.874*	0.589	0.002	-3.033	-0.715
	10Fvs.Q16	-2.226*	0.626	0.000	-3.457	-0.995
	10Fvs.Q17	-1.164	0.654	0.076	-2.450	0.122
	10Fvs.Q18	-1.568*	0.654	0.017	-2.854	-0.282
	10Fvs.Q19	-2.312*	0.693	0.001	-3.675	-0.948
	10Fvs.A20	-1.017	0.626	0.105	-2.248	0.214
	10Fvs.A22	-0.435	0.605	0.472	-1.626	0.755
	10Fvs.A23	-0.805	0.605	0.184	-1.996	0.385
	10Fvs.A24	-1.974*	0.626	0.002	-3.205	-0.743
	10Fvs.A25	-1.577*	0.605	0.010	-2.767	-0.386
	10Fvs.A26	0.509	0.626	0.416	-0.722	1.740
	10Fvs.A27	-0.849	0.693	0.222	-2.213	0.515
	10Fvs.A28	-0.536	0.654	0.413	-1.822	0.750
	10Fvs.A29	-1.500*	0.654	0.022	-2.786	-0.214
	10Fvs.A31	-0.163	0.589	0.783	-1.322	0.996
	10Fvs.A32	-0.614	0.589	0.298	-1.773	0.545
	10Fvs.A33	0.302	0.654	0.644	-0.984	1.588
	10Fvs.A35	-0.494	0.654	0.450	-1.780	0.792
	10Fvs.A36	-1.037	0.605	0.088	-2.227	0.154
	10Fvs.A37	-1.274	0.654	0.052	-2.560	0.012
	10Fvs.A39	-1.688*	0.605	0.006	-2.879	-0.498
	10Fvs.1F	-0.056	0.654	0.932	-1.342	1.230

Based on estimated marginal means

*. The mean difference is significant at the 0.05 level.

b. Adjustment for multiple comparisons: Least Significant Difference (equivalent to no adjustments).

APPENDIX G.

Table G. Contains the location and length of unique SVs found in isolate O7 along with their functional domain. In this genome the majority of SVs were located in intergenic regions, except for the SV located in Chromosome 4, at 859,107 with 2,619 bp length, that was found in gene sscle_04g034550. This SV is highlighted in blue light color.

Table G. Overview of unique Structural Variants in *Sclerotinia sclerotiorum* isolate O7: Genomic locations, neighboring genes, and functional domain of neighboring genes.

Chr.	End position (bp)	SV length (bp)	Gene in hotspot	Transcript ID	db_xref	Domain/Process	Gene in hotspot	Transcript ID	Uniparc	Protein
1	13,362	5,363					sscle_01g000060	APA05236	UPI0008DBC34D	FAD-binding FR-type domain-containing protein
1	2,503,508	4,925	sscle_01g007290	APA05959	UPI000159DF2C	PPM-type phosphatase domain-containing protein	sscle_01g007300	APA05960	UPI000159DF2B	DUF614 domain protein
2	2,740,295	5,888	sscle_02g019610	APA07191	UPI000159E4AE	CCHC-type domain-containing protein	sscle_011810	APA07282	UPI00015A09F9	Uncharacterized protein
2	3,048,966	6,302	sscle_02g020510	APA07281	UPI0008DBD808	Uncharacterized protein	sscle_02g020520	APA07282	UPI00015A09F9	Uncharacterized protein
3	639,862	6,301	sscle_03g024140	APA07644	UPI0008DB8703	HTH CENPB-type domain-containing protein	sscle_03g024150	APA07645	UPI000159DB8	BZIP domain-containing protein
3	647,229	5,303	sscle_03g024150	APA07645	UPI000159DB8	BZIP domain-containing protein	sscle_03g024160	APA07646	UPI0008DB8B75	Cytochrome b5 heme-binding domain-containing protein
3	1,692,051	6,025	sscle_03g027280	APA07958	UPI000159D952	Uncharacterized protein	sscle_03g027290	APA07959	UPI000159D951	SMP-30/Gluconolactonase/LRE-like region domain-containing protein
4	859,107	2,619	sscle_04g034550 (in gene)	APA08684	UPI0008DB91BC	DUF676 domain-containing protein				
6	1,077,780	5,752	sscle_06g051490	APA10379	UPI0008DBB0B5	MADS-box domain-containing protein	sscle_06g051500	APA10380	UPI000159F36B	beta-glucosidase
6	1,801,698	5,725	sscle_06g053550	APA10585	UPI00015A0987	Uncharacterized protein	sscle_06g053560	APA10586	UPI00015A094B	Uncharacterized protein
6	1,802,888	4,505	sscle_06g053550	APA10585	UPI00015A0987	Uncharacterized protein	sscle_06g053560	APA10586	UPI00015A094B	Uncharacterized protein
7	1,385,843	5,854	sscle_07g059030	APA11133	UPI000159E1A0	Uncharacterized protein	sscle_07g059040	APA11134	UPI00015A0209	Uncharacterized protein
8	1,887,397	2,954	sscle_08g067510	APA11981	UPI0008DBBC43	Cysteine-rich transmembrane CYSTM domain-containing protein	sscle_08g067520	APA11982	UPI0008DBA1D0	Reverse transcriptase domain-containing protein
9	242,070	6,679	sscle_09g069200	APA12150	UPI0008DBBCBD	Nitric oxide dioxygenase	sscle_09g069210	APA12151	UPI000159FF95	Uncharacterized protein

11	1,798,365	5,289	sscle_11g085960	APA13826	UPI00015A0D0E	Tripeptidyl-peptidase II	sscle_11g085970	APA13827	UPI00015A0D3D	Cytochrome P450 monooxygenase
15	1,066,586	4,024	sscle_15g105250	APA15755	UPI0008DB9E94	Uncharacterized protein	sscle_15g105260	APA15756	UPI000159FD56	BZIP domain-containing protein
15	1,291,052	11,810	sscle_15g105870	APA15817	UPI000159FC01	Reverse transcriptase	sscle_15g105880	APA15818	UPI000159FC00	Uncharacterized protein
15	1,545,048	3,739	sscle_15g106640	APA15894	UPI000159FA8B	Uncharacterized protein	sscle_15g106650	APA15895	UPI0008DBD619	FAD/NAD(P)-binding domain-containing protein
15	1,558,203	4,972	sscle_15g106680	APA15989	UPI000159FA85	Protein kinase domain-containing protein	sscle_15g106690	APA15899	UPI0008DBBDC6	Pectate lyase superfamily protein domain-containing protein
15	1,705,938	13,024	sscle_15g107120	APA15942	UPI0008DBC03C	Uncharacterized protein	sscle_15g107130	APA15943	UPI0008DBC782	BZIP domain-containing protein
16	253,340	9,419	sscle_16g108040	APA16034	UPI00015A003F	Uncharacterized protein	sscle_16g108050	APA16035	UPI0008DBAA38	HotDog ACOT-type domain-containing protein

APPENDIX H.

Table H. Contains the location and length of unique SVs found in isolate Q12 along with their functional domain. In this genome all SVs were located in intergenic regions.

Table G. Overview of unique Structural Variants in *Sclerotinia sclerotiorum* isolate Q12: Genomic locations, neighboring genes, and functional domain of neighboring genes.

Chr.	End position (bp)	SV length (bp)	Gene in hotspot	Transcript ID	db_xref	Protein	Gene in hotspot	Transcript ID	db_xref	Protein
1	2,503,508	3,561	sscle_01g007290	APA05959	UPI000159DF2C	PPM-type phosphatase domain-containing protein	sscle_01g007300	APA05960	UPI000159DF2B	DUF614 domain protein
1	2,782,279	5,458	sscle_01g008110	APA06041	UPI0008DB97D0	Methyltransferase type 11 domain-containing protein	sscle_01g008120	APA06042	UPI0008DBB382	Cation efflux protein cytoplasmic domain-containing protein
1	3,225,096	5,289	sscle_01g009420	APA06172	UPI000159DB16	DUF803 domain membrane protein	sscle_01g009430	APA06173	UPI0008DBB366	Jacalin-type lectin domain-containing protein
2	2,740,295	4,201	sscle_02g019610	APA07191	UPI000159E4AE	CCHC-type domain-containing protein	sscle_011810	Not annotated		
2	3,048,966	5,080	sscle_02g020510	APA07281	UPI0008DBD808	Uncharacterized protein	sscle_02g020520	APA07282	UPI00015A09F9	Uncharacterized protein
4	2,869,111	3,644	sscle_04g040280	APA09258	UPI00015A0EE5	EKC/KEOPS complex subunit BUD32				
7	1,385,860	4,549	sscle_07g059030	APA11133	UPI000159E1A0	Uncharacterized protein	sscle_07g059040	APA11134	UPI00015A0209	Uncharacterized protein
8	1,887,393	9,056	sscle_08g067510	APA11981	UPI0008DBBC43	Cysteine-rich transmembrane CYSTM domain-containing protein	sscle_08g067520	APA11982	UPI0008DBA1D0	Reverse transcriptase domain-containing protein
11	1,748,257	5,814	sscle_11g085800	APA13810	UPI00015A0CC2	GPR1/FUN34/YaaH-class plasma membrane protein	sscle_012570	Not annotated		

15	85,462	2,726	sscle_15g102500	APA15480	UPI0008DBE61A	alcohol dehydrogenase	sscle_15g102510	APA15481	UPI0008DBC938	Uncharacterized protein
15	1,066,586	5,219	sscle_15g105250	APA15755	UPI0008DB9E94	Uncharacterized protein	sscle_15g105260	APA15756	UPI00015FD56	BZIP domain-containing protein
15	1,086,292	7,125	sscle_15g105290	APA15759	UPI0008DBE502	Uncharacterized protein	sscle_15g105300	APA15760	UPI00015FD18	DDE-1 domain-containing protein
15	1,705,938	8,651	sscle_15g107120	APA15942	UPI0008DBC03C	Uncharacterized protein	sscle_15g107130	APA15943	UPI0008DBC782	BZIP domain-containing protein
15	1,763,214	5,536	sscle_15g107310	APA15961	UPI0008DBDD02	HMA domain-containing protein				
16	253,340	6,103	sscle_16g108040	APA16034	UPI00015A003F	Uncharacterized protein	sscle_16g108050	APA16035	UPI0008DBAA38	HotDog ACOT-type domain-containing protein